THE UNIVERSITY OF QUEENSLAND

AUSTRALIA

Tailorable Nanocarrier Emulsion for Drug Delivery

Bijun Zeng

A thesis submitted for the degree of Doctor of Philosophy at

The University of Queensland in 2014

Australian Institute for Bioengineering and Nanotechnology

Abstract

Close to 40-percent of new pharmaceuticals and over 30-percent of pipeline drugs exhibit poor water solubility which provides challenges in drug delivery, such as the delivery of therapeutic levels of drugs to specific biological targets to achieve a desired therapeutic outcome. The challenge of increasing drug therapeutic efficacy, with a concurrent minimization of side effects, can be tackled through proper design and engineering of a suitable drug delivery system (DDS). There is a high demand for DDS that are easy to prepare in the absence of non-pharmaceutical solvents, can carry a variety of drugs, have appropriate pharmacokinetic properties including stability under biological conditions and/or can deliver a drug to a particular tissue or receptor. The development of nanotechnology and bioengineered nanomaterials has greatly increased the potential of nanocarriers for drug delivery. Motivated by the challenges experienced with modular design of effective nanocarrier, this PhD project aims to develop a platform tailorable nanocarrier emulsion (TNE) with combined long circulating and target specific properties, using only biological components and facile processes. Nanoemulsions are a promising nanocarrier class for enhancement of solubility and bioavailability of poorly soluble drugs. They are emulsions that have extremely small droplet size ranging from 10 nm to 200 nm with narrow size distribution. The enormous interfacial area formed by nano-sized droplets provides further engineering opportunities for sustained and controlled drug delivery. Peptide surfactant AM1 was shown to have good emulsification properties and can stabilize oil-in-water emulsions prepared from a range of oils. Recent works from our laboratory have shown that AM1 stabilized emulsion can be used to deliver a hydrophobic molecule to knock down an intracellular protein target *in vitro*. In this PhD work, we tested our hypotheses that a recently-reported biosurfactant protein DAMP4, which comprises four repeating sequences closely related to AM1, could be used to functionalize the interface of AM1 stabilized oil-in-water emulsion through non-covalent self-assembly by addressing the following: (1) Utilization of DAMP4 modified with polyethylene glycol (PEG) to investigate whether DAMP4 can display PEG at the interface and impart altered cell association to the nanoemulsion; (2) Utilization of DAMP4 modified with monoclonal antibody (mAb) against the $CD8^+$ dendritic cells (DCs) specific receptor Clec9A to design a nanocarrier emulsion that is able to target $Clec9A^+$ DCs; (3) Encapsulation of a model antigen within the immune evading and $Clec9A^+$ DCs targeting emulsion to investigate the immune function in a relevant animal model. This work, to our best knowledge, introduces the first DC targeting and immune-evading tailorable nanocarrier emulsion (TNE) made using only biological components and assembled in a bottom-up fashion. Simple top-

down sequential addition of immune evading and receptor-specific Ab elements conjugated to DAMP4 promotes self-assembly at an interface previously formed in the presence of peptide surfactant AM1, leading to a functional display at the interface through non-covalent molecular self-assembly. Model antigen delivered by TNE can be presented by both MHC I and II molecules, leading to CD4 and CD8 T cell activation *in vivo*. Knowledge gained from this work lays a foundation on which to develop a TNE platform for vaccines to deliver both humoral and T cell mediated immunity.

Declaration by author

This thesis is composed of my original work, and contains no material previously published or written by another person except where due reference has been made in the text. I have clearly stated the contribution by others to jointly-authored works that I have included in my thesis.

I have clearly stated the contribution of others to my thesis as a whole, including statistical assistance, survey design, data analysis, significant technical procedures, professional editorial advice, and any other original research work used or reported in my thesis. The content of my thesis is the result of work I have carried out since the commencement of my research higher degree candidature and does not include a substantial part of work that has been submitted to qualify for the award of any other degree or diploma in any university or other tertiary institution. I have clearly stated which parts of my thesis, if any, have been submitted to qualify for another award.

I acknowledge that an electronic copy of my thesis must be lodged with the University Library and, subject to the General Award Rules of The University of Queensland, immediately made available for research and study in accordance with the *Copyright Act 1968*.

I acknowledge that copyright of all material contained in my thesis resides with the copyright holder(s) of that material. Where appropriate I have obtained copyright permission from the copyright holder to reproduce material in this thesis.

Publications during candidature

CHUAN, Y. P., ZENG, B. Y., O'SULLIVAN, B., THOMAS, R. & MIDDELBERG, A. P. J. 2011. Co-delivery of antigen and a lipophilic anti-inflammatory drug to cells via a tailorable nanocarrier emulsion. *Journal of Colloid and Interface Science,* 368**,** 616-624.

ZENG, B. J., CHUAN, Y. P., O'SULLIVAN, B., CAMINSCHI, I., LAHOUD, M. H., THOMAS, R. & MIDDELBERG, A. P. J. 2013. Receptor-Specific Delivery of Protein Antigen to Dendritic Cells by a Nanoemulsion Formed Using Top-Down Non-Covalent Click Self-Assembly. *Small,* 9**,** 3736-3742.

SAINSBURY, F., ZENG, B. & MIDDELBERG, A. P. J. 2014. Towards designer nanoemulsions for precision delivery of therapeutics. *Current Opinion in Chemical Engineering,* 4**,** 11-17.

Publications included in this thesis

ZENG, B. J., CHUAN, Y. P., O'SULLIVAN, B., CAMINSCHI, I., LAHOUD, M. H., THOMAS, R. & MIDDELBERG, A. P. J. 2013. Receptor-Specific Delivery of Protein Antigen to Dendritic Cells by a Nanoemulsion Formed Using Top-Down Non-Covalent Click Self-Assembly. *Small,* 9**,** 3736-3742.

-incorporated as part of Chapter 3, 4 and 5.

-incorporated as Appendix A

Contributor	Statement of contribution
Author ZENG, B. J. (Candidate)	Designed experiments (70%) Conducted experiments (90%) Wrote the paper (60%)
Author CHUAN, Y.P. and MIDDELBERG, A.P.J.	Designed experiments (15%) Wrote and edited paper (30%)
Author O'SULLIVAN, B. and THOMAS, R.	Designed experiments (10%) Wrote and edited paper (5%)
Author CAMINSCHI, I. and LAHOUD, M.H.	Designed experiments (5%) Conducted experiments (10%) Wrote and edited paper (5%)

CHUAN, Y. P., ZENG, B. Y., O'SULLIVAN, B., THOMAS, R. & MIDDELBERG, A. P. J. 2011. Co-delivery of antigen and a lipophilic anti-inflammatory drug to cells via a tailorable nanocarrier emulsion. *Journal of Colloid and Interface Science,* 368**,** 616-624.

-incorporated as Appendix B

Contributor	Statement of contribution
Author CHUAN, Y.P.	Designed experiments (70%) Conducted experiments (70%) Wrote the paper (70%)
Author ZENG, B. Y. (Candidate)	Designed experiments (10%) Conducted experiments (30%) Wrote the paper (5%)
Author MIDDELBERG, A.P.J.	Designed experiments (10%) Wrote the paper (20%)
Author O'SULLIVAN, B. and THOMAS, R.	Designed experiments (10%) Wrote and edited paper (5%)

Contributions by others to the thesis

Dr. Irina Caminschi and Dr. Mireille Lahoud contributed to the design and production of DAMP4-mAb conjugates.

Figure 1-1 and **Figure 3-1** were designed by Dr. Yap Pang Chuan

Statement of parts of the thesis submitted to qualify for the award of another degree

None.

Acknowledgements

My time as a PhD student has been a special period of my life to remember, thanks to many people around me who have inspired and encouraged me to conquer this long journey. Firstly I would like to thank my supervisors, Prof. Anton Middelberg and Prof. Ranjeny Thomas, for their patience, guidance, encouragement and trust over the course of my PhD. A very special thank-you goes to my former supervisor Dr. Yap Pang Chuan, who played a significant role in the direction and success of my PhD. I am grateful to the members of the Centre for Biomolecular Engineering, especially my fellow PhD students Melisa Anggraeni and Wendy Chen, for their constant support and companionship in depressive times.

I was financially supported by a University of Queensland Research Scholarship, and top up scholarship from Australian Institute of Bioengineering and Nanotechnology. Therefore I would like to thank these organizations for financially supporting my study.

And finally, I would like to thank my family and friends back home in China as well as in Australia for their continuous support, which are vital in the maintenance of my sanity. I would not have been able to go through the long and desperate PhD candidature without all of you.

Keywords

nanocarrier, emulsion, dendritic cells, drug delivery, protein antigen, PEGylation, receptor-specific, targeted

Australian and New Zealand Standard Research Classifications (ANZSRC)

ANZSRC code: 100709 Nanomedicine, 60%

ANZSRC code: 100708 Nanomaterials, 20%

ANZSRC code: 090301 Biomaterials, 20%

Fields of Research (FoR) Classification

FoR code: 1007 Nanotechnology, 80%

FoR code: 0903 Biomedical Engineering, 20%

Table of contents

List of abbreviation

ADME Adsorption, distribution, metabolism and excretion

CHO Chinese hamster ovary cells

CLRs C-type lectins receptors

CMC Critical micelle concentration

CTL Cytotoxic T lymphocytes

DCs Dendritic cells

DDS Drug delivery systems

D_H Hydrodynamic diameter

DiI Tetramethylindocarbocyanine perchlorate

DSA Drop shape analysis

EPR Enhanced permeability and retention

FDA Food and drug administration

GI Gastrointestinal

HEPES 4-(2-hydroxyethyl)-1-piperazineethanesulfonic acid

hPBMC Human peripheral blood mononuclear cells

IEX Ion exchange

IMAC Immobilized metal affinity chromatography

LCT Long-chain triglyceride

LMWS Low molecular weight surfactants

LN Lymph nodes

mAbs Monoclonal antibodies

MCT Medium-chain triglyceride

MHC Major histocompatibility complex

MPS Mononuclear phagocyte system

MSP Mesoporous silica nanoparticles

NCE New chemical entities

NF-κB Nuclear factor kappa B

NK Natural killer

NLRs NOD-like receptors

NNLS Non-negatively constrained least squares

O/W	Oil-in-water
OVA	Ovalbumin
PBS	Phosphate buffered saline
PEG	Polyethylene glycol
PIT	Phase inversion temperature
PLA	Polylactide
PLGA	Polylactide co-glycolide
PRRs	Pattern recognition receptors
R&D	Research and development
RES	Reticuloendothelial system
RGD	Arginine-glycine-aspartic acid
S/O	Solid-in-oil
S/O/W	Solid-in-oil-in-water
SAP	Surface active peptide
scFv	Single chain variable fragments
SMDs	Small molecule drugs
TLRs	Toll-like receptors
TNE	Tailorable nanocarrier emulsion
TNF	Tumor necrosis factor
W/O	Water-in-oil
W/O/W	Water-in-oil-in-water

List of Figures

List of Tables

Chapter 1 Introduction

1.1. Background

Biotechnology and biomedical advances have led to the discovery and development of new drugs that will change the way we treat disease. The most common small molecule drugs (SMDs), which are normally chemically-manufactured molecular substances, are traditionally processed into ingestible tablets or capsules for oral administration. Upon administration, the SMDs dissolve in the gastrointestinal (GI) tract, penetrate the intestinal wall and reach their active biological site through the blood stream. A majority (~ 90 %) of new chemical entities (NCEs) are discovered to be lipophilic and exhibit poor water solubility (Hauss, 2007). In addition, most SMDs used in or designed for cancer and autoimmune disease treatments possess unfavourable side effects. Increased systemic administration of these anti-cancer SMDs increases potential for adverse side effects.

Another hot topic in pharmaceutical research and development (R&D) is biomolecular drugs (also referred to biologics), which make up more than 30 % of the current licensed pharmaceutical products (Leader et al., 2008, Swinney and Anthony, 2011). This class of drugs are mostly active components created through biotechnology, such as monoclonal antibodies (mAbs), protein therapeutics, growth factors and cytokines (Sathish et al., 2013). Nevertheless, wide adoption of biologics in clinical application is limited by their intrinsic instability. Furthermore, most of these drugs cannot be packaged into traditional capsules for oral administration as they are susceptible to *in vivo* enzymatic degradation (Sathish et al., 2013).

Owing to the issues stated above, two strategies for improving the therapeutic efficacy of drugs have emerged over the past several decades. The first is to design new derivatives of therapeutics with enhanced pharmacological properties, e.g. solubility and bioavailability (Collins and Workman, 2006). These new derivatives have significantly extended R&D timeframes and require high financial input. The other more feasible and economical strategy is to formulate therapeutics with novel drug delivery systems (DDS) so that they can be used to cater for specific medication needs (Duncan, 2006, Ferrari, 2005, Peer et al., 2007).

DDS are vehicles by which therapeutic substances are introduced to the body and shuttled to their site of action. They are designed to improve therapeutic efficacy and reduce the potential of side-effects. In addition to the demand of suitable DDS for new drugs, pharmaceutical companies are also looking to re-package blockbuster drugs that are approaching the end of patent life into new DDS in order to maintain their lead in the market. The global DDS market in 2010 was $131.6 billion and is expected to reach $224.2 billion by the end of 2017 (2011). There is great demand for novel DDS and the prospects for this market are truly promising.

1.2. Colloidal nanocarriers for drug delivery

The challenge of increasing drug therapeutic efficacy, with a concurrent minimization of side effects, can be tackled through proper design and engineering of a suitable DDS. The development of nanotechnology and bioengineered nanomaterials has greatly increased the potential of nanocarriers for drug delivery. An ideal nanocarrier can protect delicate drugs from enzymatic degradation, prolong circulation half-life, with targeting characteristics that allow for site-specific delivery. Rational design of advanced nanocarrier DDS requires the coordinating behaviour of three components, the vehicle that carriers the drug, a targeting or/and immune-evading moiety that recognizes and binds the target, and the drug that provides therapeutic action at the specific site.

Colloidal nanocarriers DDS holds great promise to address the stated requirements above (Ferrari, 2005, Moghimi et al., 2005, Boyd, 2008). Drugs with poor water-solubility and instability under external or enzymatic environments can be encapsulated within the hydrophobic compartments of the nanocarriers, such as liposomes, emulsions and micelles (Yekollu et al., 2011, Ashley et al., 2011, Han et al., 2013, Howell et al., 2013). Obstacles arising from aberrant side effects and inability to cross biological barriers could be tackled by surface engineering with immune evading polymers and biologically reactive ligands (Boyd, 2008). Current well-studied DDS nanocarriers include but are not limited to liposomes, nanoparticles, micelles, nanocapsules, nanospheres and emulsions (Hu et al., 2011, Ashley et al., 2011, Kaaki et al., 2011, Kukowska-Latallo et al., 2005, Liu et al., 2010, Mathew et al., 2012, Reddy et al., 2006, Yoshida et al., 2012, Shroff and Kokkoli, 2012). Doxil® was the first FDA approved liposome based therapeutic nanocarrier for cancer treatment (Petros and DeSimone, 2010).

1.2.1. Potential of nanoemulsions for drug delivery

While liposomes and nanoparticles laid the foundation for nanocarriers research and represent well-studied platforms for cell-specific delivery, they often require complex preparation procedures, use solvents not suitable for pharmaceutical use and/or result in polydisperse structures that are difficult to define and characterize to a level that allows simple pharmaceutical registration. The compositional complexity of these delivery systems also hinders FDA approval for clinical application. At the other end of the application spectrum, nanoemulsions are a promising nanocarrier class for enhancement of solubility and bioavailability of poorly soluble drugs (Anton et al., 2008, Anton et al., 2010, Constantinides et al., 2004, Constantinides et al., 2000, Davis et al., 1987, Ganta and Amiji, 2009, Ghai and Sinha, 2012). They are emulsions that have an extremely small droplet size ranging from 10 nm to 200 nm with narrow size distribution (Solans et al., 2003). Nanoemulsions are non-equilibrium systems, which means they have a tendency to separate into the constituent phases (Gutiérrez et al., 2008). Nevertheless, nanoemulsions can stay kinetically stable over a long period of time (Solans et al., 2003). Compared to common polymeric micellar nanocarriers, nanoemulsions have higher drug loading capacity and longer shelf life (Sadurní et al., 2005, Tadros et al., 2004). Lipophilic drugs can be solubilized within the oil droplets to increase their bioavailability and enable facile packaging. The enormous interfacial area formed by nano-sized droplets provides further engineering opportunities for sustained and controlled drug delivery (Thanos et al., 2003, Chuan et al., 2011).

1.3. Previous relevant research in the lab and hypothesis

Emulsions and nanoemulsions have already found widespread use in clinical application. However, in most cases they do not encode sophisticated function, for example the ability to specifically target a given cell population *in vivo* (Ganta and Amiji, 2009, Santos-Magalhães et al., 2000, Makidon et al., 2008, Kukowska-Latallo et al., 2005, Sigward et al., 2013). This limitation arises from the difficulty of engineering the emulsion interface, which is usually populated by mixed chemical species including surfactants, and is less physically and chemically defined than the solid counterpart. The challenges of developing a targeted nanocarrier emulsion lie in 1) the ease of manufacturing steps in the absence of non-pharmaceutical solvents; 2) the ability to deliver a variety of pharmaceuticals with appropriate pharmacokinetic properties to their site of action; 3) controlled and target specific delivery of concentrated pharmaceutical ingredients to the site of desired action. In this thesis I develop a new DDS that overcomes these challenges, as follows.

Peptide surfactant AM1 (Dexter et al., 2006) belongs to a biosurfactant family developed in the Centre for Biomolecular Engineering (CBE) at The University of Queensland, and is a short helix-forming sequence based on the peptide Lac21(Middelberg et al., 2000) which only differs from Lac21 by two histidine residues. The histidine residues within AM1 allow binding of transition metal ions, *eg.* Zn(II), which enhance intermolecular interactions to create a cohesive interfacial network having measurable mechanical properties and known structure (Middelberg et al., 2008). Surface active peptides (SAP) like AM1 exhibit stimuli-responsive interfacial behavior in that they are capable of converting between a cohesive 'film state' and a mobile 'detergent state' at a fluid-fluid interface (Dexter and Middelberg, 2007). At neutral pH in the presence of Zn (II), AM1 has good emulsification properties and can stabilize oil-in-water emulsions prepared from a range of oils. In addition, a tunable emulsion interface can be achieved by changing either the sequence of these SAP or the physical conditions of the buffer, *e.g.* pH and ionic character (Malcolm et al., 2009). AM1 comes with the possibility of low-cost bio-production which offers the combined advantages of biocompatibility and sustainability (Kaar et al., 2009).

Using an AM1-stabilised nanoemulsion, we reported the preparation of a tailorable nanocarrier emulsion (TNE) for the co-delivery of a small lipophilic drug and an animal model relevant antigen to antigen presenting cells (APCs) *in vitro* (Chuan et al., 2011). The reported TNE comprised a core that is a pharmaceutical-grade oil stabilized by AM1 (Dexter et al., 2006), rendered stable in physiological conditions by electrostatic deposition of the antigen of interest onto the TNE outer surface using a well-established layer-by-layer approach. The chosen excipient for this first-generation TNE (Miglyol® 812) is a medium-chain fatty acid triglyceride approved by the FDA and commonly used as an excipient in pharmaceutical formulations (Chuan et al., 2011). The study showed successful packaging of a hydrophobic molecule within the oil droplet and co-delivery to cells, with dose-dependent knock-down of an intracellular protein target.

While this first TNE study showed successful delivery to cells, it did not encode stealth or targeting capability which would be necessary for effective *in vivo* use. The *in vivo* function of the TNE will likely be limited by the rapid uptake of intravenously injected colloidal drug carriers by cells in the mononuclear phagocyte system (MPS) (Klibanov et al., 1990, Mosqueira et al., 2001). Secondly, it will be desirable to specifically deliver active cargo to a target site to minimize unnecessary side effects

associated with uptake by non-target cells. Additionally, layer-by-layer assembly confused the cargo and stabilizing functions (the delivered model antigen, BSA, was also used to provide colloidal stability). The research challenge addressed in this thesis was to devise new approaches not dependent on layer-by-layer assembly that would allow an AM1-stabilised nanoemulsion to deliver active ingredient to cells, *in vivo*, in a way that evades non-specific uptake yet targets a specific subset of cells. Additionally, it was desired to not confuse the cargo and stabilization functions, so that the active compound is encapsulated within the oil core rather than located on the colloidal surface.

Several mechanisms of surface functionalization for nanocarriers are available in the literature, but typically involve the physical or chemical addition of agents to the surface of a nanocarrier (Kamphuis et al., 2010, Wang et al., 2010). These options are available for the TNE, as the surface is based on peptides thus the tools of protein conjugation are available. However, such an approach would require complex chemical steps and may still require the use of protein for colloidal stabilization.

Inspired by the chemical similarity of a recently-reported protein biosurfactant DAMP4 (Middelberg and Dimitrijev-Dwyer, 2011), Professor Anton Middelberg, who is also the principal supervisor of this PhD project, hypothesized that DAMP4 would integrate into or onto the surface of an AM1-stabilised oil-water interface, and that modification of DAMP4 with another entity (e.g. antibody or polymer) would enable display of that entity at the interface by non-covalent “click chemistry” self-assembly. Neutron reflectometry studies, subsequent to the start of this doctoral research, confirmed interfacial mixing of DAMP4 with a small peptide surfactant closely related to AM1 (Dwyer et al., 2013). The hypothesis that DAMP4 could be used to engineer the interface of the TNE through non-covalent self-assembly laid the foundation for this doctoral project. Figure 1-1 shows the schematic representation of such hypothesis.

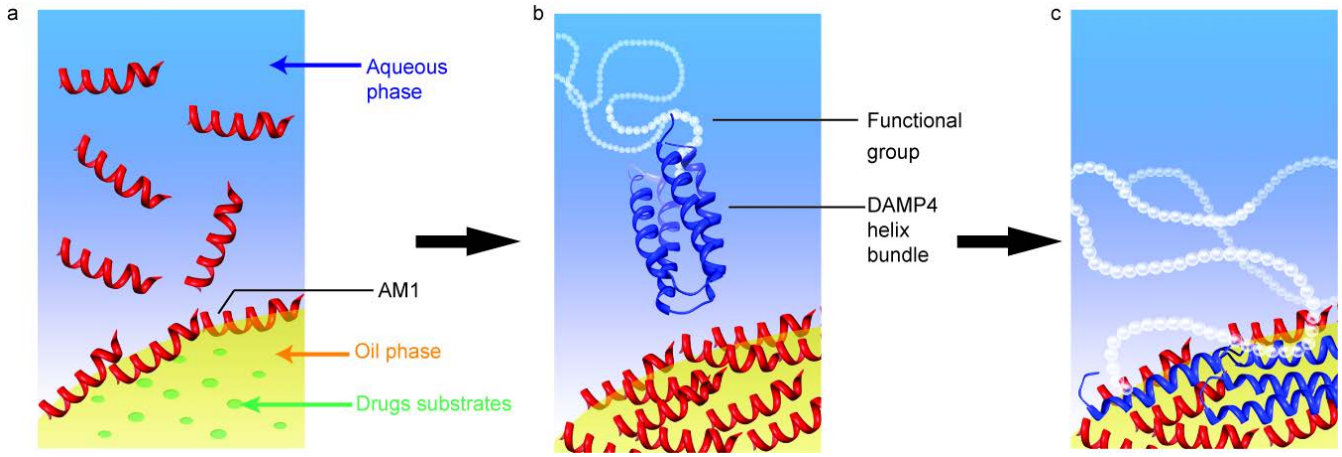

Figure 1-1. Schematic representation of hypothesis that DAMP4 could be used to engineer a TNE interface. a) Rapid adsorption of peptide surfactant AM1 (red) onto the oil-water interface results in a stable TNE oil core (yellow). Incorporating the oil-solubilized protein antigen (light green) into oil phase at the time of emulsion formation enables its facile packaging; b) Functional groups conjugated to DAMP4 protein (dark blue) introduced to a solution containing the preformed AM1 peptide stabilized TNE oil core results in c) DAMP4 integration to the oil-water interface and functional display of its conjugated group at the interface.

1.4. Project aims and objectives

The overall aim of this doctoral work was to explore the above hypothesis and solve obvious challenges along the way, to ultimately decouple the biological (cargo) and physical design (stabilization) criteria for nanoemulsions through an entirely novel emulsion nano-engineering approach based on non-covalent self-assembly at the oil-water interface. This aim was achieved through the following objectives:

1. to investigate whether DAMP4 modified with functional moieties (e.g. the polymer PEG) can display those moieties at the interface and impart function (e.g. altered cell binding) to the nanoemulsion;
2. to design a stable, long circulating nanocarrier emulsion able to target dendritic cells, using DAMP4 as an interfacial anchor;
3. to investigate the cellular uptake efficiency of the resulting nanoemulsion and conduct formulation optimization to enhance target specificity;

4. to encapsulate a model antigen within the nanoemulsion and evaluate immune function in a relevant animal model;
5. to assess the possibility of tuning the immune response elicited by antigen-loaded nanoemulsion by varying suitable design parameters.

As an initial test of the hypothesis, I modified DAMP4 with polyethylene glycol (PEG, a non-toxic and non-immunogenic highly elastic polymer) and evaluated the immune evading ability of a nanoemulsion modified with the PEG-DAMP4 hybrid molecule. PEG is a well-studied polymer that has been approved by the US Food and Drug Administration (FDA) for pharmaceutical use (Harris et al., 2001), thus it was selected in this work as the immune evading molecule. If the hypothesis is correct, conjugation of PEG to DAMP4 prior to introduction of such a hybrid molecule to a preformed AM1-stabilized TNE core would result in a TNE having an elastic interface and enhanced immune-evading characteristics. For the targeting moiety, I decorated the nanoemulsion with DAMP4 modified with antibody against Clec9A, a recently-identified surface receptor highly exclusive to a subset of DCs in both human and mouse (Caminschi et al., 2008, Lahoud et al., 2011, Sancho et al., 2009). Antibody bound to Clec9A has been found to be internalized efficiently and *in vivo* delivery of antigen coupled to this antibody results in antigen cross presentation by $CD8^+$ DCs (Caminschi et al., 2008, Sancho et al., 2009). This background made Clec9A a superior targeting choice for delivering drugs to DCs.

1.5. Thesis structure

Following this introduction, this thesis is comprised of five main chapters including a literature review and four experimental chapters.

Chapter 2 presents a critical review of the topics relevant to this research project and provides the relevant conceptual background needed.

The comprehensive development of a new TNE is documented in Chapters 3 to 6, organized by the increased complexity of the TNE composition. Chapter 3 addressed objective 1 by describing a simple, unique chemistry that allows for one-step non-covalent conjugation of PEG to the AM1 pre-stabilized TNE core for enhanced immune evading function. We first evaluate the hypothesis of DAMP4 mediating TNE functionalization by conducting sudden bubble contraction experiments. PEG-modified

DAMP4 formed an elastic film on an AM1 pre-occupied oil-water interface, suggesting a flexible layer of PEG was anchoring on the interface via DAMP4. A PEGylated TNE was prepared from PEG modified DAMP4 via sequential reagent addition process. *In vitro* stability and the immune evading ability of such PEGylated TNE are also described in this chapter.

Having proved DAMP4 was able to bring conjugated PEG into a pre-formed AM1 stabilized oil-water interface, an immune-evading TNE was fabricated using a top-down non-covalent click chemistry strategy. With this in mind, Chapter 4 addressed objectives 2 and 3 by examining whether the same method could be applied to add a target-specific homing characteristic to the TNE. *In vitro* TNE-cell association and the formulation optimization of the constructed TNE is discussed in this chapter.

The need for highly-efficient DDS for vaccines led us to consider this system for delivery of protein based therapeutics. Hence we address objectives 4 and 5 in Chapters 5 and 6. The PEG layer of the TNE is expected to promote passive targeting through enhanced permeability and retention (EPR) effect, while the targeting mAb allowed highly specific delivery to DCs to activate the required immune response. Chapter 5 describes the process of incorporating a model protein antigen (Ag) ovalbumin (OVA) into the TNE. The efficiency of TNE targeting delivery of Ag to dendritic cells (DCs) was evaluated by by an *in vitro* T cell proliferation assay. Having in mind *in vivo* drug delivery applications, such studies are an essential first steps to assess the potential of TNE for the delivery of protein and drugs.

Chapter 6 assesses the efficiency of TNE delivering Ag to DCs *in vivo*. Ag encapsulated within TNE was specifically delivered to DCs, correctly processed and cross-presented to Ag specific T cell subsets. Cytotoxic T lymphocytes (CTL) assay revealed that Ag delivered by TNE to $CD8^+$ DCs leads to endogenous production of effectors CTLs. Tunable immune response could be obtained by varying the TNE formulation composition.

Finally, the major outcomes of developing a TNE, the potential of further development for translating the TNE platform into clinical application and the shortcomings of such a platform are summarized in Chapter 7.

The patented research (Middelberg and Zeng) findings in this body of work are related to the development of a new drug delivery system that has the potential to be exploited in further clinical application. The use of top-down non-covalent click self-assembly to form a nanoemulsion harnessing the chemical similarity of novel surface peptide surfactant may eventually form the basis of flexible drug delivery platform that can be tailored to address unmet medical need in a personalized fashion.

2011. MarketsandMarkets: Global Top 10 Drug Delivery Technologies Market to be US$ 81.5 Billion by 2015. *PR Newswire Europe Including UK Disclose*.

ANTON, N., BENOIT, J.-P. & SAULNIER, P. 2008. Design and production of nanoparticles formulated from nano-emulsion templates—A review. *Journal of Controlled Release,* 128**,** 185-199.

ANTON, N., MOJZISOVA, H., PORCHER, E., BENOIT, J.-P. & SAULNIER, P. 2010. Reverse micelle-loaded lipid nano-emulsions: New technology for nano-encapsulation of hydrophilic materials. *International Journal of Pharmaceutics,* 398**,** 204-209.

ASHLEY, C. E., CARNES, E. C., PHILLIPS, G. K., PADILLA, D., DURFEE, P. N., BROWN, P. A., HANNA, T. N., LIU, J., PHILLIPS, B., CARTER, M. B., CARROLL, N. J., JIANG, X., DUNPHY, D. R., WILLMAN, C. L., PETSEV, D. N., EVANS, D. G., PARIKH, A. N., CHACKERIAN, B., WHARTON, W., PEABODY, D. S. & BRINKER, C. J. 2011. The targeted delivery of multicomponent cargos to cancer cells by nanoporous particle-supported lipid bilayers. *Nat Mater,* 10**,** 389-397.

BOYD, B. J. 2008. Past and future evolution in colloidal drug delivery systems. *Expert Opinion on Drug Delivery,* 5**,** 69-85.

CAMINSCHI, I., PROIETTO, A. I., AHMET, F., KITSOULIS, S., TEH, J. S., LO, J. C. Y., RIZZITELLI, A., WU, L., VREMEC, D., VAN DOMMELEN, S. L. H., CAMPBELL, I. K., MARASKOVSKY, E., BRALEY, H., DAVEY, G. M., MOTTRAM, P., DE VELDE, N. V., JENSEN, K., LEW, A. M., WRIGHT, M. D., HEATH, W. R., SHORTMAN, K. & LAHOUD, M. H. 2008. The dendritic cell subtype-restricted C-type lectin Clec9A is a target for vaccine enhancement. *Blood,* 112**,** 3264-3273.

CHUAN, Y. P., ZENG, B. Y., O'SULLIVAN, B., THOMAS, R. & MIDDELBERG, A. P. J. 2011. Co-delivery of antigen and a lipophilic anti-inflammatory drug to cells via a tailorable nanocarrier emulsion. *Journal of Colloid and Interface Science,* 368**,** 616-624.

COLLINS, I. & WORKMAN, P. 2006. New approaches to molecular cancer therapeutics. *Nat Chem Biol,* 2**,** 689-700.

CONSTANTINIDES, P. P., LAMBERT, K. J., TUSTIAN, A. K., SCHNEIDER, B., LALJI, S., MA, W. W., WENTZEL, B., KESSLER, D., WORAH, D. & QUAY, S. C. 2000. Formulation development and antitumor activity of a filter-sterilizable emulsion of paclitaxel. *Pharmaceutical Research,* 17**,** 175-182.

CONSTANTINIDES, P. P., TUSTIAN, A. & KESSLER, D. R. 2004. Tocol emulsions for drug solubilization and parenteral delivery. *Advanced Drug Delivery Reviews,* 56**,** 1243-1255.

DAVIS, S. S., WASHINGTON, C., WEST, P., ILLUM, L., LIVERSIDGE, G., STERNSON, L. & KIRSH, R. 1987. Lipid Emulsions as Drug Delivery Systems. *Annals of the New York Academy of Sciences,* 507**,** 75-88.

DEXTER, A. F., MALCOLM, A. S. & MIDDELBERG, A. P. J. 2006. Reversible active switching of the mechanical properties of a peptide film at a fluid-fluid interface. *Nat Mater,* 5**,** 502-506.

DEXTER, A. F. & MIDDELBERG, A. P. J. 2007. Switchable Peptide Surfactants with Designed Metal Binding Capacity. *The Journal of Physical Chemistry C,* 111**,** 10484-10492.

DUNCAN, R. 2006. Polymer conjugates as anticancer nanomedicines. *Nat Rev Cancer,* 6**,** 688-701.

DWYER, M. D., HE, L. Z., JAMES, M., NELSON, A. & MIDDELBERG, A. P. J. 2013. Insights into the role of protein molecule size and structure on interfacial properties using designed sequences. *Journal of the Royal Society Interface,* 10.

FERRARI, M. 2005. Cancer nanotechnology: opportunities and challenges. *Nat Rev Cancer,* 5**,** 161-171.

GANTA, S. & AMIJI, M. 2009. Coadministration of Paclitaxel and Curcumin in Nanoemulsion Formulations To Overcome Multidrug Resistance in Tumor Cells. *Molecular Pharmaceutics,* 6**,** 928-939.

GHAI, D. & SINHA, V. R. 2012. Nanoemulsions as self-emulsified drug delivery carriers for enhanced permeability of the poorly water-soluble selective β1-adrenoreceptor blocker Talinolol. *Nanomedicine: Nanotechnology, Biology and Medicine,* 8**,** 618-626.

GUTIÉRREZ, J. M., GONZÁLEZ, C., MAESTRO, A., SOLÈ, I., PEY, C. M. & NOLLA, J. 2008. Nano-emulsions: New applications and optimization of their preparation. *Current Opinion in Colloid & Interface Science,* 13**,** 245-251.

HAN, H. S., LEE, J., KIM, H. R., CHAE, S. Y., KIM, M., SARAVANAKUMAR, G., YOON, H. Y., YOU, D. G., KO, H., KIM, K., KWON, I. C., PARK, J. C. & PARK, J. H. 2013. Robust PEGylated hyaluronic acid nanoparticles as the carrier of doxorubicin: Mineralization and its effect on tumor targetability in vivo. *Journal of Controlled Release,* 168**,** 105-114.

HARRIS, J. M., MARTIN, N. E. & MODI, M. 2001. Pegylation - A novel process for modifying pharmacokinetics. *Clinical Pharmacokinetics,* 40**,** 539-551.

HAUSS, D. J. 2007. Oral lipid-based formulations. *Advanced Drug Delivery Reviews,* 59**,** 667-676.

HOWELL, M., MALLELA, J., WANG, C., RAVI, S., DIXIT, S., GARAPATI, U. & MOHAPATRA, S. 2013. Manganese-loaded lipid-micellar theranostics for simultaneous drug and gene delivery to lungs. *Journal of Controlled Release,* 167**,** 210-218.

HU, J., QIAN, Y., WANG, X., LIU, T. & LIU, S. 2011. Drug-Loaded and Superparamagnetic Iron Oxide Nanoparticle Surface-Embedded Amphiphilic Block Copolymer Micelles for Integrated Chemotherapeutic Drug Delivery and MR Imaging. *Langmuir,* 28**,** 2073-2082.

KAAKI, K., HERVÉ-AUBERT, K., CHIPER, M., SHKILNYY, A., SOUCÉ, M., BENOIT, R., PAILLARD, A., DUBOIS, P., SABOUNGI, M.-L. & CHOURPA, I. 2011. Magnetic Nanocarriers of Doxorubicin Coated with Poly(ethylene glycol) and Folic Acid: Relation between Coating Structure, Surface Properties, Colloidal Stability, and Cancer Cell Targeting. *Langmuir,* 28**,** 1496-1505.

KAAR, W., HARTMANN, B. M., FAN, Y., ZENG, B., LUA, L. H. L., DEXTER, A. F., FALCONER, R. J. & MIDDELBERG, A. P. J. 2009. Microbial bio-production of a recombinant stimuli-responsive biosurfactant. *Biotechnology and Bioengineering,* 102**,** 176-187.

KAMPHUIS, M. M. J., JOHNSTON, A. P. R., SUCH, G. K., DAM, H. H., EVANS, R. A., SCOTT, A. M., NICE, E. C., HEATH, J. K. & CARUSO, F. 2010. Targeting of Cancer Cells Using Click-Functionalized Polymer Capsules. *Journal of the American Chemical Society,* 132**,** 15881-15883.

KLIBANOV, A. L., MARUYAMA, K., TORCHILIN, V. P. & HUANG, L. 1990. Amphipathic polyethyleneglycols effectively prolong the circulation time of liposomes. *Febs Letters,* 268**,** 235-237.

KUKOWSKA-LATALLO, J. F., CANDIDO, K. A., CAO, Z., NIGAVEKAR, S. S., MAJOROS, I. J., THOMAS, T. P., BALOGH, L. P., KHAN, M. K. & BAKER, J. R. 2005. Nanoparticle Targeting of Anticancer Drug Improves Therapeutic Response in Animal Model of Human Epithelial Cancer. *Cancer Research,* 65**,** 5317-5324.

LAHOUD, M. H., AHMET, F., KITSOULIS, S., WAN, S. S., VREMEC, D., LEE, C. N., PHIPSON, B., SHI, W., SMYTH, G. K., LEW, A. M., KATO, Y., MUELLER, S. N., DAVEY, G. M., HEATH, W. R., SHORTMAN, K. & CAMINSCHI, I. 2011. Targeting Antigen to Mouse Dendritic Cells via Clec9A Induces Potent CD4 T Cell Responses Biased toward a Follicular Helper Phenotype. *J. Immunol,* 187**,** 842-850.

LEADER, B., BACA, Q. J. & GOLAN, D. E. 2008. Protein therapeutics: a summary and pharmacological classification. *Nat Rev Drug Discov,* 7**,** 21-39.

LIU, Y., LI, K., PAN, J., LIU, B. & FENG, S.-S. 2010. Folic acid conjugated nanoparticles of mixed lipid monolayer shell and biodegradable polymer core for targeted delivery of Docetaxel. *Biomaterials,* 31**,** 330-338.

MAKIDON, P. E., BIELINSKA, A. U., NIGAVEKAR, S. S., JANCZAK, K. W., KNOWLTON, J., SCOTT, A. J., MANK, N., CAO, Z., RATHINAVELU, S., BEER, M. R., WILKINSON, J. E., BLANCO, L. P., LANDERS, J. J. & BAKER, J. R., JR. 2008. Pre-Clinical Evaluation of a Novel Nanoemulsion-Based Hepatitis B Mucosal Vaccine. *PLoS ONE,* 3**,** e2954.

MALCOLM, A. S., DEXTER, A. F., KATAKDHOND, J. A., KARAKASHEV, S. I., NGUYEN, A. V. & MIDDELBERG, A. P. J. 2009. Tuneable Control of Interfacial Rheology and Emulsion Coalescence. *ChemPhysChem,* 10**,** 778-781.

MATHEW, A., FUKUDA, T., NAGAOKA, Y., HASUMURA, T., MORIMOTO, H., YOSHIDA, Y., MAEKAWA, T., VENUGOPAL, K. & KUMAR, D. S. 2012. Curcumin Loaded-PLGA Nanoparticles Conjugated with Tet-1 Peptide for Potential Use in Alzheimer's Disease. *PLoS ONE,* 7**,** e32616.

MIDDELBERG, A. P. J. & DIMITRIJEV-DWYER, M. 2011. A Designed Biosurfactant Protein for Switchable Foam Control. *ChemPhysChem,* 12**,** 1426-1429.

MIDDELBERG, A. P. J., HE, L., DEXTER, A. F., SHEN, H.-H., HOLT, S. A. & THOMAS, R. K. 2008. The interfacial structure and Young's modulus of peptide films having switchable mechanical properties. *Journal of the Royal Society Interface,* 5**,** 47-54.

MIDDELBERG, A. P. J., RADKE, C. J. & BLANCH, H. W. 2000. Peptide interfacial adsorption is kinetically limited by the thermodynamic stability of self association. *Proceedings of the National Academy of Sciences,* 97**,** 5054-5059.

MIDDELBERG, A. P. J. & ZENG, B. *Nanoemulsions*. International Patent Application No.: PCT/AU2013/000630, International Filing Date: 13 June 2012.

MOGHIMI, S. M., HUNTER, A. C. & MURRAY, J. C. 2005. Nanomedicine: current status and future prospects. *The FASEB Journal,* 19**,** 311-330.

MOSQUEIRA, V. C. F., LEGRAND, P., MORGAT, J. L., VERT, M., MYSIAKINE, E., GREF, R., DEVISSAGUET, J. P. & BARRATT, G. 2001. Biodistribution of long-circulating PEG-grafted nanocapsules in mice: Effects of PEG chain length and density. *Pharmaceutical Research,* 18**,** 1411-1419.

PEER, D., KARP, J. M., HONG, S., FAROKHZAD, O. C., MARGALIT, R. & LANGER, R. 2007. Nanocarriers as an emerging platform for cancer therapy. *Nat. Nanotechnol.,* 2**,** 751-760.

PETROS, R. A. & DESIMONE, J. M. 2010. Strategies in the design of nanoparticles for therapeutic applications. *Nat Rev Drug Discov,* 9**,** 615-627.

REDDY, S. T., REHOR, A., SCHMOEKEL, H. G., HUBBELL, J. A. & SWARTZ, M. A. 2006. In vivo targeting of dendritic cells in lymph nodes with poly(propylene sulfide) nanoparticles. *Journal of Controlled Release,* 112**,** 26-34.

SADURNÍ, N., SOLANS, C., AZEMAR, N. & GARCÍA-CELMA, M. J. 2005. Studies on the formation of O/W nano-emulsions, by low-energy emulsification methods, suitable for pharmaceutical applications. *European Journal of Pharmaceutical Sciences,* 26**,** 438-445.

SANCHO, D., JOFFRE, O. P., KELLER, A. M., ROGERS, N. C., MARTINEZ, D., HERNANZ-FALCON, P., ROSEWELL, I. & SOUSA, C. R. E. 2009. Identification of a dendritic cell receptor that couples sensing of necrosis to immunity. *Nature,* 458**,** 899-903.

SANTOS-MAGALHÃES, N. S., PONTES, A., PEREIRA, V. M. W. & CAETANO, M. N. P. 2000. Colloidal carriers for benzathine penicillin G: Nanoemulsions and nanocapsules. *International Journal of Pharmaceutics,* 208**,** 71-80.

SATHISH, J. G., SETHU, S., BIELSKY, M.-C., DE HAAN, L., FRENCH, N. S., GOVINDAPPA, K., GREEN, J., GRIFFITHS, C. E. M., HOLGATE, S., JONES, D., KIMBER, I., MOGGS, J., NAISBITT, D. J., PIRMOHAMED, M., REICHMANN, G., SIMS, J., SUBRAMANYAM, M., TODD, M. D., VAN DER LAAN, J. W., WEAVER, R. J. & PARK, B. K. 2013. Challenges and approaches for the development of safer immunomodulatory biologics. *Nat Rev Drug Discov,* 12**,** 306-324.

SHROFF, K. & KOKKOLI, E. 2012. PEGylated Liposomal Doxorubicin Targeted to α5β1-Expressing MDA-MB-231 Breast Cancer Cells. *Langmuir,* 28**,** 4729-4736.

SIGWARD, E., MIGNET, N., RAT, P., DUTOT, M., MUHAMED, S., GUIGNER, J. M., SCHERMAN, D., BROSSARD, D. & CRAUSTE-MANCIET, S. 2013. Formulation and cytotoxicity evaluation of new self-emulsifying multiple W/O/W nanoemulsions. *International Journal of Nanomedicine,* 8**,** 611-625.

SOLANS, C., ESQUENA, J., FORGIARINI, A. M., USÓN, N., MORALES, D., IZQUIERDO, P., AZEMAR, N. & GARCIA-CELMA, M. J. 2003. Nano-emulsions: Formation, properties and applications. *Adsorption and Aggregation of Surfactants in Solution,* 109**,** 525-554.

SWINNEY, D. C. & ANTHONY, J. 2011. How were new medicines discovered? *Nat Rev Drug Discov,* 10**,** 507-519.

TADROS, T., IZQUIERDO, P., ESQUENA, J. & SOLANS, C. 2004. Formation and stability of nano-emulsions. *Advances in Colloid and Interface Science,* 108–109**,** 303-318.

THANOS, C. G., LIU, Z., REINEKE, J., EDWARDS, E. & MATHIOWITZ, E. 2003. Improving Relative Bioavailability of Dicumarol by Reducing Particle Size and Adding the Adhesive PolyFumaric-Co-Sebacic Anhydride. *Pharmaceutical Research,* 20**,** 1093-1100.

WANG, Y., WANG, Y. Q., XIANG, J. N. & YAO, K. T. 2010. Target-Specific Cellular Uptake of Taxol-Loaded Heparin-PEG-Folate Nanoparticles. *Biomacromolecules,* 11**,** 3531-3538.

YEKOLLU, S. K., THOMAS, R. & O'SULLIVAN, B. 2011. Targeting Curcusomes to Inflammatory Dendritic Cells Inhibits NF-κB and Improves Insulin Resistance in Obese Mice. *Diabetes,* 60**,** 2928-2938.

YOSHIDA, M., TAKIMOTO, R., MURASE, K., SATO, Y., HIRAKAWA, M., TAMURA, F., SATO, T., IYAMA, S., OSUGA, T., MIYANISHI, K., TAKADA, K., HAYASHI, T., KOBUNE, M. & KATO, J. 2012. Targeting Anticancer Drug Delivery to Pancreatic Cancer Cells Using a Fucose-Bound Nanoparticle Approach. *PLoS ONE,* 7**,** e39545.

Chapter 2 Literature Review

2.1. Background

2.1.1. Nanotechnology

The emergence of nanotechnology was spawned by expanding knowledge and the enhanced ability to manipulate materials at the nanoscale. Worldwide annual public funding into nanotechnology research has ballooned exponentially from under $500 million in 1997 to $17.8 billion in 2011 (John, 2013). Nanotechnology is an interdisciplinary field that covers a wide range of areas, including physics, chemistry, biology, engineering and medicine (Roco, 2004). The conceptual foundation of nanotechnology was laid by physicist Richard Feynman in his 1959 lecture, where he stated "There's plenty of room at the bottom".

The prefix "nano" derives from the Greek word for "dwarf" (Emerich and Thanos, 2003). The National Nanotechnology Initiative (NNI) of the United States government defines nanotechnology as "research and technology development at the atomic, molecular or macromolecular scale, leading to the controlled creation and use of structures, devices and systems with a length of 1-100 nm" (McNeil, 2005, Medina et al., 2007). One nanometer is equal to 10 Ångström, or one-billionth of a meter. Nanotechnologies have great potential to bring benefits in a myriad of areas, ranging from water decontamination, information and communication technologies, mining, chemical products and drug development. A complete list of the potential application of nanotechnologies is too diverse to discuss in detail, but without doubt nanotechnology is beneficial for developing new and effective medical treatments (Shaffer, 2005, Peer et al., 2007, Safari and Zarnegar, 2014). The ability to manipulate materials at the nano-scale had catalyzed the development of novel diagnostics and imaging devices for treating disease in a way that has never before been possible.

2.1.2. Nanotechnology in medicine

Drug delivery system (DDS) are formulations or devices that enable the introduction of a therapeutic substance at the biological site of action with enhanced efficacy and safety in a controlled manner, while minimizing interactions with the rest of the body. An ideal DDS requires the interactions from three aspects: the administration of the therapeutic substance, the release of active ingredients from

delivery the vehicle and the subsequent transportation of the active ingredients across biological barriers to the site of action. Better design of DDS provides better treatments for diseases. For example, in cancer therapy, systemic administration of cytotoxic anti-cancer drugs leads to substantial indiscriminant toxicity to tissues other than tumor tissues (Scripture and Figg, 2006). Administration of chemotherapeutic agents to treat cancer can benefit from repacking these highly toxic molecules into a more favorably distributing DDS (Sharma and Straubinger, 1994, Zamboni, 2005). Moreover, advancements in biotechnology have led to the discovery and rational design of new drug candidates. However, the translation of these drug candidates into clinical applications has been limited by their poor solubility, high toxicity, nonspecific delivery, low bioavailability and short circulating half-lives. Effective drug delivery has become the key factor for better treatment. The need to develop specific drug delivery methods to promote the utilization of these new drugs in clinical effectiveness has become greater than ever.

Nanomedicine is defined as the use of nanoscale materials in medicine, by harnessing their unique properties when applied in medical application (Wagner et al., 2006). Nanomedicine covers a broad range of research areas, ranging from nanocarriers for drug delivery, self-assembled bionanomaterials for tissue regeneration, to nanoscale device for *in vivo* imaging and disease detection (Wagner et al., 2006, Kabanov and Gendelman, 2007, Bawa and Johnson, 2007). Drug delivery is currently dominating the field of nanomedicine research, comprising the highest number of scientific papers and patents (Wagner et al., 2006). Nanotechnology has great potential to revolutionize traditional DDS, by enabling the development of functionalized nanocarriers acting as a vehicle for the drug payload with release by a controlled mechanism at a specific biological site of action. Nanocarriers such as liposomes have been shown to be a biocompatible DDS with increased bioavailability, provided by the prolonged circulation time of drugs and higher accumulation of drugs at the target site due to the enhanced permeability and retention (EPR) effect. Furthermore, the enormous surface area of these nanocarriers provides opportunities for surface engineering with a homing device, such as a ligand specific for receptors over-expressed at pathological sites or to facilitate receptor-mediated endocytosis into targeted tissues.

Various nanocarriers had been constructed from a variety of materials, including polymers, lipids and metals. Therapeutics can be encapsulated either within the internal compartments, adsorbed or grafted onto the surface of the nanocarriers. The characteristics regarding drug loading capacity and stability,

target specificity and drug release rate differ for these nanocarriers; however, therapeutic nanocarriers should satisfy the following essential criteria: biodegradability, biocompatibility, non-immunogenicity and physical stability in blood for an intravenously injected formulation. The concept of the "magic bullet" proposed a century ago by Paul Enrlich (Strebhardt and Ullrich, 2008) inspired the development of targeting drugs for better treatment, which has been made possible by using various types of nanomaterials. Since the first therapeutic liposome was introduced by Gregoriadis in 1974 (Gregoriadis et al., 1974), research in the field of therapeutic nanocarriers had grown tremendously. A few of the therapeutic nanocarriers under intensive study are discussed here.

2.1.2.1. Liposome

Liposomes are spherical vesicles comprising one or multiple bilayered phospholipid membrane (Torchilin, 2005) (**Figure 2-1**). The predominant physical and chemical properties of a liposome are determined by the net properties of the constituent phospholipids (Bawarski et al., 2008). Amphiphilic phospholipids self-assemble into bilayers and form liposomes spontaneously. The biphasic character of liposomes makes them ideal carriers for both lipophilic and hydrophilic drugs. The nature of their amphipathic membrane structure enables liposomes to encapsulate hydrophobic or lipophilic molecules between two phospholipid layers; meanwhile, any hydrophilic molecule can be incorporated within the aqueous core. Drugs can be loaded into liposomes through: i) conventional methods such as thin-film rehydration and the freezing-and-thawing method, where liposomes were formed in the aqueous phase saturated with soluble drugs (Szoka and Papahadjopoulos, 1980, Lasic, 1988, Woodle and Papahadjopoulos, 1989) or ii) the more widely used remote or active loading approach, where drugs are loaded into a preformed liposome by a driving force caused by the trans-membrane gradient (Clerc and Barenholz, 1995, Clerc and Barenholz, 1998, Haran et al., 1993). Using such a method, various drugs had been successfully loaded into liposome based on pH (Nichols and Deamer, 1976, Qiu et al., 2008, Dos Santos et al., 2004, Swenson et al., 2001) or ion gradient (Lasic et al., 1995, Wasserman et al., 2007, Clerc and Barenholz, 1998). Intravenously injected liposomes are varied in size, but most of them are smaller than 400 nm to facilitate extravasation into the interstitial space from the bloodstream. One of the drawbacks of using liposomal formulations is the rapid elimination from the blood by the mononuclear phagocyte system (MPS) system. Polyethylene glycol (PEG) is often incorporated within the formulation to create a repulsive barrier and to reduce opsonization and the subsequent clearance of liposomes (Klibanov et al., 1990). Doxil®, which is a long-circulating PEGylated liposomal

formulation of the anti-cancer drug doxorubicin, is one of the exceptional success stories (Gabizon, 2001, Uziely et al., 1995, Barenholz et al., 1993, Barenholz et al., 1996, Emanuel et al., 1996). By modifying the phospholipid structure, monoclonal antibodies (mAbs) fragments or ligands could be grafted onto the liposome surface and form "immunoliposomes" to enhance selective accumulation of therapeutics at desired biological sites (Chang et al., 2009, Wang et al., 2012, Penate Medina et al., 2011).

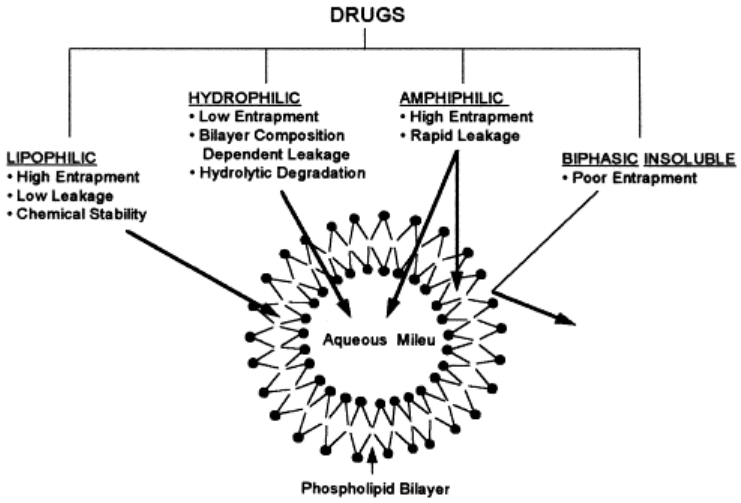

Figure 2-1. Drugs with varying solubility and their incorporation site within liposomal carrier. Taken from (Gulati et al., 1998).

Although it has been almost 50 years since the concept of the liposome was introduced (Bangham et al., 1965), only a handful of successful liposome-based drug formulations have entered the drug market (Mross et al., 2004, Moen et al., 2009, Jaeckle et al., 2002). Myocet® and Caelyx® are doxorubicin liposomal formulations for the treatment of metastatic ovarian cancer and breast cancer respectively (Gabizon and Papahadjopoulos, 1988). Marqibo® was the latest vincristine sulfate encapsulated liposome approved by the FDA in 2012 for the treatment of adult patients with lymphoblastic leukemia (O'Brien et al., 2012). Major limitations of the manufacturing and development of liposome are related to their stability, poor batch-to-batch reproducibility, difficulties in sterilization and poor drug loading capacity.

2.1.2.2. Polymeric nanoparticles

Polymer-based nanoparticles have been studied extensively as drug delivery vehicles. Most polymeric nanoparticles are engineered from biocompatible and biodegradable polymers, with functional moieties for active targeting anchoring on the surface. A number of synthetic and natural polymers such as polylactide (PLA) (Essa et al., 2010), lactide co-glycolide (PLGA) (Danhier et al., 2012), chitosan (Agnihotri et al., 2004) and alginate (Sæther et al., 2008) have been exploited to formulate nanoparticles for the sustained release of a drug at a target site. The polymeric nanoparticle surface facilitates the conjugation of functional groups and ligands to target specific drug delivery (Gu et al., 2009, Swami et al., 2012). According to the stucture of the nanoparticles, loading of drugs can be achieved via either i) entrapment of water soluble drugs within the nanoscale structure such as nanocapsules and nanospheres (Bajpai et al., 2008) or ii) chemical linkage of drugs to the polymer backbone so that they can be hydrolyzed in vivo for subsequent drug release. Polymeric nanoparticles have shown some potential as DDS (Cho et al., 2012, Hu et al., 2011, Mieszawska et al., 2013). Wide adoption of nanoparticles into clinical application has been limited by the tedious preparation steps, which require harsh chemical solvents that can potentially compromise therapeutic activities, as well as the low drug loading capacity.

2.1.2.3. Mesoporous silica nanoparticles

Ordered mesoporous silica materials were first reported over 20 years ago (Kresge et al., 1992). Since then, significant developments have been made in this field regarding control of morphology, pore size adjustment and composition variation (Wan and Zhao, 2007, Ying et al., 1999). Using mesoporous silica nanoparticles (MSP) as drug nanocarriers is of particular interest. The exceptionally high surface area of MSP enables the encapsulation of a relatively high level of drugs with MSP compared to other nanocarriers, such as liposomes or micelles. The tunable surface chemistry makes possible for further surface engineering for enhanced biofunctionality. Functional groups can be introduced into the MSP by covalent bonding or electrostatic interactions (Ferris et al., 2011, Xia et al., 2009). Due to the high pore capacity, MSPs have been used to deliver drugs that are poorly soluble in water or with low bioavailability (Meng et al., 2011b, Chen et al., 2009, Lu et al., 2007, Gu et al., 2010). Target specific delivery of MSPs can be facilitated by attaching targeting moieties to the surface of MSPs (Liong et al., 2008, Rosenholm et al., 2008, Ferris et al., 2011). MSPs have shown great potential as nanocarriers, and it is encouraging that multimodal silica nanoparticles have been approved by the FDA for the first-ever clinical trial (Friedman, 2011, Benezra et al., 2011). However, the clinical application of MSPs

still has a long way to go, as issues related to safety and therapeutic efficacy are yet to be addressed (Mai and Meng, 2012).

2.1.2.4. Polymeric micelles

Polymeric micelles are nano-sized closed lipid monolayers with a hydrophobic core and hydrophilic shell. Micelles are usually formed spontaneously by self-assembly of an amphiphilic polymer in a liquid as a result of hydrophobic or ion pair interactions between polymer segments. Polyethylene glycol (PEG) is commonly used as the hydrophilic block while poly (propylene oxide) and poly (ester) are mostly used as the hydrophobic blocks (Miyata et al., 2011, Torchilin et al., 1995). Micelles are ideal nanocarriers for delivering water insoluble molecules with improved stability (Batrakova and Kabanov, 2008, Marczylo et al., 2007, Sahu et al., 2011). These aspects probably contribute to their nanoscale size and hydrophobic shells that impair the uptake by the RES. NK105 is a polymeric micellar paclitaxel formulation under phase III evaluation (Hamaguchi et al., 2005, Kato et al., 2012). NK105 was constructed from a block copolymer consisting of PEG and polyaspartate (Hamaguchi et al., 2005). NK106, which has paclitaxel encapsulating its inner hydrophobic core, was evaluated for treating gastric cancer (Kato et al., 2012). Another micellar carrier NK911, which contains doxorubicin, was evaluated for metastatic pancreatic cancer treatment (Matsumura et al., 2004). One of the shortcomings of using micelles as drug nanocarriers is their relatively low drug loading capacity and drug molecules may gradually diffuse out of the micelles before they reach the site of action (Kim et al., 2010). In addition, micelles are unstable upon high dilution, for example intravenous administration, under which circumstance micelles may be diluted below their critical micelle concentration (CMC) and disassemble into individual copolymers (Torchilin, 2001) . There are several issues that need to be addressed before translating micellar nanocarrier research into clinical applications.

In summary, each of the systems discussed above has advantages and disadvantages regarding the versatile requirements for therapeutic applications. With the rapid development of nanotechnology, the range of building blocks that can be applied for nanocarrier platforms has also expanded tremendously over the past few decades. Each nanocarrier platform has its own unique advantage and intrinsic limitations, such as insufficient drug loading capacity or low stability. Thus a DDS with combined advantageous characteristics is in high demand.

2.2. Nanocarrier emulsions for drug delivery

2.2.1. Background of emulsion science

Emulsions are colloidal dispersions of immiscible fluids, with one fluid phase dispersed as droplet within the other (Becher, 2001 , Walstra, 2003, Schramm, 2006). The dispersed phase is called the "dispersed/internal phase" and therefore the other one is called the continuous/external phase (Barnes and Gentle, 2005). An oil-in-water (O/W) emulsion can be described as oil droplets (dispersed phase) dispersed in water (continuous phase); vise versa for an water-in-oil (W/O) emulsion (Becher, 2001). In addition to the normal two phase emulsions, there are also the so-called "double emulsion" systems consist of multiple phase, such as a W/O/W emulsion (Hanson et al., 2008, Pradhan and Rousseau, 2012, Benichou et al., 2004) (**Figure 2-2**). Emulsions are thermodynamically unfavorable systems, in which the dispersed phase tends to coalesce and flocculate over time. Thus a third component called emulsifier or surfactant is needed to stabilize the emulsion. Surfactants can lower the interfacial tension and reduce the thermodynamic forces driving towards coalescence, resulting in long-term stability exceeding that of liposomal formulaitons (Barnes and Gentle, 2005, Becher, 2001).

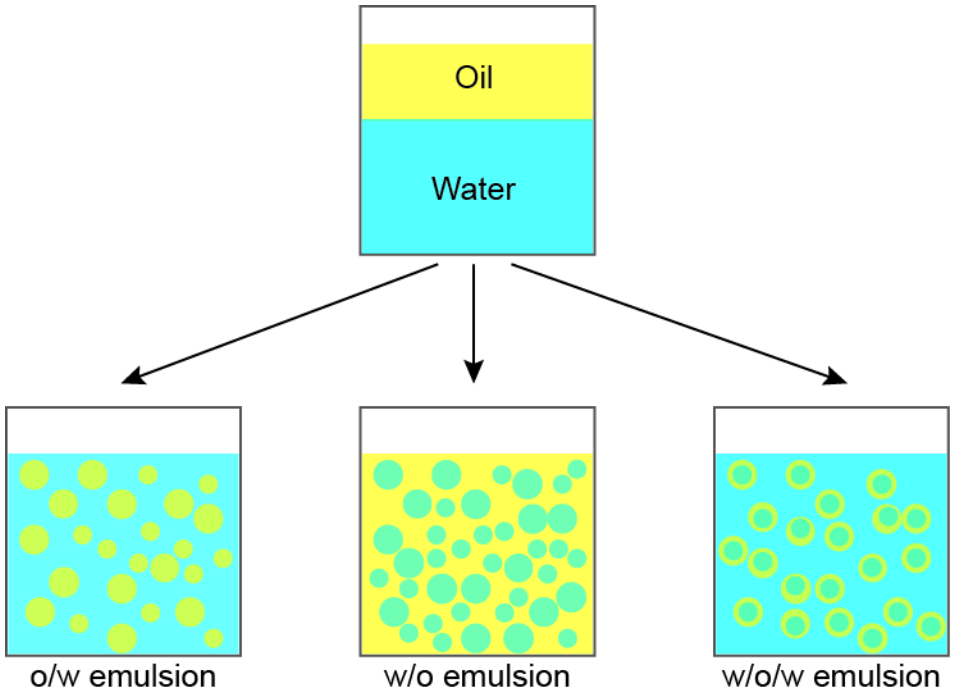

Figure 2-2. Different types of emulsions according to the nature of the dispersed and continuous phases.

Nowadays, emulsions are used in a wide range of industrial applications and products ranging from mineral ore extraction, food products, domestic cleaning products and pharmaceuticals. Particularly in the pharmaceutical industry, parenteral emulsions are used for a variety of purpose, namely, nutrition, controlled delivery of drugs and as vaccine adjuvant (Pan et al., 2003, Tamilvanan, 2004, Makidon et al., 2008, Stanberry et al., 2012, Lawrence and Rees, 2000).

2.2.2. Nanoemulsions

Over the past few decades, there has been a growing interest in the field of nanoemulsion research, as evidenced by a large number of research papers and comprehensive literature reviews (Solans and Solé, 2012, Gutiérrez et al., 2008, Fryd and Mason, 2012, Anton et al., 2008). Particularly, nanoemulsions have been intensively studied for pharmaceutical and food applications (Beck-Broichsitter et al., 2010, Anton et al., 2010, Calderó et al., 2011, Morral-Ruíz et al., 2012, Ghai and Sinha, 2012, MacHado et al., 2012, Rao and McClements, 2010, Henry et al., 2010, Silva et al., 2012). The term nanoemulsion has been quite widely used, but not with a consistent definition. It is often used interchangeably with different terms such as submicron emulsion, unstable microemulsions, miniemulisions and ultrafine emulsions in the literatures (Flanagan and Singh, 2006, Gutiérrez et al., 2008). Most studies agree that nanoemulsions are emulsions with an extremely small droplet size ranging from 10 nm to 200 nm with a narrow size distribution (Solans et al., 2003). Nanoemulsions are non-equilibrium or thermodynamically unstable systems, which means that such systems have a tendency to separate into the constituent phases (Gutiérrez et al., 2008). Nevertheless, nanoemulsions can be kinetically stable, provided an optimized composition and surfactants are in place (Solans et al., 2003). The distinction between conventional emulsions and nanoemulsions is not arbitrary. The advantages or properties of nanoemulsion systems over conventional emulsions include:

- Superior stability against creaming/sedimentation: the small droplet sizes of nanoemulsion significantly reduce the gravity force, leading to increased Brownian motion to overcome gravity (Izquierdo et al., 2002).
- The small droplet size of a nanoemulsion provides a higher surface area, which potentially provides a higher drug adsorption rate (Tadros et al., 2004). The small size distribution also provides the possibility of intravenous administration of nanoemulsion drug formulations. Conventional emulsions with a size distribution over 4 μm will cause vascular blockage and

affect blood pressure (Floyd, 1999, Nielloud and Marti-Mestres, 2000b). Emulsion formulations for intravenous injection must be below 500 nm in diameter (Driscoll et al., 2009), making nanoemulsion an ideal candidate.

2.2.3. Therapeutic nanoemulsion

Advanced DDS are required to be compatible with processes in the body as well as with the drug to be delivered. A DDS alters the biodistribution and pharmacokinetics of the associated drug; that is, the time-dependent percentage of the administered dose in different organs of the body. Furthermore, obstacles arising from low drug solubility, environmental or enzymatic degradation, rapid clearance rates, non-specific toxicity, the inability to cross biological barriers, just to mention a few, can be addressed by DDS. Nanoemulsions share many properties with liposomes as drug carriers, but are superior to liposome regarding the aspects of production cost and formulation stability. DDS based on nanoemulsions that are currently on the market are listed in **Table 2-1** (Bunjes, 2010, Hippalgaonkar et al., 2010, Marti-Mestres and Nielloud, 2002, Tamilvanan, 2009). The major advantages of nanoemulsions as DDS include:

- Production of a nanoemulsion is easy to scale up, as equipment has been developed in the food and cosmetics sectors. Also, nanoemulsions are relatively cost-effective compared to other DDS.
- Nanoemulsion formulations are insensitive to dilution. On the other hand, micellar systems become unstable when diluted below their CMC, leading to drug leakage, making them unsuitable for certain routes of administration that require dilution, *e.g.* oral and intravenous.
- The system composition of a nanoemulsion is relatively less complicated than other lipid systems. Nanoemulsions usually present less complex physicochemical behavior (Bunjes, 2010).

Brand name	Drug	Adminstration route	Producer
Diazeparm-Lipuro	Diazepam	i.v.	B.Braun Melsungen
Diprivan	Propofol	i.v.	AstraZeneca
Lipo-NASID	Flurbiprofen axetil	i.v.	Kaken Pharma.
Cleviprex	Clevidipine Butyrate	i.v.	Medicines Co.
Etomidat-Lipuro	Etomidate	i.v.	B.Braun Melsungen
Restasis	Cyclosporin A	Ocular topical use	Allergan
Gengraf	Cyclosporin A	Oral	Abbott
Stesolid	Diazepam	i.v.	Dumex
Vitalipid	Lipophilic vitamins	i.v.	Fresenius Kabi

Table 2-1. Nanoemulsion drug formulations in the market.

In recent decades, research has been performed to investigate nanoemulsions as DDS for the prevention and treatment for cancer (Anuchapreeda et al., 2012, Ganta and Amiji, 2009, Trang et al., 2011), inflammatory disease (M. H. F et al., 2010, Chuan et al., 2011), and infectious disease (Hwang et al., 2013, Makidon et al., 2008). Nanoemulsions have been shown to be effective in delivering aqueous insoluble or lipophilic molecules (Ganta and Amiji, 2009, Ganta et al., 2010, Patlolla and Vobalaboina, 2005). Using nanoemulsion formulations for controlled drug delivery and targeting is of particular interest. However, current applications of therapeutic nanoemulsion often employ egg lecithin or Cremorphor EL as the surfactant. For example, Texol®, one of the most effective anticancer drugs on the market is formulated with Cremophor® EL (polyethoxylated caster oil). Cremophor® EL, a commonly used surfactant for lipophilic compounds, has been associated with bronchospasms, hypotension and other hypersensitivity reaction (Constantinides et al., 2004). Also, it is important to

note that there are individuals who are allergic to egg lecithin, the most common surfactant for lipid-based therapeutic nanoemulsion formulation (Hofer et al., 2003). Additionally, these standard formulations make it difficult to do anything other than create a “not-so-smart” emulsion; the full power of nanotechnology cannot be brought to bear by adding targeting domains in a controlled fashion. Thus, there is a need for new formulations of nanoemulsions that are efficacious and less toxic than currently available commercial products.

2.3. Emulsion stability

2.3.1. Emulsion destabilization process

Emulsions are thermodynamically unstable systems; however, nanoemulsions can remain highly kinetically stable over a long period of time. Generally speaking, emulsions and nanoemulsions can be destabilized by the following mechanisms: creaming or sedimentation (Becher, 2001), flocculation (Petsev et al., 1995, Verwey and Overbeek, 1948), coalescence (Kabalnov and Wennerstrom, 1996) and Ostwald ripening (Taylor, 1998) (**Figure 2-3**).

Creaming or sedimentation (**Figure 2-3 i**) is caused by the density differences of the two immiscible liquids, which leads to the formation of a layer with an increased concentration of dispersed phase droplets (Schramm, 2006). For instance, creaming may occur in an o/w emulsion where the oil phase has a lower density than the aqueous phase. Creaming is often followed by flocculation and/or coalescence as droplets come into close proximity, depending on the colloidal barriers that exist in a given system.

Flocculation (**Figure 2-3 ii**) is the process whereby disperse droplets come together and form aggregates without losing their integrity as individual droplets (Schramm, 2006). The term flocculation is often interchangeable with coagulation or aggregation, but in some studies, flocculation refers to the formation of a loose aggregation of disperse droplets whereas coagulation refers to the formation of a closer aggregation of the dispersed phase (Barnes and Gentle, 2005).

Ostwald ripening (**Figure 2-3 iii**) occurs in an emulsion in which the dispersed phase has limited solubility in the continuous phase, whereby larger droplets grow at the expense of smaller ones. This

occurs due to the transfer of the soluble liquid from the smaller droplets to the larger ones through the continuous phase (Schramm, 2006). Ostwald ripening primarily affects nanoemulsions and is the main instability process of nanoemulsion (Tadros et al., 2004). Ostwald ripening can be minimized as in this thesis by choosing two phases that are highly immiscible.

Coalescence (**Figure 2-3 iv**) is a phenomenon whereby discrete droplets merge and create larger droplets, thereby reducing the total interfacial area of the system (Schramm, 2006). The ultimate end-point of coalescence is complete phase separation. In coalescence, discrete droplets first become closely associated with sufficient energy to overcome any barriers to droplet approaches, and this leads to droplet fusion if insufficient resistance to colliding droplets is provided by the surfactant layer. Coalescence of a nanoemulsion can be prevented by a thick surfactant film adsorbed at the interface, which inputs electrostatic and steric stabilization. (Fast and Mecozzi, 2009).

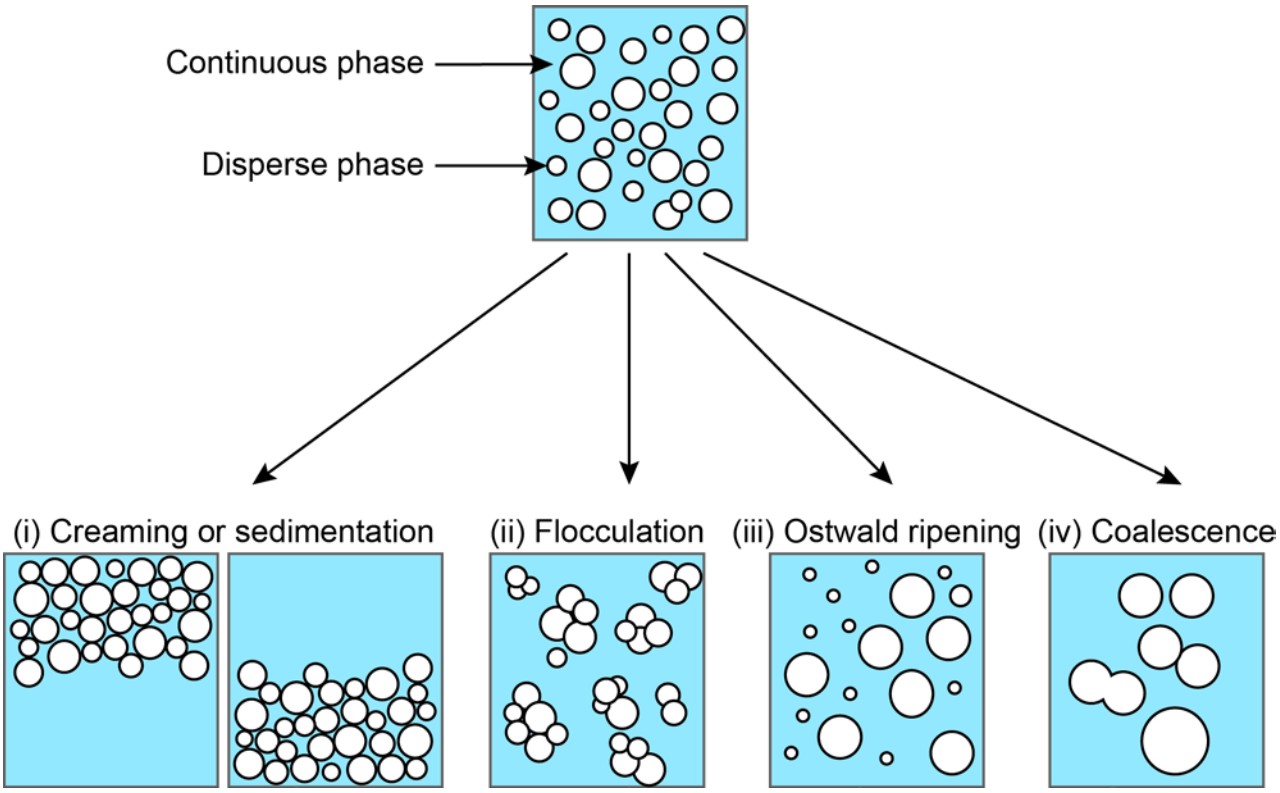

Figure 2-3. **Schematic representation of emulsion stabilization.** i) In creaming or sedimentation, the droplets rise to the surface or settle at the bottom of the continuous phase, depending on the density gradient between the two phases. ii) In flocculation, droplets come together and form aggregates. iii) Ostwald ripening occurs when large droplets grow and smaller droplets decrease in size and is prevalent when the dispersed phase is partly soluble in the continuous phase allowing molecular

movement. iv) Coalescence is a phenomenon where droplets merge to create larger droplets, thereby reducing the interfacial area of the system.

It is worth noting that the mechanisms discussed above can also combine and influence each other, *e.g.* creaming and flocculation can lead to coalescence as droplets are brought into close contact; flocculation can lead to creaming as the aggregates of droplets are large enough to be influenced by gravity rather than by Brownian motion. Thus mechanisms of destabilization are well understood, and can all be controlled by appropriate formulations.

2.3.2. DLVO theory

Generally speaking, the formation of an emulsion requires the presence of a surfactant to lower the interfacial tension. However, the stabilization of an emulsion is related to more factors than just the surfactant, and such factors can be termed as colloidal interaction theory. The DLVO theory on the stability of colloidal dispersion, which was developed based on the fundamental work performed by Derjaguin, Landau, Vervey and Overbeek (Derjaguin and Landau, 1941, Verwey and Overbeek, 1948), can be applied to emulsion stability (Barnes and Gentle, 2005, Becher, 2001). In DLVO theory, the net interaction energy between two particles is taken as a summation of the van der Waals forces of attraction and the electrostatic forces of repulsion arising from the presence of electrical double-layers. Hence, the total energy of interaction (V_T) is calculated as the sum of two components: an attractive one (V_A) and a repulsive one (V_R):

$$\boldsymbol{V_T = V_R + V_A}$$

Equation 2-1

The resulting V_T is dependent on the distance between the particles and is the decisive factor for the stability of colloidal system (**Figure 2-4**). The net energy potential indicates whether the interaction between two particles will be repulsive (i.e. favor colloid stability) or attractive (i.e. favor colloid aggregation). The combined forces acting on two interacting particles is repulsive at greater distances, while the attractive force dominates the repulsive force when the distance between particles approaches zero.

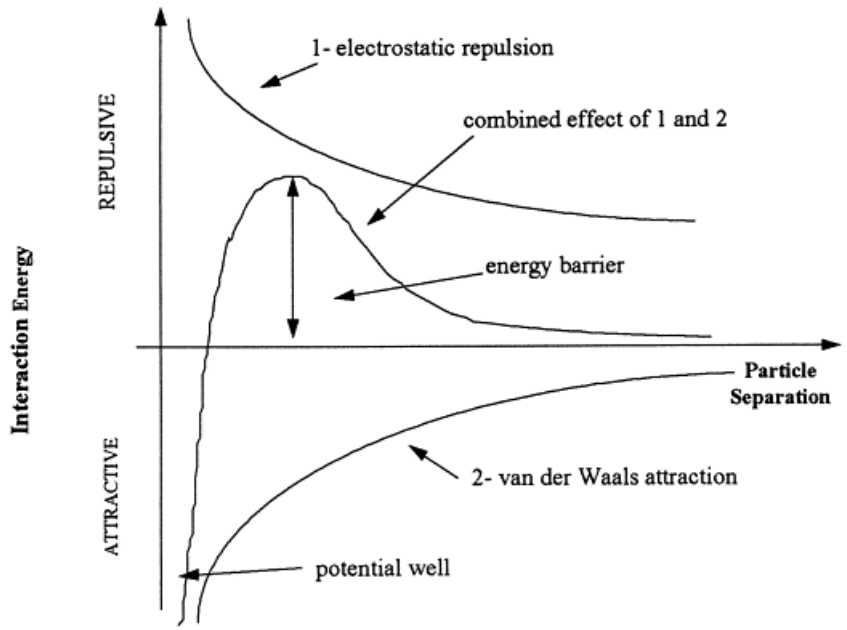

Figure 2-4. Representation of DLVO theory. Figure taken from *Thomas and Judd* (Thomas et al., 1999). The net energy can be summarized as the sum of the electrostatic repulsion and the van der Waals attractive forces that particles experience as they approach one another.

2.3.3. Emulsion stabilization

Based on DLVO theory, in order to maintain the stability of a colloidal system like an emulsion, the repulsive force needs to be dominant. There are two major mechanisms that contribute to the stability of a colloidal system: steric stabilization and electrostatic stabilization.

2.3.3.1. Steric stabilization

Steric hindrance is one of the major factors that contributes to the stability of emulsion droplets against aggregation and coalescence (Barnes and Gentle, 2005). Steric hindrance is caused by the increase in the free energy that occurs when two colloidal particles which are fully covered by strongly attached polymer appoach each other (Goodwin, 2009). Steric stabilization is achieved by attaching polymer-like moieties to the surface of emulsion droplets to form a corona, which provides a repulsive force and prevents droplets from coming into close contact (Goodwin, 2009) (**Figure 2-5**).

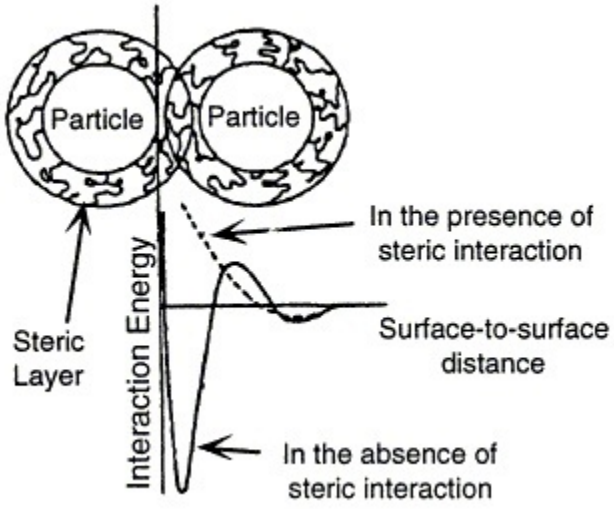

Figure 2-5. Steric stabilization by adsorption of a polymer onto nanoparticles (Aiken Iii and Finke, 1999)**.** The presence of a polymer corona around the particle provides a large barrier preventing particle interaction.

2.3.3.2. Electrostatic stabilization

Emulsions stabilized by ionic surfactants will have an electric charge on the droplet surface and thus attract a layer of counter-ions from the continuous phase, known as an electric double layer (Birdi, 2010). The electric double layer consists of three parts: i) the surface charge caused by charged ions adsorbed on the particle surface; ii) the Stern layer, which is the counter-ions attracted to the particle surface by the electrostatic force; and iii) the diffuse layer, which is the remaining region of charge adjacent to the particle, which contains free ions with a higher concentration of counterions (Birdi, 2010). When emulsion droplets move within the continuous phase, a layer of the surrounding liquid remains attached to the particle; the boundary of this layer called the slipping plane. The zeta-potential (ζ potential) is defined as the value of the electric potential at the slipping plane (Goodwin, 2009). The ζ potential is a useful indicator of the degree of repulsion between emulsion droplets in the continuous phase. Strong electrical repulsion between droplets leads to a high ζ potential, which suggests a stable suspension. When the ζ potential is close to zero, emulsion droplets may approach each other to a point where they will be attracted by van der Waals forces, i.e. when there is no steric hindrance present in the system.

2.4. Surfactants

2.4.1. Overview

Although nanoemulsions are thermodynamically unstable, the presence of a surfactant can keep this system kinetically stable by lowering the interfacial tension and preventing droplets from fusing together. Surfactants are surface active species that tend to accumulate at an interface due to their intrinsic amphiphilic nature (Barnes and Gentle, 2005). An amphiphile is a substance that contains both hydrophilic (water soluble) and hydrophobic (water insoluble) moieties and will adsorb at an interface to move the hydrophobic moieties away from the aqueous phase. In general, surfactants of industrial importance fall into two categories: (i) low molecular weight surfactants (LMWS) including chemical surfactants and detergents, and (ii) proteins and other high molecular weight surfactants (Schramm, 2006, McClements, 2005, Walstra, 2003, Dalgleish, 1997). LMWS, e.g. polysorbates and lecithins, have molecular masses in the range of 500-1300 Da, while proteins surfactants have molecular masses of tens of kDa (Dalgleish, 1997).

Common LMWS are usually synthetic organic compounds consisting of a hydrophilic head group and a hydrophobic tail. LMWS tends to quickly adsorb at interface (e.g. air-water or oil-water) by arranging the hydrophilic head in the water phase and leaving the hydrophobic tail in the non-aqueous phase. This group of surfactants efficiently stabilizes foams or emulsions by reducing the interfacial tension (Pugnaloni et al., 2004). Compared to LMWS, protein surfactants are complex amphiphilic macromolecules consisting of a chain of amino acids (Garrett and Grisham, 2005, Wilde et al., 2004, Dickinson, 1999, A. Bos and van Vliet, 2001). The polar, non-polar and ionic amino acids constitute the hydrophilic and hydrophobic groups of proteins. In an aqueous solution, a protein tends to fold in a coil-like structure known as tertiary structure; this maximizes the exposure of its hydrophilic groups (Berg et al., 2002). Due to their structural complexity, proteins take a longer amount of time to diffuse and adsorb onto an interface compared to LMWS. When adsorbed at an interface, proteins have the potential to partially unfold and orientate their hydrophobic groups towards the non-aqueous phase. A cohesive protein network forms at the interface as a result of the large degree of intermolecular interactions with the interfacially adsorbed protein, including van der Waals forces, covalent bonds, hydrophobic attractions and metal ion coordination (A. Bos and van Vliet, 2001, Dickinson, 1999, Dickinson, 2001). Such a cohesive protein network is essential for long-term stability of emulsions and foams (Martin et al., 2002, Rouimi et al., 2005).

2.4.2. Surface active peptides and proteins

Due to the non-renewable and non-biodegradable nature of petrochemical-based chemical surfactants and high petroleum prices, industries are looking for greener and more eco-friendly alternatives. However, combining high performance with cheaper and sustainable surfactants remains a hurdle for researchers. Recent advancement in biotechnology and nanotechnology have opened up opportunities for developing new classes of peptide surfactants through rational design. Peptides and small polypeptides are less complicated in structure than proteins, and display characteristics of both LMWS and proteins; these characteristics make them promising building blocks for the self-assembly of stimuli-responsive materials (Constantinides et al., 2000, Mart et al., 2006).

A group of surface active peptide or protein surfactants are of specific relevance to this PhD project. The design of these surface active peptides was inspired by the peptide Lac21 (Ac-MKQLADS LMQLARQ VSRLESA-$CONH_2$), which was derived from the naturally-occurring bacteria Lac repressor protein (Fairman et al., 1995). Lac21 contains a seven residue repeating motif with hydrophobic residues that enable this peptide to form an α-helical structure when adsorbed at an air-water or oil-water interface (**Figure 2-6 a**). Middelberg et al. showed that even though Lac21 was highly surface active, it did not form a mechanical strong interfacial network required for stabilizing foams and emulsions (Middelberg et al., 2000, Jones and Middelberg, 2002, Dexter and Middelberg, 2007). The sequence of peptide AM1 (Ac-MKQLADS LHQLARQ VSRLEHA-$CONH_2$) was designed based on the sequence of Lac21, but with the 9^{th} and 20^{th} residues replaced with metal ion binding histidine residues (**Figure 2-6 b**) (Dexter et al., 2006). The histidine residues were strategically placed within the AM1 sequence such that they will be oriented towards neighboring adsorbed peptides, allowing cross-linkage with other peptides via metal ion bridging. In the presence of zinc ions, AM1 shows greater interfacial elasticity and foam stabilization ability than Lac21, and such characteristics were switchable by changing the bulk solution pH or the addition of metal chelating agent such as EDTA (Dexter et al., 2006). Despite being a promising peptide surfactant, the application of chemically synthesized AM1 at the industrial scale is restrained by its production cost. The bio-production of GAM1, which is molecularly equivalent to AM1, requires this small peptide to be produced first as a recombinant protein followed by downstream removal of its high molecular weight fusion tag (Kaar et al., 2009). This is a common procedure in small peptide production in a biofactory system in order to

avoid issues related to low expression rates and cytotoxicity to the host system (Anangi et al., 2012, Wright et al., 2012, Meng et al., 2011a). However, it is not an economical or sustainable choice as the removal of the large fusion tag not only complicated the production process, but also generates a large amount of waste.

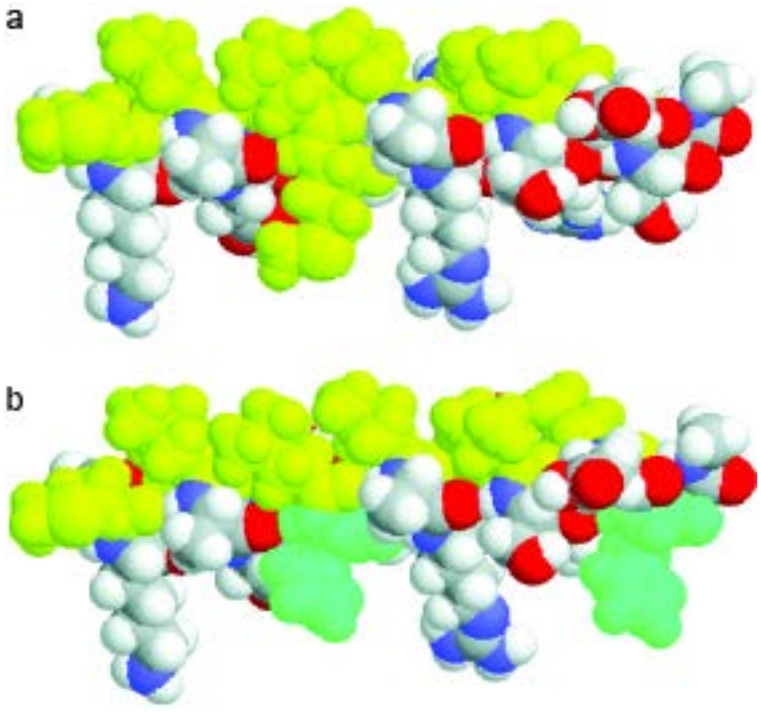

Figure 2-6. Diagram showing the 3D structure of the peptide Lac21 (a) and AM1 (b). Diagram adopted from *Dexter and Middelberg* 2007 (Dexter and Middelberg, 2007). Hydrophobic residues (methionine, leucine and valine) are shown in yellow and metal-binding histidine residues in green.

Inspired by the interfacial activities of AM1 and motivated by the need to address the aforementioned issues relate to small peptide production, a new generation biosurfactant protein DAMP4, was designed based on AM1. DAMP4 comprises four repeating sequences closely related to AM1 (named DAMP1) linked by an acid cleavable aspartyl proline serine (DPS) side: MD(PSMKQLADS LHQLARQ VSRLEHAD)$_4$ (**Figure 2-7 a, b**) (Dimitrijev-Dwyer et al., 2012, Middelberg and Dimitrijev-Dwyer, 2011). DAMP4 can be mass-produced from the industrially relevant bacterium *E.coli* without a recombinant expression fusion tag (Dimitrijev Dwyer et al., 2014). DAMP4 is surface active and produces stable foams under alkaline conditions which can be controlled through a small pH shift

(Middelberg and Dimitrijev-Dwyer, 2011). The acid cleavable DPS linker within the DAMP4 sequence allows down-stream cleavage for the production of peptides similar to AM1. Neutron reflectometry studies have shown that DAMP4 forms a monolayer with similar thickness that formed by DAMP1 at an air-water interface, suggesting that the DAMP4 four-helix bundle unfolds into a chain of four DAMP1 chain at an air-water interface (Dwyer et al., 2013). Using the same techniques, it was also revealed as that despite having a slower adsorption rate compared to DAMP1 due to its higher molecular weight, the free energy of adsorption of DAMP4 was similar to its monomer DAMP1 (Dwyer et al., 2013). DAMP4 is able to co-populate an interface with DAMP1 and at equilibrium the interfacial composition mirrors that in the underlying bulk solution (**Figure 2-7 c**). These findings support the hypothesis that motivated this PhD project: DAMP4 should be able to adsorb onto the interface pre-formed by AM1, as it shares similar chemistry with the DAMP4 monomer DAMP1. If DAMP4 was pre-conjugated to a molecule of interest (e.g. a targeting mAb or stealth agent), the adsorption of DAMP4 to the interface should lead to the functional display of its conjugated molecule. The biofunctionalization of an AM1-stabilized emulsion core can be facilitated by surface engineering with different functional moieties, using DAMP4 as an anchor.

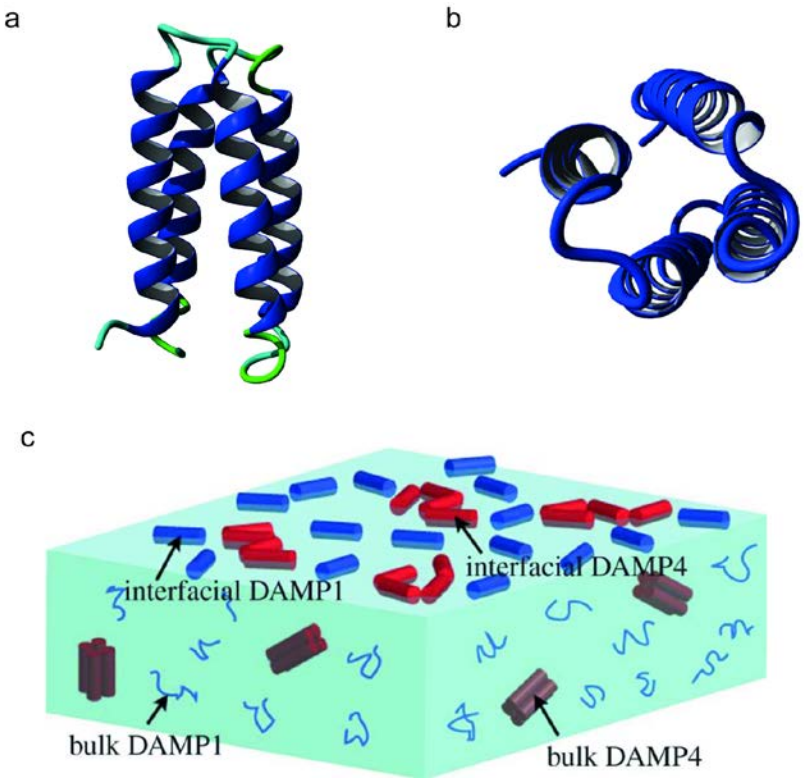

Figure 2-7. Cartoon image of the front (a) and top (b) view of the DAMP4 four-helix bundle, generated using VMC software, available at: http://www.ks.uiuc.edu/research/vmd. (c) Cartoon of the DAMP4 four-helix bundle unfolding at an interface. DAMP4 unfolds from a four-helix bundle in the bulk into a chain of four connected DAMP1 monomers. Unstructured DAMP1 and unfolded DAMP4 co-adsorb at an air-water interface. The figure was adopted from Dwyer *et al* (Dwyer et al., 2013).

2.4.2.1. Peptide surfactant-stabilized emulsion for delivering lipophilic drugs

Our lab reported a new approach to drug delivery based on surface peptide AM1-stabilized emulsions, motivated by the need to co-deliver a protein antigen and a lipophilic drug for specific inhibition of nuclear factor kappa B (NF-κB) in antigen presenting cells (APCs) (Chuan et al., 2011). Curcumin is a lipophilic molecule and inhibits NE-κB activity, which is closely associated with inflammation, making curcumin an ideal candidate drug for treating rheumatoid arthritis (Bharti et al., 2003, Singh and Aggarwal, 1995). However, curcumin in its free form exhibits low bioavailability and is poorly soluble in water (Cheng et al., 2001). Thus, there is a great need to encapsulate curcumin within a nanocarrier for enhanced delivery efficacy. We used AM1 to prepare a nano-sized emulsion with defined surface properties predictable from its sequence. Incorporating curcumin into the oil phase at the time of emulsion formation enabled its facile packaging. AM1 simultaneously charged the stabilized

interface, enabling the addition of an animal model-relevant antigen via electrostatic deposition (**Figure 2-8** upper panel). *In vitro* data showed that the tailorable nanocarrier emulsion (TNE) prepared in this way was internalized and well-tolerated by a model APC RAW 264.7 (**Figure 2-8** lower panel), and good suppression of nuclear factor- κB (NE-κB) expression was achieved. This work reports a new type of nanotechnology-based carrier emulsion, which can potentially be tailored for co-delivery of multiple therapeutic components, and can be made using simple methods using only biocompatible materials.

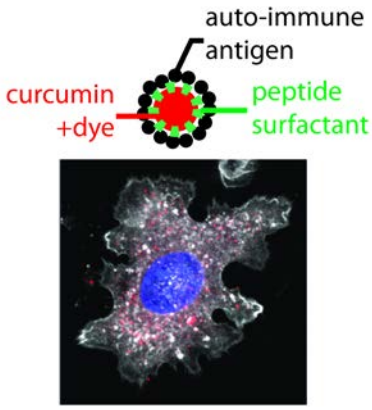

Figure 2-8. Schematic representation of a tailorable nanocarrier emulsion (TNE) for delivering a small lipophilic drug molecule. Upper panel: TNE was assembled through electrostatic adsorption of auto-immune relevant antigens onto charged emulsion droplets stabilized by a designer peptide surfactant. A lipophilic small molecule drug, curcumin, was incorporated within the TNE oil core. Lower panel: Confocal image showing the TNE (red) internalized by model cells. The cell membrane is shown in white and the nucleus is shown in blue.

As stated in Section 1.3 of **Chapter 1**, the first generation TNE did not possess the stealth or targeting capability required for effective *in vivo* use. A more sophisticated approach that was not dependent on layer-by-layer assembly for delivering an active ingredient to cells became the central research challenge for this PhD project.

2.5. Nanoemulsion formation

High energy and low energy methods can be used to prepare nanoemulsion. With the high energy methods, nanoemulsions are prepared using an apparatus (e.g. ultrasound sonicator or high pressure

homogenizer) able to produce intense disruptive forces to increase the oil/water interfacial area (Meleson et al., 2004). In this process, the oil and water phases of an emulsion are brought into contact with each other in the presence of an emulsifying agent, then high speed mixing or vigorous agitation is applied to break one of the phases into small droplets and disperse into the other one (Meleson et al., 2004, McClements, 2005). High-pressure homogenizers are the most popular machine for emulsification in industry, as they provide homogeneous flow for emulsification in at short period of time (Solans et al., 2005). Ultrasound sonication is also very efficient in producing nanoemulsions, but it is not suitable for scaled-up manufacturing processes. In contrast, low energy emulsification methods harness the internal chemical energy of the system, and allow the formation of nano-size emulsions by spontaneous emulsification without any high energy input (Anton et al., 2008, Sajjadi, 2006, Forgiarini et al., 2001). The phase inversion temperature (PIT) method is the most widely used low-energy emulsification method in industry (Shinoda and Saito, 1968, Förster and Rybinski 1998). Nevertheless, both types of methods can be used to produce homogenous nanoemulsions by choosing the optimal system and composition variables (Yang et al., 2012). However, low energy emulsification methods have attracted considerable research interest in recent years as they are thought to be more energy efficient than the established high energy methods.

2.6. Considerations for nanoemulsion formulation:

Nanoemulsions are ideal DDS to increase the bioavailability and efficacy of lipophilic compounds (Ganta et al., 2008, Ganta et al., 2010, Patlolla and Vobalaboina, 2005). Thus, this section will discuss the formulation considerations for designing nanocarriers emulsions. Therapeutic nanocarriers emulsions are required to be sterile, isotonic, biodegradable and physicochemically stable (Benita and Levy, 1993). The selection of the excipient, as well as emulsion characterization including assessments of the size distribution and surface charge should be carefully considered, as these factors could affect the pharmaceutical performance of the emulsion.

2.6.1. Excipient selection

The excipient of an emulsion, such as the oil phase and emulsifiers, need to be carefully selected so that the resulting formulation will comply with the requirements for a therapeutic emulsion. The oil phase of a therapeutic emulsion is generally of natural origin. Intralipid®, a fat emulsion formulated with 10,

20 or 30% (v/v) soybean oil, 1.2% egg phophatides and 2.5% glycerol, was the first fat emulsion for human intravenous injection that reached the market in 1962 (Hallberg et al., 1985). A common oil phase used for therapeutic emulsion is long-chain triglycerides (LCT) from vegetable sources, including soybean, safflower and cottonseed oils (Davis et al., 1987). Medium-chain triglycerides (MCT), such as Miglyol® 812, have also been reported as the oil phase for therapeutic emulsion (Chuan et al., 2011, Kovacevic et al., 2011, Sanad et al., 2010, Zeng et al., 2013). Regardless of the origin, the oil phase needs to be purified to remove any known contaminants (oxidative decomposition products, herbicides, pesticides *etc*.) (Malmesten, 2002).

The most common emulsifier used in parenteral emulsion formulations is phospholipids, especially those from egg or soybean sources. Such emulsifiers are relatively safe and stable (Floyd, 1999). Synthetic emulsifiers such as fatty acid esters of sorbitans (Span™) and polyoxyethylene sorbitans (Tweens™) are also considered or employed for use in parenteral emulsion drug delivery. One study has shown that an appropriately composed oil phase could aid in increasing the encapsulation rate of a drug due to the optimization of drug solubility within the inner oil phase (Klang et al., 1996). Another consideration regarding the excipient of an emulsion is the additives used. Electrolytes (*e.g.* NaCl), reducing sugars (*e.g.* glucose) and glycerol are sometimes needed to adjust the emulsion to physiological pH (Dawes and Groves, 1978, Kawilarang et al., 1980, Washington et al., 1990, Washington et al., 1989).

2.6.2. Emulsion particle size

Emulsion size is the main characteristic that governs interactions with the biological environment. Particles with diameters greater than 7 μm are clinically unacceptable as they will cause capillary blockage (Illum et al., 1987). Generally, particles with a larger size are more likely to be retained by the reticuloendothelial system (RES) after intravenous injection (Tamilvanan, 2004). Emulsions with a droplet size below 100 nm will escape from the vascular system via the capillary endothelium, thus making it difficult to reach any site of action in the extravascular space. One study has shown that emulsions with a droplet size larger than 200 nm could effectively inhibit the drug from entering the bone marrow, small intestine and other non-RES organs hence toxicities caused by many cytotoxic compounds can be avoided (Kurihara et al., 1996). However, therapeutic nanocarrier emulsions need to

be sterile before application to humans or animals. As most of the emulsion components are susceptible to heat sterilization, filter sterilization with a 0.22 μm filter device is more practical.

2.6.3. Surface Characteristics

The cellular uptake, biodistribution and stability of emulsions are also affected by their physiochemical characteristics, including surface charge and hydrophobicity/hydrophilicity. Emulsions with a neutral droplet surface are taken up by macrophages more slowly than those with a charged droplet surface (Stossel et al., 1972). Negatively charged emulsions are more easily cleared from the blood stream and distributed in the liver and spleen, while the positively charged emulsion droplets are expected to have high cell association as a result of electrostatic adhesion between the droplets and the negatively charged cell membrane (Nielloud and Marti-Mestres, 2000a). The hydrophobicity/hydrophilicity of emulsion oil droplets could also affect their uptake by MPS. A hydrophobic surface coating significantly reduces macrophage uptake as a result of decreased blood component opsonization onto the emulsion droplet surface, together with a steric stabilization effect from the hydrophobic surface coating (Illum et al., 1987). Coating emulsion droplets with hydrophilic polymers such as polyethylene glycol (PEG) has been found to improve emulsion stability in the plasma through steric stabilization and increased blood circulation time (Han et al., 2004).

2.6.4. Administration route

It is important to consider the route of administration for nanocarrier as this parameter will have impact on the drug delivery efficiency and safety. Intravenous (i.v.) injection still remains the standard form of application for formulations that require being bioavailable immediately or distribution to a biological site which is difficult to access by other means. However, i.v. injected nanocarrier need to escape the engulfment of the mononuclear phagocyte system (MPS) (Vonarbourg et al., 2006). Strategies that could improve the delivery efficiency of i.v. injected nanocarrier will be discussed in next section. In contrast to i.v. administration, intraperitoneal (i.p.) administration can directly delivers injected nanocarriers to peritoneal pathogenic-relevant macrophages and serves as a depot for subsequent systemic dissemination (Howard et al., 2008). PLGA particles i.p. injected to mice are found to be primary up-taken by macrophages, whereas intrademal injection (i.d.) of the same particles resulted in increased DCs association in draining lymph nodes (Newman et al., 2002). I.p. injection showed

reduced toxicity as the peritoneal cavity acts as a barrier to the injected nanocarrier entering the blood-brain-barrier (Sadauskas et al., 2007).

2.7. Targeting strategies

Targeting therapeutic nanocarriers to an active biological site provides several advantages over their non-targeted counterparts. Targeted delivery of a therapeutic compound could potentially circumvent the side-effects on healthy tissues and enhance pharmaceutical efficiency (Minko et al., 2004). The current targeting strategies fall into two main areas: passive and active targeting.

2.7.1. Passive targeting

Passive targeting exploits the normal biodistribution that nanocarriers will take upon administration. In general, intravenously injected unadorned nanocarriers are rapidly removed from the circulation by opsonization and the mononuclear phagocytic system (MPS) and eventually accumulate within the spleen and liver (Owens Iii and Peppas, 2006). Hence, the rapid clearance of nanocarriers can be exploited for targeting professional antigen presenting cells (APCs) or treating hepatic disorders (Durand et al., 1997, Yekollu et al., 2011, Chuan et al., 2011). The potential of a passively targeted nanocarrier in cancer treatment has been well studied. Nanocarriers can passively accumulate within solid tumors due to the leaky vasculature network and aberrant lymphatic system that limits the drainage of molecules from tumor tissues (Matsumura and Maeda, 1986, Peer et al., 2007).

Although rapid clearance by the MPS had been exploited as a passive targeting strategy, treatment of other diseases, like tumors, requires that drug loaded nanocarriers escape from opsonization and MPS arrest for drug delivery to non-MPS tissues. In addition, the non-specific uptake of nanocarriers prevents the use of emulsions for controlled release of the drug within the vasculature. To circumvent this, nanocarriers have been modified with polyethylene glycol (PEG), a process known as PEGylation; this has been widely investigated and shown to increase the bioavailability and biodistribution of nanocarriers (Gref et al., 2000, Kim et al., 2009). A corona of hydrophilic PEG on the surface of nanocarriers creates a repulsive barrier that prevents the absorption of opsonins (Klibanov et al., 1990, Maruyama et al., 1991). Therapeutics encapsulated in long-circulating nanocarriers can escape from MPS clearance and accumulate within the blood stream. Thus, the required therapeutic level can be

maintained (termed as enhanced permeability and retention effect, also known as the EPR effect or passive targeting) (Maeda et al., 2000).

2.7.1.1. PEGylation

Polyethylene glycol (PEG) is formed by linking repeating units of ethylene glycol in either linear or branched structures (**Figure 2-9**). The process of covalently coupling PEG to a carrier of choice is called PEGylation. Activated PEG, with a functional group at one or both termini can be coupled to a molecule via different chemistries. One should choose the functional group based on the type of available reactive amino acids on the molecule to which PEG is conjugated. Conjugating PEG to lysine and N-terminal amino acid groups is the most common route for the PEGylation of a protein or peptide (Roberts et al., 2002), since lysine is the most prevalent amino acid in proteins.

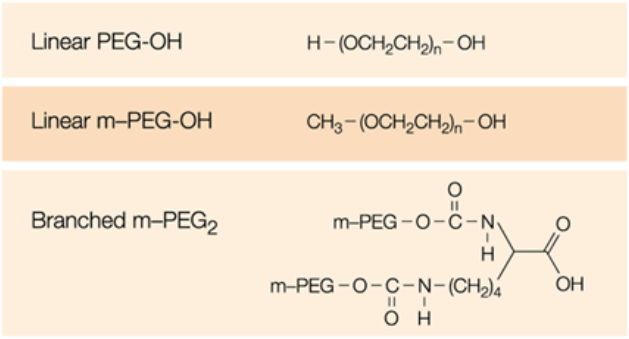

Figure 2-9. Structural formulation of the polyethylene glycol (PEG) molecule (Harris and Chess, 2003).

PEGylation studies were initiated in the late 1970s by Davis and colleagues who succeeded in protecting proteins from enzymatic degradation during drug delivery by PEGylation (Abuchowski et al., 1977a, Abuchowski et al., 1977b). The literature is now replete with reports on the PEGylation of various applications, namely increased stability and half-life, enhanced drug solubility, reduced toxicity and immunogenicity (Veronese and Pasut, 2005). PEG provides a steric barrier that surrounds its conjugated drugs or particles, which protect them from enzymatic degradation, excretion by the kidneys, MPS clearance, and cell surface protein interactions and thereby eliminating adverse allergic reactions (Harris and Chess, 2003, Davis et al., 1978). PEGylation also enhances the stability of DDS over a range of pH and temperature, compared to non-PEGylated counterparts (Monfardini et al., 1995).

It is worth noting that PEG derivatives with a molecular weight lower than 40 kDa can be excreted from the body via the kidneys (Caliceti and Veronese, 2003). The most commonly used PEG molecules for drug nanocarrier modification are those with a molecular weight from 1000 to 20,000 Da (Torchilin, 2006). Owing to the above mentioned properties, the FDA has approved PEG for application in foods, cosmetics and pharmaceuticals (Harris and Chess, 2003). The first PEGylated protein to enter the pharmaceutical market was ADAGEN®, a PEGylated adenosine deaminase (ADA) for treating severe combined immunodeficiency disease (SCID).

2.7.2. Active targeting

Active targeting is a strategy that relies on specific interactions at target sites, such as antibody-antigen or ligand-receptor interactions. Inspired by Paul Ehrlich's "magic bullet" theory back in the early 20th century (Strebhardt and Ullrich, 2008), the active targeting strategy involves modifying nanocarriers with a targeting moiety to facilitate the homing, binding and internalization of the therapeutic agent by cells at the biological site of action. Various moieties have been examined as targeting agents, including antibodies and their fragments (Fay and Scott, 2011, Han and Davis, 2013, Marega et al., 2012), peptides (Agemy et al., 2011, Hansen et al., 2013, Stefanick et al., 2013, Choi et al., 2010), proteins (Huang et al., 2010, Wiley et al., 2013, Pitek et al., 2012, Carrillo-Conde et al., 2011), DNA aptamers (Boyacioglu et al., 2013, Yu et al., 2011, Li et al., 2012), and vitamins, in particular folate (Werner et al., 2011a, Werner et al., 2011b).

The most common strategy for preparing targeting nanocarriers takes advantage of the well-known molecular recognition in antibody-antigen binding. Certain antigens are over-expressed in specific tumor cells and nanocarriers modified with monoclonal antibodies (mAbs) have been shown to effectively accumulate within tumor tissues. For instance, the use of anti-HER2 immunoliposomes leads to significantly higher drug accumulation within the tumor site compared to their non-targeting counterparts (Park et al., 2002, Reynolds et al., 2012, Nielsen et al., 2002). Nonetheless, the use of a full-length mAb as the targeting moiety for nanocarriers is limited by their relatively high molecular weight, which will potentially lead to poor quality control and incorrect orientation on the nanocarriers surface after conjugation. These shortcomings have led to a new trend of using targeting moieties, such as Fab fragments (Sapra et al., 2004) or single chain variable fragments (scFv) (Iyer et al., 2011) of antibodies, proteins over-expressed on tumor cells like transferrin (Iinuma et al., 2002, Li et al., 2009,

Ishida et al., 2001), DNA-based aptamers (Boyacioglu et al., 2013, Li et al., 2013, Xiong et al., 2013), and peptides such as arginine–glycine–aspartic acid (RGD) (Li et al., 2004, Danhier et al., 2009). The relatively smaller hydrodynamic radius of these targeting moieties enables higher ligand density and more flexible multivalent surface engrafting.

2.7.2.1. Receptor mediated endocytosis

Once the drug delivery nanocarriers have reached their target site and been taken up by cells, subsequent drug release may occur in the intracellular space. There are several cellular uptake mechanisms that depend on the cell type (e.g. phagocytic vs. non-phagocytic cells), physicochemical properties of the internalized entity and the mode of activation such as receptor-mediated endocytosis.

Endocytosis is a process by which cells engulf macromolecules, which can be sub-divided into two categories, namely phagocytosis and pinocytosis depending on the physical state of the internalized objects (Xiao and Gan, 2013, Conner and Schmid, 2003). Phagocytosis corresponds to the uptake of large solid macromolecules, *e.g.* bacteria or dead cell debris; while pinocytosis is the uptake of a large volume of extracellular material or a small volume of fluids (Hansen and Nichols, 2009). Meanwhile, receptor-mediated or clathrin-dependent endocytosis is a specific process for cells to acquire bulk quantities of specific substances, including hormones, growth factors, and plasma proteins (Goldstein et al., 1979, Xiao and Gan, 2013). In receptor mediated endocytosis, extracellular molecules are recognized by specific receptors on the cell membrane. Interactions of these molecules with surface receptors lead to their internalization into cells by the engulfment plasma membrane vesicles through coated pits, a term that refers to a clustering of receptors in specific regions the cell membrane (Goldstein et al., 1979). Then, the coated pit pinches off from the cell membrane and forms an endosome for subsequent lysosomal degradation and drug release (Lodish, 2008). Meanwhile, endocytic receptor released from the endosome returns to the cell membrane to start a second round of receptor mediated endocytosis (**Figure 2-10**).

Whether the targeting nanocarrier can be internalized after binding to target cells is an important criterion in the selection of targeting ligands. Drugs that enter the cytoplasm by means of receptor mediated endocytosis may avoid recognition by the P-glycoprotein efflux pump, which is known for being related to P-glycoprotein mediated drug resistance (Gottesman et al., 2002, Wong et al., 2006).

Encapsulating drugs within a nanocarrier engineered with a targeting moiety which specifically binds to an endocytic receptor can potentially overcome drug resistance in cancer.

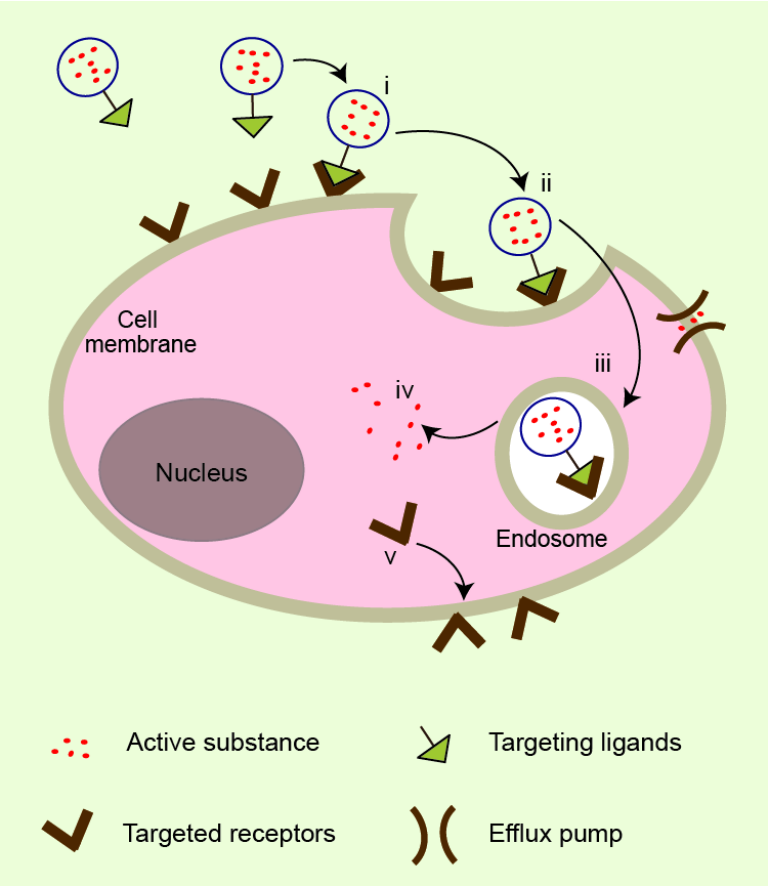

Figure 2-10. Schematic representation of receptor-mediated endocytosis of a targeting nanocarrier. Once the targeting nanocarriers reach the extracellular space of the target cells, (i) they bind to specific receptors; (ii) membrane invagination occurs and the targeting nanocarriers is engulfed by the cell through a coated pit; (iii) drug release is initiated by the acidic pH environment of the endosome; (iv) the drugs are released from the endosomal compartment into the cytoplasm. (v) Receptors then recycle back to the cell membrane. Meanwhile, efflux pumps express on the cell membrane may clear free drugs and leads to multidrug resistant (Kapse-Mistry et al., 2014).

In summary, combining targeted ligands with protecting polymers such as PEG within a single nanocarrier platform will be beneficial for the following reasons: i) the presence of a sterically-protecting polymer like PEG could compensate for MPS clearance caused by the attached ligands on

the nanocarrier surface and ii) the longevity of a ligand-bearing nanocarrier may allow for greater accumulation even at target sites expressing a low level of the receptor. The rationale for combining passive and active targeting strategies in single nanocarrier platform to enhance drug delivery efficacy has been demonstrated by PEGylated liposomal doxorubicin (Yamada et al., 2008). The greatest antitumor efficacy was found in animals treated with PEGylated, folate-modified liposomal doxorubicin, compared to that of animal treated with untargeted PEGylated liposome or non-PEGylated PEGylated liposomes modified with folate. However, one should also consider that the target recognition moiety may be shielded by the steric barriers created by the protective polymer. Studies in the field of targeting nanocarriers have shown that the particle size and surface ligand density are critical to their performance (Jiang et al., 2008, Huang et al., 2009, Wang et al., 2010, Elias et al., 2013, Bandyopadhyay et al., 2011). Hence, the optimization of these parameters, in combination with PEGylation and targeting moiety density, are crucial to ensure that the functionality of nanocarriers is not compromised. As stated in **Section 1.4** of **Chapter 1**, **Objective 5** of this PhD project was to investigate whether varied design parameters have an effect on eliciting an immune response, and to use the research outcome to design an optimized drug delivery vehicle with enhanced immunogenicity.

2.8. Our body's defense against foreign invaders

The human immune defense is a complex system involving specialized lymphoid tissues and various types of cells, which closely interact with each other to defend the body against foreign invaders. There are three major defense mechanisms involved in the human immune system (Janeway, 2005, Moser and Leo, 2010). The first mechanism is comprised of external barriers, including physical (such as skin and mucous membranes) and chemical (such as stomach acids) barriers that provide the first line of defense against foreign intruders. The second mechanism is innate immunity, which is induced immediately once a pathogen enters the body. A range of cells are involved in innate immunity, including natural killer (NK) cells, macrophages, granulocytes and dendritic cells that are specialized in the recognition and destruction of common pathogens (Moser and Leo, 2010, Haaheim, 2009). Several receptors are also involved in the recognition of pathogens, such as pattern recognition receptors (PRRs), Toll-like receptors (TLRs) and NOD-like receptors (NLRs) (Janeway, 2005). Antigen presenting cells, including macrophages, dendritic cells and granulocytes, will take up, destroy and process the invading pathogen through these receptors. However, the innate immune system cannot

defend the body against all pathogens and is not capable of immunological memory. Thus, a more versatile means of defense, termed adaptive immunity, constitutes the third mechanism of defense. Immature dendritic cells encounter and capture pathogens in infected tissues and thereby initiate the adaptive immune response. Adaptive immunity consists of humoral and cell mediated immunity. Humoral immunity is mediated by B cell-secreted antibodies, while cell-mediated immunity is mediated by T lymphocytes which target and destroy pathogens that antibodies do not have access to.

2.8.1. Dendritic cells in the immune system

Dendritic cells (DCs) are a group of professional antigen presenting cells (APCs) specialized in capturing, processing and cross-presenting antigens (Banchereau and Steinman, 1998). DCs play a central role in regulating the innate and adaptive immune systems. As a key regulator of the immune response, DCs comprise a complex network of APCs that regulates T cell mediated immunity and tolerance. DCs are also responsible for inducing the differentiation of B cells into antibody-producing plasma cells. While B cells can directly recognize native antigen through their B cell receptors and secrete the corresponding antibody, T lymphocytes need the antigen to be processed and presented to them by APCs. In most tissue, DCs are present in their immature state and are incapable of stimulating T cell due to the lack of requisite accessory signals for T cell activation, *e.g.* CD40, CD54 and CD86. However, they are highly efficient in capturing antigens, which is essential for their full maturation and mobilization (Banchereau and Steinman, 1998). DCs take up particles and microbes by phagocytosis (Inaba et al., 1993, Moll et al., 1993), take in high volumes of fluid or solutes via macropinocytosis (Sallusto et al., 1995) and express receptors that mediate adsorptive endocytosis such as C-type lectin receptors (Sancho et al., 2009) and macrophage mannose receptor (Sallusto et al., 1995). An encounter with antigen stimulates the maturation and differentiation of DCs, which then rapidly lose their ability to capture antigen. On the other hand, this process up-regulates the antigen processing and presentation ability of DCs, as well as their expression of co-stimulatory molecules and the secretion of cytokines. DCs undergo a complex process of maturation into antigen-presenting cells. There are two types of major histocompatibility complexes (MHC) on the surface of APCs that can bind to the antigen: MHC class I and MHC class II, responsible for stimulating cytotoxic T cells (CTLs) and helper T cells respectively. To generate CTLs, mature DCs present intracellular MHC class I loaded with antigenic peptides. Extracellular antigens are processed within the APC endocytic pathway and presented by MHC class II to T helper cells to initiate an immune response (Banchereau and Steinman, 1998). In

summary, DCs are mobile sentinels that bring antigen to T cells and initiate the immune response (**Figure 2-11**).

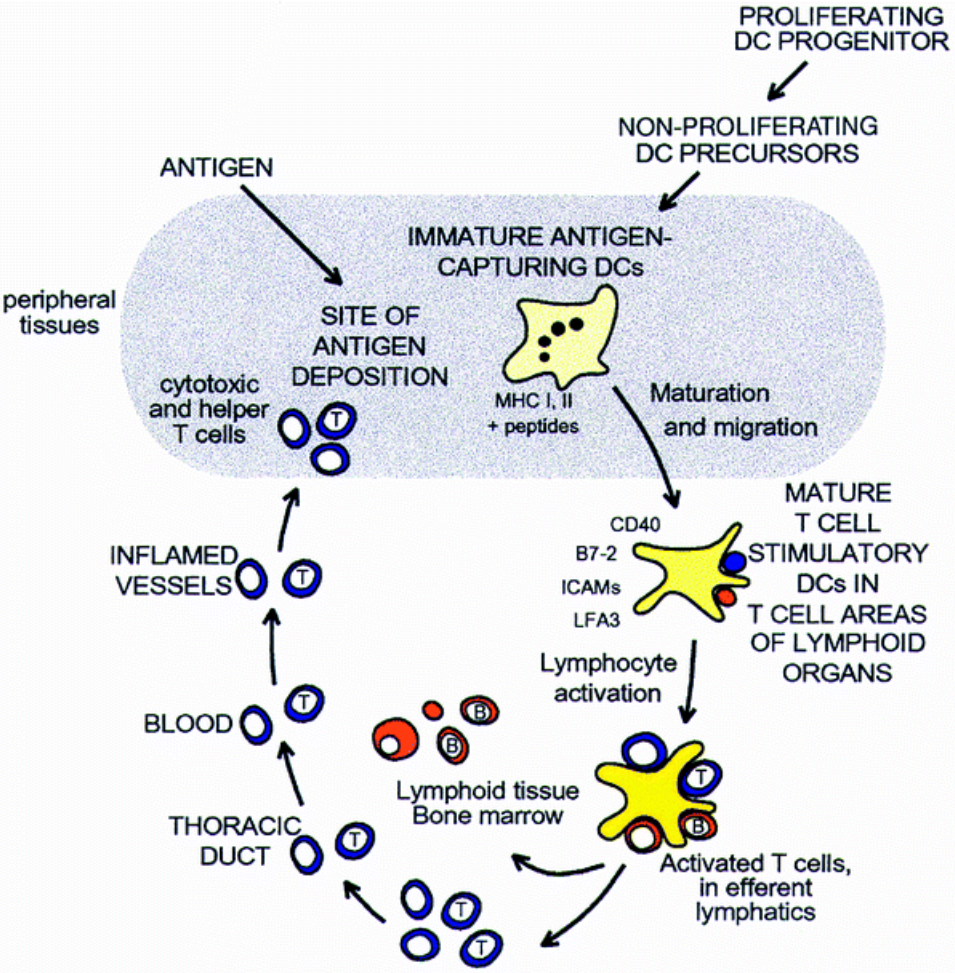

Figure 2-11. A brief illustration for antigen presentation in vivo. Immature DCs capture antigen in peripheral tissues followed by the formation of MHC-peptide complexes. After an encounter with antigen, immature DCs derived from proliferating DC progenitors begin to mature and express cytokines to stimulate and bind T cells. In cases where the antigen was bound to B cells, then both T cells (blue) and B cells (orange) can cluster with DCs and leave the T-cell area of the lymph nodes. Eventually, B cells will arrive at bone marrow and other lymphoid tissues, such as the medulla of lymph node. Figure taken from (Banchereau and Steinman, 1998).

2.8.2. Types of DCs in mice, CD8+ DC and cross presentation

Numerous studies have shown that mouse DCs comprise several subsets with distinct phenotypes and functionalities (Ganguly et al., 2013b). DCs can be subdivided into two major subsets: conventional (myeloid) DC (cDC) and plasmacytoid DC (pDC) that differ in the expression of their Toll-like receptor (Shortman and Liu, 2002, Caminschi et al., 2012). In addition to cDCs and pDCs, two small subsets of DCs, namely monocyte derived DCs (moDCs) and langerhans cells (LCs) had also been reported (Chorro et al., 2009, Domínguez and Ardavín, 2010).

In the steady-state, cDC progenitors in bone marrow migrate through the blood to non-hematopoietic tissues and secondary lymphoid organs. cDCs are dedicated in internalizing, processing and presenting antigen and the subsequent naïve T cell activation. The lymphoid-resident cDCs in the spleen and lymph nodes can be sub-categorized as CD8α and CD4. CD8+ DCs are the primary DCs found in the thymus which express CD8α but no CD4, while the CD4+ DCs express CD4 but not CD8α. In addition, there are double negative (DN) DC express neither CD8α nor CD4 surface molecules (Vremec et al., 2000). The CD8+ DCs subset is highly efficient at presenting exogenous antigen on MHC class I molecules to cytotoxic CD8+ T cells (Ganguly et al., 2013a). Such mechanism is called cross-presentation and is vital for the induction of cytotoxic T lymphocytes and efficient T-cell mediated anti-tumor immunity(Caminschi et al., 2009). The reason for CD8+ DCs superior to CD4+ DCs at cross-presenting exogenous antigen lies in the selective expression of phagocytics receptors and their endocytic pathways (Caminschi et al., 2012, Segura et al., 2013). In CD8+ DCs endocytotic pathway, proteolysis is limited different mechanisms, including the inhibition of acidification in endosomes and phagosomes through production of reactive oxygen species (ROS), by which degradation of potential epitopes can be avoided(Savina et al., 2009). CD4+ DCs are believed to be professional in presenting MHC class II-restricted antigens to CD4+ T cells (Ganguly et al., 2013a).

2.8.3. Targeting delivery to DCs via Clec9A

As stated in the previous section, DCs are professional APCs that detect and destroy invading pathogens. Receptors such as Toll-like receptors (TLRs), nucleotide-binding oligomerization domain (NOD) proteins and C-type lectin receptors on the immature DCs surface are vital for the recognition, communication and activation of DCs (Villadangos and Schnorrer, 2007). C-type lectins (also known as C-type lectin receptors (CLRs) are a protein family involved in cell adhesion, endocytosis, natural-

killer-cell target recognition and dendritic-cell activation (Robinson et al., 2006, Villadangos and Schnorrer, 2007). One of the C-type lectins, Clec9A (C-type lectin domain family 9A; also known as DNGR1) is the most recently identified receptor and is expressed in many tissues (Caminschi et al., 2009, Huysamen et al., 2008, Sancho et al., 2009). In mouse, Clec9A is highly restricted to $CD8^+$ dendritic cells (Sancho et al., 2009, Huysamen et al., 2008). The equivalent human ortholog of mouse Clec9a was found on the human dendritic cell subtype $BDCA3^+$ (Huysamen et al., 2008). The cytoplasmic tail of Clec9A contains a tyrosine residue with a sequence similar to the immunoreceptor tyrosine-based activation motifs (ITAMs), allowing the recruitment and activation of spleen tyrosine kinase (Syk) by Clec9A (Sancho et al., 2009). Clec9A functions as an activation receptor that induces inflammatory cytokine production and signaling via Syk kinase (Huysamen et al., 2008).

DCs play a central role in the immune system and orchestrate a wide repertoire of immune responses, ranging from resistance to infection and tolerance to self (Steinman and Banchereau, 2007). Being a key player in regulating immunity, DCs are the natural focus for immune therapy. Targeting an antigen to CLRs on DCs represents an attractive strategy to enhance vaccine efficacy. This is because most of the CLRs are endocytic receptors, i.e. they are highly specialized for the internalization of antigens and processing and influence antigen routing and presentation on MHC class I and II. Depending on the CLR targeted, either $CD4^+$ or $CD8^+$ T cell response can be specifically induced (Caminschi et al., 2009). In order to facilitate highly specific targeting delivery, it is important to choose a CLR that is highly exclusive to a certain subset of DCs. Expression of Clec9A is highly restricted to certain DC subsets in both mice and humans compared to other C-type lectins. Antigen coupled to an mAb recognizing a DC surface molecule like Clec9A could potentially be cross-presented to the $CD8^+$ DCs. Several studies have been done to show that Clec9A is an effective target for delivering antigen to DCs. Sancho et al have shown that along with adjuvant, targeting a tumor antigen conjugated to a mouse Clec9A specific antibody elicits a robust CTL response. In another study done by Caminschi et al, even without the presence of adjuvant, an antigen targeted to Clec9A produced a striking enhancement in antibody responses, and the required amount of antibody was much lower than that of the free antigen to preduce a positive titer (Caminschi et al., 2008). All these findings suggest that targeting DCs using Clec9A as a target could potentially enhance the effectiveness of vaccines. One of the reasons why Clec9A is such an effective target could be due to the fact that $CD8^+$ DCs, which express Clec9A, are believed to be capable of recognizing necrotic cells and cross-presenting antigen to T cells via MHC class I molecules (Villadangos and Schnorrer, 2007). Antigens that target $CD8^+$ via Clec9A seemed to

fall into the regular biological process of DCs for processing exogenous antigens (Caminschi et al., 2009).

2.9. Summary

In this chapter, the literatures relating to this PhD projects were critically reviewed. Effective drug delivery is key to better disease treatment. With a high proportion of drug candidates characterized by poor bioavailability and biodistribution, there is a great need to develop new drug delivery systems that can improve the intrinsic adsorption, distribution, metabolism and excretion (ADME) of drugs. Nanocarriers are emerging as safer and more effective drug delivery options compared to the traditional counterparts, *i.e.* capsules and tablets. They have shown numerous favorable features including a long circulation halftime, target specificity, intracellular delivery through endocytosis, high drug loading capacity and co-delivery of multiple therapeutic substrates to cater personal medication needs. The delivery of therapeutic agents through nanocarriers diminishes the unfavorable site effect in healthy tissues and enables enhanced accumulation at the biological site of action. The use of antigens exclusive to certain subset of cells is an effective targeting strategy. However, current strategies for surface engineering with functional moieties usually required a stringent reaction environment, which is potentially compromising to the activity of the therapeutic payload. The search for new strategies for targeting and nanocarrier stabilization will advance our ability to improve delivery efficacy.

The next chapter presents the study on constructing a PEGylated TNE with enhanced immune evading ability. It demonstrates a simple one-step PEGylation step for TNE using DAMP4 as anchor. The result from this part of the work provides a strong evidence base to support the hypothesis stated in Chapter 1 that laid the foundation of this PhD project. Subsequent chapters develop the PEGylated nanoemulsion further to input targeting and to demonstrate desirable biological outcomes *in vivo*.

2.10. References

A. BOS, M. & VAN VLIET, T. 2001. Interfacial rheological properties of adsorbed protein layers and surfactants: a review. *Advances in Colloid and Interface Science,* 91**,** 437-471.

ABUCHOWSKI, A., MCCOY, J. R., PALCZUK, N. C., VANES, T. & DAVIS, F. F. 1977a. Effect of covalent attachment of polyethylene glycol on immunogenicity and circulating life of bovine liver catalase. *Journal of Biological Chemistry,* 252**,** 3582-3586.

ABUCHOWSKI, A., VANES, T., PALCZUK, N. C. & DAVIS, F. F. 1977b. Alteration of immunological properties of bovine serum albumin by covalent attachment of polyethylene glycol. *Journal of Biological Chemistry,* 252**,** 3578-3581.

AGEMY, L., FRIEDMANN-MORVINSKI, D., KOTAMRAJU, V. R., ROTH, L., SUGAHARA, K. N., GIRARD, O. M., MATTREY, R. F., VERMA, I. M. & RUOSLAHTI, E. 2011. Targeted nanoparticle enhanced proapoptotic peptide as potential therapy for glioblastoma. *Proceedings of the National Academy of Sciences*.

AGNIHOTRI, S. A., MALLIKARJUNA, N. N. & AMINABHAVI, T. M. 2004. Recent advances on chitosan-based micro- and nanoparticles in drug delivery. *Journal of Controlled Release,* 100**,** 5-28.

AIKEN III, J. D. & FINKE, R. G. 1999. A review of modern transition-metal nanoclusters: their synthesis, characterization, and applications in catalysis. *Journal of Molecular Catalysis A: Chemical,* 145**,** 1-44.

ANANGI, R., RASH, L. D., MOBLI, M. & KING, G. F. 2012. Functional Expression in Escherichia coli of the Disulfide-Rich Sea Anemone Peptide APETx2, a Potent Blocker of Acid-Sensing Ion Channel 3. *Marine Drugs,* 10**,** 1605-1618.

ANTON, N., BENOIT, J.-P. & SAULNIER, P. 2008. Design and production of nanoparticles formulated from nano-emulsion templates—A review. *Journal of Controlled Release,* 128**,** 185-199.

ANTON, N., MOJZISOVA, H., PORCHER, E., BENOIT, J.-P. & SAULNIER, P. 2010. Reverse micelle-loaded lipid nano-emulsions: New technology for nano-encapsulation of hydrophilic materials. *International Journal of Pharmaceutics,* 398**,** 204-209.

ANUCHAPREEDA, S., FUKUMORI, Y., OKONOGI, S. & ICHIKAWA, H. 2012. Preparation of Lipid Nanoemulsions Incorporating Curcumin for Cancer Therapy. *Journal of Nanotechnology,* 2012.

BAJPAI, A. K., SHUKLA, S. K., BHANU, S. & KANKANE, S. 2008. Responsive polymers in controlled drug delivery. *Progress in Polymer Science,* 33**,** 1088-1118.

BANCHEREAU, J. & STEINMAN, R. M. 1998. Dendritic cells and the control of immunity. *Nature,* 392**,** 245-252.

BANDYOPADHYAY, A., FINE, R. L., DEMENTO, S., BOCKENSTEDT, L. K. & FAHMY, T. M. 2011. The impact of nanoparticle ligand density on dendritic-cell targeted vaccines. *Biomaterials,* 32**,** 3094-3105.

BANGHAM, A. D., STANDISH, M. M. & WATKINS, J. C. 1965. Diffusion of univalent ions across the lamellae of swollen phospholipids. *Journal of Molecular Biology,* 13**,** 238-IN27.

BARENHOLZ, Y., AMSELEM, S., GOREN, D., COHEN, R., GELVAN, D., SAMUNI, A., GOLDEN, E. B. & GABIZON, A. 1993. STABILITY OF LIPOSOMAL DOXORUBICIN FORMULATIONS - PROBLEMS AND PROSPECTS. *MEDICINAL RESEARCH REVIEWS,* 13**,** 449-491.

BARENHOLZ, Y., BOLOTIN, E., COHEN, R. & GABIZON, A. 1996. Sterically stabilized doxorubicin loaded liposomes (DOX-SL(TM)): From basics to the clinics. *PHOSPHORUS SULFUR AND SILICON AND THE RELATED ELEMENTS,* 109**,** 293-296.

BARNES, G. T. & GENTLE, I. R. 2005. *Interfacial Science - An Introduction,* New York, Oxford University Press Inc.

BATRAKOVA, E. V. & KABANOV, A. V. 2008. Pluronic block copolymers: Evolution of drug delivery concept from inert nanocarriers to biological response modifiers. *Journal of Controlled Release,* 130**,** 98-106.

BAWA, R. & JOHNSON, S. 2007. The ethical dimensions of nanomedicine. *The Medical clinics of North America,* 91**,** 881-887.

BAWARSKI, W. E., CHIDLOWSKY, E., BHARALI, D. J. & MOUSA, S. A. 2008. Emerging nanopharmaceuticals. *Nanomedicine: Nanotechnology, Biology and Medicine,* 4**,** 273-282.

BECHER, P. 2001 *Emulsions: Theory and practice.,* Washington, D.C. Oxford, American Chemical Society; Oxford University Press.

BECK-BROICHSITTER, M., RYTTING, E., LEBHARDT, T., WANG, X. & KISSEL, T. 2010. Preparation of nanoparticles by solvent displacement for drug delivery: A shift in the "ouzo region" upon drug loading. *European Journal of Pharmaceutical Sciences,* 41**,** 244-253.

BENEZRA, M., PENATE-MEDINA, O., ZANZONICO, P. B., SCHAER, D., OW, H., BURNS, A., DESTANCHINA, E., LONGO, V., HERZ, E., IYER, S., WOLCHOK, J., LARSON, S. M., WIESNER, U. & BRADBURY, M. S. 2011. Multimodal silica nanoparticles are effective cancer-targeted probes in a model of human melanoma. *The Journal of Clinical Investigation,* 121**,** 2768-2780.

BENICHOU, A., ASERIN, A. & GARTI, N. 2004. Double emulsions stabilized with hybrids of natural polymers for entrapment and slow release of active matters. *Advances in Colloid and Interface Science,* 108–109**,** 29-41.

BENITA, S. & LEVY, M. Y. 1993. Submicron emulsions as colloidal drug carriers for intravenous administration: comprehensive physicochemical characterization. *Journal of Pharmaceutical Sciences,* 82**,** 1069-1079.

BERG, J. M., TYMOCZKO, J. L. & STRYER, L. 2002. *Biochemistry,* New York, W.H. Freeman and Company.

BHARTI, A. C., DONATO, N., SINGH, S. & AGGARWAL, B. B. 2003. Curcumin (diferuloylmethane) down-regulates the constitutive activation of nuclear factor-kappa B and I kappa B alpha kinase in human multiple myeloma cells, leading to suppression of proliferation and induction of apoptosis. *Blood,* 101**,** 1053-1062.

BIRDI, K. S. 2010. *Surface and colloid chemistry: principles and applications,* Boca Raton, CRC Press/Taylor & Francis Group.

BOYACIOGLU, O., STUART, C. H., KULIK, G. & GMEINER, W. H. 2013. Dimeric DNA Aptamer Complexes for High-capacity-targeted Drug Delivery Using pH-sensitive Covalent Linkages. *Mol Ther Nucleic Acids,* 2**,** e107.

BUNJES, H. 2010. Lipid nanoparticles for the delivery of poorly water-soluble drugs. *The Journal of pharmacy and pharmacology,* 62**,** 1637-1645.

CALDERÓ, G., GARCÍA-CELMA, M. J. & SOLANS, C. 2011. Formation of polymeric nano-emulsions by a low-energy method and their use for nanoparticle preparation. *Journal of Colloid and Interface Science,* 353**,** 406-411.

CALICETI, P. & VERONESE, F. M. 2003. Pharmacokinetic and biodistribution properties of poly(ethylene glycol)-protein conjugates. *Advanced Drug Delivery Reviews,* 55**,** 1261-1277.

CAMINSCHI, I., LAHOUD, M. H. & SHORTMAN, K. 2009. Enhancing immune responses by targeting antigen to DC. *Eur. J. Immunol.,* 39**,** 931-938.
CAMINSCHI, I., MARASKOVSKY, E. & HEATH, W. R. 2012. Targeting dendritic cells in vivo for cancer therapy. *Frontiers in Immunology,* 3.
CAMINSCHI, I., PROIETTO, A. I., AHMET, F., KITSOULIS, S., TEH, J. S., LO, J. C. Y., RIZZITELLI, A., WU, L., VREMEC, D., VAN DOMMELEN, S. L. H., CAMPBELL, I. K., MARASKOVSKY, E., BRALEY, H., DAVEY, G. M., MOTTRAM, P., DE VELDE, N. V., JENSEN, K., LEW, A. M., WRIGHT, M. D., HEATH, W. R., SHORTMAN, K. & LAHOUD, M. H. 2008. The dendritic cell subtype-restricted C-type lectin Clec9A is a target for vaccine enhancement. *Blood,* 112**,** 3264-3273.
CARRILLO-CONDE, B., SONG, E.-H., CHAVEZ-SANTOSCOY, A., PHANSE, Y., RAMER-TAIT, A. E., POHL, N. L. B., WANNEMUEHLER, M. J., BELLAIRE, B. H. & NARASIMHAN, B. 2011. Mannose-Functionalized "Pathogen-like" Polyanhydride Nanoparticles Target C-Type Lectin Receptors on Dendritic Cells. *Molecular Pharmaceutics,* 8**,** 1877-1886.
CHANG, D.-K., LIN, C.-T., WU, C.-H. & WU, H.-C. 2009. A Novel Peptide Enhances Therapeutic Efficacy of Liposomal Anti-Cancer Drugs in Mice Models of Human Lung Cancer. *PLoS ONE,* 4**,** e4171.
CHEN, A. M., ZHANG, M., WEI, D., STUEBER, D., TARATULA, O., MINKO, T. & HE, H. 2009. Co-delivery of Doxorubicin and Bcl-2 siRNA by Mesoporous Silica Nanoparticles Enhances the Efficacy of Chemotherapy in Multidrug-Resistant Cancer Cells. *Small,* 5**,** 2673-2677.
CHENG, A. L., HSU, C. H., LIN, J. K., HSU, M. M., HO, Y. F., SHEN, T. S., KO, J. Y., LIN, J. T., LIN, B. R., WU, M. S., YU, H. S., JEE, S. H., CHEN, G. S., CHEN, T. M., CHEN, C. A., LAI, M. K., PU, Y. S., PAN, M. H., WANG, Y. J., TSAI, C. C. & HSIEH, C. Y. 2001. Phase I clinical trial of curcumin, a chemopreventive agent, in patients with high-risk or pre-malignant lesions. *Anticancer Research,* 21**,** 2895-2900.
CHO, H., BAE, J., GARRIPELLI, V. K., ANDERSON, J. M., JUN, H.-W. & JO, S. 2012. Redox-sensitive polymeric nanoparticles for drug delivery. *Chemical Communications,* 48**,** 6043-6045.
CHOI, C. H. J., ALABI, C. A., WEBSTER, P. & DAVIS, M. E. 2010. Mechanism of active targeting in solid tumors with transferrin-containing gold nanoparticles. *Proceedings of the National Academy of Sciences,* 107**,** 1235-1240.
CHORRO, L., SARDE, A., LI, M., WOOLLARD, K. J., CHAMBON, P., MALISSEN, B., KISSENPFENNIG, A., BARBAROUX, J.-B., GROVES, R. & GEISSMANN, F. 2009. Langerhans cell (LC) proliferation mediates neonatal development, homeostasis, and inflammation-associated expansion of the epidermal LC network. *The Journal of Experimental Medicine,* 206**,** 3089-3100.
CHUAN, Y. P., ZENG, B. Y., O'SULLIVAN, B., THOMAS, R. & MIDDELBERG, A. P. J. 2011. Co-delivery of antigen and a lipophilic anti-inflammatory drug to cells via a tailorable nanocarrier emulsion. *Journal of Colloid and Interface Science,* 368**,** 616-624.
CLERC, S. & BARENHOLZ, Y. 1995. Loading of amphipathic weak acids into liposomes in response to transmembrane calcium acetate gradients. *Biochimica et Biophysica Acta (BBA) - Biomembranes,* 1240**,** 257-265.
CLERC, S. & BARENHOLZ, Y. 1998. A Quantitative Model for Using Acridine Orange as a Transmembrane pH Gradient Probe. *Analytical Biochemistry,* 259**,** 104-111.
CONNER, S. D. & SCHMID, S. L. 2003. Regulated portals of entry into the cell. *Nature,* 422**,** 37-44.
CONSTANTINIDES, P. P., LAMBERT, K. J., TUSTIAN, A. K., SCHNEIDER, B., LALJI, S., MA, W. W., WENTZEL, B., KESSLER, D., WORAH, D. & QUAY, S. C. 2000. Formulation development and

antitumor activity of a filter-sterilizable emulsion of paclitaxel. *Pharmaceutical Research,* 17**,** 175-182.
CONSTANTINIDES, P. P., TUSTIAN, A. & KESSLER, D. R. 2004. Tocol emulsions for drug solubilization and parenteral delivery. *Advanced Drug Delivery Reviews,* 56**,** 1243-1255.
DALGLEISH, D. G. 1997. Adsorption of protein and the stability of emulsions. *Trends in Food Science & Technology,* 8**,** 1-6.
DANHIER, F., ANSORENA, E., SILVA, J. M., COCO, R., LE BRETON, A. & PRÉAT, V. 2012. PLGA-based nanoparticles: An overview of biomedical applications. *Journal of Controlled Release,* 161**,** 505-522.
DANHIER, F., VROMAN, B., LECOUTURIER, N., CROKART, N., POURCELLE, V., FREICHELS, H., JÉRÔME, C., MARCHAND-BRYNAERT, J., FERON, O. & PRÉAT, V. 2009. Targeting of tumor endothelium by RGD-grafted PLGA-nanoparticles loaded with Paclitaxel. *Journal of Controlled Release,* 140**,** 166-173.
DAVIS, F. F., ABUCHOWSKI, A., ES, T., PALCZUK, N. C., CHEN, R., SAVOCA, K. & WIEDER, K. 1978. Enzyme-Polyethylene Glycol Adducts: Modified Enzymes with Unique Properties. *In:* BROUN, G., MANECKE, G. & WINGARD, L., JR. (eds.) *Enzyme Engineering.* Springer US.
DAVIS, S. S., WASHINGTON, C., WEST, P., ILLUM, L., LIVERSIDGE, G., STERNSON, L. & KIRSH, R. 1987. Lipid Emulsions as Drug Delivery Systems. *Annals of the New York Academy of Sciences,* 507**,** 75-88.
DAWES, W. H. & GROVES, M. J. 1978. The effect of electrolytes on phospholipid-stabilized soyabean oil emulsions. *International Journal of Pharmaceutics,* 1**,** 141-150.
DERJAGUIN, B. & LANDAU, L. 1941. Theory of the stability of strongly charged lyophobic sols and of the adhesion of strongly charged particles in solutions of electrolytes. *Acta Physico Chemica URSS,* 14**,** 633-662.
DEXTER, A. F., MALCOLM, A. S. & MIDDELBERG, A. P. J. 2006. Reversible active switching of the mechanical properties of a peptide film at a fluid-fluid interface. *Nat Mater,* 5**,** 502-506.
DEXTER, A. F. & MIDDELBERG, A. P. J. 2007. Switchable Peptide Surfactants with Designed Metal Binding Capacity. *The Journal of Physical Chemistry C,* 111**,** 10484-10492.
DICKINSON, E. 1999. Adsorbed protein layers at fluid interfaces: interactions, structure and surface rheology. *Colloids and Surfaces B: Biointerfaces,* 15**,** 161-176.
DICKINSON, E. 2001. Milk protein interfacial layers and the relationship to emulsion stability and rheology. *Colloids and Surfaces B: Biointerfaces,* 20**,** 197-210.
DIMITRIJEV-DWYER, M., HE, L., JAMES, M., NELSON, A., WANG, L. & MIDDELBERG, A. P. J. 2012. The effects of acid hydrolysis on protein biosurfactant molecular, interfacial, and foam properties: pH responsive protein hydrolysates. *Soft Matter,* 8**,** 5131-5139.
DIMITRIJEV DWYER, M., BRECH, M., YU, L. & MIDDELBERG, A. P. J. 2014. Intensified expression and purification of a recombinant biosurfactant protein. *Chemical Engineering Science,* 105**,** 12-21.
DOMÍNGUEZ, P. M. & ARDAVÍN, C. 2010. Differentiation and function of mouse monocyte-derived dendritic cells in steady state and inflammation. *Immunological Reviews,* 234**,** 90-104.
DOS SANTOS, N., COX, K. A., MCKENZIE, C. A., VAN BAARDA, F., GALLAGHER, R. C., KARLSSON, G., EDWARDS, K., MAYER, L. D., ALLEN, C. & BALLY, M. B. 2004. pH gradient loading of anthracyclines into cholesterol-free liposomes: enhancing drug loading rates through use of ethanol. *Biochimica et Biophysica Acta (BBA) - Biomembranes,* 1661**,** 47-60.

DRISCOLL, D. F., LING, P.-R. & BISTRIAN, B. R. 2009. Pharmacopeial compliance of fish oil-containing parenteral lipid emulsion mixtures: Globule size distribution (GSD) and fatty acid analyses. *International Journal of Pharmaceutics,* 379**,** 125-130.

DURAND, R., PAUL, M., RIVOLLET, D., HOUIN, R., ASTIER, A. & DENIAU, M. 1997. Activity of pentamidine-loaded methacrylate nanoparticles against Leishmania infantum in a mouse model. *International Journal for Parasitology,* 27**,** 1361-1367.

DWYER, M. D., HE, L. Z., JAMES, M., NELSON, A. & MIDDELBERG, A. P. J. 2013. Insights into the role of protein molecule size and structure on interfacial properties using designed sequences. *Journal of the Royal Society Interface,* 10.

ELIAS, D. R., POLOUKHTINE, A., POPIK, V. & TSOURKAS, A. 2013. Effect of ligand density, receptor density, and nanoparticle size on cell targeting. *Nanomedicine: Nanotechnology, Biology and Medicine,* 9**,** 194-201.

EMANUEL, N., KEDAR, E., BOLOTIN, E. M., SMORODINSKY, N. I. & BARENHOLZ, Y. 1996. Preparation and characterization of doxorubicin-loaded sterically stabilized immunoliposomes. *Pharmaceutical Research,* 13**,** 352-359.

EMERICH, D. F. & THANOS, C. G. 2003. Nanotechnology and medicine. *Expert Opinion on Biological Therapy,* 3**,** 655-663.

ESSA, S., RABANEL, J. M. & HILDGEN, P. 2010. Effect of polyethylene glycol (PEG) chain organization on the physicochemical properties of poly(d, l-lactide) (PLA) based nanoparticles. *European Journal of Pharmaceutics and Biopharmaceutics,* 75**,** 96-106.

FAIRMAN, R., CHAO, H.-G., MUELLER, L., LAVOIE, T. B., SHEN, L., NOVOTNY, J. & MATSUEDA, G. R. 1995. Characterization of a new four-chain coiled-coil: Influence of chain length on stability. *Protein Science,* 4**,** 1457-1469.

FAST, J. & MECOZZI, S. 2009. Nanoemulsions for Intravenous Drug Delivery. *In:* VILLIERS, M., ARAMWIT, P. & KWON, G. (eds.) *Nanotechnology in Drug Delivery.* Springer New York.

FAY, F. & SCOTT, C. J. 2011. Antibody-targeted nanoparticles for cancer therapy. *Immunotherapy,* 3**,** 381-394.

FERRIS, D. P., LU, J., GOTHARD, C., YANES, R., THOMAS, C. R., OLSEN, J.-C., STODDART, J. F., TAMANOI, F. & ZINK, J. I. 2011. Synthesis of Biomolecule-Modified Mesoporous Silica Nanoparticles for Targeted Hydrophobic Drug Delivery to Cancer Cells. *Small,* 7**,** 1816-1826.

FLANAGAN, J. & SINGH, H. 2006. Microemulsions: A Potential Delivery System for Bioactives in Food. *Critical Reviews in Food Science and Nutrition,* 46**,** 221-237.

FLOYD, A. G. 1999. Top ten considerations in the development of parenteral emulsions. *Pharmaceutical Science & Technology Today,* 2**,** 134-143.

FORGIARINI, A., ESQUENA, J., GONZÁLEZ, C. & SOLANS, C. 2001. Formation of Nano-emulsions by Low-Energy Emulsification Methods at Constant Temperature. *Langmuir,* 17**,** 2076-2083.

FÖRSTER, T. & RYBINSKI , W. V. 1998. Applications of Emulsions. *In:* BINKS, B. (ed.) *Modern aspects of emulsion science.* Cambridge: The Royal society of Chemistry.

FRIEDMAN, R. 2011. Nano Dot Technology Enters Clinical Trials. *Journal of the National Cancer Institute,* 103**,** 1428-1429.

FRYD, M. M. & MASON, T. G. 2012. Advanced Nanoemulsions. *Annual Review of Physical Chemistry,* 63**,** 493-518.

GABIZON, A. & PAPAHADJOPOULOS, D. 1988. Liposome formulations with prolonged circulation time in blood and enhanced uptake by tumors. *Proceedings of the National Academy of Sciences,* 85**,** 6949-6953.

GABIZON, A. A. 2001. Pegylated liposomal doxorubicin: metamorphosis of an old drug into a new form of chemotherapy. *Cancer investigation,* 19**,** 424-436.
GANGULY, D., HAAK, S., SISIRAK, V. & REIZIS, B. 2013a. The role of dendritic cells in autoimmunity. *Nature reviews.Immunology,* 13**,** 566-577.
GANGULY, D., HAAK, S., SISIRAK, V. & REIZIS, B. 2013b. The role of dendritic cells in autoimmunity. *Nat Rev Immunol,* 13**,** 566-577.
GANTA, S. & AMIJI, M. 2009. Coadministration of Paclitaxel and Curcumin in Nanoemulsion Formulations To Overcome Multidrug Resistance in Tumor Cells. *Molecular Pharmaceutics,* 6**,** 928-939.
GANTA, S., DEVALAPALLY, H., BAGULEY, B. C., GARG, S. & AMIJI, M. 2008. Microfluidic preparation of chlorambucil nanoemulsion formulations and evaluation of cytotoxicity and pro-apoptotic activity in tumor cells. *Journal of Biomedical Nanotechnology,* 4**,** 165-173.
GANTA, S., SHARMA, P., PAXTON, J. W., BAGULEY, B. C. & GARG, S. 2010. Pharmacokinetics and pharmacodynamics of chlorambucil delivered in long-circulating nanoemulsion. *Journal of Drug Targeting,* 18**,** 125-133.
GARRETT, R. H. & GRISHAM, C. M. 2005. *Biochemistry,* Belmont, Thomson Brooks/Cole.
GHAI, D. & SINHA, V. R. 2012. Nanoemulsions as self-emulsified drug delivery carriers for enhanced permeability of the poorly water-soluble selective β1-adrenoreceptor blocker Talinolol. *Nanomedicine: Nanotechnology, Biology and Medicine,* 8**,** 618-626.
GOLDSTEIN, J. L., ANDERSON, R. G. W. & BROWN, M. S. 1979. Coated pits, coated vesicles, and receptor-mediated endocytosis. *Nature,* 279**,** 679-685.
GOODWIN, J. W. 2009. *Colloids and interfaces with surfactants and polymers,* Hoboken, NJ U6 - ctx_ver=Z39.88-2004&ctx_enc=info%3Aofi%2Fenc%3AUTF-8&rfr_id=info:sid/summon.serialssolutions.com&rft_val_fmt=info:ofi/fmt:kev:mtx:book&rft.genre=book&rft.title=Colloids+and+interfaces+with+surfactants+and+polymers&rft.au=Goodwin%2C+James+W&rft.date=2009-01-01&rft.pub=Wiley&rft.externalDBID=n%2Fa&rft.externalDocID=b2490918x&paramdict=en-US U7 - eBook U8 - FETCH-uq_catalog_b2490918x1, Wiley.
GOTTESMAN, M. M., FOJO, T. & BATES, S. E. 2002. Multidrug resistance in cancer: role of ATP-dependent transporters. *Nat Rev Cancer,* 2**,** 48-58.
GREF, R., LÜCK, M., QUELLEC, P., MARCHAND, M., DELLACHERIE, E., HARNISCH, S., BLUNK, T. & MÜLLER, R. H. 2000. 'Stealth' corona-core nanoparticles surface modified by polyethylene glycol (PEG): influences of the corona (PEG chain length and surface density) and of the core composition on phagocytic uptake and plasma protein adsorption. *Colloids and Surfaces B: Biointerfaces,* 18**,** 301-313.
GREGORIADIS, G., SWAIN, C. P., WILLS, E. J. & TAVILL, A. S. 1974. DRUG-CARRIER POTENTIAL OF LIPOSOMES IN CANCER CHEMOTHERAPY. *The Lancet,* 303**,** 1313-1316.
GU, F., LANGER, R. & FAROKHZAD, O. 2009. Formulation/Preparation of Functionalized Nanoparticles for In Vivo Targeted Drug Delivery. *In:* FOOTE, R. S. & LEE, J. W. (eds.) *Micro and Nano Technologies in Bioanalysis.* Humana Press.
GU, J., SU, S., LI, Y., HE, Q., ZHONG, J. & SHI, J. 2010. Surface Modification−Complexation Strategy for Cisplatin Loading in Mesoporous Nanoparticles. *The Journal of Physical Chemistry Letters,* 1**,** 3446-3450.
GULATI, M., GROVER, M., SINGH, S. & SINGH, M. 1998. Lipophilic drug derivatives in liposomes. *International Journal of Pharmaceutics,* 165**,** 129-168.

GUTIÉRREZ, J. M., GONZÁLEZ, C., MAESTRO, A., SOLÈ, I., PEY, C. M. & NOLLA, J. 2008. Nano-emulsions: New applications and optimization of their preparation. *Current Opinion in Colloid & Interface Science,* 13**,** 245-251.
HAAHEIM, L. R. 2009. Basic influenza virology and immunology. Wallingford, UK: CABI.
HALLBERG, D., SCHUBERTH, O. & WRETLIND, A. 1985. Nutrition Classics - Experimental and clinical -studies with fat emulsion for intravenous nutrition. *Nutrition Reviews,* 43**,** 26-28.
HAMAGUCHI, T., MATSUMURA, Y., SUZUKI, M., SHIMIZU, K., GODA, R., NAKAMURA, I., NAKATOMI, I., YOKOYAMA, M., KATAOKA, K. & KAKIZOE, T. 2005. NK105, a paclitaxel-incorporating micellar nanoparticle formulation, can extend in vivo antitumour activity and reduce the neurotoxicity of paclitaxel. *Br J Cancer,* 92**,** 1240-1246.
HAN, H. & DAVIS, M. E. 2013. Single-Antibody, Targeted Nanoparticle Delivery of Camptothecin. *Molecular Pharmaceutics,* 10**,** 2558-2567.
HAN, J. H., DAVIS, S. S., PAPANDREOU, C., MELIA, C. D. & WASHINGTON, C. 2004. Design and evaluation of an emulsion vehicle for paclitaxel. I. physicochemical properties and plasma stability. *Pharmaceutical Research,* 21**,** 1573-1580.
HANSEN, C. G. & NICHOLS, B. J. 2009. Molecular mechanisms of clathrin-independent endocytosis. *Journal of cell science,* 122**,** 1713-1721.
HANSEN, L., UNMACK LARSEN, E. K., NIELSEN, E. H., IVERSEN, F., LIU, Z., THOMSEN, K., PEDERSEN, M., SKRYDSTRUP, T., NIELSEN, N. C., PLOUG, M. & KJEMS, J. 2013. Targeting of peptide conjugated magnetic nanoparticles to urokinase plasminogen activator receptor (uPAR) expressing cells. *Nanoscale,* 5**,** 8192-8201.
HANSON, J. A., CHANG, C. B., GRAVES, S. M., LI, Z., MASON, T. G. & DEMING, T. J. 2008. Nanoscale double emulsions stabilized by single-component block copolypeptides. *Nature,* 455**,** 85-88.
HARAN, G., COHEN, R., BAR, L. K. & BARENHOLZ, Y. 1993. Transmembrane ammonium sulfate gradients in liposomes produce efficient and stable entrapment of amphipathic weak bases. *Biochimica et Biophysica Acta (BBA) - Biomembranes,* 1151**,** 201-215.
HARRIS, J. M. & CHESS, R. B. 2003. Effect of pegylation on pharmaceuticals. *Nat Rev Drug Discov,* 2**,** 214-221.
HENRY, J. V. L., FRYER, P. J., FRITH, W. J. & NORTON, I. T. 2010. The influence of phospholipids and food proteins on the size and stability of model sub-micron emulsions. *Food Hydrocolloids,* 24**,** 66-71.
HIPPALGAONKAR, K., MAJUMDAR, S. & KANSARA, V. 2010. Injectable lipid emulsions-advancements, opportunities and challenges. *Aaps Pharmscitech,* 11**,** 1526-1540.
HOFER, K. N., MCCARTHY, M. W., BUCK, M. L. & HENDRICK, A. E. 2003. Possible anaphylaxis after propofol in a child with food allergy. *Annals of Pharmacotherapy,* 37**,** 398-401.
HOWARD, K. A., PALUDAN, S. R., BEHLKE, M. A., BESENBACHER, F., DELEURAN, B. & KJEMS, J. 2008. Chitosan/siRNA Nanoparticle-mediated TNF-[alpha] Knockdown in Peritoneal Macrophages for Anti-inflammatory Treatment in a Murine Arthritis Model. *Mol Ther,* 17**,** 162-168.
HU, C.-M. J., ZHANG, L., ARYAL, S., CHEUNG, C., FANG, R. H. & ZHANG, L. 2011. Erythrocyte membrane-camouflaged polymeric nanoparticles as a biomimetic delivery platform. *Proceedings of the National Academy of Sciences*.
HUANG, R. K., STEINMETZ, N. F., FU, C.-Y., MANCHESTER, M. & JOHNSON, J. E. 2010. Transferrin-mediated targeting of bacteriophage HK97 nanoparticles into tumor cells. *Nanomedicine,* 6**,** 55-68.

HUANG, Y.-F., LIU, H., XIONG, X., CHEN, Y. & TAN, W. 2009. Nanoparticle-Mediated IgE−Receptor Aggregation and Signaling in RBL Mast Cells. *Journal of the American Chemical Society,* 131**,** 17328-17334.

HUYSAMEN, C., WILLMENT, J. A., DENNEHY, K. M. & BROWN, G. D. 2008. CLEC9A is a novel activation C-type lectin-like receptor expressed on BDCA3(+) dendritic cells and a subset of monocytes. *Journal of Biological Chemistry,* 283**,** 16693-16701.

HWANG, Y. Y., RAMALINGAM, K., BIENEK, D. R., LEE, V., YOU, T. & ALVAREZ, R. 2013. Antimicrobial Activity of Nanoemulsion in Combination with Cetylpyridinium Chloride in Multidrug-Resistant Acinetobacter baumannii. *Antimicrobial Agents and Chemotherapy,* 57**,** 3568-3575.

IINUMA, H., MARUYAMA, K., OKINAGA, K., SASAKI, K., SEKINE, T., ISHIDA, O., OGIWARA, N., JOHKURA, K. & YONEMURA, Y. 2002. Intracellular targeting therapy of cisplatin-encapsulated transferrin-polyethylene glycol liposome on peritoneal dissemination of gastric cancer. *International Journal of Cancer,* 99**,** 130-137.

ILLUM, L., DAVIS, S. S., MULLER, R. H., MAK, E. & WEST, P. 1987. The organ distribution and circulation time of intravenously injected colloidal carriers sterically stabilized with a blockcopolymer - poloxamine 908. *Life Sciences,* 40**,** 367-374.

INABA, K., INABA, M., NAITO, M. & STEINMAN, R. M. 1993. Dendritic cell progenitors phagocytose particulates, including bacillus Calmette-Guerin organisms, and sensitize mice to mycobacterial antigens in vivo. *Journal of Experimental Medicine,* 178**,** 479-488.

ISHIDA, O., MARUYAMA, K., TANAHASHI, H., IWATSURU, M., SASAKI, K., ERIGUCHI, M. & YANAGIE, H. 2001. Liposomes Bearing Polyethyleneglycol-Coupled Transferrin with Intracellular Targeting Property to the Solid Tumors In Vivo. *Pharmaceutical Research,* 18**,** 1042-1048.

IYER, A. K., SU, Y., FENG, J., LAN, X., ZHU, X., LIU, Y., GAO, D., SEO, Y., VANBROCKLIN, H. F., COURTNEY BROADDUS, V., LIU, B. & HE, J. 2011. The effect of internalizing human single chain antibody fragment on liposome targeting to epithelioid and sarcomatoid mesothelioma. *Biomaterials,* 32**,** 2605-2613.

IZQUIERDO, P., ESQUENA, J., TADROS, T. F., DEDEREN, C., GARCIA, M. J., AZEMAR, N. & SOLANS, C. 2002. Formation and stability of nano-emulsions prepared using the phase inversion temperature method. *Langmuir,* 18**,** 26-30.

JAECKLE, K., BATCHELOR, T., O'DAY, S., PHUPHANICH, S., NEW, P., LESSER, G., COHN, A., GILBERT, M., AIKEN, R., HEROS, D., ROGERS, L., WONG, E., FULTON, D., GUTHEIL, J., BAIDAS, S., KENNEDY, J., MASON, W., MOOTS, P., RUSSELL, C., SWINNEN, L. & HOWELL, S. 2002. An Open Label Trial of Sustained-release Cytarabine (DepoCyt™) for the Intrathecal Treatment of Solid Tumor Neoplastic Meningitis. *Journal of Neuro-Oncology,* 57**,** 231-239.

JANEWAY, C. A. 2005. *Immunobiology: the immune system in health and disease,* New York, Garland Science/Churchill Livingstone.

JIANG, W., KIMBETTY, Y. S., RUTKA, J. T. & CHANWARREN, C. W. 2008. Nanoparticle-mediated cellular response is size-dependent. *Nat Nano,* 3**,** 145-150.

JOHN, F. 2013. *The National nanotechnology Initiative: Overview, Reauthorization, and Appropriations Issues* [Online]. Congressional Research Service. Available: http://www.fas.org/sgp/crs/misc/RL34401.pdf [Accessed 11-Sep 2013].

JONES, D. B. & MIDDELBERG, A. P. J. 2002. Mechanical Properties of Interfacially Adsorbed Peptide Networks. *Langmuir,* 18**,** 10357-10362.

KAAR, W., HARTMANN, B. M., FAN, Y., ZENG, B., LUA, L. H. L., DEXTER, A. F., FALCONER, R. J. & MIDDELBERG, A. P. J. 2009. Microbial bio-production of a recombinant stimuli-responsive biosurfactant. *Biotechnology and Bioengineering,* 102**,** 176-187.
KABALNOV, A. & WENNERSTROM, H. 1996. Macroemulsion stability: The oriented wedge theory revisited. *Langmuir,* 12**,** 276-292.
KABANOV, A. V. & GENDELMAN, H. E. 2007. Nanomedicine in the diagnosis and therapy of neurodegenerative disorders. *Progress in Polymer Science,* 32**,** 1054-1082.
KAPSE-MISTRY, S., GOVENDER, T., SRIVASTAVA, R. & YERGERI, M. 2014. Nanodrug delivery in reversing multidrug resistance in cancer cells. *Frontiers in Pharmacology,* 5**,** 159.
KATO, K., CHIN, K., YOSHIKAWA, T., YAMAGUCHI, K., TSUJI, Y., ESAKI, T., SAKAI, K., KIMURA, M., HAMAGUCHI, T., SHIMADA, Y., MATSUMURA, Y. & IKEDA, R. 2012. Phase II study of NK105, a paclitaxel-incorporating micellar nanoparticle, for previously treated advanced or recurrent gastric cancer. *Investigational New Drugs,* 30**,** 1621-1627.
KAWILARANG, C. R. T., GEORGHIOU, K. & GROVES, M. J. 1980. The effect of additives on the physical properties of a phospholipid-stabilized soybean oil emulsion. *Journal of Clinical and Hospital Pharmacy,* 5**,** 151-160.
KIM, J.-Y., KIM, J.-K., PARK, J.-S., BYUN, Y. & KIM, C.-K. 2009. The use of PEGylated liposomes to prolong circulation lifetimes of tissue plasminogen activator. *Biomaterials,* 30**,** 5751-5756.
KIM, S., SHI, Y., KIM, J. Y., PARK, K. & CHENG, J.-X. 2010. Overcoming the barriers in micellar drug delivery: loading efficiency, in vivo stability, and micelle-cell interaction. *Expert Opinion on Drug Delivery,* 7**,** 49-62.
KLANG, S. H., BASZKIN, A. & BENITA, S. 1996. The stability of piroxicam incorporated in a positively-charged submicron emulsion for ocular administration. *International Journal of Pharmaceutics,* 132**,** 33-44.
KLIBANOV, A. L., MARUYAMA, K., TORCHILIN, V. P. & HUANG, L. 1990. Amphipathic polyethyleneglycols effectively prolong the circulation time of liposomes. *FEBS Letters,* 268**,** 235-237.
KOVACEVIC, A., SAVIC, S., VULETA, G., MULLER, R. H. & KECK, C. M. 2011. Polyhydroxy surfactants for the formulation of lipid nanoparticles (SLN and NLC): Effects on size, physical stability and particle matrix structure. *International Journal of Pharmaceutics,* 406**,** 163-172.
KRESGE, C. T., LEONOWICZ, M. E., ROTH, W. J., VARTULI, J. C. & BECK, J. S. 1992. Ordered mesoporous molecular sieves synthesized by a liquid-crystal template mechanism. *Nature,* 359**,** 710-712.
KURIHARA, A., SHIBAYAMA, Y., MIZOTA, A., YASUNO, A., IKEDA, M. & HISAOKA, M. 1996. Pharmacokinetics of highly lipophilic antitumor agent palmitoyl rhizoxin incorporated in lipid emulsions in rats. *Biological & Pharmaceutical Bulletin,* 19**,** 252-258.
LASIC, D. D. 1988. The mechanism of vesicle formation. *The Biochemical journal,* 256**,** 1-11.
LASIC, D. D., ČEH, B., STUART, M. C. A., GUO, L., FREDERIK, P. M. & BARENHOLZ, Y. 1995. Transmembrane gradient driven phase transitions within vesicles: lessons for drug delivery. *BBA - Biomembranes,* 1239**,** 145-156.
LAWRENCE, M. J. & REES, G. D. 2000. Microemulsion-based media as novel drug delivery systems. *Advanced Drug Delivery Reviews,* 45**,** 89-121.
LI, J., JI, J., HOLMES, L. M., BURGIN, K. E., BARTON, L. B., YU, X., WAGNER, T. E. & WEI, Y. 2004. Fusion protein from RGD peptide and Fc fragment of mouse immunoglobulin G inhibits angiogenesis in tumor. *Cancer Gene Ther,* 11**,** 363-370.

LI, L.-L., XIE, M., WANG, J., LI, X., WANG, C., YUAN, Q., PANG, D.-W., LU, Y. & TAN, W. 2013. A vitamin-responsive mesoporous nanocarrier with DNA aptamer-mediated cell targeting. *Chemical Communications,* 49**,** 5823-5825.

LI, L.-L., YIN, Q., CHENG, J. & LU, Y. 2012. Polyvalent Mesoporous Silica Nanoparticle-Aptamer Bioconjugates Target Breast Cancer Cells. *Advanced Healthcare Materials,* 1**,** 567-572.

LI, X., DING, L., XU, Y., WANG, Y. & PING, Q. 2009. Targeted delivery of doxorubicin using stealth liposomes modified with transferrin. *International Journal of Pharmaceutics,* 373**,** 116-123.

LIONG, M., LU, J., KOVOCHICH, M., XIA, T., RUEHM, S. G., NEL, A. E., TAMANOI, F. & ZINK, J. I. 2008. Multifunctional Inorganic Nanoparticles for Imaging, Targeting, and Drug Delivery. *ACS Nano,* 2**,** 889-896.

LODISH, H. F. 2008. *Molecular cell biology,* New York, W.H. Freeman.

LU, J., LIONG, M., ZINK, J. I. & TAMANOI, F. 2007. Mesoporous Silica Nanoparticles as a Delivery System for Hydrophobic Anticancer Drugs. *Small,* 3**,** 1341-1346.

M. H. F, S., M. F, Y., S. M, E., A. S, M. & M. N, A. 2010. Anti-inflammatory and Analgesic Effects of Ketoprofen in Palm Oil Esters Nanoemulsion. *Journal of Oleo Science,* 59**,** 667-671.

MACHADO, A. H. E., LUNDBERG, D., RIBEIRO, A. J., VEIGA, F. J., LINDMAN, B., MIGUEL, M. G. & OLSSON, U. 2012. Preparation of calcium alginate nanoparticles using water-in-oil (W/O) nanoemulsions. *Langmuir,* 28**,** 4131-4141.

MAEDA, H., WU, J., SAWA, T., MATSUMURA, Y. & HORI, K. 2000. Tumor vascular permeability and the EPR effect in macromolecular therapeutics: a review. *Journal of Controlled Release,* 65**,** 271-284.

MAI, W. X. & MENG, H. 2012. Mesoporous silica nanoparticles: A multifunctional nano therapeutic system. *Integrative biology : quantitative biosciences from nano to macro,* 5**,** 19-28.

MAKIDON, P. E., BIELINSKA, A. U., NIGAVEKAR, S. S., JANCZAK, K. W., KNOWLTON, J., SCOTT, A. J., MANK, N., CAO, Z., RATHINAVELU, S., BEER, M. R., WILKINSON, J. E., BLANCO, L. P., LANDERS, J. J. & BAKER, J. R., JR. 2008. Pre-Clinical Evaluation of a Novel Nanoemulsion-Based Hepatitis B Mucosal Vaccine. *PLoS ONE,* 3**,** e2954.

MALMESTEN, M. 2002. Surfactants and Polymers in Drug Delivery. *Marcel Dekker, Inc., New York, Basel,* 122.

MARCZYLO, T. H., VERSCHOYLE, R. D., COOKE, D. N., MORAZZONI, P., STEWARD, W. P. & GESCHER, A. J. 2007. Comparison of systemic availability of curcumin with that of curcumin formulated with phosphatidylcholine. *Cancer Chemotherapy and Pharmacology,* 60**,** 171-177.

MAREGA, R., KARMANI, L., FLAMANT, L., NAGESWARAN, P. G., VALEMBOIS, V., MASEREEL, B., FERON, O., BORGHT, T. V., LUCAS, S., MICHIELS, C., GALLEZ, B. & BONIFAZI, D. 2012. Antibody-functionalized polymer-coated gold nanoparticles targeting cancer cells: an in vitro and in vivo study. *Journal of Materials Chemistry,* 22**,** 21305-21312.

MART, R. J., OSBORNE, R. D., STEVENS, M. M. & ULIJN, R. V. 2006. Peptide-based stimuli-responsive biomaterials. *Soft Matter,* 2**,** 822-835.

MARTI-MESTRES, G. & NIELLOUD, F. 2002. Emulsions in Health Care Applications—An Overview. *Journal of Dispersion Science and Technology,* 23**,** 419-439.

MARTIN, A. H., GROLLE, K., BOS, M. A., STUART, M. A. C. & VAN VLIET, T. 2002. Network Forming Properties of Various Proteins Adsorbed at the Air/Water Interface in Relation to Foam Stability. *Journal of Colloid and Interface Science,* 254**,** 175-183.

MARUYAMA, K., YUDA, T., OKAMOTO, A., ISHIKURA, C., KOJIMA, S. & IWATSURU, M. 1991. Effect of molecular weight in amphipathic polyethyleneglycol on prolonging the circulation time of large unilamellar liposomes. *Chemical & Pharmaceutical Bulletin,* 39**,** 1620-1622.

MATSUMURA, Y., HAMAGUCHI, T., URA, T., MURO, K., YAMADA, Y., SHIMADA, Y., SHIRAO, K., OKUSAKA, T., UENO, H., IKEDA, M. & WATANABE, N. 2004. Phase I clinical trial and pharmacokinetic evaluation of NK911, a micelle-encapsulated doxorubicin. *Br J Cancer,* 91**,** 1775-1781.

MATSUMURA, Y. & MAEDA, H. 1986. A New Concept for Macromolecular Therapeutics in Cancer Chemotherapy: Mechanism of Tumoritropic Accumulation of Proteins and the Antitumor Agent Smancs. *Cancer Research,* 46**,** 6387-6392.

MCCLEMENTS, D. J. 2005. *Food emulsions: principles, practice, and techniques,* Boca Raton, CRC Press.

MCNEIL, S. E. 2005. Nanotechnology for the biologist. *Journal of Leukocyte Biology,* 78**,** 585-594.

MEDINA, C., SANTOS-MARTINEZ, M. J., RADOMSKI, A., CORRIGAN, O. I. & RADOMSKI, M. W. 2007. Nanoparticles: pharmacological and toxicological significance. *British Journal of Pharmacology,* 150**,** 552-558.

MELESON, K., GRAVES, S. & MASON, T. G. 2004. Formation of Concentrated Nanoemulsions by Extreme Shear. *Soft Materials,* 2**,** 109-123.

MENG, E., CAI, T.-F., LI, W.-Y., ZHANG, H., LIU, Y.-B., PENG, K., LIANG, S. & ZHANG, D.-Y. 2011a. Functional Expression of Spider Neurotoxic Peptide Huwentoxin-I in <italic>E. coli</italic>. *PLoS ONE,* 6**,** e21608.

MENG, H., XUE, M., XIA, T., JI, Z., TARN, D. Y., ZINK, J. I. & NEL, A. E. 2011b. Use of Size and a Copolymer Design Feature To Improve the Biodistribution and the Enhanced Permeability and Retention Effect of Doxorubicin-Loaded Mesoporous Silica Nanoparticles in a Murine Xenograft Tumor Model. *ACS Nano,* 5**,** 4131-4144.

MIDDELBERG, A. P. J. & DIMITRIJEV-DWYER, M. 2011. A Designed Biosurfactant Protein for Switchable Foam Control. *Chemphyschem,* 12**,** 1426-1429.

MIDDELBERG, A. P. J., RADKE, C. J. & BLANCH, H. W. 2000. Peptide interfacial adsorption is kinetically limited by the thermodynamic stability of self association. *Proceedings of the National Academy of Sciences,* 97**,** 5054-5059.

MIESZAWSKA, A. J., KIM, Y., GIANELLA, A., VAN ROOY, I., PRIEM, B., LABARRE, M. P., OZCAN, C., CORMODE, D. P., PETROV, A., LANGER, R., FAROKHZAD, O. C., FAYAD, Z. A. & MULDER, W. J. M. 2013. Synthesis of Polymer–Lipid Nanoparticles for Image-Guided Delivery of Dual Modality Therapy. *Bioconjugate chemistry*.

MINKO, T., DHARAP, S. S., PAKUNLU, R. I. & WANG, Y. 2004. Molecular targeting of drug delivery systems to cancer. *Current Drug Targets,* 5**,** 389-406.

MIYATA, K., CHRISTIE, R. J. & KATAOKA, K. 2011. Polymeric micelles for nano-scale drug delivery. *Reactive and Functional Polymers,* 71**,** 227-234.

MOEN, M., LYSENG-WILLIAMSON, K. & SCOTT, L. 2009. Liposomal Amphotericin B. *Drugs,* 69**,** 361-392.

MOLL, H., FUCHS, H., BLANK, C. & ROLLINGHOFF, M. 1993. Langerhans cells transport Leishmania major from the infected skin to the draining lymph node for presentation to antigen-specific T cells. *European Journal of Immunology,* 23**,** 1595-1601.

MONFARDINI, C., SCHIAVON, O., CALICETI, P., MORPURGO, M., HARRIS, J. M. & VERONESE, F. M. 1995. A branched monomethoxypoly(ethylene glycol) for protein modification. *Bioconjugate chemistry,* 6**,** 62-69.

MORRAL-RUÍZ, G., SOLANS, C., GARCÍA, M. L. & GARCÍA-CELMA, M. J. 2012. Formation of pegylated polyurethane and lysine-coated polyurea nanoparticles obtained from O/W nano-emulsions. *Langmuir,* 28**,** 6256-6264.

MOSER, M. & LEO, O. 2010. Key concepts in immunology. *Vaccine,* 28**,** C2-C13.

MROSS, K., NIEMANN, B., MASSING, U., DREVS, J., UNGER, C., BHAMRA, R. & SWENSON, C. 2004. Pharmacokinetics of liposomal doxorubicin (TLC-D99; Myocet) in patients with solid tumors: an open-label, single-dose study. *Cancer Chemotherapy and Pharmacology,* 54**,** 514-524.

NEWMAN, K. D., ELAMANCHILI, P., KWON, G. S. & SAMUEL, J. 2002. Uptake of poly(D,L-lactic-co-glycolic acid) microspheres by antigen-presenting cells in vivo. *Journal of Biomedical Materials Research,* 60**,** 480-486.

NICHOLS, J. W. & DEAMER, D. W. 1976. Catecholamine uptake and concentration by liposomes maintaining pH gradients. *Biochimica et Biophysica Acta (BBA) - Biomembranes,* 455**,** 269-271.

NIELLOUD, F. & MARTI-MESTRES, G. 2000a. Pharmaceutical Emulsions and Suspensions. *Marcel Dekker, Inc., New York, USA,* 105.

NIELLOUD, F. O. & MARTI-MESTRES, G. 2000b. *Pharmaceutical emulsions and suspensions,* New York, Marcel Dekker, Inc.

NIELSEN, U. B., KIRPOTIN, D. B., PICKERING, E. M., HONG, K., PARK, J. W., REFAAT SHALABY, M., SHAO, Y., BENZ, C. C. & MARKS, J. D. 2002. Therapeutic efficacy of anti-ErbB2 immunoliposomes targeted by a phage antibody selected for cellular endocytosis. *Biochimica et Biophysica Acta (BBA) - Molecular Cell Research,* 1591**,** 109-118.

O'BRIEN, S., SCHILLER, G., LISTER, J., DAMON, L., GOLDBERG, S., AULITZKY, W., BEN-YEHUDA, D., STOCK, W., COUTRE, S., DOUER, D., HEFFNER, L. T., LARSON, M., SEITER, K., SMITH, S., ASSOULINE, S., KURIAKOSE, P., MANESS, L., NAGLER, A., ROWE, J., SCHAICH, M., SHPILBERG, O., YEE, K., SCHMIEDER, G., SILVERMAN, J. A., THOMAS, D., DEITCHER, S. R. & KANTARJIAN, H. 2012. High-Dose Vincristine Sulfate Liposome Injection for Advanced, Relapsed, and Refractory Adult Philadelphia Chromosome–Negative Acute Lymphoblastic Leukemia. *JOURNAL OF CLINICAL ONCOLOGY*.

OWENS III, D. E. & PEPPAS, N. A. 2006. Opsonization, biodistribution, and pharmacokinetics of polymeric nanoparticles. *International Journal of Pharmaceutics,* 307**,** 93-102.

PAN, G. L., SHAWER, M., OIE, S. & LU, D. R. 2003. In vitro gene transfection in human glioma cells using a novel and less cytotoxic artificial lipoprotein delivery system. *Pharmaceutical Research,* 20**,** 738-744.

PARK, J. W., HONG, K., KIRPOTIN, D. B., COLBERN, G., SHALABY, R., BASELGA, J., SHAO, Y., NIELSEN, U. B., MARKS, J. D., MOORE, D., PAPAHADJOPOULOS, D. & BENZ, C. C. 2002. Anti-HER2 Immunoliposomes: Enhanced Efficacy Attributable to Targeted Delivery. *Clinical Cancer Research,* 8**,** 1172-1181.

PATLOLLA, R. R. & VOBALABOINA, V. 2005. Pharmacokinetics and tissue distribution of etoposide delivered in parenteral emulsion. *Journal of Pharmaceutical Sciences,* 94**,** 437-445.

PEER, D., KARP, J. M., HONG, S., FAROKHZAD, O. C., MARGALIT, R. & LANGER, R. 2007. Nanocarriers as an emerging platform for cancer therapy. *Nat. Nanotechnol.,* 2**,** 751-760.

PENATE MEDINA, O., HAIKOLA, M., TAHTINEN, M., SIMPURA, I., KAUKINEN, S., VALTANEN, H., ZHU, Y., KUOSMANEN, S., CAO, W., REUNANEN, J., NURMINEN, T., SARIS, P. E. J., SMITH-JONES, P., BRADBURY, M., LARSON, S. & KAIREMO , K. 2011. Liposomal Tumor Targeting

in Drug Delivery Utilizing MMP-2- and MMP-9-Binding Ligands. *Journal of Drug Delivery,* 2011.
PETSEV, D. N., DENKOV, N. D. & KRALCHEVSKY, P. A. 1995. Flocculation of Deformable Emulsion Droplets II. Interaction Energy. *Journal of Colloid and Interface Science,* 176**,** 201-201.
PITEK, A. S., O'CONNELL, D., MAHON, E., MONOPOLI, M. P., BALDELLI BOMBELLI, F. & DAWSON, K. A. 2012. Transferrin Coated Nanoparticles: Study of the Bionano Interface in Human Plasma. *PLoS ONE,* 7**,** e40685.
PRADHAN, M. & ROUSSEAU, D. 2012. A one-step process for oil-in-water-in-oil double emulsion formation using a single surfactant. *Journal of Colloid and Interface Science,* 386**,** 398-404.
PUGNALONI, L. A., DICKINSON, E., ETTELAIE, R., MACKIE, A. R. & WILDE, P. J. 2004. Competitive adsorption of proteins and low-molecular-weight surfactants: computer simulation and microscopic imaging. *Advances in Colloid and Interface Science,* 107**,** 27-49.
QIU, L., JING, N. & JIN, Y. 2008. Preparation and in vitro evaluation of liposomal chloroquine diphosphate loaded by a transmembrane pH-gradient method. *International Journal of Pharmaceutics,* 361**,** 56-63.
RAO, J. & MCCLEMENTS, D. J. 2010. Stabilization of phase inversion temperature nanoemulsions by surfactant displacement. *Journal of Agricultural and Food Chemistry,* 58**,** 7059-7066.
REYNOLDS, J. G., GERETTI, E., HENDRIKS, B. S., LEE, H., LEONARD, S. C., KLINZ, S. G., NOBLE, C. O., LÜCKER, P. B., ZANDSTRA, P. W., DRUMMOND, D. C., OLIVIER JR, K. J., NIELSEN, U. B., NIYIKIZA, C., AGRESTA, S. V. & WICKHAM, T. J. 2012. HER2-targeted liposomal doxorubicin displays enhanced anti-tumorigenic effects without associated cardiotoxicity. *Toxicology and Applied Pharmacology,* 262**,** 1-10.
ROBERTS, M. J., BENTLEY, M. D. & HARRIS, J. M. 2002. Chemistry for peptide and protein PEGylation. *Advanced Drug Delivery Reviews,* 54**,** 459-476.
ROBINSON, M. J., SANCHO, D., SLACK, E. C., LEIBUNDGUT-LANDMANN, S. & SOUSA, C. R. E. 2006. Myeloid C-type lectins in innate immunity. *Nat Immunol,* 7**,** 1258-1265.
ROCO, M. C. 2004. Nanoscale Science and Engineering: Unifying and Transforming Tools. *AIChE Journal,* 50**,** 890-897.
ROSENHOLM, J. M., MEINANDER, A., PEUHU, E., NIEMI, R., ERIKSSON, J. E., SAHLGREN, C. & LINDÉN, M. 2008. Targeting of Porous Hybrid Silica Nanoparticles to Cancer Cells. *ACS Nano,* 3**,** 197-206.
ROUIMI, S., SCHORSCH, C., VALENTINI, C. & VASLIN, S. 2005. Foam stability and interfacial properties of milk protein–surfactant systems. *Food Hydrocolloids,* 19**,** 467-478.
SADAUSKAS, E., WALLIN, H., STOLTENBERG, M., VOGEL, U., DOERING, P., LARSEN, A. & DANSCHER, G. 2007. Kupffer cells are central in the removal of nanoparticles from the organism. *Particle and Fibre Toxicology,* 4**,** 10.
SÆTHER, H. V., HOLME, H. K., MAURSTAD, G., SMIDSRØD, O. & STOKKE, B. T. 2008. Polyelectrolyte complex formation using alginate and chitosan. *Carbohydrate Polymers,* 74**,** 813-821.
SAFARI, J. & ZARNEGAR, Z. 2014. Advanced drug delivery systems: Nanotechnology of health design A review. *Journal of Saudi Chemical Society,* 18**,** 85-99.
SAHU, A., KASOJU, N., GOSWAMI, P. & BORA, U. 2011. Encapsulation of Curcumin in Pluronic Block Copolymer Micelles for Drug Delivery Applications. *J Biomater Appl***,** 0885328209357110.
SAJJADI, S. 2006. Nanoemulsion Formation by Phase Inversion Emulsification: On the Nature of Inversion. *Langmuir,* 22**,** 5597-5603.

SALLUSTO, F., CELLA, M., DANIELI, C. & LANZAVECCHIA, A. 1995. Dendritic cells use macropinocytosis and the mannose receptor to concentrate macromolecules in the major histocompatibility complex class II compartment: downregulation by cytokines and bacterial products. *Journal of Experimental Medicine,* 182**,** 389-400.

SANAD, R. A., ABDELMALAK, N. S., ELBAYOOMY, T. S. & BADAWI, A. A. 2010. Formulation of a Novel Oxybenzone-Loaded Nanostructured Lipid Carriers (NLCs). *Aaps Pharmscitech,* 11**,** 1684-1694.

SANCHO, D., JOFFRE, O. P., KELLER, A. M., ROGERS, N. C., MARTINEZ, D., HERNANZ-FALCON, P., ROSEWELL, I. & SOUSA, C. R. E. 2009. Identification of a dendritic cell receptor that couples sensing of necrosis to immunity. *Nature,* 458**,** 899-903.

SAPRA, P., MOASE, E. H., MA, J. & ALLEN, T. M. 2004. Improved Therapeutic Responses in a Xenograft Model of Human B Lymphoma (Namalwa) for Liposomal Vincristine versus Liposomal Doxorubicin Targeted via Anti-CD19 IgG2a or Fab′ Fragments. *Clinical Cancer Research,* 10**,** 1100-1111.

SAVINA, A., PERES, A., CEBRIAN, I., CARMO, N., MOITA, C., HACOHEN, N., MOITA, L. F. & AMIGORENA, S. 2009. The Small GTPase Rac2 Controls Phagosomal Alkalinization and Antigen Crosspresentation Selectively in CD8+ Dendritic Cells. *Immunity,* 30**,** 544-555.

SCHRAMM, L. L. 2006. *Emulsions, Foams, and Suspensions,* Weinheim, Wiley-VCH Verlag GmbH & Co. KGaA.

SCRIPTURE, C. D. & FIGG, W. D. 2006. Drug interactions in cancer therapy. *Nat Rev Cancer,* 6**,** 546-558.

SEGURA, E., DURAND, M. & AMIGORENA, S. 2013. Similar antigen cross-presentation capacity and phagocytic functions in all freshly isolated human lymphoid organ–resident dendritic cells. *The Journal of Experimental Medicine,* 210**,** 1035-1047.

SHAFFER, C. 2005. Nanomedicine transforms drug delivery. *Drug Discovery Today,* 10**,** 1581-1582.

SHARMA, A. & STRAUBINGER, R. M. 1994. Novel taxol formulations: preparation and characterization of taxol-containing liposomes. *Pharmaceutical Research,* 11**,** 889-896.

SHINODA, K. & SAITO, H. 1968. The effect of temperature on the phase equilibria and the types of dispersions of the ternary system composed of water, cyclohexane, and nonionic surfactant. *Journal of Colloid and Interface Science,* 26**,** 70-74.

SHORTMAN, K. & LIU, Y.-J. 2002. Mouse and human dendritic cell subtypes. *Nat Rev Immunol,* 2**,** 151-161.

SILVA, H. D., CERQUEIRA, M. A. & VICENTE, A. A. 2012. Nanoemulsions for Food Applications: Development and Characterization. *Food and Bioprocess Technology,* 5**,** 854-867.

SINGH, S. & AGGARWAL, B. B. 1995. Activation of transcription factor. NF-kappaB is suppressed by curcumin (diferulolylmethane). *Journal of Biological Chemistry,* 270**,** 24995-25000.

SOLANS, C., ESQUENA, J., FORGIARINI, A. M., USÓN, N., MORALES, D., IZQUIERDO, P., AZEMAR, N. & GARCIA-CELMA, M. J. 2003. Nano-emulsions: Formation, properties and applications. *Adsorption and Aggregation of Surfactants in Solution,* 109**,** 525-554.

SOLANS, C., IZQUIERDO, P., NOLLA, J., AZEMAR, N. & GARCIA-CELMA, M. J. 2005. Nano-emulsions. *Current Opinion in Colloid & Interface Science,* 10**,** 102-110.

SOLANS, C. & SOLÉ, I. 2012. Nano-emulsions: Formation by low-energy methods. *Current Opinion in Colloid & Interface Science,* 17**,** 246-254.

STANBERRY, L. R., SIMON, J. K., JOHNSON, C., ROBINSON, P. L., MORRY, J., FLACK, M. R., GRACON, S., MYC, A., HAMOUDA, T. & BAKER JR, J. R. 2012. Safety and immunogenicity of a novel

nanoemulsion mucosal adjuvant W805EC combined with approved seasonal influenza antigens. *Vaccine,* 30**,** 307-316.
STEFANICK, J. F., ASHLEY, J. D. & BILGICER, B. 2013. Enhanced Cellular Uptake of Peptide-Targeted Nanoparticles through Increased Peptide Hydrophilicity and Optimized Ethylene Glycol Peptide-Linker Length. *ACS Nano*.
STEINMAN, R. M. & BANCHEREAU, J. 2007. Taking dendritic cells into medicine. *Nature,* 449**,** 419-426.
STOSSEL, T. P., VAUGHAN, M., MASON, R. J. & HARTWIG, J. 1972. Quantitative studies of phagocytosis by polymorphonuclear leukocytes: use of emulsions to measure the initial rate of phagocytosis. *Journal of Clinical Investigation,* 51**,** 615-&.
STREBHARDT, K. & ULLRICH, A. 2008. Paul Ehrlich's magic bullet concept: 100 years of progress. *Nat Rev Cancer,* 8**,** 473-480.
SWAMI, A., SHI, J., GADDE, S., VOTRUBA, A., KOLISHETTI, N. & FAROKHZAD, O. 2012. Nanoparticles for Targeted and Temporally Controlled Drug Delivery. *In:* SVENSON, S. & PRUD'HOMME, R. K. (eds.) *Multifunctional Nanoparticles for Drug Delivery Applications.* Springer US.
SWENSON, C. E., PERKINS, W. R., ROBERTS, P. & JANOFF, A. S. 2001. Liposome technology and the development of Myocet™ (liposomal doxorubicin citrate). *The Breast,* 10, Supplement 2**,** 1-7.
SZOKA, F. & PAPAHADJOPOULOS, D. 1980. Comparative Properties and Methods of Preparation of Lipid Vesicles (Liposomes). *Annual Review of Biophysics and Bioengineering,* 9**,** 467-508.
TADROS, T., IZQUIERDO, P., ESQUENA, J. & SOLANS, C. 2004. Formation and stability of nano-emulsions. *Advances in Colloid and Interface Science,* 108–109**,** 303-318.
TAMILVANAN, S. 2004. Oil-in-water lipid emulsions: implications for parenteral and ocular delivering systems. *Progress in Lipid Research,* 43**,** 489-533.
TAMILVANAN, S. 2009. Formulation of multifunctional oil-in-water nanosized emulsions for active and passive targeting of drugs to otherwise inaccessible internal organs of the human body. *International Journal of Pharmaceutics,* 381**,** 62-76.
TAYLOR, P. 1998. Ostwald ripening in emulsions. *Advances in Colloid and Interface Science,* 75**,** 107-163.
THOMAS, D. N., JUDD, S. J. & FAWCETT, N. 1999. Flocculation modelling: a review. *Water Research,* 33**,** 1579-1592.
TORCHILIN, V. P. 2001. Structure and design of polymeric surfactant-based drug delivery systems. *Journal of Controlled Release,* 73**,** 137-172.
TORCHILIN, V. P. 2005. Recent advances with liposomes as pharmaceutical carriers. *Nat Rev Drug Discov,* 4**,** 145-160.
TORCHILIN, V. P. 2006. Multifunctional nanocarriers. *Advanced Drug Delivery Reviews,* 58**,** 1532-1555.
TORCHILIN, V. P., TRUBETSKOY, V. S., WHITEMAN, K. R., CALICETI, P., FERRUTI, P. & VERONESE, F. M. 1995. New synthetic amphiphilic polymers for steric protection of liposomes in vivo. *Journal of Pharmaceutical Sciences,* 84**,** 1049-1053.
TRANG, P., WIGGINS, J. F., DAIGE, C. L., CHO, C., OMOTOLA, M., BROWN, D., WEIDHAAS, J. B., BADER, A. G. & SLACK, F. J. 2011. Systemic Delivery of Tumor Suppressor microRNA Mimics Using a Neutral Lipid Emulsion Inhibits Lung Tumors in Mice. *Mol Ther,* 19**,** 1116-1122.

UZIELY, B., JEFFERS, S., ISACSON, R., KUTSCH, K., WEITSAO, D., YEHOSHUA, Z., LIBSON, E., MUGGIA, F. M. & GABIZON, A. 1995. LIPOSOMAL DOXORUBICIN - ANTITUMOR-ACTIVITY AND UNIQUE TOXICITIES DURING 2 COMPLEMENTARY PHASE-I STUDIES. *JOURNAL OF CLINICAL ONCOLOGY,* 13**,** 1777-1785.

VERONESE, F. M. & PASUT, G. 2005. PEGylation, successful approach to drug delivery. *Drug Discovery Today,* 10**,** 1451-1458.

VERWEY, E. J. W. & OVERBEEK, J. T. G. 1948. *Theory of the stability of lyophobic colloids,* Amsterdam, Elsevier

VILLADANGOS, J. A. & SCHNORRER, P. 2007. Intrinsic and cooperative antigen-presenting functions of dendritic-cell subsets in vivo. *Nature Reviews Immunology,* 7**,** 543-555.

VONARBOURG, A., PASSIRANI, C., SAULNIER, P. & BENOIT, J.-P. 2006. Parameters influencing the stealthiness of colloidal drug delivery systems. *Biomaterials,* 27**,** 4356-4373.

VREMEC, D., POOLEY, J., HOCHREIN, H., WU, L. & SHORTMAN, K. 2000. CD4 and CD8 Expression by Dendritic Cell Subtypes in Mouse Thymus and Spleen. *The Journal of Immunology,* 164**,** 2978-2986.

WAGNER, V., DULLAART, A., BOCK, A.-K. & ZWECK, A. 2006. The emerging nanomedicine landscape. *Nat Biotech,* 24**,** 1211-1217.

WALSTRA, P. 2003. *Physical Chemistry of Foods,* New York, Marcel Dekker.

WAN, Y. & ZHAO 2007. On the Controllable Soft-Templating Approach to Mesoporous Silicates. *Chemical Reviews,* 107**,** 2821-2860.

WANG, Y., WANG, Y. Q., XIANG, J. N. & YAO, K. T. 2010. Target-Specific Cellular Uptake of Taxol-Loaded Heparin-PEG-Folate Nanoparticles. *Biomacromolecules,* 11**,** 3531-3538.

WANG, Z., YU, Y., DAI, W., LU, J., CUI, J., WU, H., YUAN, L., ZHANG, H., WANG, X., WANG, J., ZHANG, X. & ZHANG, Q. 2012. The use of a tumor metastasis targeting peptide to deliver doxorubicin-containing liposomes to highly metastatic cancer. *Biomaterials,* 33**,** 8451-8460.

WASHINGTON, C., ATHERSUCH, A. & KYNOCH, D. J. 1990. The electrokinetic properties of phospholipids-stabilized fat emulsions. IV. The effect of glucose and pH. *International Journal of Pharmaceutics,* 64**,** 217-222.

WASHINGTON, C., CHAWLA, A., CHRISTY, N. & DAVIS, S. S. 1989. The electrokinetic properties of phospholipid-stabilized fat emulsions. *International Journal of Pharmaceutics,* 54**,** 191-197.

WASSERMAN, V., KIZELSZTEIN, P., GARBUZENKO, O., KOHEN, R., OVADIA, H., TABAKMAN, R. & BARENHOLZ, Y. 2007. The antioxidant tempamine: in vitro antitumor and neuroprotective effects and optimization of liposomal encapsulation and release. *Langmuir : the ACS journal of surfaces and colloids,* 23**,** 1937-1947.

WERNER, M. E., COPP, J. A., KARVE, S., CUMMINGS, N. D., SUKUMAR, R., LI, C., NAPIER, M. E., CHEN, R. C., COX, A. D. & WANG, A. Z. 2011a. Folate-Targeted Polymeric Nanoparticle Formulation of Docetaxel Is an Effective Molecularly Targeted Radiosensitizer with Efficacy Dependent on the Timing of Radiotherapy. *ACS Nano,* 5**,** 8990-8998.

WERNER, M. E., KARVE, S., SUKUMAR, R., CUMMINGS, N. D., COPP, J. A., CHEN, R. C., ZHANG, T. & WANG, A. Z. 2011b. Folate-targeted nanoparticle delivery of chemo- and radiotherapeutics for the treatment of ovarian cancer peritoneal metastasis. *Biomaterials,* 32**,** 8548-8554.

WILDE, P., MACKIE, A., HUSBAND, F., GUNNING, P. & MORRIS, V. 2004. Proteins and emulsifiers at liquid interfaces. *Advances in Colloid and Interface Science,* 108–109**,** 63-71.

WILEY, D. T., WEBSTER, P., GALE, A. & DAVIS, M. E. 2013. Transcytosis and brain uptake of transferrin-containing nanoparticles by tuning avidity to transferrin receptor. *Proceedings of the National Academy of Sciences,* 110**,** 8662-8667.
WONG, H. L., BENDAYAN, R., RAUTH, A. M., XUE, H. Y., BABAKHANIAN, K. & WU, X. Y. 2006. A Mechanistic Study of Enhanced Doxorubicin Uptake and Retention in Multidrug Resistant Breast Cancer Cells Using a Polymer-Lipid Hybrid Nanoparticle System. *Journal of Pharmacology and Experimental Therapeutics,* 317**,** 1372-1381.
WOODLE, M. C. & PAPAHADJOPOULOS, D. 1989. Liposome preparation and size characterization. *Methods in enzymology,* 171**,** 193-217.
WRIGHT, O., YOSHIMI, T. & TUNNACLIFFE, A. 2012. Recombinant production of cathelicidin-derived antimicrobial peptides in Escherichia coli using an inducible autocleaving enzyme tag. *New Biotechnology,* 29**,** 352-358.
XIA, T., KOVOCHICH, M., LIONG, M., MENG, H., KABEHIE, S., GEORGE, S., ZINK, J. I. & NEL, A. E. 2009. Polyethyleneimine Coating Enhances the Cellular Uptake of Mesoporous Silica Nanoparticles and Allows Safe Delivery of siRNA and DNA Constructs. *ACS Nano,* 3**,** 3273-3286.
XIAO, G. & GAN, L.-S. 2013. Receptor-Mediated Endocytosis and Brain Delivery of Therapeutic Biologics. *International Journal of Cell Biology,* 2013**,** 14.
XIONG, X., LIU, H., ZHAO, Z., ALTMAN, M. B., LOPEZ-COLON, D., YANG, C. J., CHANG, L.-J., LIU, C. & TAN, W. 2013. DNA Aptamer-Mediated Cell Targeting. *Angewandte Chemie International Edition,* 52**,** 1472-1476.
YAMADA, A., TANIGUCHI, Y., KAWANO, K., HONDA, T., HATTORI, Y. & MAITANI, Y. 2008. Design of Folate-Linked Liposomal Doxorubicin to its Antitumor Effect in Mice. *Clinical Cancer Research,* 14**,** 8161-8168.
YANG, Y., MARSHALL-BRETON, C., LESER, M. E., SHER, A. A. & MCCLEMENTS, D. J. 2012. Fabrication of ultrafine edible emulsions: Comparison of high-energy and low-energy homogenization methods. *Food Hydrocolloids,* 29**,** 398-406.
YEKOLLU, S. K., THOMAS, R. & O'SULLIVAN, B. 2011. Targeting Curcusomes to Inflammatory Dendritic Cells Inhibits NF-κB and Improves Insulin Resistance in Obese Mice. *Diabetes,* 60**,** 2928-2938.
YING, J. Y., MEHNERT, C. P. & WONG, M. S. 1999. Synthese und Anwendungen von mit supramolekularen Templaten hergestellten mesoporösen Materialien. *Angewandte Chemie,* 111**,** 58-82.
YU, C., HU, Y., DUAN, J., YUAN, W., WANG, C., XU, H. & YANG, X.-D. 2011. Novel Aptamer-Nanoparticle Bioconjugates Enhances Delivery of Anticancer Drug to MUC1-Positive Cancer Cells <italic>In Vitro</italic>. *PLoS ONE,* 6**,** e24077.
ZAMBONI, W. C. 2005. Liposomal, Nanoparticle, and Conjugated Formulations of Anticancer Agents. *Clinical Cancer Research,* 11**,** 8230-8234.
ZENG, B. J., CHUAN, Y. P., O'SULLIVAN, B., CAMINSCHI, I., LAHOUD, M. H., THOMAS, R. & MIDDELBERG, A. P. J. 2013. Receptor-Specific Delivery of Protein Antigen to Dendritic Cells by a Nanoemulsion Formed Using Top-Down Non-Covalent Click Self-Assembly. *Small,* 9**,** 3736-3742.

Chapter 3 Design, synthesis and characterization of a stealth nanocarrier emulsion using DAMP4 as an anchor

3.1. Introduction

The *in vivo* behavior of nanocarriers is dictated by their physical parameters such as size, surface charge and hydrophilicity (Laurent *et al.*, 2009, Mornet *et al.*, 2004) and any biological function encoded, for example, by antibodies on the nanocarrier surface. When nanocarriers enter the bloodstream, they encounter a complex environment filled with plasma proteins and immune cells. Based on their physiochemical nature, these nanocarriers in the blood stream will be captured by the mononuclear phagocyte system (MPS) and directed to clearance organs including the liver and spleen at various clearance rates. The capturing of nanocarriers by the MPS is known to be initiated by the electrostatic adsorption of plasma protein (opsonin) onto the surface of nanocarriers (Vonarbourg *et al*., 2006). For a nanocarrier to escape MPS capture, that is to be a "stealth" nanocarrier, opsonin adsorption on the nanocarrier surface needs to be minimized (Dobrovolskaia *et al*., 2008). Thus nanocarriers with neutral zeta-potential or zeta-potential close to zero are expected to have a lower opsonization rate. Stealth nanocarriers are expected to circulate within the bloodstream for a longer time and accumulate in the desired biological site by the EPR effect (reviewed in **Section 2.7**). To aid this, the hydrodynamic diameter (D_H) of nanocarriers is optimally between 100 to 200 nm (reviewed in **Section 2.6**).

Modifying the surface of nanocarriers with a hydrophilic polymer is another effective way to increase "stealthiness". PEG is a non-toxic, non-immunogenic, hydrophilic and highly elastic polymer approved by the FDA for pharmaceutical use. PEG is an attractive polymer for reducing opsonization due to its uncharged and hydrophilic nature (Harris and Chess, 2003, Harris *et al*., 2001). It has been shown that the presence of PEG chains on the nanocarrier surface increases both the colloidal stability in physiological conditions (Hervé *et al*., 2008) and the *in vivo* blood half-life (Krystek *et al.*, 2011). The stealthiness of a PEGylated nanocarrier can also be affected by parameters such as the polymer molecular weight, as well as its density and conformation on the nanocarrier surface (Gref *et al*., 2000, Peracchia *et al*., 1997). Therefore it is important to understand hematocompatibility during initial biological evaluation for newly designed injectable nanocarriers.

As stated in **Chapter 1**, the goal of this research is to develop an efficient emulsion nanocarrier with immune evading and target-specific characteristics for cellular delivery. Here we decouple the biological and physical design criteria through a novel emulsion nano-engineering approach. This chapter aims to address **Objective 1** stated in **Section 1.4**, which is devoted to PEG modified TNE development as the base platform having enhanced immune-evading ability. Under our first hypothesis (see **Chapter 1**), conjugation of a functional molecule to DAMP4 and addition of the conjugate to a pre-formed emulsion should functionalize the AM1-coated oil-water interface with this molecule. **Figure 3-1** shows this idea schematically. PEG (white) chemically conjugated to DAMP4 (dark blue) is introduced to a solution containing pre-formed TNE oil core (light yellow) stabilized by AM1 (red), in aqueous buffer (light blue background). The chemical similarity of DAMP4 and AM1 allows non-covalent interfacial coupling and hence integration of DAMP4 to the interface, with hydrophilic PEG projecting from its DAMP4 interfacial anchor into the aqueous phase surrounding the emulsion surface.

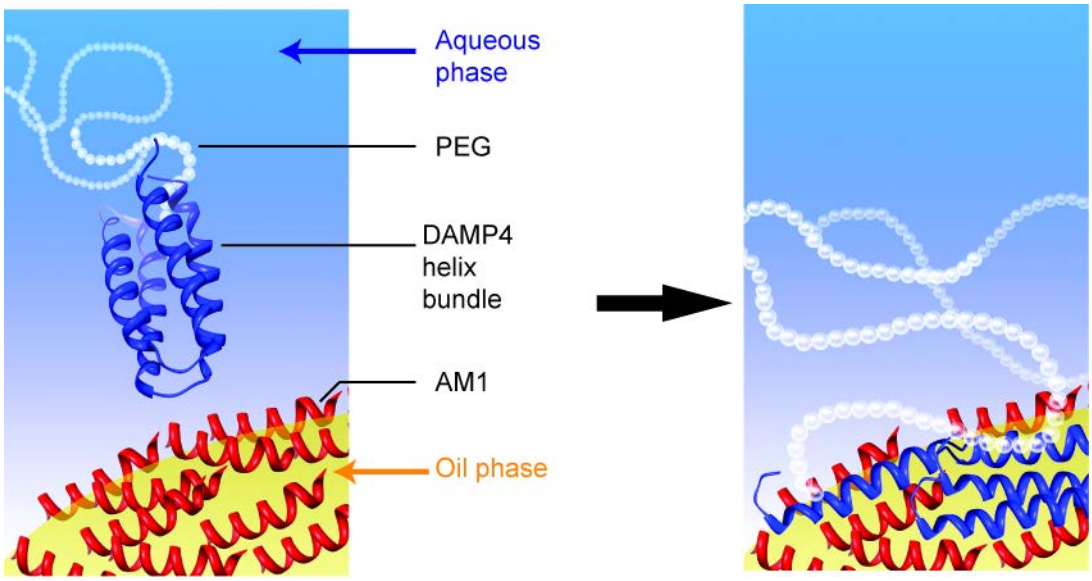

Figure 3-1. Decoration of the nanoemulsion oil-water interface with PEG by simple addition of PEGylated biosurfactant protein DAMP4 to an oil droplet previously formed in the presence of peptide surfactant AM1. Schematic representation of PEG (white) chemically conjugated to DAMP4 protein (dark blue) being introduced to a solution containing pre-formed nanoemulsion oil core (light yellow) stabilized by AM1 peptide (red), in aqueous buffer (light blue background). DAMP4 protein, which is chemically similar to AM1 peptide, is able to integrate into the oil-water interface formed between the core and the aqueous bulk. Prior conjugation of PEG to DAMP4 leads to its functional

display at the interface through non-covalent molecular self-assembly. Figure reproduced from Zeng *et al,* 2013 (Zeng *et al.*, 2013).

With reference to **Figure 3-1**, the addition of PEG to the interface will create a sheath at the interface which is expected to very significantly change the mechanical properties of the interface. By conducting a sudden contraction of the interface, we would expect the response to be quite different in the presence or absence of interfacially-anchored PEG. Thereafter, the effects of an anchored PEG coating on the *in vitro* hematocompatibility was assessed by comparison of TNE modified with various concentration of PEG. We showed that the conjugation of DAMP4 to PEG resulted in functional display of the molecule at the interface separating the oil droplet from the aqueous bulk.

3.2. Materials and methods

3.2.1. Materials

AM1 (molar mass 2473 Da, 95 % purity) was custom synthesized by Genscript (Piscataway, NJ, USA) as reported previously (Dexter *et al.*, 2006). Peptide concentration was determined by quantitative amino-acid analysis (Australian Proteome Analysis Facility, Sydney, NSW, Australia). Miglyol® 812 was purchased from AXO Industry SA (Wavre, Belgium). 1,1′-dioctadecyl-3,3,3′3′-tetramethylindocarbocyanine perchlorate (DiI), Phalloidin-AlexaFluor® 647, Hoechst 33342, CellTrace™ Violet and AlexaFluor® 700-anti-CD20 were purchased from Molecular Probes (Victoria, Australia). 4-(2-hydroxyethyl)-1-piperazineethanesulfonic acid (HEPES) and zinc chloride ($ZnCl_2$) were purchased from Sigma-Aldrich (St Louis, MO, USA) and were reagent grade. mPEG-NHS (MW 5000, PDI <1.08, purity >95 %) was purchased from Nanocs (Boston, MA, USA). RPMI-1640 and foetal calf serum (FCS) were purchased from GIBCO (Victoria, Australia). Anti-CD8-eFluor780 was purchased from eBioscience (San Diego, CA, USA). APC-ani-HLA-DR, FITC-anti-CD3, PerCP5.5-anti-CD14, PE/Cy7-anti-I-A/I-E, PerCP5.5-anti-CD8, Pacific Blue-anti-CD19 and PE/Cy7-anti-CD11c were purchased from Biolegend (San Diego, CA, USA).

3.2.2. DAMP4 expression

Protein surfactant DAMP4 sequence was cloned into pET48b vector and expressed in *E. coli* with high expression level and good solubility (conducted in Protein Expression Facility, The University of Queensland, Australia). Briefly, DAMP4 was expressed as a soluble protein in *E. coli* BL21 (DE3). Glycerol stock of the transformed cells was streaked onto an LB plate (15 g L^{-1} agar, 10 g L^{-1} peptone, 5 g L^{-1} yeast extract, 10 g L^{-1} NaCl) containing kanamycin sulphate (50 mg L^{-1}). A single colony from the plate was inoculated into 10mL LB media (10 g L^{-1} peptone, 5 g L^{-1} yeast extract, 10 g L^{-1} NaCl) and incubated for 16 h at 37 ºC as a seed culture. 400 µL of seed culture was inoculated into 400 mL LB media containing 50 mg L^{-1} of kanamycin and incubated at 37 ºC in an orbital shaker (BioLine, Alexandria, Australia) at 180 rpm. When the OD_{600} reached 0.5, cultures were induced with 1 mM Isopropyl β-D-1-thiogalactopyranoside (IPTG) (AMRESCO®, Solon, US) and incubated for another 5 h at 37 ºC. The cell pellet was collected by centrifugation for 15 min at 2000 g at 4 ºC (Beckman Coulter-Avanti® J-20 XPI) and stored at -80 ºC until further use.

3.2.3. DAMP4 purification

The purification of DAMP4 involved sequential chromatographic methods, specifically immobilized metal affinity chromatography (IMAC), ion exchange (IEX) and then reversed-phase HPLC (RP-HPLC) polishing. In brief, cell pellets were re-suspended in lysis buffer (50 mM NaCl, 25 mM Na_2PO_4, 2 mM $MgCl_2$, 0.5 % v/v Triton X-100, pH 7.5) and disrupted by ultrasonication (4 cycles of 45 s each; Branson Ultrasonics Corporation, Connecticut, USA). Homogenate was centrifuged at 8000 xg (Avanti® J-26 XPI, Beckman Coulter) at 4 ºC for 30 min and the supernatant was filtered through a Millex® 0.45 µm syringe filte unit (Millipore, Vic, Australia). Clarified cell lysate was loaded onto to a Ni^{2+} charged 5 mL HisTrap FF IMAC column (GE Healthcare Life Sciences, NSW, Australia) using an ÄKTAexplorer™ 10 chromatography system (GE Healthcare Biosciences) pre-equilibrated with five column volumes (CV) of Buffer A (50 mM NaCl, 25 mM NaH_2PO_4, pH 7.5). Unbound sample was washed out by 4 CV of Buffer A. Pre-elution was performed with 3.8 CV at 6 % (v/v) Buffer B (50 mM NaCl, 25 mM NaH_2PO_4, 500 mM imidazole, pH 7.5) and DAMP4 was eluted from the column with 80 % (v/v) Buffer B for 8 CV. Elution fractions were pooled and further purified on a HiTrap QFF 1mL column (GE Healthcare Life Sciences, NSW, Australia) coupled with a HiTrap SP FF 1 mL column (GE Healthcare Life Sciences, NSW, Australia). Only flow-through fractions were collected from this step. DAMP4 collected from IEX was further purified on semi-preparative RP-HPLC using a Jupiter

C5 10 μm 300 Å 250 mm × 10 mm column (Phenomenex, NSW, Australia). The solvent system comprised 99.9 % ultrapure water and 0.1 % (v/v) TFA as Buffer A and 90 % acetonitrile, 0.1 % (v/v) TFA as Buffer B. DAMP4-containing fractions were lyophilized and stored at -80 ºC until PEGylation. Quantification of DAMP4 was performed on RP-HPLC using a standard curve established in our lab previously.

3.2.4. DAMP4 PEGylation

Methyoxyl N-hydroxylsuccinamide (NHS) functionalized polyethylene glycol (mPEG-NHS) (average MW 5000, PDI <1.08, purity >95 %) was purchased from Nanocs (New York, USA). Lyophilized DAMP4 was dissolved in 25 mM HEPES, pH 7.0 and a known amount of mPEG-NHS (molar ratio of mPEG : DAMP4 = 20 : 1) was added to the solution, and the conjugation reaction was performed for 12 h at 4°C. The reaction product, which contained PEGylated DAMP4 (PEG-DAMP4), unmodified DAMP4 and free PEG, was analyzed by SDS-PAGE using Novex® 10 % SDS-PAGE tricine gel (Life technologies, Vic, Australia).

3.2.5. Sudden inverted oil drop contraction experiment

A drop shape tensiometer (DSA-10, KRÜSS GmbH, Hamburg, Germany) was used to record images. An 8 mL quartz cuvette (Hellma GmbH, Mülheim, Germany) was filled with AM1 peptide (final concentration 5 μM) and zinc chloride (100 μM) in HEPES (25 mM, pH 7.0). An inverted needle fitted to a gas-tight glass syringe (SGE Analytical Science Pty Ltd, Ringwood, Australia) was submerged into the cuvette and Miglyol® 812 as injected to form a droplet. Miglyol® 812 droplets were first aged for 10 min before PEGylated DAMP4 (10 μM) or an equivalent volume of HEPES buffer (25 mM, pH 7.0) was added. Droplets were then aged for another 30 min before a sudden reduction in droplet volume was performed by withdrawing Miglyol® 812 back into the syringe.

3.2.6. TNE preparation

To prepare TNE core, lyophilized AM1 (final concentration 400 μM) was dissolved in 980 μL HEPES (25 mM, pH 7.0) containing $ZnCl_2$ (800 μM). Twenty microliters of Miglyol® 812 was added to give an oil volume fraction of 2 % (v/v). The mixture was homogenized using a Branson Sonifier 450

ultrasonicator for four 45 s bursts at 60 W. To prepare P_{20}-TNE, TNE (500 µL) was added to PEGylated DAMP4 solution (500 µL, 40 µM) followed by 60 s of vigorous stirring using a magnetic stirrer. To prepare P_{200}-P_{20}-TNE, P_{20}-TNE (500 µL) was added to PEGylated DAMP4 solution (500 µL, 400 µM) followed by 60 seconds of vigorous stirring using a magnetic stirrer.

3.2.7. Particle size and zeta potential analysis

TNE was diluted 100-fold into water or phosphate buffered saline (PBS, 137 mM NaCl, 2.7 mM KCl, 10 mM Na_2HPO_4, 2 mM KH_2PO_4, pH 7.4) prior to analysis to avoid multiple scattering effects. Particle size and zeta potential measurements were performed using a Malvern Zetasizer Nano ZS (Malvern, Worcestershire, UK) equipped with a He-Ne laser (633 nm). Data analysis was with DTS software (Malvern, version 4.2), using a non-negatively constrained least squares (NNLS) fitting algorithm. Dispersant refractive index and viscosity of the dispersant were assumed to be 1.45 and 1.02 cP, respectively.

3.2.8. Analysis of in vitro *cell uptake*

RAW264.7 mouse macrophage cells were cultured in RPMI-1640 medium supplemented with FCS (5 %, v/v). One day before the uptake experiment, cells (2.5×10^5 cells per well) were seeded into a 24-well flat bottom tissue culture plate (Greiner Bio-One, Frickenhausen, Germany) with 12-mm diameter glass slips and incubated at 37°C with 5 % (v/v) CO_2 supplied. The following day, DiI labelled BSA-TNE (25 µL) or P_{20}-TNE (25 µL) or P_{200}-P_{20}-TNE (50 µL) was added to the corresponding well and co-cultured with cells for 2 h at 37°C with 5 % (v/v) CO_2 supplied. Cells were fixed with 4 % (v/v) paraformaldehyde. Cell nuclei were stained with Hoechst 33342 and cell membrane was stained with Phalloidin-AlexaFluor® 647. Mounted glass slips were imaged on an Apotome microscope (Carl-Ziess, Sydney, Australia). For *in vitro* uptake in human peripheral blood mononuclear cells (PBMC, collected from health donors with approval from the Human Research Ethics Committee of the Princess Alexandra Hospital), cells (5×10^5 cells per well) were seeded into a 24-well flat bottom tissue culture plate in 1 mL of RPMI-1640 medium supplemented with FCS (5 %, v/v). DiI labelled BSA-TNE (25 µL) or P_{20}-TNE (25 µL) or P_{200}-P_{20}-TNE (50 µL) was added to the corresponding wells and co-cultured with cells for 3 h at 37°C with 5 % (v/v) CO_2 supplied. After washing with PBS, cells were stained with APC-anti-HLA-DR and PE/Cy7-anti-CD11c (DCs), FITC-anti-CD3 (T cells), PerCP5.5-anti-

CD14 (monocytes) and Pacific Blue-anti-CD20 (B cells). Cell uptake was analyzed on a Beckman Coulter Gallios™ Flow Cytometer.

3.3. Results and discussion

3.3.1. DAMP4 PEGylation

A variety of chemistries can be used for the covalent attachment of PEG to proteins and peptides (Veronese and Pasut, 2005, Roberts *et al.*, 2002). The most common method is to conjugate PEG to the primary amino group of lysine using PEG modified with an active NHS ester. SDS-PAGE is a widely used method for PEG-protein characterization (Sun *et al.*, 2003, Moosmann *et al.*, 2009, Colonna *et al.*, 2008). Theoretically there are five NHS-reactive sites in the DAMP4 sequence (4 lysine residues plus 1 N-terminus group per DAMP4 molecule). As shown in **Figure 3-2**, the additional band at size 17 kDa suggests that the majority of DAMP4 had been conjugated with PEG. However, the molecular mass of the PEGylated DAMP4 could not be determined due to the band broadening and, for most cases, the electrophoretic mobility of PEGylated proteins is not strictly related to their molecular weight (Kurfürst, 1992).

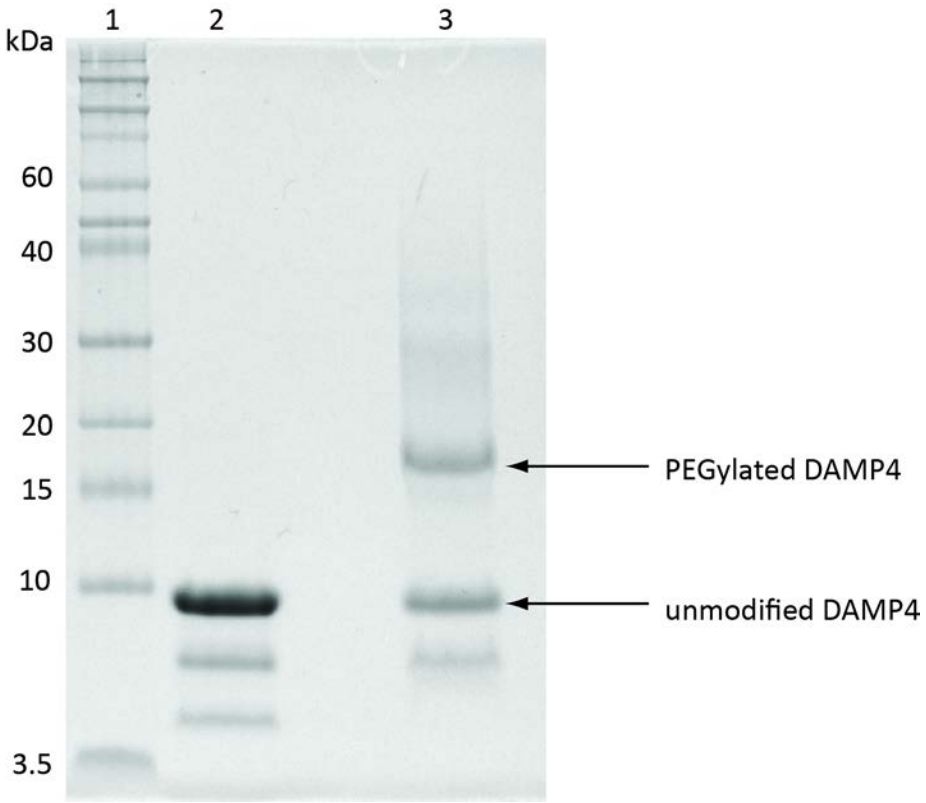

Figure 3-2. Photographic representation of an SDS-PAGE gel showing samples from a PEGylation reaction of DAMP4. Lane 1: Novex® Sharp Pre-stained Protein Standard (Novex®, Mulgrave, Australia); Lane 2: Lyophilized DAMP4 re-dissolved in HEPES (25 mM, pH 7.0); Lane 3: DAMP4 PEGylation reaction mixture.

3.3.2. DAMP4 carries its conjugated PEG onto an AM1 pre-adsorbed oil-water interface

An inverted oil drop within an aqueous buffer solution comprising AM1 was formed and allowed to form a cohesive interfacial network at the oil-water interface. PEGylated DAMP4 was then added to the buffer and aged for 30 min. When a sudden contraction of the oil drop interface was imposed, the oil-water-PEG interface wrinkled as the oil drop relaxed and the effect persisted for more than 10 min (**Figure 3-3a**). In the absence of PEGylated DAMP4, the oil drop relaxed to a spherical shape in less than 6 s (**Figure 3-3b**). The strikingly distinct interfacial behavior mediated by PEGylated DAMP4 is characteristic of an elastic interface (Malcolm *et al.*, 2009), likely due to the presence of the additional elastic PEG film connected to the oil-water interface by DAMP4, in keeping with our hypotheses.

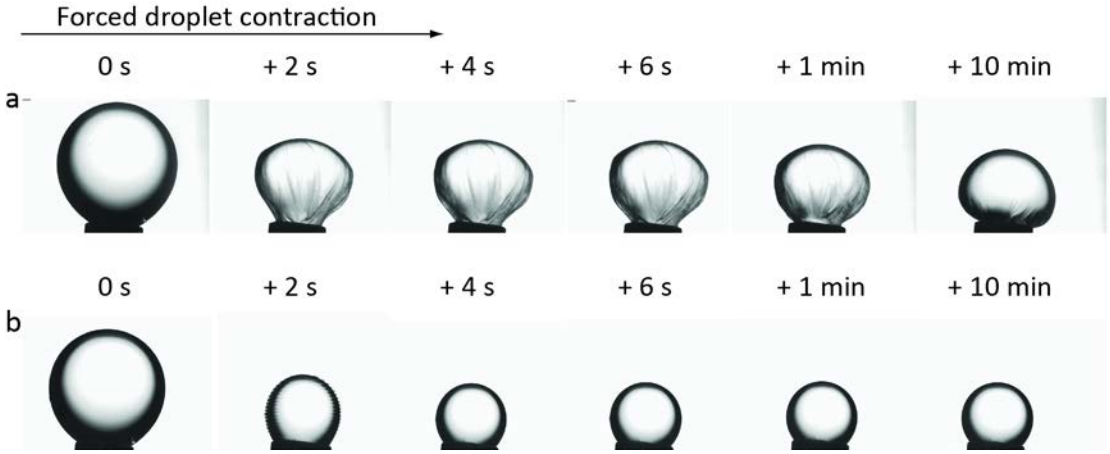

Figure 3-3. Photographs of a 10 min old Miglyol 812 oil drop formed from an inverted needle in peptide AM1 solution, further aged for 30 min following the addition of either (a) PEGylated DAMP4 or (b) HEPES buffer. The oil drops were subjected to a sudden contraction in volume and images were acquired using a drop shape tensiometer.

3.3.3. DAMP4 mediated TNE PEGylation

Nanocarriers for intravenous administration should ideally have colloidal stability within a biological environment. AM1-stablized TNE core forms large flocculates rapidly when diluted in PBS as a result of removal of the electrostatic barrier by the high ionic strength of PBS. These then proceed to quickly coalesce at a rate dependent on the interfacial mechanical properties.(Chuan *et al.*, 2011, Malcolm *et al.*, 2009). On the other hand, the anchoring of the polymer PEG at the interface would create a repulsive steric barrier thus imparting additional stability to the nanoemulsion even under conditions of high ionic strength. If DAMP4 really does integrate its conjugated PEG onto the AM1 stabilized oil-water interface as hypothesized, then the additional PEG layer should prevent the TNE core from flocculation and coalescence. So first we evaluated whether the PEG-modified TNE oil core could stay stable under isotonic conditions. Serial additions of PEGylated TNE were prepared by adding a range of concentrations of PEGylated DAMP4 to a pre-formed 2 % (v/v) AM1 stabilized TNE oil core and the size distribution of the resulting PEGylated TNE in isotonic phosphate buffered solution (PBS) was measured by DLS.

As shown in **Figure 3-4**, AM1-stabilized TNE core modified with PEGylated DAMP4 at a concentration ranging from 20 μM to 560 μM was flocculation-stable in PBS and maintained a Z-average diameter of approximately 180 nm, even at low levels of added PEGylated DAMP4. Only when TNE core was mixed with PEGylated DAMP4 at a concentration lower than 20 μM was a polydispersed size distribution, with large droplets, observed. This result suggested that as little as 20 μM of PEGylated DAMP4 was sufficient to create steric repulsion around the pre-formed AM1 stabilized TNE oil core, preventing them from flocculating and coalescing under high ionic strength conditions.

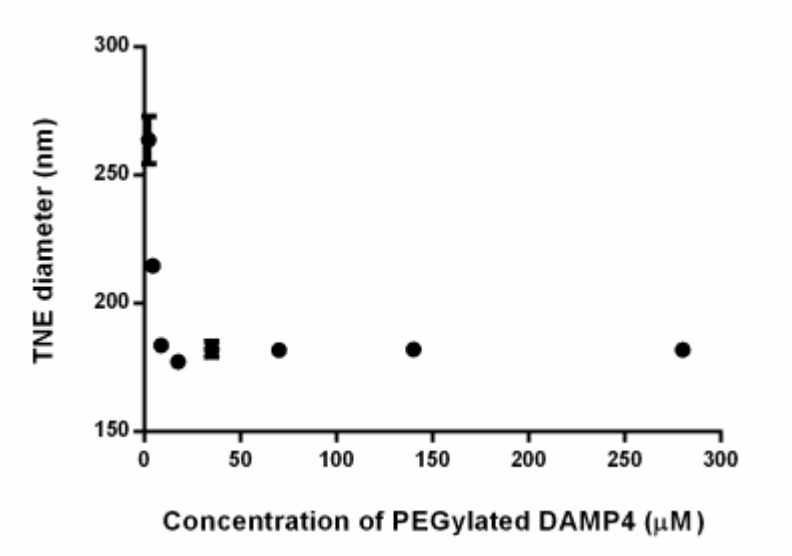

Figure 3-4. The effect of concentration of PEGylated DAMP4 on TNE stability following dilution from water into isotonic buffer. 10 μL of freshly prepared TNE was diluted into 990 μL of PBS for DLS measurements. All measurements were done in triplicates. Data was shown as mean with SD.

3.3.4. PEGylated TNE escapes APC phagocytosis

We further tested the biological function of the TNE oil core modified with PEGylated DAMP4, by assessing whether the expected reduction in phagocytosis due to core PEGylation, indeed occurred. We constructed a PEGylated TNE by adding 20 μM of PEGylated DAMP4 to a pre-formed 2 % (v/v) AM1-stabilized TNE oil core (termed P_{20}-TNE, noting that the formulation comprises an AM1-stabilised core modified by addition of 20 μM PEG to the surrounding bulk aqueous phase). Further addition of 200 μM PEGylated DAMP4 to P_{20}-TNE created a modified TNE which notionally had a higher PEG surface coverage (P_{200}-P_{20}-TNE, i.e. P_{20}-TNE with a further 200 μM of PEG added to the surrounding bulk aqueous phase after prior addition of 20 μM PEG). Size distribution and zeta-potential of the resulting TNE were measured by DLS. As shown in **Table 3-1**, following the addition of 20 μM of PEGylated DAMP4 to the pre-formed AM1 stabilized oil core, the emulsion size was slightly larger, but remained mono-dispersed at 174 ± 2.4 nm. The zeta potential of the emulsion surface decreased to 30.2 ± 0.6 mV as a result of decoration of the PEG polymer shielding the effective positive charge of AM1 stabilized interface. Further addition of PEGylated DAMP4 to P_{20}-TNE (P_{200}-P_{20}-TNE) did not increase the size significantly, but further decreased the Z-potential to 18.9 ± 0.7 mV as a consequence of more PEG being introduced to the oil core surface shielding the positively charged AM1 network.

	Zeta average d.nm	Zeta potential mV
AM1 stabilized oil core	166.7 ± 3.9	39.4 ± 3.1
P_{20} - TNE	174.3 ± 2.4	30.2 ± 0.6
P_{200} - P_{20} - TNE	179.9 ± 2.0	18.9 ± 0.7

Table 3-1 Size distribution and Z-potential of TNE measured. TNE was diluted 1 in 100 in ultra-pure water, size distribution and zeta potential were measured using a Malvern Zetasizer Nano ZS (Malvern, Worcestershire, UK). Data were collected from three experiments and expressed as average with Standard Deviation.

The P_{20}-TNE and P_{200}-P_{20}-TNE were co-cultured with RAW264.7 macrophages for 2 h. The previously-reported BSA-coated TNE (Chuan *et al.*, 2011) was also incubated with the same cell line for comparison. Uptake of TNE was monitored with intensity of the DiI dye used to label the emulsion. Compared with uptake of a BSA-stabilized but non-PEGylated TNE, uptake of P_{20}-TNE appeared to be reduced (**Figure 3-5**), although significant uptake occurred in both cases. Further addition of 200 μM PEGylated DAMP4 to P_{20}-TNE created a modified TNE (P_{200}-P_{20}-TNE) which notionally had a higher PEG surface coverage. *In vitro* testing confirmed that P_{200}-P_{20}-TNE exhibited reduced uptake by macrophages compared to P_{20}-TNE (**Figure 3-5**), providing evidence that the core TNE is amenable to successive PEGylation via simple, top-down sequential addition of PEGylated DAMP4.

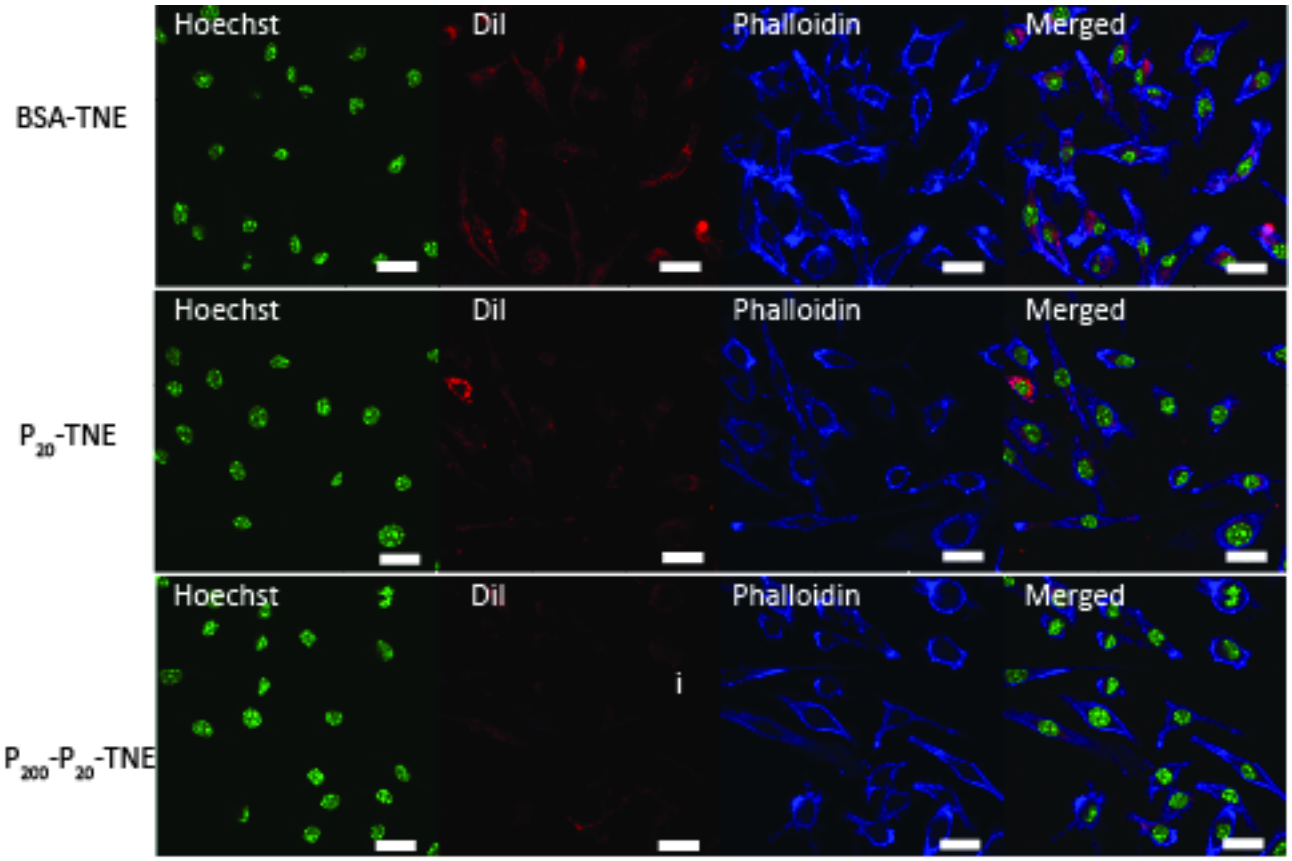

Figure 3-5 Confocal images showing uptake of BSA-TNE (a negative control reported previously, lacking PEG), P_{20}-TNE (an interface coated with a low amount of PEG) and P_{200}-P_{20}-TNE (nanoemulsion with a higher level of PEG interfacial coverage) by murine macrophage cell line (RAW264.7) after 2 h incubation and then washing to remove unbound TNE. Nanoemulsions were labeled with fluorescent dye DiI (red). Cell nuclei were stained with Hoechst 33342 (green) and cell membrane was stained with Alexa Fluor® 647 conjugated phalloidin (blue). Scale bar 20 µm;

We then sought to evaluate the PEGylated TNE in a more complex system. To mimic injection of PEGylated TNE into the bloodstream, clearance by immune cells was investigated *in vitro* by co-culturing the same set of TNEs with human peripheral blood mononuclear cells (hPBMC), predominantly comprising T and B cells, monocytes and dendritic cells (DCs). **Figure 3-6** shows that uptake of P_{200}-P_{20}-TNE was consistently lower than that of the simple and previously-reported BSA-TNE across all of these cell types, with 40 % and 20 % reduction in internalization by monocytes and HLA-DR^{hi} $CD11c^{+}$ DCs, respectively. This result shows that the nanoemulsion, when appropriately covered with self-assembled PEG, is able to avoid non-specific cell uptake.

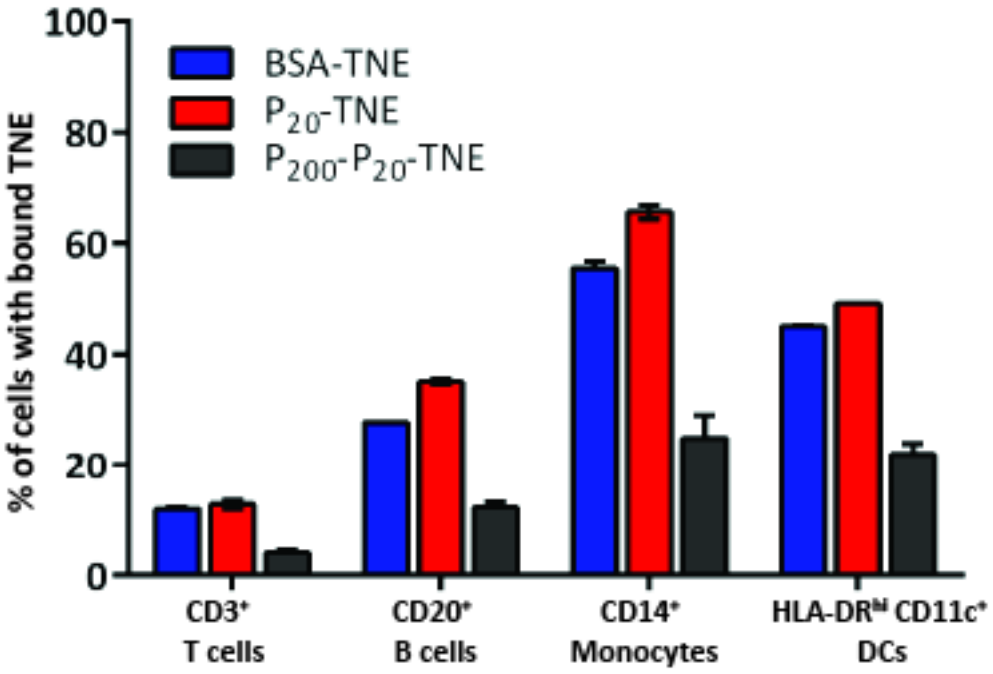

Figure 3-6. Uptake of BSA-TNE, P_{20}-TNE and P_{200}-P_{20}-TNE by cell sub-populations within human peripheral blood mononuclear cells (PBMC). Gating strategy: T cells: $CD3^+$ CD20; B cells: $CD20^+$ CD3; monocytes: $CD14^+$, DCs: HLA-$DR^{hi}CD11c^+$. Percentage of cells with bound TNE (DiI positive cells) was calculated using baseline set against FMO. Results are expressed as mean with standard deviation (for N=2), and demonstrate a clear down-regulation of non-specific binding for PEGylated nanoemulsion versus BSA-TNE.

3.4. Conclusions

The goal of this Chapter was to address **Objective 1** stated in **Section 1.4**, by using DAMP4 as anchor for TNE PEGylation based on the hypothesis stated in **Section 1.3**, which comprises three steps that are closely associated with each other: 1) DAMP4 four-helical bundle pre-conjugated to PEG unfolds in the sub-interfacial region; 2) The unfolded DAMP4 integrates into the AM1 pre-occupied interface and anchors its conjugated PEG molecule there, and 3) functionally displays PEG on the surface of TNE oil core. By conducting a sudden inverted oil drop contraction experiment, we demonstrated that the addition of PEGylated DAMP4 to an oil-in-water interface pre-adsorbed with AM1 created an elastic

PEG film connected to the interface, consistent with the first part of our hypothesis that the DAMP4 bundle unfolds and integrates into the AM1-coated interface.

In its unmodified form, the AM1 stabilized TNE core was not stable against flocculation in isotonic buffer as the positively-charged AM1 network will be neutralized eventually leading to emulsion destabilization through flocculation and coalescence under physiological levels of salt. We developed a simple sequential reagent addition approach for preparing PEGylated TNE that enables the non-covalent attachment of PEG to the surface of the AM1-stabilized TNE core. We prepared a range of PEGylated TNEs formulated with a range of concentrations of PEG-DAMP4 conjugate. The addition of PEG-DAMP4 conjugate into the TNE system led to the formation of PEGylated TNE. PEGylation imparts steric stability to the TNE oil core in isotonic conditions, as can be seen from the consistent size distribution when PEGylated TNE was exposed in isotonic PBS (**Table 3-1),** suggesting such formulation would be suitable for intravenous injection and intracellular delivery. Another consequence of PEGylation is partial charge screening. Unmodified TNE is positively charge due to the presence of positively charge amino acid residues R, H and K within the AM1 sequence (AM1 is reviewed in **Section 2.4.2**), as well as the presence of zinc ions in the interfacial network. The magnitude of positive charge reduces with the concentration of PEG-DAMP4 within the system as the non-covalent grafting of PEG-DAMP4 shields the positively charged AM1 network (**Figure 3-4**). This result further supports the second hypothesis, that DAMP4 brings PEG to the AM1 pre-occupied interface as evident by the reduction in PEGylated TNE surface charge.

Armed with this PEGylated TNE, we proceeded to test the immune evading ability *in vitro*. The PEGylated TNE, P_{200}-P_{20}-TNE, showed reduced non-specific cell-association compared to its non-PEGylated (BSA-TNE) or TNE with lower PEG content (P_{20}-TNE) counterparts (**Figure 3-5, 3-6**). Others have already demonstrated that the rapid MPS clearance of nanocarriers can be significantly reduced by modifying their surface with a hydrophilic polymer such as PEG (topic reviewed in **Section 2.7.1**). The presence of PEG on the TNE surface can protect a TNE from capture by macrophages (Gaur *et al.*, 2000, Ozcan *et al.*, 2010). Such a reduction in MPS clearance of the PEGylated nanocarrier is mainly due to reduced interactions between the nanocarrier and the protein opsonin within the blood stream. Consistent with literature, the presented results in this Chapter confirm that the cell-association of TNE is dependent on the PEG content within the TNE system, further proving the

third part of our hypotheis, that PEG was functionally displayed on the TNE oil/water interface by DAMP4.

Results from this experimental chapter confirm the hypothesis that the integration of DAMP4 into the AM1 stabilized oil droplet surface would lead to the functional display of conjugated PEG at the interface of the TNE oil core. This was evidenced by the elastic properties of the film during inverted oil drop contraction. When appropriately covered with self-assembled PEG using DAMP4 as an anchor, nanoemulsion is able to avoid, almost completely, non-specific cell uptake.

The long term goal of this PhD project was to develop an efficient emulsion nanocarrier for targeting intracellular delivery. However, the PEGylated TNE presented in this chapter does not contain any targeting ligand which is necessary for a nanocarrier to enter cancerous cells (reviewed in **Section 2.7.2**). For nanocarrier to work for intracellular delivery, it must be internalized by the target cells in significant quantities. Hence in the next Chapter (**Chapter 4)**, we further investigated whether the same process can be applied to functionalize a TNE with a receptor-specific homing device (an antibody), to simultaneously increase its target specificity while reducing clearance by immune cells through PEGylation as demonstrated in this Chapter.

CHUAN, Y. P., ZENG, B. Y., O'SULLIVAN, B., THOMAS, R. & MIDDELBERG, A. P. J. 2011. Co-delivery of antigen and a lipophilic anti-inflammatory drug to cells via a tailorable nanocarrier emulsion. *Journal of Colloid and Interface Science,* 368**,** 616-624.

COLONNA, C., CONTI, B., PERUGINI, P., PAVANETTO, F., MODENA, T., DORATI, R., IADAROLA, P. & GENTA, I. 2008. Site-directed PEGylation as successful approach to improve the enzyme replacement in the case of prolidase. *International Journal of Pharmaceutics,* 358**,** 230-237.

DEXTER, A. F., MALCOLM, A. S. & MIDDELBERG, A. P. J. 2006. Reversible active switching of the mechanical properties of a peptide film at a fluid-fluid interface. *Nat Mater,* 5**,** 502-506.

DOBROVOLSKAIA, M. A., AGGARWAL, P., HALL, J. B. & MCNEIL, S. E. 2008. Preclinical studies to understand nanoparticle interaction with the immune system and its potential effects on nanoparticle biodistribution. *Molecular Pharmaceutics,* 5**,** 487-495.

GAUR, U., SAHOO, S. K., DE, T. K., GHOSH, P. C., MAITRA, A. & GHOSH, P. K. 2000. Biodistribution of fluoresceinated dextran using novel nanoparticles evading reticuloendothelial system. *International Journal of Pharmaceutics,* 202**,** 1-10.

GREF, R., LÜCK, M., QUELLEC, P., MARCHAND, M., DELLACHERIE, E., HARNISCH, S., BLUNK, T. & MÜLLER, R. H. 2000. 'Stealth' corona-core nanoparticles surface modified by polyethylene glycol (PEG): influences of the corona (PEG chain length and surface density) and of the core composition on phagocytic uptake and plasma protein adsorption. *Colloids and Surfaces B: Biointerfaces,* 18**,** 301-313.

HARRIS, J. M. & CHESS, R. B. 2003. Effect of pegylation on pharmaceuticals. *Nat Rev Drug Discov,* 2**,** 214-221.

HARRIS, J. M., MARTIN, N. E. & MODI, M. 2001. Pegylation - A novel process for modifying pharmacokinetics. *Clinical Pharmacokinetics,* 40**,** 539-551.

HERVÉ, K., DUBOIS, P., CHOURPA, I., DOUZIECH-EYROLLES, L., MUNNIER, E., COHEN-JONATHAN, S., SOUCÉ, M., MARCHAIS, H., LIMELETTE, P., WARMONT, F. & SABOUNGI, M. L. 2008. The development of stable aqueous suspensions of PEGylated SPIONs for biomedical applications. *Nanotechnology,* 19**,** 465608.

KRYSTEK, P., OOMEN, A. G., RAYAVARAPU, R. G., LEEUWEN, V. T. G., JONG, D. W. H., MANOHAR, S., LANKVELD, D. P. K. & VERHAREN, H. W. 2011. Blood clearance and tissue distribution of PEGylated and non-PEGylated gold nanorods after intravenous administration in rats. *Nanomedicine,* 6**,** 339-349.

KURFÜRST, M. M. 1992. Detection and molecular weight determination of polyethylene glycol-modified hirudin by staining after sodium dodecyl sulfate-polyacrylamide gel electrophoresis. *Analytical Biochemistry,* 200**,** 244-248.

LAURENT, S., BOUTRY, S., MAHIEU, I., VANDER ELST, L. & MULLER, R. N. 2009. Iron Oxide Based MR Contrast Agents: from Chemistry to Cell Labeling. *CURRENT MEDICINAL CHEMISTRY,* 16**,** 4712-4727.

MALCOLM, A. S., DEXTER, A. F., KATAKDHOND, J. A., KARAKASHEV, S. I., NGUYEN, A. V. & MIDDELBERG, A. P. J. 2009. Tuneable Control of Interfacial Rheology and Emulsion Coalescence. *ChemPhysChem,* 10**,** 778-781.

MOOSMANN, A., CHRISTEL, J., BOETTINGER, H. & MUELLER, E. 2009. Analytical and preparative separation of PEGylated lysozyme for the characterization of chromatography media. *Journal of Chromatography A,* 1217**,** 209-215.

MORNET, S., VASSEUR, S., GRASSET, F. & DUGUET, E. 2004. Magnetic nanoparticle design for medical diagnosis and therapy. *Journal of Materials Chemistry,* 14**,** 2161-2175.

OZCAN, I., SEGURA-SÁNCHEZ, F., BOUCHEMAL, K., SEZAK, M., OZER, O., GÜNERI, T. & PONCHEL, G. 2010. Pegylation of poly(γ-benzyl-L-glutamate) nanoparticles is efficient for avoiding mononuclear phagocyte system capture in rats. *International Journal of Nanomedicine*, 5**,** 1103-1111.

PERACCHIA, M. T., VAUTHIER, C., PASSIRANI, C., COUVREUR, P. & LABARRE, D. 1997. Complement consumption by poly(ethylene glycol) in different conformations chemically coupled to poly(isobutyl 2-cyanoacrylate) nanoparticles. *Life Sciences,* 61**,** 749-761.

ROBERTS, M. J., BENTLEY, M. D. & HARRIS, J. M. 2002. Chemistry for peptide and protein PEGylation. *Advanced Drug Delivery Reviews,* 54**,** 459-476.

SUN, X., YANG, Z., LI, S., TAN, Y., ZHANG, N., WANG, X., YAGI, S., YOSHIOKA, T., TAKIMOTO, A., MITSUSHIMA, K., SUGINAKA, A., FRENKEL, E. P. & HOFFMAN, R. M. 2003. In Vivo Efficacy of Recombinant Methioninase Is Enhanced by the Combination of Polyethylene Glycol Conjugation and Pyridoxal 5 鈥?Phosphate Supplementation. *Cancer Research,* 63**,** 8377-8383.

VERONESE, F. M. & PASUT, G. 2005. PEGylation, successful approach to drug delivery. *Drug Discovery Today,* 10**,** 1451-1458.

VONARBOURG, A., PASSIRANI, C., SAULNIER, P. & BENOIT, J.-P. 2006. Parameters influencing the stealthiness of colloidal drug delivery systems. *Biomaterials,* 27**,** 4356-4373.

ZENG, B. J., CHUAN, Y. P., O'SULLIVAN, B., CAMINSCHI, I., LAHOUD, M. H., THOMAS, R. & MIDDELBERG, A. P. J. 2013. Receptor-Specific Delivery of Protein Antigen to Dendritic Cells by a Nanoemulsion Formed Using Top-Down Non-Covalent Click Self-Assembly. *Small*.

Chapter 4 Design, synthesis and characterization of a TNE targeting dendritic cells

4.1. Introduction

In **Chapter 3** we demonstrated that addition of PEG-DAMP4 conjugate to a pre-formed AM1-stabilized TNE core resulted in an elastic layer being coated on the oil core, which creates a steric barrier for stabilizing the TNE under isotonic conditions. The PEGylated TNE, P_{200}-P_{20}-TNE, showed enhanced immune evading characteristics, compared to P_{20}-TNE which had less PEG displayed on the TNE oil core. Reasons for the enhanced stealthiness, which is the ability of a nanocarrier to escape mononuclear phagocyte (MPS) capture, could be due to the possibility that DAMP4 carries its conjugated PEG and co-adsorbs at the AM1-stabilized TNE core interface, which then imparts a repulsive barrier that repels the attachment of opsonins onto the TNE surface. It has been demonstrated that PEGylation can increase the bioavailability and biodistribution of a nanocarrier, hence it is a common strategy for passive targeting (reviewed in **Section 2.7.1**). In Chapter 3, I accomplished **Objective 1** as stated in **Section 1.4**, by demonstrating that DAMP4 could display its conjugated PEG on a TNE surface to achieve a PEGylated TNE having enhanced immune-evading ability.

A novel drug delivery system (DDS) should not only have immune evading ability, but also have superior *in situ* targeting ability for precise intracellular delivery, which is the so called "active targeting" strategy (**reviewed in Section 2.7.2**). Take cancer treatment, for example; current cancer therapy usually involves the application of cytotoxic anti-cancer drugs. Systemic administration of these drugs leads to undesired site-effects; hence they are given to patients at sub-optimal dosages and potentially result in treatment failure (Allen, 2002). Concentrated dosage of these cytotoxic drugs can be given to patients by encapsulation into a nanocarrier, and a passive targeting strategy, *e.g.* PEGylation, can increase the circulation half time of the nanocarrier. Adding a targeting moiety to the long-circulating nanocarrier could further improve its "homing" ability, *i.e.* the ability to discriminate between healthy and malignant cells. Targeting moiety incorporation facilitates intracellular delivery via receptor-mediated endocytosis, whereby their drug payloads can be released to provide a therapeutic action.

Liposome nanocarriers and nanoparticles represent well-studied platforms for cell-specific delivery both *in vitro* and *in vivo* (Ashley et al., 2011, Hu et al., 2011, Kaaki et al., 2011, Kukowska-Latallo et al., 2005, Liu et al., 2010, Mathew et al., 2012, Reddy et al., 2006, Shroff and Kokkoli, 2012, Yoshida et al., 2012). These systems can encode complex functionality, for example immune targeting and immune evasion, but often suffer from a lack of stability, limited cargo capacity, cellular processing through non-functional pathways, or a general loss of intended function simply due to the complexity of the *in vivo* environment (Kim et al., 2009). In the last chapter, I demonstrated that PEGylation of a TNE can be achieved by non-covalent "click" chemistry by using DAMP4 as an anchor and a simple, sequential, reagent addition method. In this chapter, I aim to address **Objectives 2** and **3** stated in **Section 1.4**, to construct a long circulating nanocarrier emulsion that has superior *in situ* targeting ability, by using the non-covalent TNE functionalization procedure I developed and demonstrated in **Chapter 3**. Although active targeting of the nanocarrier by engineering a site-specific moiety on a long-circulating nanocarrier's surface can potentially increase intracellular delivery, exposure of the targeting moieties may counteract the shielding effect of the polymeric coating. Therefore it is vital to maintain a balance between these two categories of functional groups (**Objective 3**). Hence I also investigate the effect of tuning the ratio of PEG to targeting moiety on the *in vitro* target selectivity of the constructed TNE platform.

For the targeting moiety, we choose dendritic cells (DCs) as the model target cell, and an antibody against the highly DC-restricted receptor Clec9A (Caminschi et al., 2008, Huysamen et al., 2008) as the homing device on the nanoemulsion (**Clec9A was reviewed in Section 2.8.2**). In this chapter, we demonstrate that the constructed P_{200}-Ab-P_{20}-TNE specifically targets Clec9A presented on the surface of Chinese hamster ovary (CHO) cells *in vitro*. In addition, we show superior *in situ* targeting with the constructed targeting TNE in comparison with its non-targeted counterparts.

4.2. Materials and methods

4.2.1. Materials

Refer to **Section 3.2.1**.

4.2.2. Preparation of DAMP4 fused with antibody

Preparation of antibody against Clec9A or an isotype antibody fused to DAMP4 was done by . Irina Caminschi in the Walter and Eliza Hall Institute, Melbourne, Australia. Briefly, the cDNA encoding heavy and light chains of (anti-Clec9A clone 24/04-10B4; rat IgG2a isotype control clone GL117) were amplified from the original hybridomas (Caminschi et al., 2008) and cloned by RACE amplification as previously described (Lahoud et al., 2011). The cDNA antibody heavy chains were subcloned into a pcDNA 3.1 vector modified to contain an Ala-Ala-Ala linker fused to DAMP4 cDNA. This construct enabled the generation of a single fusion protein where the C-terminal region of the heavy chain is fused to an alanine linker and then to DAMP4. The antibody light chains were cloned into pcDNA3.1. Plasmid DNA was prepared using the GigaPrep Plasmid DNA extraction kit (Qiagen, Hilden, Germany), and plasmids encoding the kappa chain, and the heavy chain linked to OVA were transiently co-transfected into freestyle 293F cells (Invitrogen) using 293Fectin transfection reagent as per manufacturer's recommendations. Culture supernatant containing the recombinant antibodies was harvested, and antibodies purified by affinity chromatography using Protein G Sepharose. Recombinant antibodies were validated for their ability to bind Clec9A on transfectant cells as previously described (Caminschi et al., 2008). DAMP4 fused to anti-Clec9A mAb was termed as DAMP4-mAb, and DAMP4 fused to isotype mAb was termed as DAMP4-Isotype.

4.2.3. TNE preparation

P_{20}-TNE was prepared following the protocol detailed in **Section 3.2.6**. For preparation of P_{200}-Ab-P_{20}-TNE, mAb-DAMP4 (36 µL, 3 µM) was added to P_{20}-TNE (200 µL) followed by 60 seconds of vigorous stirring using a magnetic stirrer to prepare Ab-P_{20}-TNE; subsequently Ab-P_{20}-TNE (200 µL) was added to PEGylated DAMP4 (200 µL, 400 µM), followed by 60 seconds of vigorous stirring. TNE size was measured by Malvern Zetasizer Nano ZS (Malvern, Worcestershire, UK) equipped with a He-Ne laser (633 nm). Data analysis was with DTS software (Malvern, version 6.2), using a non-negatively constrained least squares (NNLS) fitting algorithm. Dispersant refractive index and viscosity of the dispersant were assumed to be 1.45 and 1.02 cP, respectively. For each sample, 10 runs of 10s were performed.

4.2.4. CHO-Clec9A cells binding test

Chinese hamster ovary (CHO)-Clec9A cell line, which was CHO-K1 cell line transfected with Clec9A, was provided by the Walter and Eliza Hall Institute (WEHI, NSW Australia). Cells were grown in RPMI 1640 medium supplemented with heat inactivated 5 % fetal calf serum. G418 antibiotic (500 µg mL^{-1}) was added to medium to maintain selection pressure. One day before the binding experiment, cells (2.5×10^5 cells per well) were seeded into a 24-well flat bottom tissue culture plate (Greiner Bio-One, Frickenhausen, Germany) with 12-mm diameter glass slips and incubated at 37°C with 5 % CO_2 supplied. The following day, DiI labelled P_{20}-TNE or Ab-P_{20}-TNE (25 µL) or P_{200}-P_{20}-TNE or P_{200}-Ab-P_{20}-TNE (50 µL) was added to the corresponding well and co-cultured with cells for 1 h at 4°C. Cells were fixed with 4 % paraformaldehyde. Cell nuclei were stained with Hoechst 33342 and cell membrane was stained with Phalloidin-AlexaFluor® 647. Mounted glass slips were imaged on an Apotome microscope (Carl-Ziess, Sydney, Australia).

For testing the effects of PEG on TNE target specificity, CHO-Clec9A cells were first labeled with Hoechst 33342 before mixing with CHO-K1 cells at a ratio of 1:10 (CHO-Clec9A to CHO-K1). Fifty microliter of DiI TNE sample was added to 1 mL of mix cell population containing 2.5×10^5 of cells. Cells were kept at 4°C all the time to prevent internalization. Cells and TNE mixture were incubated for 1 h before acquiring data on a Gallios™ Flow Cytometer. Percentage of TNE bound cells was calculated from DiI positive cells from each cell population.

4.2.5. Mouse splenocyte binding test

Spleens from C57Bl/6 mice were harvested and digested with Collagenase Type III (Worthington) for 25 min at room temperature. Digested tissue was passed through a cell strainer and then centrifuged at 800 x*g* for 2 min before removing red blood cells by incubation in ACK lysis buffer (150 mM NH_4Cl, 1 mM $KHCO_3$, 0.1 mM Na_2EDTA). Cell pellet was re-suspended in RPMI1640 medium supplemented with 5 % FCS. Cells (10^6 in 1 mL) were added to tubes and co-cultured with 50 µL of P_{200}-Isotype-P_{20}-TNE or P_{200}-Ab-P_{20}-TNE for 1 h at 4°C. Cells were washed with PBS and stained with anti-I-A/I-E-PE/Cy7, anti-CD11c-PerCP5.5 and anti-CD8-eFluor780. Cells were analyzed on a Beckman Coulter Gallios™ Flow Cytometer. $CD8^+$ DCs were gated as I-A/I-$E^{hi}CD11c^+CD8^+$ and $CD8^-$ DCs were gated as I-A/I-$E^{hi}CD11c^+CD8^-$.

4.2.6. Analysis of in vivo *specificity*

Two hundred micro liters of DiI labelled P_{200}-Ab-P_{20}-TNE or P_{200}-Isotype-P_{20}-TNE was injected intraperitoneally into C57BL/6 mice. Twenty four hours post injection, spleens were removed and digested with Collagenase Type III (Worthington) for 25 min at room temperature. Digested tissue was passed through a cell strainer and then centrifuged at 800 x*g* for 2 min before removing red blood cells by incubation in ACK lysis buffer (150 mM NH_4Cl, 1 mM $KHCO_3$, 0.1 mM Na_2EDTA). Single cell suspension was stained with anti-I-A/I-E-PE/Cy7, anti-CD11c-PerCP5.5 and anti-CD8-eFluor780. Cells were analysed on a Beckman Coulter Gallios™ Flow Cytometer. $CD8^+$ DCs were gated as I-A/I-$E^{hi}CD11c^+CD8^+$ and $CD8^-$ DCs were gated as I-A/I-$E^{hi}CD11c^+CD8^-$.

4.3. Results and discussion

4.3.1. Functionalized TNE with Clec9A mAb via DAMP4

In this chapter we examined whether the top-down approach for sequential self-assembly of components of the oil-water interface of the nanoemulsion, which had been used to construct an immune-evading TNE in **Chapter 3**, could be applied to simultaneously down-regulate phagocytosis by generic immune cells via PEGylation, and up-regulate specific delivery to target cells. Here, the anti-Clec9A mAb was first fused to DAMP4 (mAb-DAMP4) at the DNA level (see **Section 4.2.2**). A self-assembled nanoemulsion bearing the anti-Clec9A mAb and PEG on its surface was then created by first adding 270 nM mAb-DAMP4 to P_{20}-TNE to form Ab-P_{20}-TNE. Further addition of 200 μM PEGylated DAMP4 Ab-P_{20}-TNE led to the formation of P_{200}-Ab-P_{20}-TNE, enabling the sequence of additions to be easily identified. **Table 4-1** shows the size distribution and zeta-potential of the constructed TNE measured by dynamic lights scattering. Addition of DAMP4-Ab conjugate to P_{20}-TNE did not cause an increase in size distribution, but decreased the Z-potential from 30.1 ± 0.7 mV to 26.3 ± 2.4 mV. This reduction could due to the attachment of the negatively-charged DAMP4-Ab onto the oil droplet surface reducing the net positive charge on the AM1-stabilized oil-water interface. Further addition of PEGylated DAMP4 reduced the zeta-potential to 18.9 ± 0.7 mV, suggesting the additional attachment of neutral PEG to the interface shielded the positively-charged AM1 network.

	Z-average d.nm	Z-potential mV
AM1 stabilized oil core	153 ± 1.5	39 ± 3.1
P_{20} - TNE	171 ± 2.4	30 ± 0.7
Ab - P_{20} - TNE	171 ± 2.9	26 ± 2.4
P_{200} - Ab - P_{20} - TNE	180 ± 2.0	19 ± 0.7

Table 4-1 Size distribution of zeta-potential of TNEs measured by dynamic light scattering (DLS). TNE samples were 1 in 100 diluted in ultrapure water. Data were collected from three experiments and expressed as average with Standard Deviation.

4.3.2. Effect of adding anti-Clec9A-mAb into TNE on binding to CHO-Clec9A cells

After having constructed the P_{200}-Ab-P_{20}-TNE and characterizing its physicochemical properties, we next examined their targeting ability, particularly against Chinese hamster ovary (CHO)-K1 cells that were transfected to express surface Clec9A (CHO-Clec9A) (Caminschi et al., 2008) . TNE was labeled with a fluorescence dye (DiI) for *in vitro* tracking purpose. Labeled TNE was incubated with CHO-Clec9A cells for 1 h at 4°C to allow association between TNE and cells. Isotype-P_{20}-TNE and P_{200}-Isotype-P_{20}-TNE, which were constructed using the same method as for Ab-P_{20}-TNE and P_{200}-Ab-P_{20}-TNE, but with a non-targeting mAb isotype, were used as negative controls. The binding profile was evaluated by confocal microscopy. The overlay of the red and blue fluorescence suggests that the TNE bound to the cell membrane. **Figure 4-1** shows the confocal images of the binding of TNE to CHO-Clec9A. As expected, the non-targeting, non-immune evading TNE, P_{20}-TNE which carries the lowest amount of PEG on the surface, showed the strongest cell-association out of the all TNE constructs tested here. Addition of Clec9A targeting mAb to P_{20}-TNE (Ab-P_{20}-TNE) did not significantly affect the binding extent. Though slightly reduced binding was observed when cells were incubated with P_{200}-Ab-P_{20}-TNE, suggesting that the addition of further PEG into the targeting but not immune evading Ab-P_{20}-TNE aided in reducing non-specific cell interactions, meanwhile not compromising the Clec9A ligand mediated cell-TNE association. This was further proved by incubating cells with immune-evading P_{200}-P_{20}-TNE, as a minimal level of DiI-labeled TNE was observed co-localizing with cell membrane (**Figure 4-1a**). In contrast, the non-specific binding of Isotype-P_{20}-TNE to CHO-Clec9A (**Figure 4-1b**) was significantly reduced by the further addition of PEGylated DAMP4 to the same

formulation (P_{200}-Isotype-P_{20}-TNE), as reduced DiI fluorescence was observed in cells incubated with P_{200}-Isoype-P_{20}-TNE (**Figure 4-1c**). This selective targeting could only be attributed to the complementary binding to the Clec9A antigens by the anti-Clec9A mAb on the surface of P_{200}-Ab-P_{20}-TNE, as compared to the binding profile of the non-targeting TNE in the same cell line. Such a mechanism could potentially enhance drug delivery efficiency through receptor-mediated endocytosis which facilitates particle internalization (Goldstein et al., 1979, Jiang et al., 2008). After the TNE is taken up by the target cells, it may release its drug payload to show therapeutic activity, though this remains to be shown in later chapters.

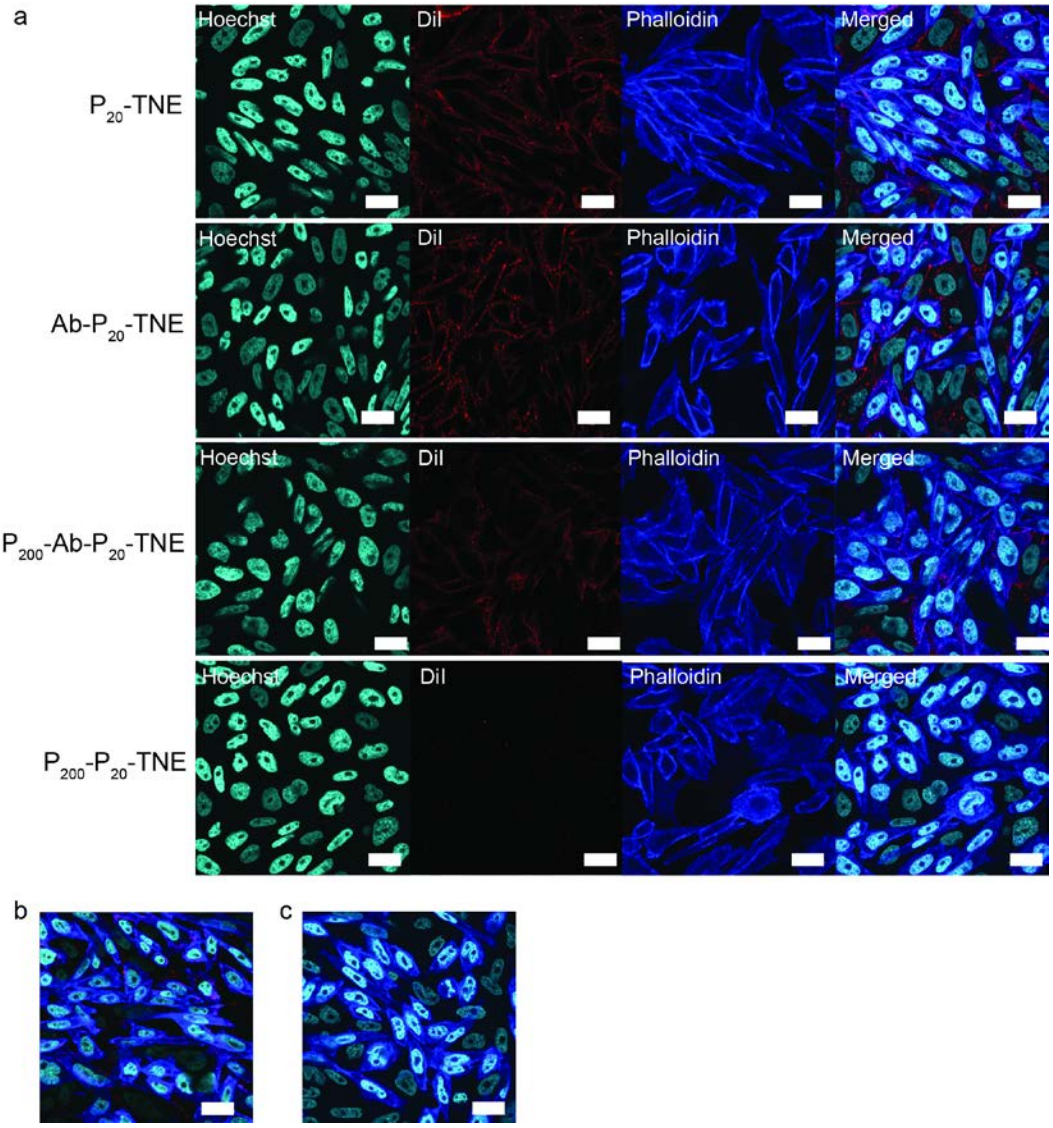

Figure 4-1. Confocal images showing binding of TNE to CHO-Clec9A cells which have been transfected to express a dendritic-cell ligand (Clec9A) on the cell surface. TNEs were labeled with

fluorescent dye DiI (red) for *in vitro* tracking. Cell membrane was stained with phalloidin (blue) and cell nuclei with Hoechst 33342 (green). a) Binding of targeting P_{200}-Ab-P_{20}-TNE to CHO-Clec9A cells; (b) Binding of non-targeting Isoypte-P_{20}-TNE, and; (c) P_{200}-Isoype-P_{20}-TNE to CHO-Clec9A cells. Scale bar: 10 µm.

4.3.3. Effect of PEG on TNE target specificity

The generic binding of P_{200}-Ab-P_{20}-TNE was tested in a mixed cell population comprised of CHO-K1 with (Clec9A$^+$) and without (Clec9A$^-$) surface-expressed Clec9A receptors in a 1:10 number ratio (**Figure 4-2**). P_{200}-Ab-P_{20}-TNE exhibited striking selectivity for Clec9A$^+$ cells, binding to more than 85% of this sub-population, which represented only 10 % of the total population. Binding to Clec9A$^-$ cells was significantly less (only 26 %), even though these cells dominated the culture numerically. This result shows clear ability to target cells in a mixed population and in a receptor-specific fashion. As expected, P_{20}-TNE was present in over 95 % of both the Clec9A$^+$ and Clec9A$^-$ cells, showing no cell selectivity. P_{200}-P_{20}-TNE, on the other hand, almost completely avoided cell binding, likely due to the high PEG surface coverage on the TNE. These findings provided evidence that the anti-Clec9A mAb was connected to the oil-water interface of P_{200}-Ab-P_{20}-TNE by DAMP4 in a functional manner, and that the presence of the mAb successfully up-regulated selectivity for targeted Clec9A-bearing CHO cells. These results suggest that cell selectivity could be adjusted by modifying the mAb to PEG ratio presented on the TNE surface. To test this theory, mAb-DAMP4 concentration was kept constant while varying the amount of PEGylated DAMP4 added in the sequential addition preparation method. **Figure 4-2** shows that cell selectivity was increased for both P_{300}-Ab-P_{20}-TNE and P_{400}-Ab-P_{20}-TNE, with the non-specific binding to Clec9A$^-$ cells almost abrogated. However, enhanced selectivity was achieved at the expense of an overall reduction in binding, decreasing the binding to Clec9A$^+$ cells to only 30-40 %. Nonetheless, these results provide a very clear demonstration that the targeted nanoemulsion was able to very selectively target a specific set of cells in a mixed population of very similar cells, in a receptor-specific fashion. The ability to control for non-specific binding by simple variation of the amount of PEG versus targeting antibody also provides an elegant nanotechnology strategy to tune specificity and thus to control bio-distribution and pharmacokinetics.

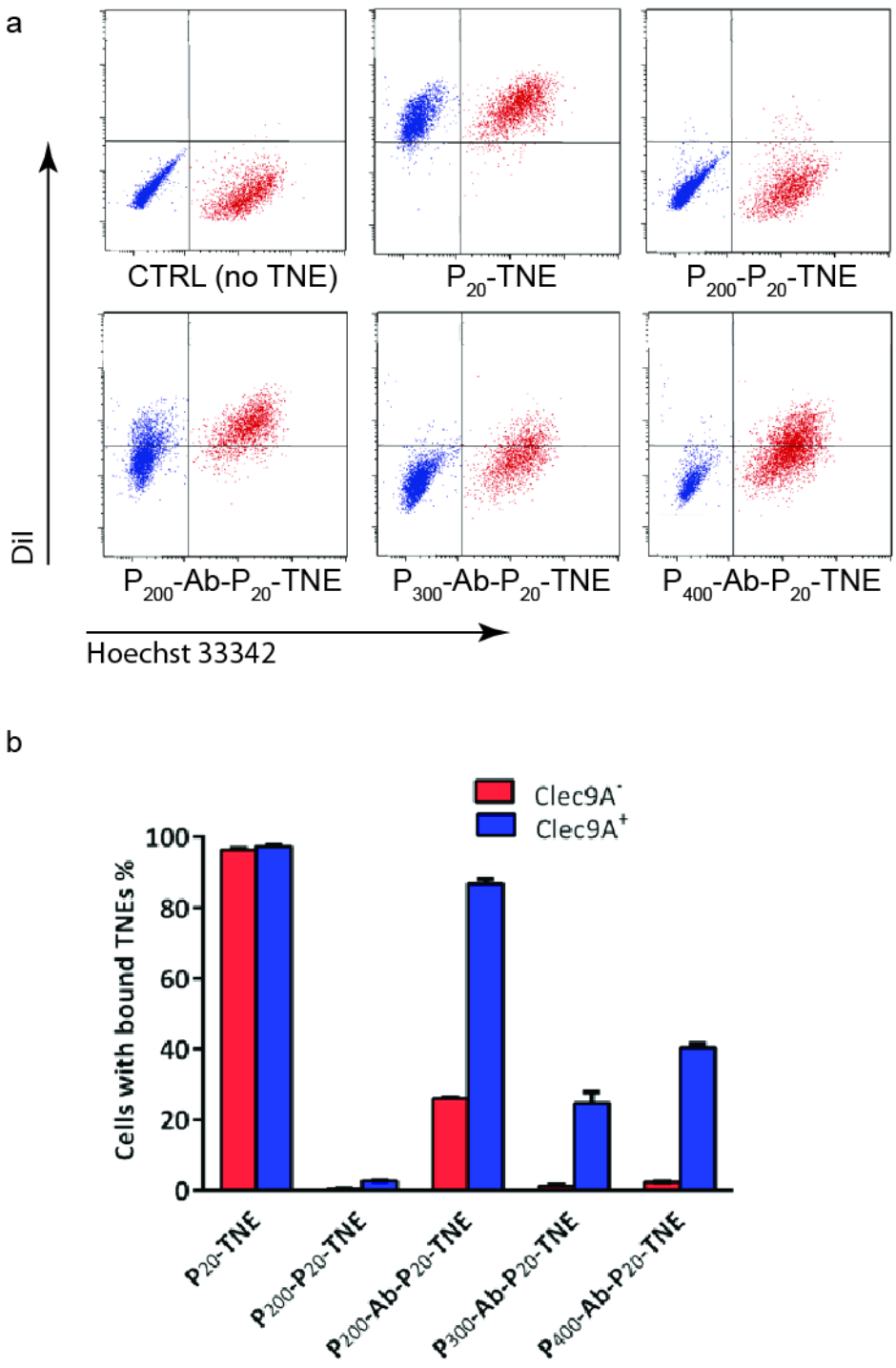

Figure 4-2. a) FACS dot plots showing binding of DiI labeled TNE to Clec9A$^-$ (blue) and Clec9A$^+$ (red) cells. DiI positive cells were gated against CTRL where no TNE was added. **b)** The percentage of Clec9A- or Clec9A+ CHO-K1 cells bound with TNE calculated from flow cytometry results showing the effects of increased PEG content in the Ab-P_{20}-TNE formulation. Results are shown as the mean of N=3 experiments with standard deviation.

4.3.4. *TNE selectively binds to CD8$^+$ DCs* in vitro

We also investigated the *in vitro* cell specific of P_{200}-Ab-P_{20}-TNE in a more complex cell population that mimics the *in vivo* environment that the i.v. injected TNE would encounter. Labeled emulsion was incubated with mouse splenic cells for 1 h at 4°C. Clec9A is highly restricted to DCs and is selectively expressed by CD8$^+$ conventional DCs and plasmacytoid DCs in mice (Caminschi et al., 2008) therefore allowing the Clec9A$^+$ cells among mouse splenocytes to be tracked using the CD8 marker. **Figure 4-3** shows that P_{200}-Ab-P_{20}-TNE selectively associated with the CD8$^+$ DC sub-population. Emulsion was detected in close to 40% of the CD8$^+$ DCs, while the non-targeting P_{200}-Isotype-P_{20}-TNE only bound to a minimum number of cells in the same population (< 5 %). This result further demonstrated the *in vitro* targeting capability of P_{200}-Ab-P_{20}-TNE in a highly-complex cell population.

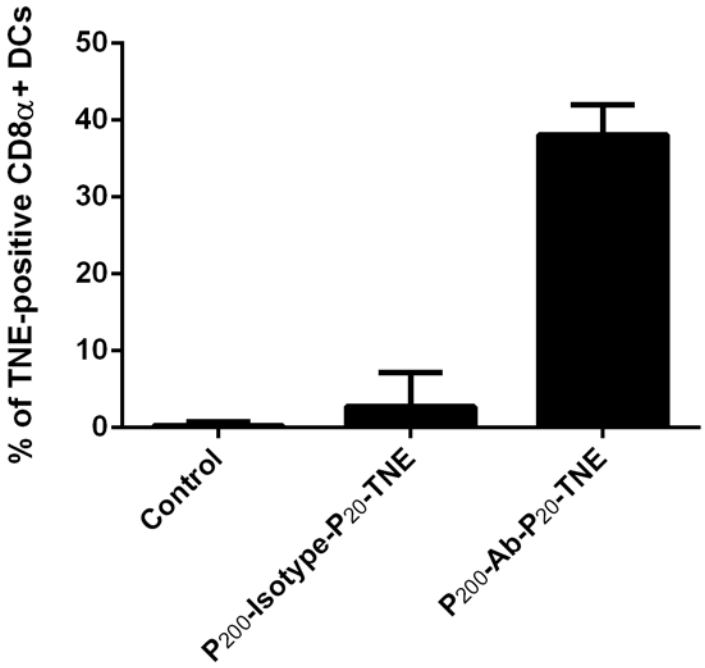

Figure 4-3. *In vitro* cellular binding of P_{200}-Ab-P_{20}-TNE and P_{200}-Isotype-P_{20}-TNE to CD8$^+$ DC. Splenocytes (10^6 in 1 mL) were added to tubes and co-cultured with 50 µL of P_{200}-Isotype-P_{20}-TNE or P_{200}-Ab-P_{20}-TNE for 1 h at 4°C. Cells were washed with PBS and stained with anti-I-A/I-E, anti-CD11c and anti-CD8. CD8$^+$ DCs were gated as I-A/I-E^{hi}CD11c$^+$CD8$^+$ and CD8$^-$ DCs were gated as I-

A/I-$E^{hi}CD11c^{+}CD8^{-}$. Cells did not incubated with TNE was used as control for baseline. Results shown are mean and standard deviation from N=3 experiments.

4.3.5. TNE targets $CD8^{+}$ DCs in vivo

We also investigated the *in vivo* distribution of P_{200}-Ab-P_{20}-TNE by i.p. injecting labeled emulsion into mice, and harvested splenocytes after 24 h. **Figure 4-4** shows that P_{200}-Ab-P_{20}-TNE associated selectively with the $CD8^{+}$ DC sub-population; the emulsion was detected in >30 % of the $CD8^{+}$ DCs but in <2 % of the $CD8^{-}$ DCs. This finding supports the *in vitro* data, demonstrating the excellent *in situ* targeted delivery capability of P_{200}-Ab-P_{20}-TNE. As expected, this level of striking cell selectivity was not exhibited by the control sample constructed in a similar way but using a non-specific isotype antibody instead of the anti-Clec9A mAb (P_{200}-Isotype-P_{20}-TNE).

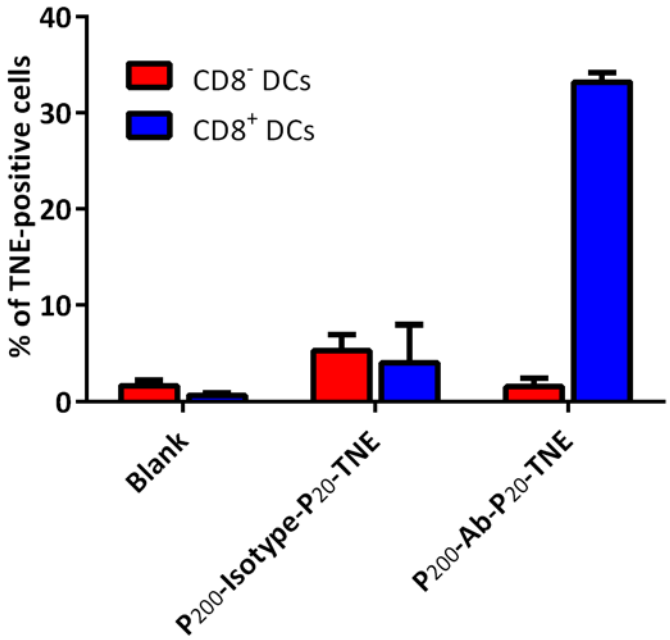

Figure 4-4. *In vivo* cellular uptake of P_{200}-Ab-P_{20}-TNE and P_{200}-Isotype-P_{20}-TNE in $CD8^{+}$ DCs and $CD8^{-}$ DCs. Results shown are mean and standard deviation from N=2 experiments.

4.4. Conclusion

The goal of this Chapter is to address **Objective 2** and **3** stated in **Section 1.4**, by constructing a long-circulating TNE that is capable of targeting Clec9A$^+$ DCs *in vivo*. A long-circulating TNE, termed as P_{200}-P_{20}-TNE, was demonstrated in the last Chapter by using DAMP4 as an anchor to functionalize the nanoemulsion oil core with immune-evading polymer PEG. This initial result supports our hypothesis, that DAMP4 carries its conjugated PEG onto an AM1 pre-stabilized oil-water interface, leading to functional display of PEG on the nanoemulsion surface. PEGylation imparts steric stability of TNE in isotonic condition and creates a repulsive barrier that repels the attachment of opsonins which leads to clearance by the mononuclear phagocyte system (MPS). In order to increase the intracellular delivery efficiency, P_{200}-P_{20}-TNE can benefit from being functionalized with a targeting moiety that enables receptor-mediated endocytosis. Targeting delivery of a nanocarrier loaded with therapeutic components, *e.g.* protein antigen, to DCs is a promising strategy to initiate antigen-specific immune response (reviewed in **Section 2.8.2**).

The coupling of anti-Clec9A mAb to PEGylated TNE oil core is based on the non-covalent "click" chemistry we developed in **Chapter 3**, which uses DAMP4 as an anchor to display mAb on the TNE surface. This approach differs from procedures used by others, which normally involves covalent conjugation chemistry (Goldstein et al., 2007, Lundberg et al., 1999, Lundberg et al., 2004). Anti-Clec9A mAb was fused to DAMP4 via molecular cloning, circumventing the potential of mAb deactivation by extreme physiochemical conditions required by covalent conjugation chemistry. Cell binding ability of targeting nanocarriers is governed by many factors, including shape, size and surface charge (Thorek and Tsourkas, 2008). Following functionalization of TNE oil core with DAMP4-PEG and mAb-DAMP4, we measured the size distribution and surface zeta-potential of each conjugate. Sequential addition of PEG-DAMP4 and DAMP4-mAb to positively-charged TNE oil core causes a decrease in the absolute value of the zeta potential (**Table 4-1**), probably due to a shielding effect from PEG-DAMP4 and the addition of negatively charged mAb-DAMP4 to the TNE system. The constructed P_{200}-mAb-P_{20}-TNE exhibits size distribution under 200 nm, which indicates it is suitable for i.v. injection.

The cell-targeting capability of P_{200}-Ab-P_{20}-TNE was first assessed by conducting *in vitro* cell-binding assays using Clec9A-transfected CHO-K1 cells (CHO-Clec9A). To assess Clec9A-mediated

differential uptake, the CHO-Clec9A cells were incubated with TNEs functionalized with DAMP4-PEG and/or Clec9A mAb-DAMP4 in 4 ˚C to prevent internalization. The cells from each sample were then washed, stained and analyzed using confocal microscopy (**Figure 4-1**). As expected, P_{20}-TNE shows high levels of non-specific binding to cells, as there is not sufficient PEG content to create a repulsive barrier that prevents cell association. And such non-specific cell association can be diminished by further adding PEG into P_{20}-TNE to create P_{200}-P_{20}-TNE. Compared to the non-targeting long circulating P_{200}-P_{20}-TNE, incubation of Clec9A targeting P_{200}-Ab-$_{P20}$-TNE resulted in a significantly high level of cell association, as evident by the co-localization of fluorescence dye labeled P_{200}-Ab-$_{P20}$-TNE with cell membrane, which indicated that the increased cell binding of P_{200}-Ab-$_{P20}$-TNE was receptor-specific (**Figure 4-1 a**). To demonstrate that the targeting effects were exclusive to TNE functionalized with Clec9A mAb, CHO-Clec9A cells were also incubated with two TNEs that been functionalized with a non-targeting isotype mAb, which was termed as Isotype-P_{20}-TNE and P_{200}-Isotype-P_{20}-TNE. The non-specific binding of Isotype-P_{20}-TNE was minimized by adding additional content of PEG to create P_{200}-Isotype-P_{20}-TNE, further suggesting that the cell-association observed in CHO-Clec9A cells incubated with P_{200}-Ab-P_{20}-TNE was mediated by Clec9A mAb that had been displayed on the TNE surface. Overall, these results confirm the receptor-specific targeting capability of Clec9A mAb functionalized TNE.

PEG density on a nanocarrier is a crucial determinant of immune evading efficacy. Increasing PEG density can significantly reduce interactions of PEGylated nanocarriers with MPS and increase their *in vivo* half-life (Gref et al., 2000, Mosqueira et al., 2001). Increased density of PEG on the surface could affect the availability of targeting ligand and alleviate potential steric hindrances. We presented a method to tune the density of PEG presented on the TNE surface by producing them with adjusted amount of PEG-DAMP4. Not surprisingly, we found that an increased amount of PEG-DAMP4 reduce the non-specific cell association of P_{300}-Ab-P_{20}-TNE and P_{400}-Ab-P_{20}-TNE, but also reduced specificity towards target cells (**Figure 4-2**). Nonetheless, we demonstrated the ability to tune the target specificity by simple variation of TNE composition, and the superior targeting selectivity of P_{200}-Ab-P_{20}-TNE compared to their non-targeting counter parts both *in vitro* and *in vivo* (**Figure 4-3** and **4-4)**.

In summary, we have successfully synthesized a nanocarrier emulsion-based TNE platform specific to Clec9A-expressing dendritic cells. Through the aid of DAMP4, which acts as anchor for displaying immune evading polymer PEG and mAb targeting Clec9A using a non-covalent “click” chemistry, thus

circumventing the need to expose the biological moieties to chemical reactions designed to form irreversible bonds. The simplicity of this functionalization scheme can potentially enable a wide array of functionalized TNE for tailored disease treatments. The capability to control and adjust density of functional moieties through DAMP4 mediated functionalization also provides versatility for platform optimization. Future studies are warranted to examine the *in vivo* implications of ligand functionalization of TNE. The targeted P_{200}-Ab-P_{20}-TNE demonstrated in this Chapter possess significant potential for targeting delivery of delicate therapeutics, *e.g.* protein based therapeutics, as the platform integrates immune-evasive moieties with a DC-targeting ligand. DCs plays a central role in immune system and orchestrate a wide repertoire of immune responses (topic reviewed in **Section 2.9.2**), thus targeting an antigen to DCs exclusive receptor, *i.e.* Clec9A, represents an attractive strategy to enhance vaccine efficacy. The following Chapters will demonstrate the process of loading a model protein antigen into P_{200}-Ab-P_{20}-TNE (**Chapter 5**), as well as the immune response and advantage of targeting antigen to DCs by P_{200}-Ab-P_{20}-TNE (**Chapter 6**) with the aim to address **Objectives 4** and **5** of this PhD project.

ALLEN, T. M. 2002. Ligand-targeted therapeutics in anticancer therapy. *Nat Rev Cancer,* 2, 750-763.

ASHLEY, C. E., CARNES, E. C., PHILLIPS, G. K., PADILLA, D., DURFEE, P. N., BROWN, P. A., HANNA, T. N., LIU, J., PHILLIPS, B., CARTER, M. B., CARROLL, N. J., JIANG, X., DUNPHY, D. R., WILLMAN, C. L., PETSEV, D. N., EVANS, D. G., PARIKH, A. N., CHACKERIAN, B., WHARTON, W., PEABODY, D. S. & BRINKER, C. J. 2011. The targeted delivery of multicomponent cargos to cancer cells by nanoporous particle-supported lipid bilayers. *Nat Mater,* 10, 389-397.

CAMINSCHI, I., PROIETTO, A. I., AHMET, F., KITSOULIS, S., TEH, J. S., LO, J. C. Y., RIZZITELLI, A., WU, L., VREMEC, D., VAN DOMMELEN, S. L. H., CAMPBELL, I. K., MARASKOVSKY, E., BRALEY, H., DAVEY, G. M., MOTTRAM, P., DE VELDE, N. V., JENSEN, K., LEW, A. M., WRIGHT, M. D., HEATH, W. R., SHORTMAN, K. & LAHOUD, M. H. 2008. The dendritic cell subtype-restricted C-type lectin Clec9A is a target for vaccine enhancement. *Blood,* 112, 3264-3273.

GOLDSTEIN, D., SADER, O. & BENITA, S. 2007. Influence of oil droplet surface charge on the performance of antibody–emulsion conjugates. *Biomedicine & Pharmacotherapy,* 61, 97-103.

GOLDSTEIN, J. L., ANDERSON, R. G. W. & BROWN, M. S. 1979. Coated pits, coated vesicles, and receptor-mediated endocytosis. *Nature,* 279, 679-685.

GREF, R., LÜCK, M., QUELLEC, P., MARCHAND, M., DELLACHERIE, E., HARNISCH, S., BLUNK, T. & MÜLLER, R. H. 2000. 'Stealth' corona-core nanoparticles surface modified by polyethylene glycol (PEG): influences of the corona (PEG chain length and surface density) and of the core composition on phagocytic uptake and plasma protein adsorption. *Colloids and Surfaces B: Biointerfaces,* 18, 301-313.

HU, C.-M. J., ZHANG, L., ARYAL, S., CHEUNG, C., FANG, R. H. & ZHANG, L. 2011. Erythrocyte membrane-camouflaged polymeric nanoparticles as a biomimetic delivery platform. *Proceedings of the National Academy of Sciences*.

HUYSAMEN, C., WILLMENT, J. A., DENNEHY, K. M. & BROWN, G. D. 2008. CLEC9A is a novel activation C-type lectin-like receptor expressed on BDCA3(+) dendritic cells and a subset of monocytes. *Journal of Biological Chemistry,* 283, 16693-16701.

JIANG, W., KIMBETTY, Y. S., RUTKA, J. T. & CHANWARREN, C. W. 2008. Nanoparticle-mediated cellular response is size-dependent. *Nat Nano,* 3, 145-150.

KAAKI, K., HERVÉ-AUBERT, K., CHIPER, M., SHKILNYY, A., SOUCÉ, M., BENOIT, R., PAILLARD, A., DUBOIS, P., SABOUNGI, M.-L. & CHOURPA, I. 2011. Magnetic Nanocarriers of Doxorubicin Coated with Poly(ethylene glycol) and Folic Acid: Relation between Coating Structure, Surface Properties, Colloidal Stability, and Cancer Cell Targeting. *Langmuir,* 28, 1496-1505.

KIM, J.-Y., KIM, J.-K., PARK, J.-S., BYUN, Y. & KIM, C.-K. 2009. The use of PEGylated liposomes to prolong circulation lifetimes of tissue plasminogen activator. *Biomaterials,* 30, 5751-5756.

KUKOWSKA-LATALLO, J. F., CANDIDO, K. A., CAO, Z., NIGAVEKAR, S. S., MAJOROS, I. J., THOMAS, T. P., BALOGH, L. P., KHAN, M. K. & BAKER, J. R. 2005. Nanoparticle Targeting of Anticancer Drug Improves Therapeutic Response in Animal Model of Human Epithelial Cancer. *Cancer Research,* 65, 5317-5324.

LAHOUD, M. H., AHMET, F., KITSOULIS, S., WAN, S. S., VREMEC, D., LEE, C. N., PHIPSON, B., SHI, W., SMYTH, G. K., LEW, A. M., KATO, Y., MUELLER, S. N., DAVEY, G. M., HEATH, W. R., SHORTMAN, K. & CAMINSCHI, I. 2011. Targeting Antigen to Mouse Dendritic Cells via Clec9A Induces Potent CD4 T Cell Responses Biased toward a Follicular Helper Phenotype. *J. Immunol,* 187, 842-850.

LIU, Y., LI, K., PAN, J., LIU, B. & FENG, S.-S. 2010. Folic acid conjugated nanoparticles of mixed lipid monolayer shell and biodegradable polymer core for targeted delivery of Docetaxel. *Biomaterials,* 31, 330-338.

LUNDBERG, B. B., GRIFFITHS, G. & HANSEN, H. J. 1999. Conjugation of an anti-B-cell lymphoma monoclonal antibody, LL2, to long-circulating drug-carrier lipid emulsions. *The Journal of pharmacy and pharmacology,* 51, 1099-1105.

LUNDBERG, B. B., GRIFFITHS, G. & HANSEN, H. J. 2004. Cellular association and cytotoxicity of anti-CD74-targeted lipid drug-carriers in B lymphoma cells. *Journal of Controlled Release,* 94, 155-161.

MATHEW, A., FUKUDA, T., NAGAOKA, Y., HASUMURA, T., MORIMOTO, H., YOSHIDA, Y., MAEKAWA, T., VENUGOPAL, K. & KUMAR, D. S. 2012. Curcumin Loaded-PLGA Nanoparticles Conjugated with Tet-1 Peptide for Potential Use in Alzheimer's Disease. *PLoS ONE,* 7, e32616.

MOSQUEIRA, V. C. F., LEGRAND, P., MORGAT, J. L., VERT, M., MYSIAKINE, E., GREF, R., DEVISSAGUET, J. P. & BARRATT, G. 2001. Biodistribution of long-circulating PEG-grafted nanocapsules in mice: Effects of PEG chain length and density. *Pharmaceutical Research,* 18, 1411-1419.

REDDY, S. T., REHOR, A., SCHMOEKEL, H. G., HUBBELL, J. A. & SWARTZ, M. A. 2006. In vivo targeting of dendritic cells in lymph nodes with poly(propylene sulfide) nanoparticles. *Journal of Controlled Release,* 112, 26-34.

SHROFF, K. & KOKKOLI, E. 2012. PEGylated Liposomal Doxorubicin Targeted to α5β1-Expressing MDA-MB-231 Breast Cancer Cells. *Langmuir,* 28, 4729-4736.

THOREK, D. L. J. & TSOURKAS, A. 2008. Size, charge and concentration dependent uptake of iron oxide particles by non-phagocytic cells. *Biomaterials,* 29, 3583-3590.

YOSHIDA, M., TAKIMOTO, R., MURASE, K., SATO, Y., HIRAKAWA, M., TAMURA, F., SATO, T., IYAMA, S., OSUGA, T., MIYANISHI, K., TAKADA, K., HAYASHI, T., KOBUNE, M. & KATO, J. 2012. Targeting Anticancer Drug Delivery to Pancreatic Cancer Cells Using a Fucose-Bound Nanoparticle Approach. *PLoS ONE,* 7, e39545.

Chapter 5 Induction of potent $CD8^+$ T cells response by TNE carrying model antigen using S/O/W emulsification method

5.1. Introduction

The two previous chapters of this thesis describe the design, construction and characterization of a nanocarrier emulsion capable of targeting a specific subset of DCs that express the C-type lectin receptor Clec9A. The targeting emulsion, P_{200}-Ab-P_{20}-TNE, was constructed using a new approach to the bottom-up self-assembly of nanoemulsion. Functional moieties such as immune evading PEG and the targeting antibody against Clec9A can be pre-conjugated to the biosurfactant (reviewed in **Section 2.4.2**) DAMP4, and the simple top-down sequential addition of such a hybrid DAMP4 molecule to an AM1-pre-stabilized nanoemulsion leads to self-assembly of the functional moieties at the emulsion interface. These two previous chapters report successful outcomes that provide evidence in support of hypothesis stated in **Chapter 1**, that DAMP4 could be used to engineer the interface of a TNE through non-covalent self-assembly.

As mentioned in **Chapter 1**, biologics is a hot topic in the pharmaceutical industry. Advances in biotechnology have led to the development of new therapeutics for various disease treatments by delivering proteins and peptides into cells (Vlieghe et al., 2010, Leader et al., 2008). Alterations in intracellular protein functions are the main course of many diseases (Carter, 2011), making protein therapeutics a potential treatment. Biologics have opened a new door for treating diseases such as cancers (Foltopoulou et al., 2010, Yarden and Sliwkowski, 2001), inflammation (Jo et al., 2005) and cerebrovascular disorders (Ogawa et al., 2009). Since the first recombinant insulin was approved by the Food and Drug Administration (FDA) for clinical use over 30 years ago, biologics currently represent a significant proportion of biopharmaceutical market (Leader et al., 2008). For example, Humira®, an engineered human tumor necrosis factor (TNF) mainly prescribed for treating rheumatoid arthritis (Bain and Brazil, 2003), was the most top-selling biologic drug of 2012 (Huggett, 2013). Compared to traditional small molecule drugs (SMDs), protein based therapeutics have higher intracellular activities and specificities, which could potentially provide more effective disease treatment. Moreover, biologics are relatively safer than alternative gene therapies, as no random or permanent genetic changes result, thus circumventing concerns of potential mutagenesis (Gu et al., 2011).

Despite their potential medical application, effective delivery of biologics to their site of action remains a challenge, due to intrinsic properties of most proteins, including high molecular weight, fragile tertiary structures and hydrophilicity (Leader et al., 2008). Moreover, the transportation of protein-based drugs through compartmental barriers is ineffective due to their short *in vivo* half-life. Translation of biologics research to clinical application is restrained by the incapability of delivering functional proteins into cells. Native protein drugs administered intravenously can suffer from serum instability and be rapidly degraded or deactivated. Mechanical delivery methods such as microinjection have been investigated for decades, nevertheless are laborious and require specialized equipment to mechanically puncture membranes thereby limiting their *in vivo* application (Zhang and Yu, 2008). On the other hand, proper design of a transport system can greatly improve the pharmacokinetics of these drugs. In order to achieve effective intracellular protein release, drug delivery systems (DDS) capable of carrying their therapeutic payloads overcoming a range of biological barriers are needed. For example, such DDS need to escape from the rapid clearance by mononuclear phagocytic system (MPS), kidney filtration, aggregation and degradation by serum proteins. In addition, protein DDS need to help their protein cargo escape from early endosomal degradation to reach the desired subcellular compartments, such as the cytosol and nucleus (Bareford and Swaan, 2007). Therefore, development of efficient and safe protein DDS is vital for the translation of these drugs into clinical application.

To date, many research groups have concentrated on the development of protein delivery systems (reviewed in Chapter 2). The enhanced ability to manipulate materials at the nanoscale enables the development of various nanocarriers for protein delivery. Protein cargos can be encapsulated in or adsorbed onto various nanocarriers to avoid premature degradation and denaturing interactions with the biological environment (Peer et al., 2007, Faraji and Wipf, 2009, Gao and Xu, 2009). The high surface-to-volume ratio of nanocarriers can potentially improve the pharmacokinetics and biodistribution of the payload (Chou et al., 2011, Gaberc-Porekar et al., 2008, Peer et al., 2007). Moreover, nanocarrier-based DDS provide tailored chemical and physical properties to facilitate cell penetration, endosomal escape, enhanced stability, target specificity and controlled release, through controlled assembly and chemical modification (Kabanov and Vinogradov, 2009, Stuart et al., 2010, Solaro, 2008). An ideal nanocarrier should incorporate the drugs without compromising bioactivity. Once administered into the human body, these nanocarriers should protect the drug payload (by concealing immunogenic epitopes) and avoid capture by the host immune system. Most importantly, the drug must be shuttled into the particular cell compartments where it can exert its therapeutic activity (Torchilin, 2006). Nanocarriers

such as micelles (Lee et al., 2009, Gao et al., 2012, Ren et al., 2013), nanocapsules (Gu et al., 2009, Yan et al., 2010, Tang et al., 2013) and liposomes (Liguori et al., 2008, Zelphati et al., 2001, Dalkara et al., 2006) have been developed for intracellular protein delivery. However, there is not a single nanocarrier or platform that can be considered ideal for all types of biologics. For example, the use of organic solvents in the preparation of some of the polymeric formulations will potentially denature the protein payload; liposomal formulations mostly suffer from low drug loading capacity and inadequate stability; inorganic nanocarriers such as quantum dots and gold nanoparticles are non-biodegradable, causing huge safety concerns in relation to their clinical administration (Gu et al., 2011). Therefore new strategies need to be explored to expand the scope of nanocarriers for effective protein delivery.

The ability of DCs to prime naïve T cells with antigens implies a critical role of DCs in mediating immunity against infectious diseases and cancers (Fonteneau et al., 2003). This thesis reports a simple method to produce a DC-targeting TNE in the last two chapters, by which stringent preparation steps are not involved. We have already shown the AM1 stabilized nanoemulsion is an ideal cargo carrier for delivering lipophilic drugs to cells (Chuan et al., 2011). Hence the TNE platform could potentially be an ideal system for intracellular protein delivery by addressing the aforementioned issues. It is possible that once P_{200}-Ab-P_{20}-TNE has been taken up by target DCs, its encapsulated protein will be released and processed by DCs and subsequently presented via the MHC class I molecules to $CD8^+$ T cells through the antigen cross-presentation pathway.

This chapter extends the previous studies into the application of TNE for intracellular delivery of protein. TNE was evaluated *in vitro* using ovalbumin (OVA) as a model antigen. Hydrophilic OVA was loaded into the oil core using the solid-in-oil (S/O) nanodispersion method (Tahara et al., 2008) (**Figure 5-1**). Briefly, an aqueous solution of protein was mixed with hexane solution of glycerol monooleate (Cithrol™ GMO HP) to form a water-in-oil (W/O) emulsion. Then a S/O nanodispersion was prepared by lyophilizing the W/O emulsion before dissolving the lyophilized surfactant-protein complex in Miglyol® 812. Subsequently protein S/O dispersion was used as the oil phase to prepare S/O/W emulsion following the same procedure for producing P_{200}-Ab-P_{20}-TNE which is described in **Chapter 4**. In this method, protein was first coated with hydrophobic surfactant molecules to form protein-surfactant complexes, to significantly increase its solubility in the oil phase and enable facile packaging into the TNE oil core. An *in vitro* cross-presentation assay was carried out as the first step to

evaluate whether antigen encapsulated within TNE could be correctly processed and cross-presented by DCs to antigen-specific T cells.

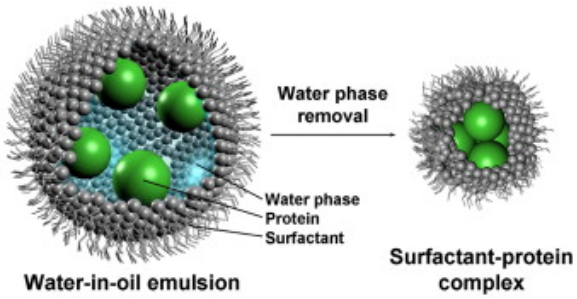

Figure 5-1. Schematic illustration of the preparation of the surfactant protein complex prepared from a W/O emulsion (Tahara et al., 2008).

5.2. Materials and methods

5.2.1. *Materials*

n-hexane and disodium salt of ethylenediaminetetraacetic acid (Na_2EDTA) were purchased from Ajax Finechem (NSW, Australia). Cithrol^{TM} GMO HP was a gift from Croda Europe Ltd (Staffordshire, United Kingdom). Other materials were as detailed in **Section 3.2.1** of **Chapter 3**.

5.2.2. *Mice*

Mice (C57Bl/6) were bred at the Diamantina Institute Biological Research Facility (BRF) at The University of Queensland under specific pathogen-free conditions. Experiments were approved by the UQ Animal Ethics Committee (ethics number 465/12).

5.2.3. *Preparation of OVA in oil dispersion*

OVA solution (8 mg mL^{-1}) was prepared by dissolving OVA (80 mg) in ultrapure water (10 mL). Cithrol^{TM} GMO HP solution (1 %, w/v) was prepared by dissolving Cithrol^{TM} GMO HP (200 mg) in hexane (20 mL). OVA solution (1 mL) and Cithrol^{TM} GMO HP solution (2 mL) were transferred into a 20 mL glass vial, and mixed by using the homogenizer at 24,000 rpm for 5 min to form stable water in oil (w/o) emulsion. The resulting emulsion was frozen rapidly on dry ice for 2 h before being

lyophilized for 24 h. The resulting OVA-Cithrol™ GMO HP pellet was dissolved in Miglyol® 812 (3 mL) to a final concentration of 2.7 mg mL^{-1} of OVA, and used as the oil phase for preparing OVA-P_{20}-Ab-P_{200}-TNE and OVA-P_{20}-Isotype-P_{200}-TNE following the same procedures detailed in **Section 4.2.3** of **Chapter 4**.

5.2.4. Dot blot assay

Dot blot analysis was performed to determine if the OVA-surfactant complex could be recognized by commercial anti-OVA mAb. Briefly, 5 µL of each protein sample was dotted onto a nitrocellulose membrane before blocking with 5 % (v/v) skim milk powder in PBS buffer containing 0.1 % (w/v) Tween 20. Commercial mouse monoclonal antibody specific to OVA (clone OVA-14, Sigma-Aldrich, NSW, Australia), was used at 1 µg mL^{-1} to bind protein. The commercial antibody was generated from mice immunized with OVA. Secondary HRP-conjugated goat anti-mouse antibody (A4416, Sigma-Aldrich, MO, USA) was used for detection. Binding of antibody to protein was detected by chemiluminescence with the Novex® ECL chemiluminescent substrate reagent kit (Invitrogen, Carlsbad, CA, USA) according to the manufacturer's protocol.

5.2.5. In vitro *cross-presentation assay*

To prepare splenocytes, spleen from C57BL/6 mouse was removed and digested with Collagenase Type III (Worthington) for 30 min at room temperature. Digested tissue was passed through a cell strainer and then centrifuged at 430 *g* for 5 min before removing erythrocytes by incubation in ACK lysis buffer (150 mM NH_4Cl, 1 mM $KHCO_3$, 0.1 mM Na_2EDTA). OT-I cells were isolated from spleen and lymph nodes (LNs) of OT-I mice and purified using Miltenyi $CD8\alpha^+$ T Cell Isolation Kit II (Miltenyi Biotec Australia Pty. Ltd., NSW, Australia). Purified OT-I cells were stained with CellTrace™ Violet for *in vitro* tracking.

Splenocytes were treated with Mitomycin C (Sigma-Aldrich, St Louis, MO, USA) to block cell division. Mitomycin C treated splenocytes (10^6 cells) were cultured with P_{200}-Ab-P_{20}-TNE, OVA-P_{200}-Ab-P_{20}-TNE or OVA-P_{200}-Isotype-P_{20}-TNE (50 µL, equivalent to 0.6 µg of OVA) for 3 h at 37°C with 5 % v/v CO_2. As positive control, splenocytes were pulsed with 1 µg of SIINFEKL peptide. At the end of the incubation, splenocytes were washed three times with RPMI-1640 supplemented with FCS (5 %

v/v) before being added to wells of a 96-well tissue culture plate at 5×10^5 cells per well in 100 µL RPMI-1640 medium supplemented with FCS (5 % v/v). OT-I cells (2.5×10^5) in 100 µL RPMI-1640 medium supplemented with FCS (5 % v/v) were then added to each well and cultured for 4 days at 37°C with 5 % v/v CO_2 supplied. Cells were harvested from the 96-well plate and stained with PerCP5.5-anti-CD8. OT-I T cell proliferation was measured as a function of CellTrace™ Violet dye dilution after gating on $CD8^+$ T cells.

5.2.6. In vivo *cross-presentation assay*

OT-I cells were isolated from lymph nodes (LNs) of $OVA_{257-264}$ specific OT-I transgenic mice and purified using Miltenyi $CD8\alpha^+$ T Cell Isolation Kit II (Miltenyi Biotec Australia Pty. Ltd., NSW, Australia). Purified OT-I cells were stained with CellTrace™ Violet (CTV) for *in vivo* tracking. Cells were washed three times with RPMI-1640 supplemented with FCS (5 % v/v) before re-suspending in sterile PBS. C57Bl/6 mice were adoptively transferred with CTV labeled OT-I cells (10^6). One day later, these mice were immunized intravenously with OVA-P_{200}-Isotype-P_{20}-TNE or OVA-P_{200}-Ab-P_{20}-TNE. Mice were sacrificed 4 days later, and the $CD3^+MHCII^-CD8^+$ OT-I T cell response was determined as the dilution in CTV fluorescence intensity.

5.3. Results and discussions

5.3.1. Preparation of OVA loaded TNE

Figure 5-2 a represents the physical difference in appearance between native OVA and its S/O dispersion counterpart in Miglyol® 812. The surfactant–FITC labeled OVA complex was highly dissolved in oil phase to give a transparent solution. In contrast, native FITC-labeled OVA without surfactant exhibited low solubility in oil and precipitated over time. The surfactant–OVA complex solubilized Miglyol® 812 used to prepare OVA-P_{200}-Ab-P_{20} TNE followed a published protocol (Zeng et al., 2013). OVA-P_{200}-Ab-P_{20} had consistent size distributions when diluted in water and PBS, with mean sizes of 187.1 ± 2 nm and 189.3 ± 3.8 nm, respectively, suggesting good stability under physiological salt (**Figure 5-2 b)**. The co-localizing of FITC-labeled OVA with the DiI-labeled AM1 stabilized TNE oil core under confocal microscopy suggested that the surfactant-OVA complex was well encapsulated within the TNE oil core (**Figure 5-2 c)**.

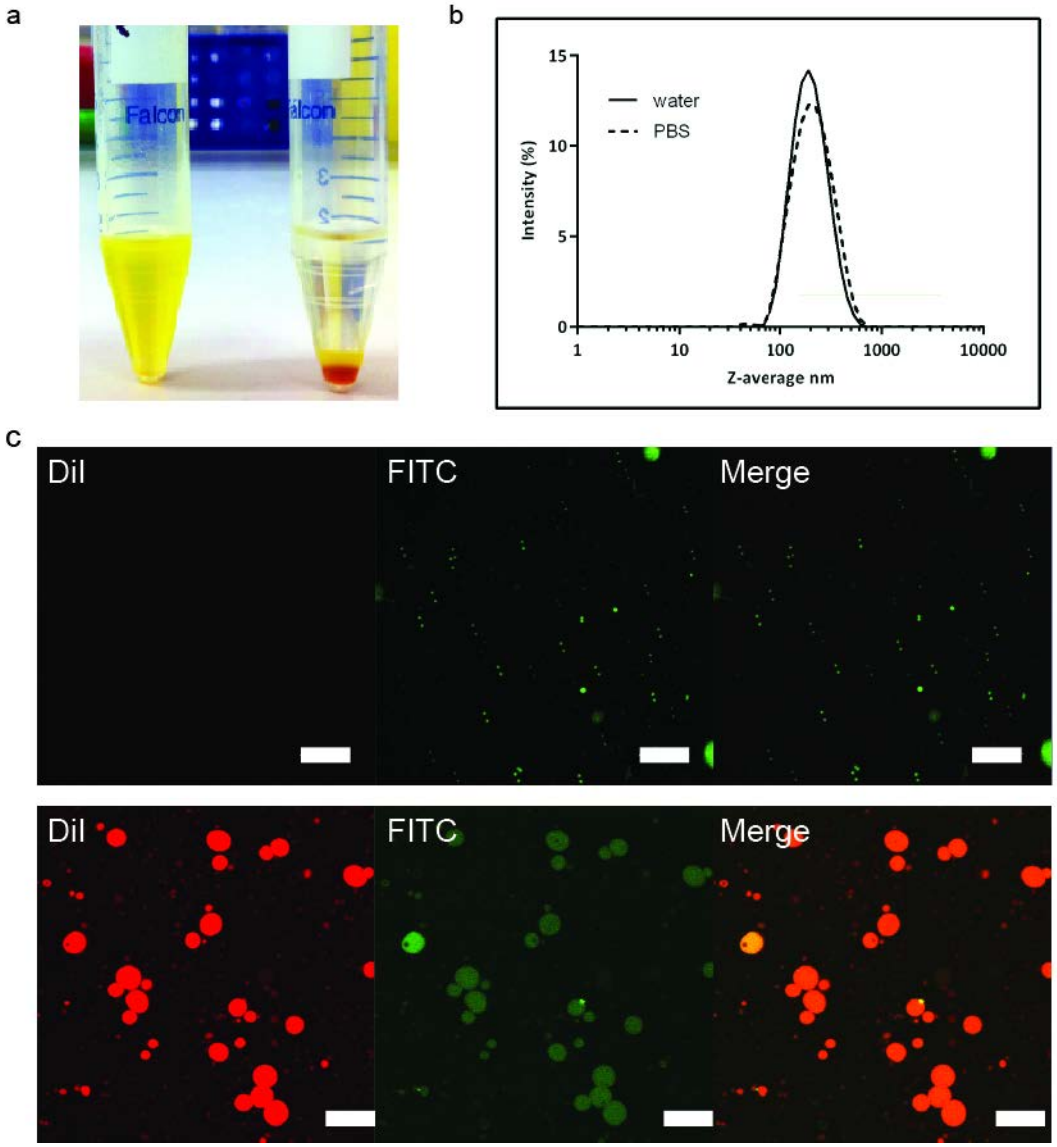

Figure 5-2. Characterization of OVA loaded TNE: a) Comparison of solubility between native FITC labeled OVA (right) and its surfactant complex (left) in Miglyol® 812; b) Particle size distribution of OVA-P_{200}-Ab-P_{20} TNE diluted in water and PBS measured by dynamic light scattering; c) Confocal images showing FITC labeled OVA (green) dissolved in oil (upper panel) or encapsulated within AM1 stabilized TNE core (lower panel), where the oil phase was pre-labeled with DiI (red). Size bar: 10 µm.

5.3.2. Dot-blot assay

Figure 5-3 shows dot blot analysis of oil-solubilized OVA-surfactant complex against commercial antibody specific to OVA antigen. Native OVA dispersed in oil, surfactant solubilized oil and oil core from surfactant encapsulated TNE were dotted as negative control. OVA-surfactant complex was first

dissolved in Miglyol® 812 to produce an OVA solid in oil (S/O) dispersion, and subsequently used as the oil phase to prepare OVA-TNE. TNE oil core was separated from the aqueous phase by high speed centrifugation. The dot blot analysis shows that both OVA S/O dispersion and the oil core from OVA-TNE were recognized by the commercial antibody, showing that the ability of OVA within the OVA-surfactant complex to be recognized by an antibody was retained. This result also demonstrated that once encapsulated within the TNE oil core, only a limited amount of lipophilic OVA-surfactant complex presented in the emulsion aqueous phase due to its limited solubility in water.

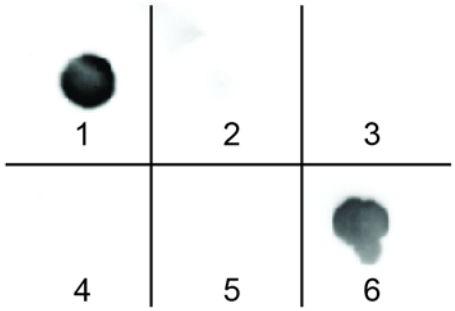

Figure 5-3. Dot blot analysis using a commercial OVA-specific antibody. Tested samples include (1) OVA-surfactant complex dissolved in Miglyol® 812 (OVA S/O dispersion); (2) Native OVA protein dispersed in oil (after centrifugation to remove aggregates); (3) Surfactant dissolved in Miglyol® 812 (negative control); (4) OVA-TNE oil core (negative control); (5) Aqueous phase of OVA-TNE (for testing residual OVA present in aqueous phase); (6) Oil phase of OVA-TNE. Only OVA S/O dispersion and OVA-TNE oil core were recognized by the commercial antibody specific to OVA, confirming appropriate loading of OVA into the oil phase of the TNE.

5.3.3. Dendritic cells response to antigen-loaded TNE

DCs are professional APCs capable of presenting exogenous antigens to cytotoxic T lymphocytes, a crucial step for the development of adaptive immunity towards infectious pathogens and tumors, which plays an important role in the elimination of cancerous cells and pathogens (Heath and Carbone, 2001). An OT-I $CD8^+$ T cell proliferation assay was performed to determine if model antigen OVA encapsulated within TNE can be correctly processed and cross-presented on MHC I via P_{200}-Ab-P_{20}-TNE, which been shown to target DCs *in vivo* (**Chapter 4**). OVA specific $CD8^+$ T cells were isolated from transgenic OT-I mice, labeled with CTV and co-cultured for 3 d with splenocytes that had been pulsed with either OVA loaded P_{200}-Ab-P_{20}-TNE (OVA- P_{200}-Ab-P_{20}-TNE) or the non-targeting P_{200}-

Isotype-P_{20}-TNE (OVA- P_{200}-Isotype-P_{20}-TNE). OT-I specific epitope $OVA_{257-264}$ peptide (SIINFEKL) was also used as a positive control. Splenocytes pulsed with SIINFEKL or OVA-P_{200}-Ab-P_{20}-TNE induced similar levels of $CD8^+$ T cell proliferation (71.4% and 77.2% T cells divided, respectively) (**Figure 5-4**). However, it is worth noting that although SIINFEKL was able to induce an OT-I T cell response, a similar level of T cell response was obtained only by using almost double the amount of native peptide (1 µg) to the one induced by OVA-P_{200}-Ab-P_{20}-TNE (containing 0.6 µg OVA protein). And as expected, splenocytes pulsed with the same amount of OVA-P_{200}-Isotype-P_{20}-TNE failed to induce T cell proliferation. These results suggest that as an antigen vehicle, P_{200}-Ab-P_{20}-TNE was superior in delivering its payload to the target subset of DCs compared to its non-targeting counterpart.

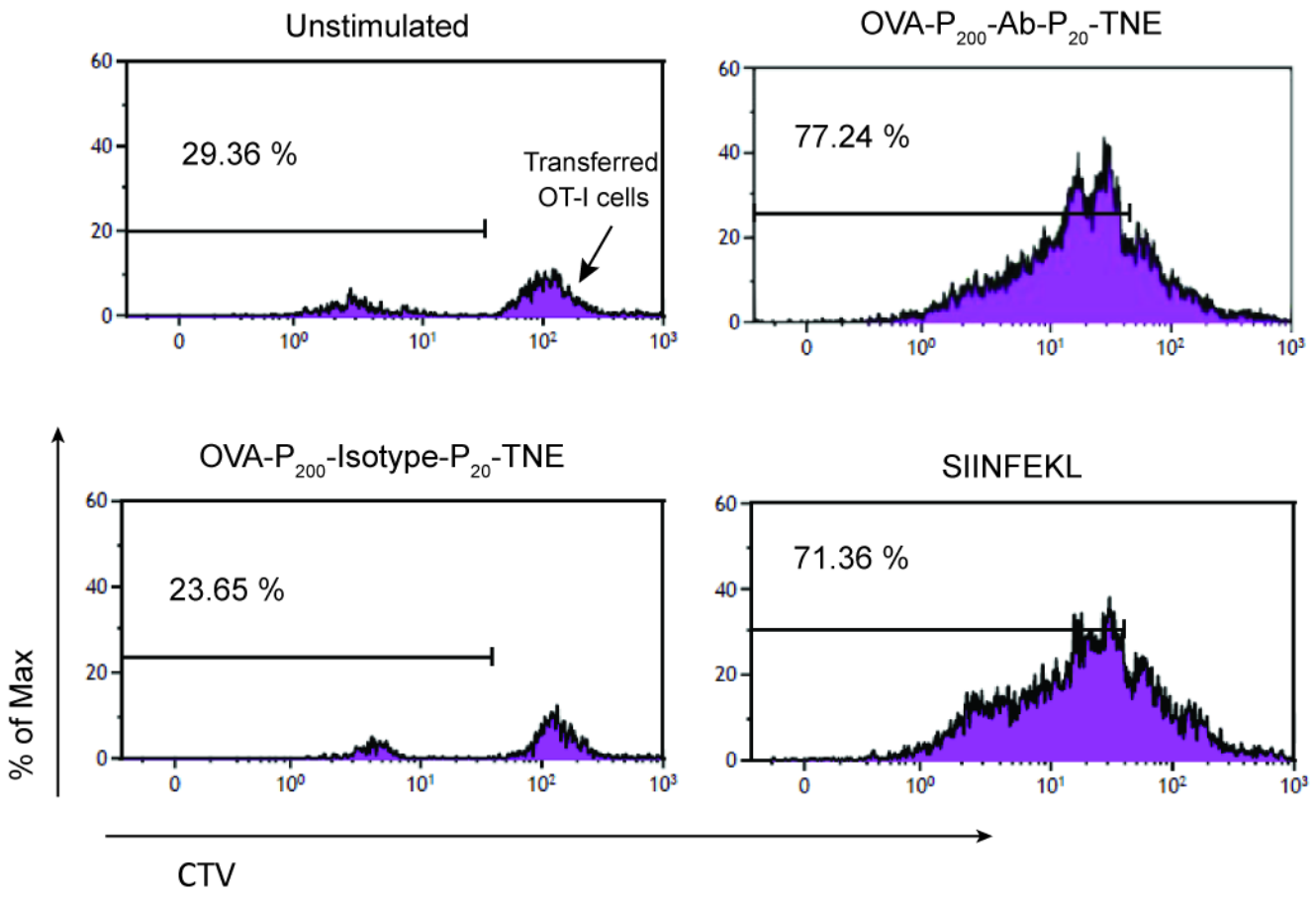

Figure 5-4. *In vitro* T cell proliferation assay. Splenocytes were pulsed with OVA (0.6 µg) loaded P_{200}-Ab-P_{20}-TNE (OVA-P_{200}-Ab-P_{20}-TNE) or P_{200}-Isotype-P_{20}-TNE (OVA-P_{200}-Isotype-P_{20}-TNE), or OVA peptide SIINFEKL (1 µg) and subsequently co-cultured with CTV labeled OT-I T cells for 4 days. T cell proliferation was assessed by dilution of CTV in the labeled T cells. Representative histogram

showing proliferation of OT-I T cells gated as MHCII-$CD3^+CD8^+$. Percentage of proliferated T cells is stated in cytograms.

5.3.4. Activation of antigen-specific $CD8^+$ T cells by OVA antigen-carrying P_{200}-Ab-P_{20}-TNE in vivo

Next we accessed whether OVA-P_{200}-Ab-P_{20}-TNE could induce an antigen-specific $CD8^+$ T cells response *in vivo*. Mice were immunized once with OVA-P_{200}-Ab-P_{20}-TNE or OVA-P_{200}-Isotype-P_{20}-TNE (both contained 2.5 µg of OVA), or left unimmunized one day after mice have been adoptively transferred with CTV-labeled OT-I T cells. Proliferation of OT-I cells was determined by the dilution of CTV fluorescence on day 4 after immunization using flow cytometry. Mice immunized with OVA-P_{200}-Ab-P_{20}-TNE displayed a significant proliferation of OVA-specific $CD8^+$ T cells (**Figure 5-5**), compared to mice that been immunized with non-targeting OVA-P_{200}-Isotype-P_{20}-TNE. In contrast, immunizing mice with OVA-P_{200}-Isotype-P_{20}-TNE did not induce noticeable OT-I T cell proliferation. Coupled with results from the *in vitro* cross presentation assay, these findings suggest that TNE was productively taken up by target $CD8^+$ DCs in a receptor-targeted fashion, and its encapsulated antigen was correctly processed and presented to $CD8^+$ T cells.

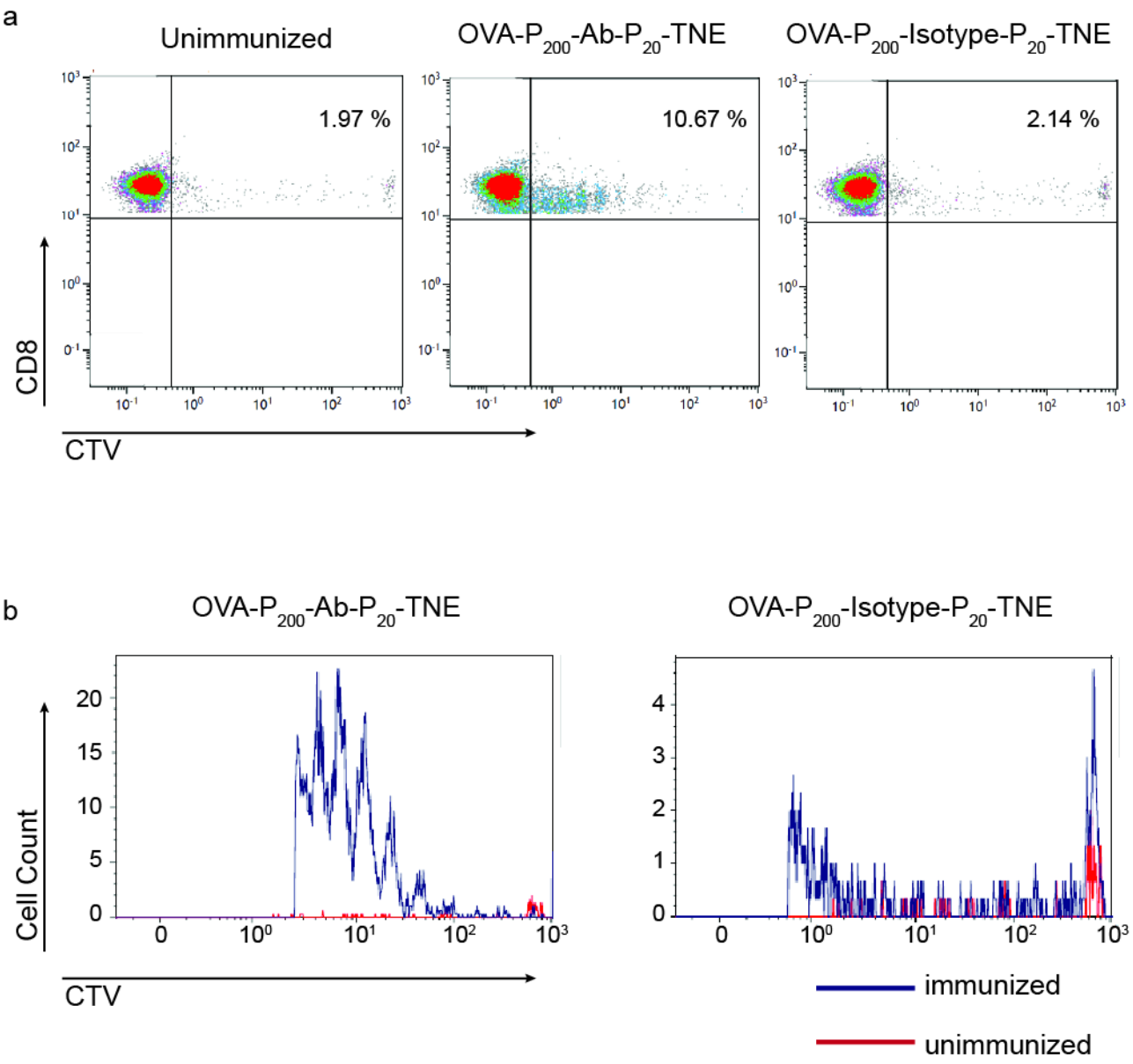

Figure 5-5. Activation of antigen-specific $CD8^+$ T cells by OVA-P_{200}-Ab-P_{20}-TNE *in vivo*. Mice were intravenously injected once with OVA-P_{200}-Ab-P_{20}-TNE or non-targeting OVA-P_{200}-Isotype-P_{20}-TNE, or left unimmunized one day after the mice had been adoptively transferred with CTV-labeled OT-I cells. Spleen cells were isolated from the mice on day 4 after immunization before staining with anti-CD3, anti-MHC II and anti-CD8 mAb. Data are expressed as (a) Flow cytometry dot plots showing the percentage of CTV^+ $CD8^+$ OT-I cells among the gated $CD3^+MHC\ II^-$ T cells as determined; The percentage of proliferated T cells is stated in each dot plot. (b) histogram showing CTV fluorescence of OT-I cells. Reduction of CTV fluorescence intensity (from right to left) depicts OVA-specific OT-I T cells proliferation.

5.4. Conclusions

Dendritic cells are considered the most effective antigen presenting cells that are professionalized in antigen uptake, processing and presentation to antigen-specific T cells (Reviewed in **Section 2.8**). Even though DCs are capable of taking up soluble proteins, peptides or DNA to induce antigen-specific immunity, these antigens alone are not sufficient to induce a potent and broad immune response. Relatively high doses of soluble proteins are needed to induce a sufficient immune response. Common methods of conjugating protein antigen to cell penetration peptide by protein engineering for intracellular delivery will potentially jeopardize the intrinsic protein function (Tahara et al., 2008). Encapsulating protein drugs within nanocarriers is an alternative and effective method for protein intracellular delivery, however most procedures require stringent conditions that may potentially compromise protein activity and are limited by the diversity of protein physiochemical properties. In **Chapters 3** and **4**, P_{200}-Ab-P_{20}-TNE that selectively targets Clec9A-expressing cells *in situ* was developed. The platform was constructed using a simple top-down sequential reagent addition method whereby stringent physiochemical preparation conditions were not required, making it an ideal carrier for delivering delicate therapeutics, *e.g.* protein, in a cell-specific manner. Hence the aim of this Chapter was to evaluate the potential of P_{200}-Ab-P_{20}-TNE as a carrier for targeting delivery of protein to DCs.

We firstly encapsulated native OVA within the TNE oil core using a S/O/W emulsification method (Tahara et al., 2008). Hydrophilic OVA was first coated with hydrophobic small molecule surfactants for increased solubility in the oil phase of emulsion. Encapsulation of protein into nanocarriers by such a method does not require any covalent conjugation that would damage the native properties. Results from dot blot assay showed that the immunogenicity of OVA protein was preserved after it had been complexed with surfactant (**Figure 5-3**). Encapsulation of OVA into TNE via S/O/W emulsification did not affect stability of the TNE in isotonic conditions (**Figure 5-2**), suggested OVA-P_{200}-Ab-P_{20}-TNE was suitable for intravenous injection.

The ability of OVA-surfactant to induce antigen specific T cell immunity was assessed first *in vitro* and then *in vivo*. We demonstrated that potent antigen presentation by DCs can be achieved, by encapsulating antigen within the DCs targeting P_{200}-Ab-P_{20}-TNE. This may be due to the unique nature

of $CD8^+$ DCs subset targeted by P_{200}-Ab-P_{20}-TNE, which are efficient in taking up exogenous antigens and cross-presenting to MHC class I (den Haan et al., 2000, Pooley et al., 2001, Schnorrer et al., 2006). Consistent with these studies, we have already shown that engineering of an mAb against $CD8^+$ DCs exclusive to surface receptor Clec9A with nanocarriers emulsion facilitating the *in situ* targeting delivery to DCs (**Chapter 4**). In this Chapter, we showed that antigen encapsulated within the targeting P_{200}-Ab-P_{20}-TNE could be correctly processed and cross-presented to antigen-specific T cells both *in vitro* and *in vivo* (**Figure 5-4 and 5-5**). As effective delivery of protein antigen is an important goal for developing vaccines for cancers and infectious disease, results in this chapter further support the hypothesis that TNE will serve as an effective DDS platform for targeting DCs. Hereby we address **Objective 4** of this PhD project as stated in **Chapter 1**.

Questions regarding whether the ability of antigen carrying TNE for inducing antigen specific T cell immunity is dependent of the TNE formulation or the amount of antigen being encapsulated and delivered to DCs is of interest of this PhD project, but yet to be addressed. Density of targeting moieties on a nanocarrier surface is important in designing effective DDS. For example, different densities of folate acid ligand on liposomal formulations have been reported in the literature for promoting association between liposome and folate receptor on cells (Shmeeda et al., 2006, Watanabe et al., 2012, Saul et al., 2003, Reddy et al., 2002, Kawano and Maitani, 2011). In the case of a TNE system, we showed the *in vitro* target specificity of TNE was decreased when increasing the PEG content on a TNE surface (**Chapter 4**), probably as the accessibility of Clec9A mAb was shielded by the increased steric hindrance of the PEG layer surrounding the TNE surface. Therefore it is important to establish the optimal density of Clec9A mAb on TNE surface *in vivo*, as such a parameter is not only crucial for designing an effective DDS, but is also important for subsequent industrial scale up as the production cost is highly related to the amount of targeting mAb required.

Targeting different DC subsets normally results in different types of immune response, *i.e.* targeting $CD8^+$ DCs is more likely to induce an antigen-specific $CD8^+$ T cell response while antigen-targeting $CD8^-$ DCs are more likely to induce a $CD4^+$ T helper cell response. However Caminschi *et al.* reported that OVA targeting to Clec9A on the $CD8^+$ DCs subsets not only led to a strong CTL response, but also induce a strong humoral immune response as a result of prolonged and efficient presentation of Ag on MHC class II (Caminschi et al., 2008). $CD4^+$ T cells play a crucial role in initiating adaptive immunity, therefore it is also worth investigating whether TNE could deliver antigen payload to DCs and induce a

comparable $CD4^+$ T cell response. In order to address the aforementioned issues, the next Chapter focuses on investigating the potential of the TNE as a tunable platform for delivering protein antigen, by evaluating the effect of Clec9A mAb density on *in vivo* cross-presentation efficiency and the ability of OVA-P_{200}-Ab-P_{20}-TNE to induce humoral immunity, with the aim to address **Objective 5** of this PhD project.

5.5. References

BAIN, B. & BRAZIL, M. 2003. Adalimumab. *Nat Rev Drug Discov,* 2**,** 693-694.

BANCHEREAU, J., BRIERE, F., CAUX, C., DAVOUST, J., LEBECQUE, S., LIU, Y.-J., PULENDRAN, B. & PALUCKA, K. 2000. Immunobiology of Dendritic Cells. *Annual review of immunology,* 18**,** 767-811.

BAREFORD, L. M. & SWAAN, P. W. 2007. Endocytic mechanisms for targeted drug delivery. *Advanced Drug Delivery Reviews,* 59**,** 748-758.

CAMINSCHI, I., PROIETTO, A. I., AHMET, F., KITSOULIS, S., TEH, J. S., LO, J. C. Y., RIZZITELLI, A., WU, L., VREMEC, D., VAN DOMMELEN, S. L. H., CAMPBELL, I. K., MARASKOVSKY, E., BRALEY, H., DAVEY, G. M., MOTTRAM, P., DE VELDE, N. V., JENSEN, K., LEW, A. M., WRIGHT, M. D., HEATH, W. R., SHORTMAN, K. & LAHOUD, M. H. 2008. The dendritic cell subtype-restricted C-type lectin Clec9A is a target for vaccine enhancement. *Blood,* 112**,** 3264-3273.

CARTER, P. J. 2011. Introduction to current and future protein therapeutics: A protein engineering perspective. *Experimental Cell Research,* 317**,** 1261-1269.

CHOU, L. Y. T., MING, K. & CHAN, W. C. W. 2011. Strategies for the intracellular delivery of nanoparticles. *Chemical Society reviews,* 40**,** 233-245.

CHUAN, Y. P., ZENG, B. Y., O'SULLIVAN, B., THOMAS, R. & MIDDELBERG, A. P. J. 2011. Co-delivery of antigen and a lipophilic anti-inflammatory drug to cells via a tailorable nanocarrier emulsion. *Journal of Colloid and Interface Science,* 368**,** 616-624.

DALKARA, D., CHANDRASHEKHAR, C. & ZUBER, G. 2006. Intracellular protein delivery with a dimerizable amphiphile for improved complex stability and prolonged protein release in the cytoplasm of adherent cell lines. *Journal of Controlled Release,* 116**,** 353-359.

DEN HAAN, J. M., LEHAR, S. M. & BEVAN, M. J. 2000. CD8(+) but not CD8(-) dendritic cells cross-prime cytotoxic T cells in vivo. *The Journal of Experimental Medicine,* 192**,** 1685-1695.

FARAJI, A. H. & WIPF, P. 2009. Nanoparticles in cellular drug delivery. *Bioorganic & Medicinal Chemistry,* 17**,** 2950-2962.

FOLTOPOULOU, P. F., TSIFTSOGLOU, A. S., BONOVOLIAS, I. D., INGENDOH, A. T. & PAPADOPOULOU, L. C. 2010. Intracellular delivery of full length recombinant human mitochondrial L-Sco2 protein into the mitochondria of permanent cell lines and SCO2 deficient patient's primary cells. *BIOCHIMICA ET BIOPHYSICA ACTA-MOLECULAR BASIS OF DISEASE,* 1802**,** 497-508.

FONTENEAU, J. F., KAVANAGH, D. G., LIRVALL, M., SANDERS, C., COVER, T. L., BHARDWAJ, N. & LARSSON, M. 2003. Characterization of the MHC class I cross-presentation pathway for cell-associated antigens by human dendritic cells. *Blood,* 102**,** 4448-4455.

GABERC-POREKAR, V., ZORE, I., PODOBNIK, B. & MENART, V. 2008. Obstacles and pitfalls in the PEGylation of therapeutic proteins. *CURRENT OPINION IN DRUG DISCOVERY & DEVELOPMENT,* 11**,** 242-250.

GAO, G. H., PARK, M. J., LI, Y., IM, G. H., KIM, J.-H., KIM, H. N., LEE, J. W., JEON, P., BANG, O. Y., LEE, J. H. & LEE, D. S. 2012. The use of pH-sensitive positively charged polymeric micelles for protein delivery. *Biomaterials,* 33**,** 9157-9164.

GAO, J. & XU, B. 2009. Applications of nanomaterials inside cells. *Nano Today,* 4**,** 37-51.

GU, Z., BISWAS, A., ZHAO, M. & TANG, Y. 2011. Tailoring nanocarriers for intracellular protein delivery. *Chemical Society reviews,* 40**,** 3638-3655.

GU, Z., YAN, M., HU, B., JOO, K.-I., BISWAS, A., HUANG, Y., LU, Y., WANG, P. & TANG, Y. 2009. Protein Nanocapsule Weaved with Enzymatically Degradable Polymeric Network. *Nano Letters,* 9**,** 4533-4538.

HEATH, W. R. & CARBONE, F. R. 2001. Cross-presentation, dendritic cells, tolerance and immunity. *Annual review of immunology,* 19**,** 47.

HUGGETT, B. 2013. Public biotech 2012[mdash]the numbers. *Nat Biotech,* 31**,** 697-703.

JO, D., LIU, D., YAO, S., COLLINS, R. D. & HAWIGER, J. 2005. Intracellular protein therapy with SOCS3 inhibits inflammation and apoptosis. *Nature medicine,* 11**,** 892-898.

KABANOV, A. V. & VINOGRADOV, S. V. 2009. Nanogels as Pharmaceutical Carriers: Finite Networks of Infinite Capabilities. *Angewandte Chemie International Edition,* 48**,** 5418-5429.

KAWANO, K. & MAITANI, Y. 2011. Effects of polyethylene glycol spacer length and ligand density on folate receptor targeting of liposomal Doxorubicin in vitro. *Journal of Drug Delivery,* 2011**,** 160967-6.

LEADER, B., BACA, Q. J. & GOLAN, D. E. 2008. Protein therapeutics: a summary and pharmacological classification. *Nat Rev Drug Discov,* 7**,** 21-39.

LEE, Y., ISHII, T., CABRAL, H., KIM, H. J., SEO, J.-H., NISHIYAMA, N., OSHIMA, H., OSADA, K. & KATAOKA, K. 2009. Charge-Conversional Polyionic Complex Micelles—Efficient Nanocarriers for Protein Delivery into Cytoplasm. *Angewandte Chemie International Edition,* 48**,** 5309-5312.

LIGUORI, L., MARQUES, B., VILLEGAS-MENDEZ, A., ROTHE, R. & LENORMAND, J.-L. 2008. Liposomes-mediated delivery of pro-apoptotic therapeutic membrane proteins. *Journal of Controlled Release,* 126**,** 217-227.

OGAWA, T., DATE, I., ONO, S., ICHIKAWA, T., ARIMITSU, S., ONODA, K., TOKUNAGA, K., SUGIU, K., TOMIZAWA, K. & MATSUI, H. 2009. Protein transduction method for cerebrovascular disorders. *Acta medica Okayama,* 63**,** 1-7.

PEER, D., KARP, J. M., HONG, S., FAROKHZAD, O. C., MARGALIT, R. & LANGER, R. 2007. Nanocarriers as an emerging platform for cancer therapy. *Nat. Nanotechnol.,* 2**,** 751-760.

POOLEY, J. L., HEATH, W. R. & SHORTMAN, K. 2001. Cutting edge: intravenous soluble antigen is presented to CD4 T cells by CD8- dendritic cells, but cross-presented to CD8 T cells by CD8+ dendritic cells. *Journal of immunology (Baltimore, Md. : 1950),* 166**,** 5327-5330.

REDDY, J. A., ABBURI, C., HOFLAND, H., HOWARD, S. J., VLAHOV, I., WILS, P. & LEAMON, C. P. 2002. Folate-targeted, cationic liposome-mediated gene transfer into disseminated peritoneal tumors. *Gene therapy,* 9**,** 1542-1550.

REN, J., ZHANG, Y., ZHANG, J., GAO, H., LIU, G., MA, R., AN, Y., KONG, D. & SHI, L. 2013. pH/Sugar Dual Responsive Core-Cross-Linked PIC Micelles for Enhanced Intracellular Protein Delivery. *Biomacromolecules*.

SAUL, J. M., ANNAPRAGADA, A., NATARAJAN, J. V. & BELLAMKONDA, R. V. 2003. Controlled targeting of liposomal doxorubicin via the folate receptor in vitro. *Journal of Controlled Release,* 92**,** 49-67.

SCHNORRER, P., MARASKOVSKY, E., BELZ, G. T., CARBONE, F. R., SHORTMAN, K., HEATH, W. R., VILLADANGOS, J. A., BEHRENS, G. M. N., WILSON, N. S., POOLEY, J. L., SMITH, C. M., EL-SUKKARI, D., DAVEY, G., KUPRESANIN, F. & LI, M. 2006. The dominant role of CD8+ dendritic cells in cross-presentation is not dictated by antigen capture. *Proceedings of the National Academy of Sciences of the United States of America,* 103**,** 10729-10734.

SHMEEDA, H., MAK, L., TZEMACH, D., ASTRAHAN, P., TARSHISH, M. & GABIZON, A. 2006. Intracellular uptake and intracavitary targeting of folate-conjugated liposomes in a mouse

lymphoma model with up-regulated folate receptors. *Molecular Cancer Therapeutics,* 5**,** 818-824.

SOLARO, R. 2008. Targeted delivery of proteins by nanosized carriers. *Journal of Polymer Science Part A: Polymer Chemistry,* 46**,** 1-11.

STUART, M. A. C., HUCK, W. T. S., GENZER, J., MULLER, M., OBER, C., STAMM, M., SUKHORUKOV, G. B., SZLEIFER, I., TSUKRUK, V. V., URBAN, M., WINNIK, F., ZAUSCHER, S., LUZINOV, I. & MINKO, S. 2010. Emerging applications of stimuli-responsive polymer materials. *Nat Mater,* 9**,** 101-113.

TAHARA, Y., HONDA, S., KAMIYA, N., PIAO, H., HIRATA, A., HAYAKAWA, E., FUJII, T. & GOTO, M. 2008. A solid-in-oil nanodispersion for transcutaneous protein delivery. *Journal of Controlled Release,* 131**,** 14-18.

TANG, R., KIM, C. S., SOLFIELL, D. J., RANA, S., MOUT, R., VELÁZQUEZ-DELGADO, E. M., CHOMPOOSOR, A., JEONG, Y., YAN, B., ZHU, Z.-J., KIM, C., HARDY, J. A. & ROTELLO, V. M. 2013. Direct Delivery of Functional Proteins and Enzymes to the Cytosol Using Nanoparticle-Stabilized Nanocapsules. *ACS Nano,* 7**,** 6667-6673.

TORCHILIN, V. P. 2006. Recent Approaches to Intracellular Delivery of Drugs and DNA and Organelle Targeting. *Annual Review of Biomedical Engineering,* 8**,** 343-375.

VLIEGHE, P., LISOWSKI, V., MARTINEZ, J. & KHRESTCHATISKY, M. 2010. Synthetic therapeutic peptides: science and market. *Drug Discovery Today,* 15**,** 40-56.

WATANABE, K., KANEKO, M. & MAITANI, Y. 2012. Functional coating of liposomes using a folate- polymer conjugate to target folate receptors. *International Journal of Nanomedicine,* 7**,** 3679-3688.

YAN, M., DU, J., GU, Z., LIANG, M., HU, Y., ZHANG, W., PRICEMAN, S., WU, L., ZHOU, Z. H., LIU, Z., SEGURA, T., TANG, Y. & LU, Y. 2010. A novel intracellular protein delivery platform based on single-protein nanocapsules. *Nat Nano,* 5**,** 48-53.

YARDEN, Y. & SLIWKOWSKI, M. X. 2001. Untangling the ErbB signalling network. *NATURE REVIEWS MOLECULAR CELL BIOLOGY,* 2**,** 127-137.

ZELPHATI, O., WANG, Y., KITADA, S., REED, J. C., FELGNER, P. L. & CORBEIL, J. 2001. Intracellular Delivery of Proteins with a New Lipid-mediated Delivery System. *Journal of Biological Chemistry,* 276**,** 35103-35110.

ZENG, B. J., CHUAN, Y. P., O'SULLIVAN, B., CAMINSCHI, I., LAHOUD, M. H., THOMAS, R. & MIDDELBERG, A. P. J. 2013. Receptor-Specific Delivery of Protein Antigen to Dendritic Cells by a Nanoemulsion Formed Using Top-Down Non-Covalent Click Self-Assembly. *Small*.

ZHANG, Y. & YU, L.-C. 2008. Microinjection as a tool of mechanical delivery. *Current Opinion in Biotechnology,* 19**,** 506-510.

Chapter 6 Efficient Targeting of protein antigen to dendritic cells via receptor Clec9A with an engineered nanoemulsion promotes potent antibody and cytotoxic T cell responses

Chapter 6 is comprised entirely of the manuscript written for the submission to Journal of Controlled Release.

Efficient targeting of protein antigen to dendritic cell receptor Clec9A with an engineered nanoemulsion promotes potent antibody and cytotoxic T cell responses

B.J.Zeng [a,d], A.P.J. Middelberg [a], I. Caminschi [c], M.H. Lahoud [c], R. Thomas [d]*

[a] Australian Institute for Bioengineering and Nanotechnology, The University of Queensland, St Lucia, QLD 4072, Australia

[b] Centre for Immunology, Burnet Institute, Melbourne, VIC 3004, Australia

[c] The Walter and Eliza Hall Institute of Medical Research, Parkville, VIC 3052, Australia

[d] Diamantina Institute, Translational Research Institute, The University of Queensland, Woolloongabba, QLD 4102, Australia

Abstract Eliciting potent antibody production and an efficacious cytotoxic T cell response represent major challenges in the field of modern vaccine development. Nanocarrier-based antigen delivery systems have great potential as an effective strategy to improve the efficacy of vaccines in order to deliver protein antigen to dendritic cell targets. In the present study, we developed a tailorable nanocarriers emulsion (TNE) encapsulated with a model protein antigen ovalbumin (OVA), termed OVA-P_{200}-Ab-P_{20}-TNE. Soluble protein antigen was encapsulated within the oil core of the emulsion by using a solid-in-oil (S/O) nanodispersion method. The emulsion oil core of the TNE was functionalized with immune-evading polymer PEG and an antibody directed against the $CD8^+$ dendritic cell-specific ligand, Clec9A, using a novel non-covalent click chemistry method involving molecular self-assembly at the oil-aqueous interface. Immunizing mice with OVA-P_{200}-Ab-P_{20}-TNE induced the proliferation of both $CD4^+$ and $CD8^+$ T cells *in vivo* and strong CTL and humoral responses, in the absence of adjuvant. These results suggest TNE is an ideal system for targeting delivery of protein antigen for induction of cell mediated immunity.

1. Introduction

Dendritic cells (DCs) are the mobile sentinels of the immune system and specialize in the capture, processing and presenting antigen to T cells via MHC I or II pathway [1]. DCs play a central role in the induction and the regulation of T- and B-cell immunity. The interaction between DCs and T cells regulates the type and magnitude of the immune response [2, 3]. Increased understanding of DC biology has inspired novel vaccines using DCs as a target for antigen (Ag) delivery, and thereby manipulating T cell responses [4, 5]. Since different subsets of DCs have distinct patterns of surface markers [6, 7], current approaches for targeting DCs include ligating Ag to monoclonal antibodies (mAbs) that specifically recognize exclusive DC subsets *in situ*. Such approach relies on a choice of suitable DC surface receptors that mediate endocytosis of bound mAb, allowing Ag to be delivered to endosomal compartments and subsequently processed for MHC presentation. To date, several DC-specific endocytic receptors have been identified, including DEC205, CD207, Clec9A and Clec12A [8-11]. Among these receptors, Clec9A or DNGR is a C-type lectin receptor expressed by $CD8\alpha^+$ DCs in mouse and $BDCA3^+$ DCs in humans. In vivo, Clec9A organizes the processing and cross-presentation of dead cell and viral antigens by MHC class I for efficient induction of cytotoxic T lymphocytes (CTLs) [12, 13]. DC-targeting using the anti-Clec9A mAb clone induces efficient antigen processing and presentation in the context of MHC class I and II to induce CD4 and CD8 proliferative responses, T follicular helper cell development and potent humoral immunity [10, 14-16].

While protein antigens ligated to Clec9A or DEC205 mAb enhanced vaccine immunogenicity, studies also found that such delivery of Ag to DCs failed to induce strong antigen-specific effector CTLs, which are essential for tumor- or infected cell-clearance, unless additional stimuli or adjuvant was applied to activate DCs for the production of co-stimulatory molecules for adequate CTL generation [11, 15, 17-19]. These findings led to the hypothesis that vaccine efficacy can be further improved by simultaneously delivering multiple vaccine components to DCs. However, options for linking a DC-specific mAb to multiple vaccine components, e.g. antigen and immune modulators, are limited. To this end, nanotechnology provides a great tool for designing better vaccines. Nanocarrier systems loaded with multiple vaccine components provide an attractive alternative to overcome the limitations of current DC-based vaccine approaches. Several types of nanocarriers have been used as vaccine carriers to entrap antigens or as adjuvant alone [20-23]. Nanocarriers are considered to be an effective vehicle for delivering antigen and have been widely investigated for their biological potential [24, 25]. Compared to its soluble counterparts, concentrated antigen and immune modulatory factors can be

encapsulated within the internal compartment of nanocarriers to avoid in vivo enzymatic degradation and to allow controlled release; targeting delivery to DCs can be facilitated by surface engineering with a DC-specific ligand. Antigen encapsulated nanocarrier systems can mimic pathogens that are recognized by professional antigen presenting cells, such as DCs and macrophages, and their subsequent processing and cross-presentation for initiating T cell immunity more efficiently.

Oil in water nanoemulsion systems have been widely used as clinical vaccine adjuvants [26-28]. Nanoemulsions have shown low toxicity and no significant adverse effect in humans [29, 30]. Nevertheless, wide adoption of nanoemulsion as a drug delivery system (DDS) into clinical applications requires these platforms to encode more sophisticated functions, such as combined long circulation half-life and in vivo targeting ability. The in vivo fate of intravenously injected nanocarriers is dictated by their physical parameters such as size, surface charge and coating [31, 32]. In particular, pharmacokinetics and bioavailability as well as the nanocarrier's ability to target a biological site are highly influenced by their surface coating [33]. Nanocarriers in the blood stream will be rapidly captured by the mononuclear phagocyte system (MPS) and directed to clearance organs like the liver and spleen. Modifying the nanocarrier surface with hydrophilic polymer such as polyethylene glycol (PEG) is an effective way to increase stealthiness, which is the ability to escape capture by the MPS. as PEG can create a steric barrier to reduce opsonization [34]. In addition, target-specific molecules can be engineered onto the nanocarrier's surface for enhanced cellular delivery. However, exposure of the targeting moieties on the nanocarrier's surface may counteract the shielding effect of the polymeric coating. Therefore it is vital to maintain a balance between these two categories of functional moieties on the surface of the nanocarrier.

We recently reported a tailorable nanocarrier emulsion (TNE) for target specific delivery of antigen to DCs [35]. Harnessing the chemical similarity between two surface active peptides and their self-assemble properties, the reported TNE was grafted with immune evading polymer PEG, which provides a steric repulsive barrier protecting the TNE from non-specific cell association. To facilitate the target specificity, anti-Clec9A mAb was also grafted onto the nanoemulsion surface using the same non-covalent click self-assemble approach. Our studies show that intraperitoneally injected TNE was able to evade the non-specific phagocytosis in blood stream and renal clearance, and was well distributed within Clec9A expressing $CD8^+$ cDCs in mouse. Moreover, OVA encapsulated within the TNE oil core induced OVA-specific $CD8^+$ T cell responses in vitro [32].

The aforementioned results, besides a promising platform nanocarrier technology, raised the question of whether Ag encapsulated within TNE could be efficiently cross-presented in the more complicated in vivo environment, which is pivotal for success of protein-based vaccines. Nanocarriers that specifically target DC-specific receptors for improved in vitro uptake have been reported, however there are few comprehensive studies demonstrating enhanced in vivo $CD8^+$ T cell activation and antigen-specific CTL responses [36, 37]. It is also been reported that the cellular association of DC-targeting nanocarriers can be influenced by ligand density on surface, and cell association can be improved with an optimal surface density [38, 39]. In this study, we examined whether OVA antigen delivered to DCs via this TNE induces $CD4^+$ and $CD8^+$ CTL cell responses in vivo. We show that OVA-encapsulated TNE target the $Clec9A^+$ DC subset, and effectively induce OVA-specific effector CTLs and Ab responses.

2. Materials and methods

2.1. Materials

AM1 (molar mass 2473, 95% purity) was custom synthesized by Genscript (Piscataway, NJ, USA) as reported previously [40]. Peptide concentration was determined by quantitative amino-acid analysis (Australian Proteome Analysis Facility, Sydney, NSW, Australia). Miglyol® 812 was purchased from AXO Industry SA (Wavre, Belgium). CellTrace™ Violet (CTV) was purchased from Molecular Probes (Victoria, Australia). 4-(2-hydroxyethyl)-1-piperazineethanesulfonic acid (HEPES), albumin from chicken egg white (OVA) and zinc chloride ($ZnCl_2$) were purchased from Sigma-Aldrich (St Louis, MO, USA). mPEG-NHS (MW 5000, PDI <1.08, purity > 95%) was purchased from Nanocs (Boston, MA, USA). RPMI-1640 and fetal calf serum (FCS) were purchased from GIBCO (Victoria, Australia). FITC-anti-CD3, APC/Cy7-anti-CD8, PE-anti-CD45.2 and PerCP5.5-anti-MHCII and APC-anti-CD4 were purchased from Biolegend (San Diego, CA, USA). Cithrol™ GMO HP was a gift from Croda Europe Ltd (Staffordshire, United Kingdom). DAMP4 fused with antibody (mAb-DAMP4) was provided by Dr. Irina Caminschi and Dr. Mireille Lahoud at the Burnet Institute (Melbourne, Australia) and was prepared using published protocol [10, 15].

2.2. Mice

Mice were purchased from the Animal Research Centre (Perth, WA) or bred at the Diamantina Institute Biological Research Facility (BRF) at The University of Queensland under specific pathogen-free conditions. Experiments were approved by the UQ Animal Ethics Committee (ethics number 465/12).

2.3. Preparation of OVA in oil dispersion

OVA solution (10 mg mL^{-1}) was prepared by dissolving endotoxin free OVA protein (MW 45 kDa, 100 mg) in ultrapure water (10 mL). Cithrol^{TM} GMO HP solution (1%, w/v) was prepared by dissolving Cithrol^{TM} GMO HP (200 mg) in hexane (20 mL). OVA solution (1 mL) and Cithrol^{TM} GMO HP solution (2 mL) were transferred into a 20 mL glass vial, and mixed by using a sonicator (Branson Sonifier® S-450A, Danbury, United State) 1 min at 20 W to form stable water in oil (w/o) emulsion. The resulting emulsion was frozen rapidly in dry ice for 2 h before being lyophilized for 24 h. The resulting OVA-Cithrol GMO HP pellet was dissolved in Miglyol 812 (2 mL) to a final concentration of 5 mg ml^{-1} of OVA, and used as oil phase for preparing OVA-P_{200}-Ab-P_{20}-TNE and OVA-P_{200}-Isotype-P_{20}-TNE.

2.4. TNE preparation and characterization

To prepare TNE core, lyophilized AM1 (400 µM) was dissolved in 980 µL HEPES (25 mM, pH 7.0) containing $ZnCl_2$ (800 µM). Twenty microliter of Miglyol 812 was added to give an oil volume fraction of 2% (v/v). The mixture was homogenized using a Branson Sonifier 450A ultrasonicator for four 45 s bursts at 60 W. To prepare P_{20}-TNE, TNE (500 µL) was added to PEGylated DAMP4 solution (500 µL, 40 µM) followed by 60 s of vigorous stirring using a magnetic stirrer. For preparation of P_{200}-Ab-P_{20}-TNE, mAb-DAMP4 (36 µL, 3 µM) was added to P_{20}-TNE (200 µL) followed by 60 seconds of vigorous stirring using a magnetic stirrer, and subsequently Ab-P_{20}-TNE (200 µL) was added to PEGylated DAMP4 (200 µL, 400 µM), followed by 60 seconds of vigorous stirring. The final concentration of OVA in OVA-P_{200}-Ab-P_{20}-TNE was 0.56 µM.

TNE size was measured by Malvern Zetasizer Nano ZS (Malvern, Worcestershire, UK) equipped with a He-Ne laser (633 nm). Data analysis was with DTS software (Malvern, version 6.2), used the non-negativity constrained least squares (NNLS) fitting algorithm. Dispersant refractive index and viscosity

of the dispersant were assumed to be 1.45 and 1.02 cP, respectively. For each sample, 10 runs of 10s were performed.

2.5. In vivo proliferation assays of transgenic T cells

B6.SJL-Ptprc^{a} mice were injected i.v. with 3×10^{6} CTV labelled lymph node cells harvested from OT-I or OT-II transgenic mice. One day later, these recipient mice were injected i.v. with 200 µL of OVA-P_{200}-Ab-P_{20}-TNE or OVA-P_{200}-Isotype-P_{20}-TNE (both formulated with 5 µg of OVA). 200 µL of empty P_{200}-Ab-P_{20}-TNE or 5 µg of soluble OVA protein were also injected i.v. into control mice. Mice were sacrificed 4 days later, and the proliferation of $CD3^{+}CD45.2^{+}CD8^{+}$ OT-I or $CD3^{+}CD45.2^{+}CD4^{+}$ OT-II T cells was visualized by dilution of CTV fluorescence.

In the Tuneable $CD8^{+}$ T cells Response experiment, TNE samples were prepared following the same protocol detailed in Section 2.4, with the modification of using different concentrations of mAb-DAMP4 to prepare P_{200}-Ab-P_{20}-TNE. Serial dilutions of 3 µM mAb-DAMP4 stock solution were made to obtain mAb-DAMP4 at concentrations of 1.5, 0.75 and 0.38 µM individually. Thirty-six microliters of 3, 1.5, 0.75 or 0.38 µM mAb-DAMP4 was added to P_{20}-TNE (200 µL) followed by 60 seconds of vigorous stirring using a magnetic stirrer, and subsequently Ab-P_{20}-TNE (200 µL) was added to PEGylated DAMP4 (200 µL, 400 µM), followed by 60 seconds of vigorous stirring to obtain P_{200}-Ab-P_{20}-TNE with mAb-DAMP4 content at 0.27, 0.14, 0.07 or 0.03 µM respectively (based on the overall solution volume). The ratio of Ag to mAb was calculated by using the molar concentration of OVA protein in P_{200}-Ab-P_{20}-TNE (0.56 µM) divided by the molar concentration of mAb-DAMP4 added to the individual P_{200}-Ab-P_{20}-TNE formulations.

2.6. In vivo cytotoxic T lymphocyte (CTL) assay

Recipient C57BL/6 mice were primed by i.v. injection of 200 µL of OVA-P_{200}-Ab-P_{20}-TNE or OVA-P_{200}-Isotype-P_{20}-TNE (both formulated with 5 µg of OVA) five days earlier. Empty P_{200}-Ab-P_{20}-TNE and soluble OVA (100 µg) were also injected to control mice. To prepare CTL targets in our in vivo CTL assay, single cell suspensions of splenocytes from C57Bl/6 mice were depleted of red cells and divided equally into two parts. Half of the splenocyte suspension (CTV^{high} population) was pulsed with $OVA_{257-264}$ (1 µg mL^{-1}) and labeled with CTV (5 µM); and the other half of the splenocytes (CTV^{low}

population) was labeled with CTV (0.5 μM). Equal numbers of cells from each population were pooled and 10^7 cells were injected i.v. into recipient mice. Twenty hours post injection, lymph nodes (LN) and spleens were harvested from the mice and the relative proportion of CTV^{high} to CTV^{low} cells was determined by flow cytometry using a Beckman Coulter Gallios™ flow cytometer and analysed using Kaluza® software. Percentage (%) specific lysis in vivo was calculated by [1-(*r* unprimed/*r* primed)] × 100, where *r* = % CTV^{low} / % CTV^{high} for each mouse.

2.7. Immunization using OVA-P200-Ab-P20-TNE and Clec9A-OVA

Constructs of OVA conjugated to anti-Clec9A mAb (Clec9A-OVA) or isotype mAb (Isotype-OVA) were provided by Dr. Irina Caminschi and Dr. Mireille Lahoud at the Burnet Institute (Melbourne, Australia) and were prepared using published protocols[10, 15]. C57Bl/6 mice were injected i.v. with 5 μg of Clec9A-OVA or OVA-P_{200}-Ab-P_{20}-TNE. Isotype-OVA, OVA-P_{200}-Isotype-P_{20}-TNE or PBS was also injected to control mice in the absence of adjuvant. Serum anti-OVA Ig reactivity was measured 1, 2 and 3 wk later by ELISA as previously described [10].

3. Results

3.1. Preparation and Characterization of OVA-encapsulated TNE

We determined the particle size of the prepared OVA-P_{200}-Ab-P_{20} by dynamic light scattering (DLS). **Figure 1** shows OVA-P_{200}-Ab-P_{20} had a similar size distribution of 187.1 ± 2 nm and 189.3 ± 4 nm, when diluted in water and isotonic PBS respectively. As stability of nanocarriers in physiological conditions is a pre-requisite for effective cellular targeting, this result suggests OVA-P_{200}-Ab-P_{20} is stable in physiological environment and suitable for i.v. injection.

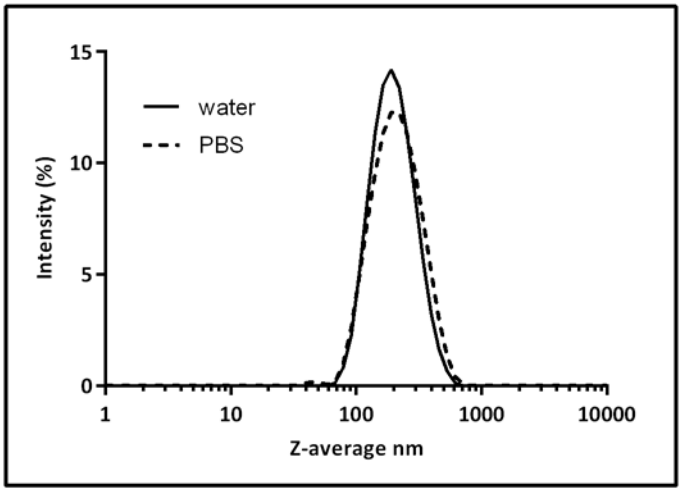

Figure 1. Particle size distribution of OVA-P_{200}-Ab-P_{20} TNE diluted in water and PBS measured by dynamic light scattering (DLS).

3.2. TNE delivers Ag to $CD8^+$ T cells

We demonstrated that OVA-P_{200}-Ab-P_{20}-TNE could induce $CD8^+$ T cell proliferation in vitro [35]. Here we investigated whether an antigen encapsulated within P_{200}-Ab-P_{20} could be delivered in vivo to $Clec9A^+CD8^+$ DCs with subsequent processing and cross-presentation to Ag-specific $CD8^+$ T cells. B6.SJL-*Ptprc*^{a} mice were adoptively transferred with CTV-labelled lymph node cells from $OVA_{257-264}$ epitope-specific OT-I TCR transgenic mice. One day later, these mice were immunized i.v. with OVA-P_{200}-Isotype-P_{20}-TNE or OVA-P_{200}-Ab-P_{20}-TNE. Empty P_{200}-Ab-P_{20}-TNE or soluble OVA protein (5 µg) in an amount equivalent to that encapsulated in TNE were injected i.v. to control mice. Seven days later the $CD8^+$ OT-I T cell response was determined as the dilution in CTV fluorescence intensity, and the expansion of $CD8^+$ OT-I cells identified by CD45.2 staining. Substantial levels of OT-I T cell proliferation were observed both in LN and spleen from mice immunized with OVA-P_{200}-Ab-P_{20}-TNE or equivalent amounts of soluble OVA (**Figure 2**). Immunization of mice with OVA-P_{200}-Ab-P_{20}-TNE resulted in significantly higher levels of OT-I T cell proliferation relative to mice treated with equivalent amounts of soluble OVA without adjuvant (**Figure 2b-d**). In contrast, OVA-P_{200}-Isotype-P_{20}-TNE, prepared using the same process but engineered with an isotype targeting mAb, and empty P_{200}-Ab-P_{20}-TNE, did not induce OT-I T cell proliferation (**Figure 2b-d**). This result indicates that the P_{200}-Ab-P_{20} TNE effectively induce OVA-specific $CD8^+$ T cell proliferation in a manner dependent on Clec9A targeting of APCs.

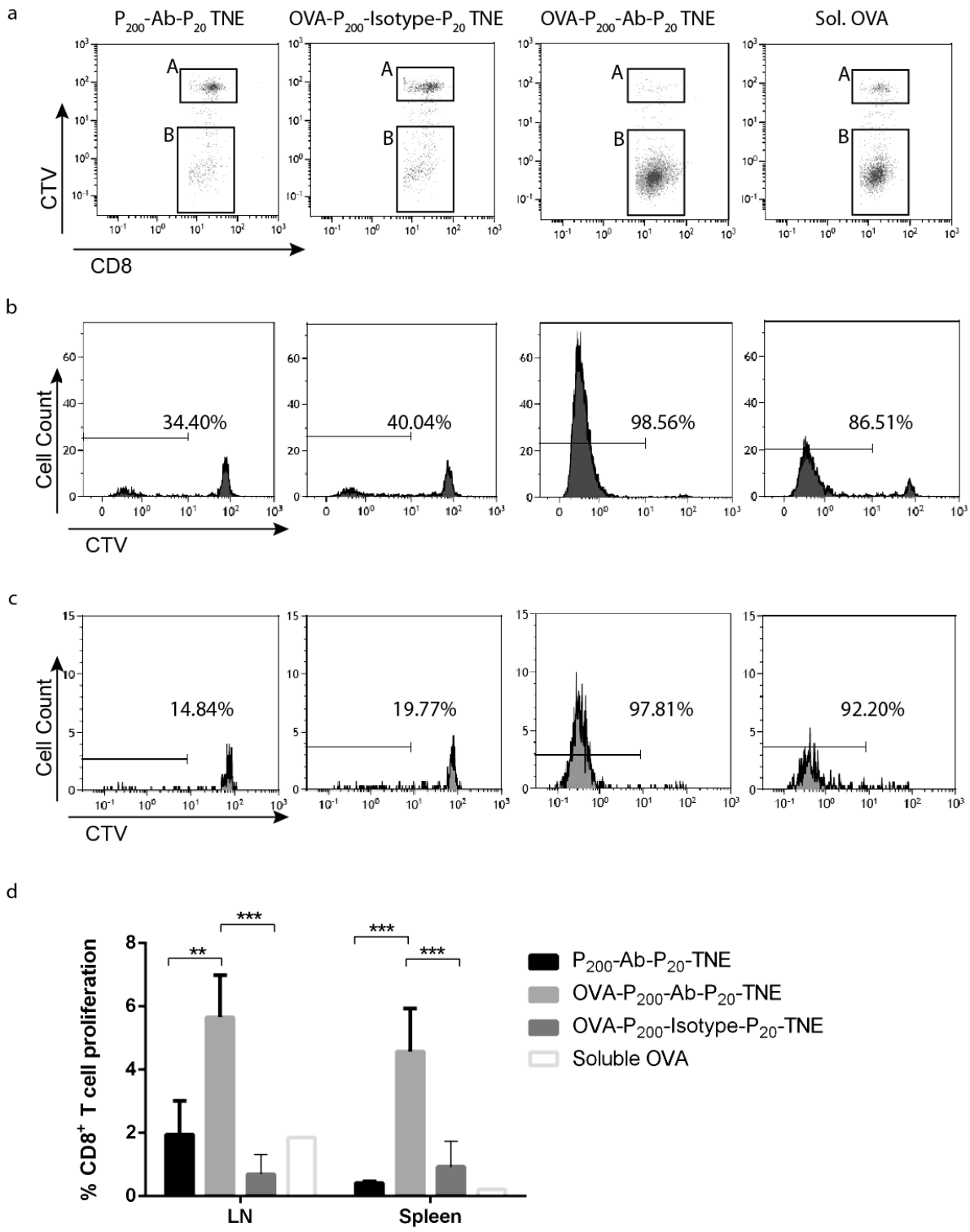

Figure 2. TNE induces CD8$^+$ T cell proliferation in LN and spleen. CTV labeled LN cells from $OVA_{257-264}$ specific OT-I transgenic mice were transferred to B6.SJL-Ptprca mice. One day later these mice were injected i.v. with 100 µg of soluble OVA, or 200 µL of P_{200}-Ab-P_{20}-TNE, OVA-P_{200}-Ab-P_{20}-TNE or OVA-P_{200}-Isotype-P_{20}-TNE (formulated with 5 µg of OVA). Six days later, LN and spleens

were removed and cell suspension were stained with anti-CD3, CD8, CD45.2 and MHC-II mAb and analyzed by flow cytometry. $CD3^+CD8^+CD45.2^+MHCII^-$ cells were gated. a) Dot-plots with rectangle gate **A** represent OVA-specific CTV^{high} parent T cells while gate **B** represent proliferated daughter T cells. b) Histogram showing dilution in CTV fluorescence intensity depicts OVA-specific T cell proliferation in LN. c) Dilution in CTV fluorescence intensity depicts OVA-specific T cell proliferation in spleen. d) Mean values ± SD of percentage $CD3^+CD8^+CD45.2^+$ proliferation. Statistical differences were determined by one-way ANOVA. *, $P < 0.05$; **, $P < 0.01$; ***, $P < 0.001$. (n=8-10 from two individual experiments).

3.3. CTL generation in vivo after Ag targeting

We further investigated whether Ag delivered by P_{200}-Ab-P_{20}-TNE to the $CD8^+$ DCs leads to the generation of effector CTLs. $OVA_{257-264}$ (SIINFEKL) induces a strong CTL response in naïve mice and is commonly used to investigate CTL-mediated immune responses. We first immunized C57BL/6 mice with OVA-P_{200}-Ab-P_{20}-TNE or OVA-P_{200}-Isotype-P_{20}-TNE (both formulations contained a total of 5 µg of OVA). Empty P_{200}-Ab-P_{20}-TNE or 5 µg of soluble OVA were injected to control mice. Five days later the mice were injected with an equal mix of syngeneic splenocytes pulsed with SIINFEKL and labelled with 5 µM of CTV (CTV^{high}), together with unpulsed splenocytes labelled with 0.5 µM of CTV (CTV^{low}). Twenty hours post injection, the residual SIINFEKL specific CTV^{high} and control CTV^{low} cells remaining in the immunized mice were analyzed by flow cytometry, which represents the killing activity of SIINFEKL-specific effector $CD8^+$ cytotoxic T lymphocytes (CTLs) in the recipient mice (**Figure 3**). Whereas no CTV^{high} target cell loss was observed in mice immunized with empty P_{200}-Ab-P_{20}-TNE, substantial loss of CTV^{high} target cells was observed in mice immunized with OVA-P_{200}-Ab-P_{20}-TNE. We found approximately 80% SIINFEKL-specific lysis in this group of mice (**Figure 3b**). In contrast, no significant increase in % specific lysis was detected in mice immunized with non-targeting OVA-P_{200}-Isotype-P_{20}-TNE or equal amount of soluble OVA (5 µg). These data indicate that OVA encapsulated within the targeting P_{200}-Ab-P_{20}-TNE effectively induces CTL with capacity to kill Ag-specific targets.

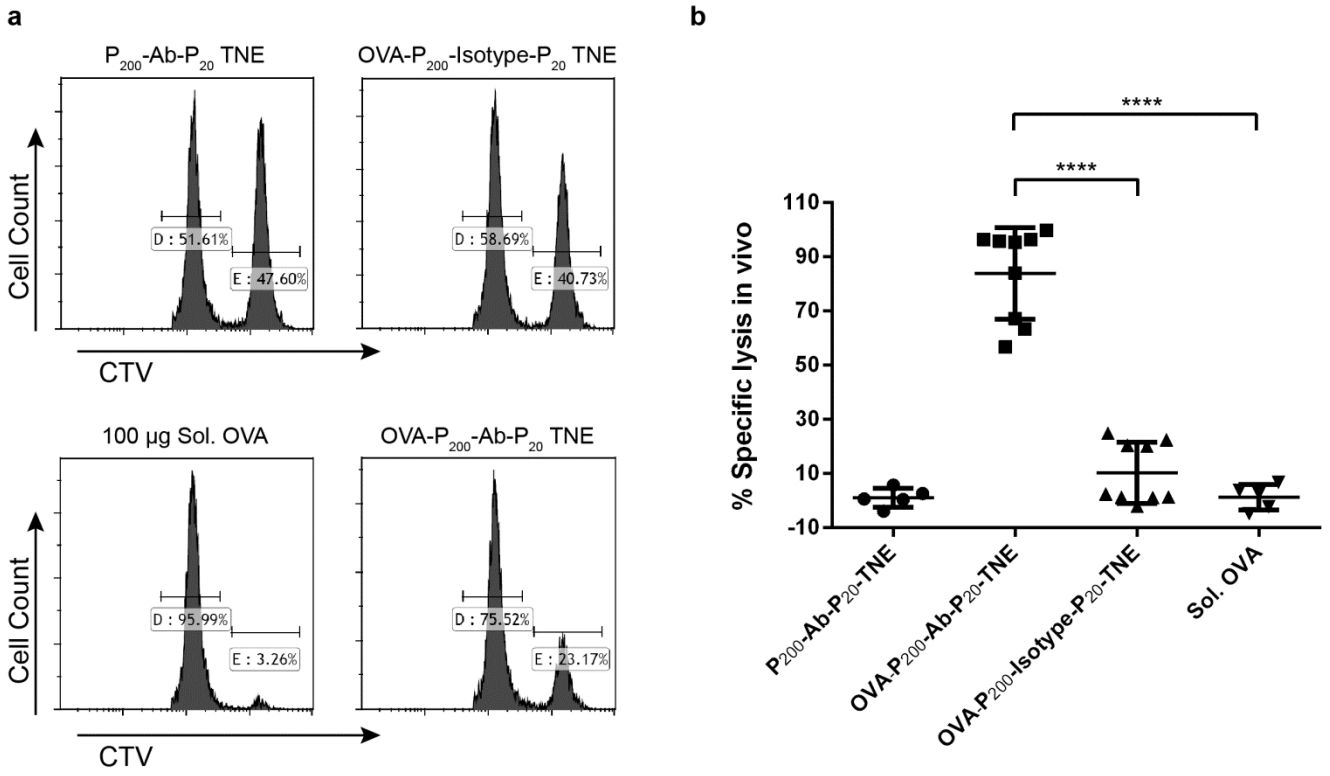

Figure 3. Targeting OVA to Clec9A induces OVA-specific cytotoxic response. C57BL/6 mice were adoptively transferred with equal number of unpulsed CTV^{low} and $OVA_{257-264}$ (SIINFEKL)-pulsed CTV^{high} target cells 5 days after i.v. injection with OVA-P_{200}-Ab-P_{20}-TNE or OVA-P_{200}-Isotype-P_{20}-TNE (both formulated with 5 µg of OVA). After 20h, spleen cells were analysed by flow cytometry to determine the ratio of CTV^{high} to CTV^{low} target cells (specific killing of target). a) Representative histograms of splenocytes of individual mouse are shown. b) Graph represents the percentage of SIINFEKL peptide specific lysis in spleen. Results are expressed as mean ± SD. Statistical differences were determined by one-way ANOVA. *, $P < 0.05$; **, $P < 0.01$; ***, $P < 0.001$, ****, $P < 0.0001$. (n=5-9 from two experiment).

3.4. Tuneable $CD8^+$ T cell response

We next investigated whether the $CD8^+$ T cell response from mice immunized with OVA-P_{200}-Ab-P_{20}-TNE was dependent on the mAb-DAMP4 within the formulation, and whether such responses could be tuned by simply changing the concentration of the targeting mAb. We generated a set of OVA-P_{200}-Ab-P_{20}-TNE which comprised varied molar ratios of OVA payload to targeting mAb, while keeping the composition of other components constant. We injected these formulations to B6.SJL-*Ptprc*^{a} mice which been adoptively transferred with CTV-labelled OT-I cells one day before. PBS and the non-

targeting OVA-P_{200}-Isotype-P_{20} TNE were injected to control mice. Expansion of OVA specific OT-I T cells was evaluated by flow cytometry 3 days later. Mice immunized with different formulations of OVA-P_{200}-Ab-P_{20}-TNE displayed varied levels of $CD8^+$ T cell response, expressed as OT-I cell expansion (**Figure 4**). Immunization with OVA-P_{200}-Ab-P_{20}-TNE formulated with lowest molar ratio of mAb (2:1) resulted in expansion of 17% of OT-I T cells in spleen and LN. Dilution of anti-Clec9A mAb 4 fold to increase in the ratio of Ag to mAb to 8:1 significantly reduced the T cell response, and 9 fold dilution essentially eliminated the T cell response. Results were similar in spleen and LN. This result further supports the conclusion that the antigen was correctly delivered and cross-presented to $CD8^+$ T cells, and this target specificity was partly dependent on the targeting Ab concentration within the TNE formulation. These data indicated that Ag-specific responses after delivery of OVA via P_{200}-Ab-P_{20}-TNE were mAb concentration dependent.

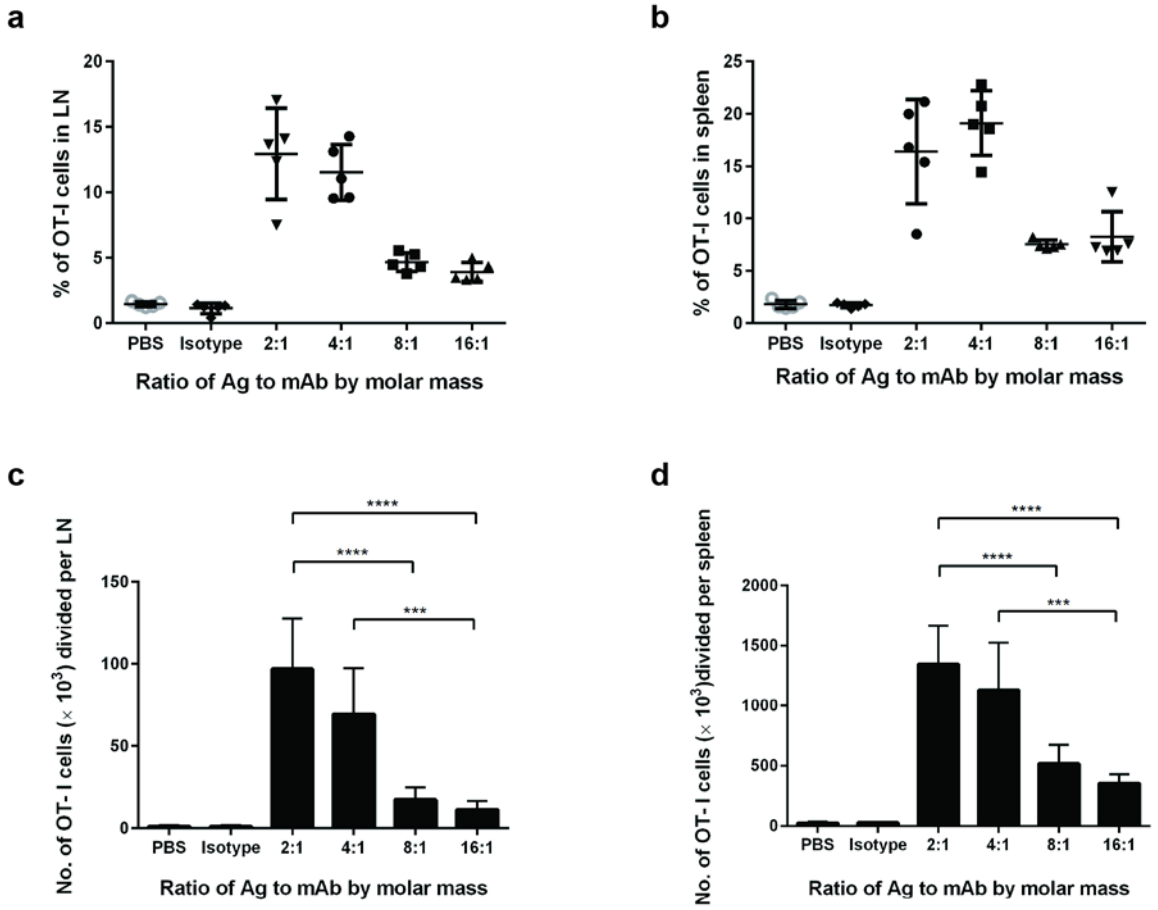

Figure 4. Tuneable $CD8^+$ T cells response by varying the concentration of targeting Ab within the TNE formulation. B6.SJL-*Ptprc*^{a} mice were adoptively transferred with CTV labelled lymph node cells from OT-I transgenic mice. One day later, the mice were injected with OVA-P_{200}-Ab-P_{20}-TNE formulated with a varied molar ratio of Ag to targeting mAb. Three days later, spleens and inguinal LN

were harvested and cells were stained with mAb against CD45.2, CD3 and CD8. Proliferation of OT-I cells ($CD3^+CD8^+CD45.2^+$) in LN (a) and spleen (b) were determined by flow cytometry. Proliferation of OT-I ($CD45.2^+CD8^+$) cells in LN (c) and Spleen (d) were enumerated. Results are expressed as mean ± SD from two separate experiments (n=8). Statistical differences were determined by one-way ANOVA. *, $P < 0.05$; **, $P < 0.01$; ***, $P < 0.001$, ****, $P < 0.0001$.

3.5. Proliferation response of $CD4^+$ T cells in vivo after targeting Ags to Clec9A by TNE

We next assessed the delivery of Ag by means of OVA-P_{200}-Ab-P_{20}-TNE to induce $CD4^+$ Ag-specific responses in vivo. CTV-labeled LN cells from transgenic OT-II mice specific for $OVA_{323-336}$ presented in the context of MHC class II were adoptively transferred into B6.SJL-*Ptprc*^{a} mice. One day later, mice were injected i.v. with OVA-P_{200}-Ab-P_{20}-TNE or the non-targeting OVA-P_{200}-Isotype-P_{20}-TNE. An equivalent amount of soluble OVA or empty P_{200}-Ab-P_{20}-TNE was injected into control mice. Six days later the proliferation of OT-II T cells was analyzed by flow cytometry (**Figure 5**). Mice immunized with OVA-P_{200}-Ab-P_{20}-TNE, which encapsulated low dose of soluble OVA (5 µg), induced vigorous OT-II cells proliferation in LN and spleen. By contrast, immunizing mice with the non-targeting OVA-P_{200}-Isotype-P_{20}-TNE, which contained the same amount of OVA, induced a significantly lower OT-II T cell response, similar to the response level from mice that had been immunized with empty P_{200}-Ab-P_{20}-TNE. Notably, mice immunized with an equivalent amount of soluble OVA alone did not induce a comparable OT-II T cell response. These data indicate that P_{200}-Ab-P_{20}-TNE delivers OVA protein effectively to APC for presentation to $CD4^+$ T cells.

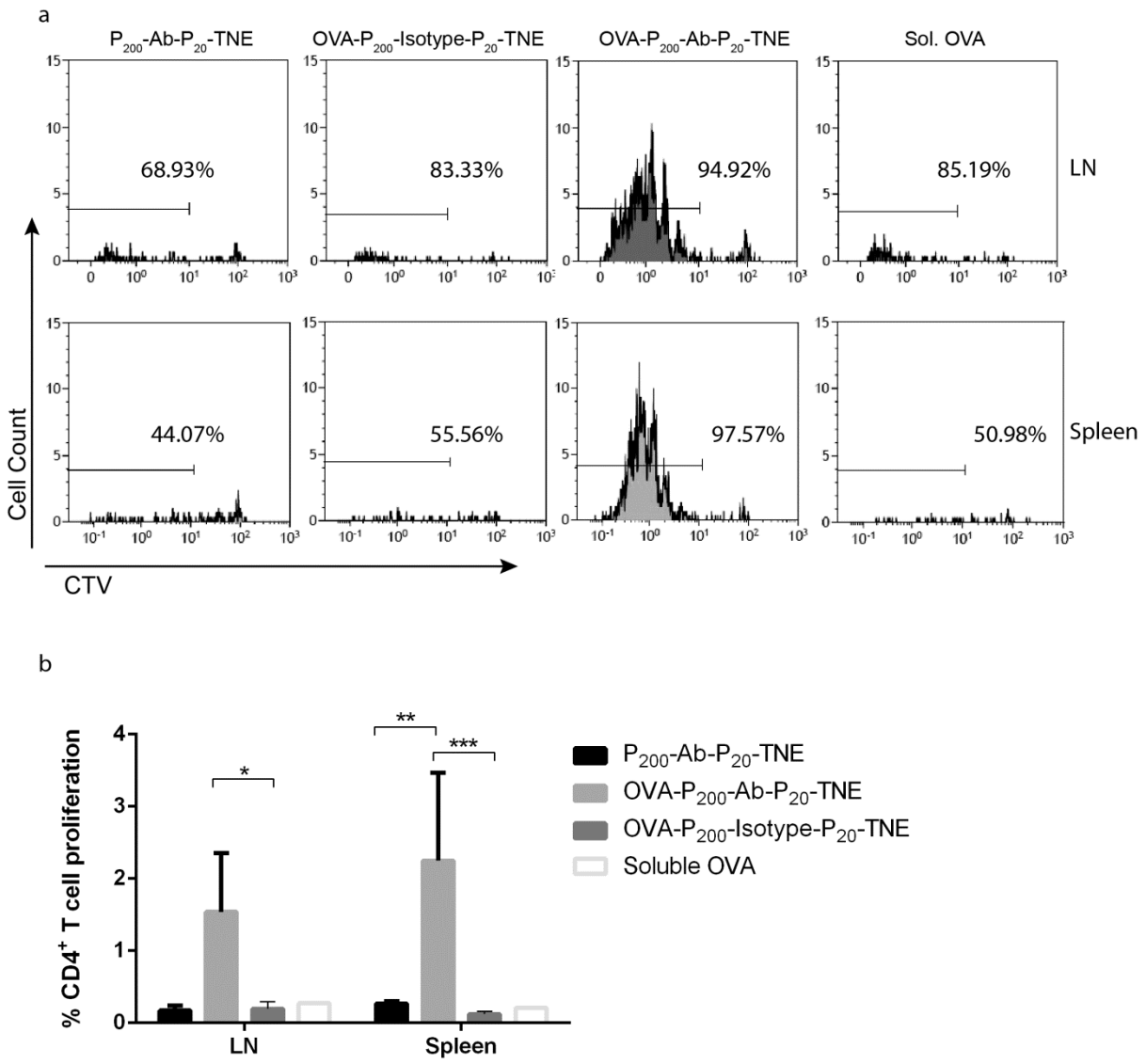

Figure 5. TNE delivery of OVA to Clec9A$^+$ DC elicits CD4$^+$ T cell proliferation. LN cells from transgenic OT-II mice (3×10^7) labeled with CTV were adoptively transferred to B6.SJL-*Ptprc*^{a} mice. One day later, mice were immunized i.v. with 200 µl of OVA-P_{200}-Ab-P_{20}-TNE or non-targeted control OVA-P_{200}-Isotype-P_{20}-TNE. Empty P_{200}-Ab-P_{20}-TNE and equivalent amount of soluble OVA were also injected i.v. to control mice. Six days later, LNs and spleens were harvested and cells were stained with mAb against CD45.2, CD3 and CD4. Proliferation of OT-II cells ($CD3^+CD4^+CD45.2^+$) was seen as the dilution of CTV fluorescence by flow cytometry. a) Histogram showing dilution in CTV fluorescence intensity depicts OVA-specific OT-II T cell proliferation in LN and spleen. b) Mean values ± SD of percentage $CD3^+CD4^+CD45.2^+$ proliferation. Statistical differences were dete rmined by one-way ANOVA. *, $P < 0.05$; **, $P < 0.01$; ***, $P < 0.001$. (n=8-10 from two experiment).

3.6. Ab responses induced by targeting Ags to Clec9A by TNE

It has been reported that targeting OVA conjugated to anti-Clec9A mAb can induce strong Ab responses in mice [10]. We tested wether Ab delivered by P_{200}-Ab-P_{20}-TNE could induce comparable anti-OVA responses to those induced by OVA conjugated to anti-Clec9A mAb (Clec9A-OVA). Mice were injected i.v. with 5 µg of OVA-P_{200}-Ab-P_{20}-TNE or Clec9A-OVA. Serum anti-OVA Ab response was quantitated over 3 consective weeks after immunization. In the absence of adjuvant, OVA-P_{200}-Ab-P_{20}-TNE induced similar anti-OVA response to that induced by Clec9A-OVA over 3 weeks post immunization (**Figure 6**). On the other hands, OVA delivered by the non-targeting P_{200}-Isotype-P_{20}-TNE or conjugated to an isotype mAb (Isotype-OVA), induced significantly lower anti-OVA responses, similar to the reponses in mice injected with PBS.

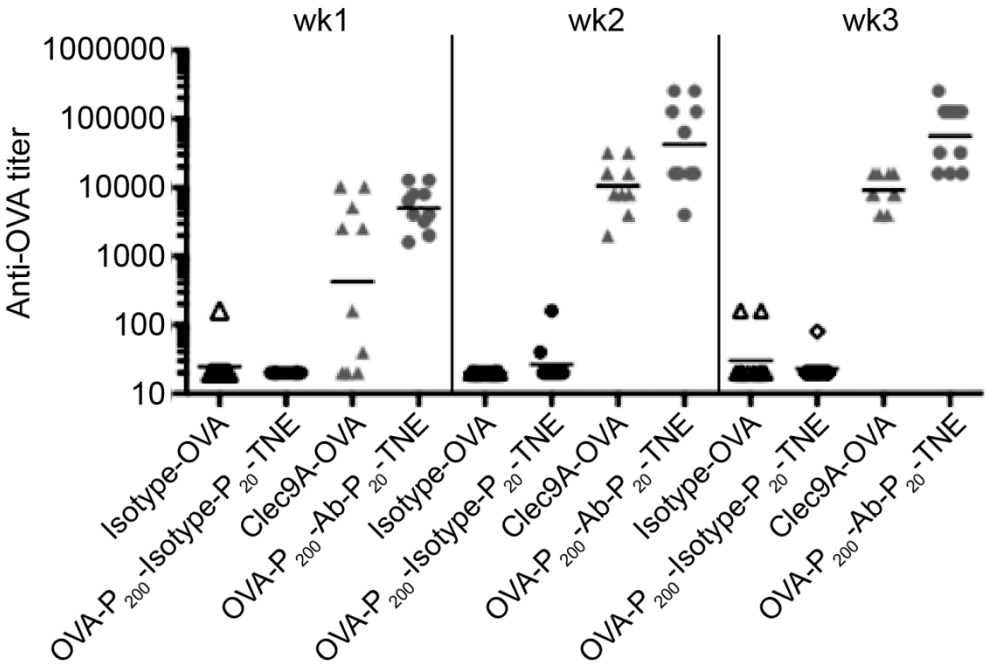

.

Figure 6. OVA delivered by TNE to Clec9A$^+$ DC induced humoral response. C57Bl/6 mice were injected i.v. with 5 µg of OVA in the form of either conjugate to anti-Clec9A mAb (Clec9A-OVA) or OVA-P_{200}-Ab-P_{20}-TNE. OVA conjugated to an isotype mAb (Isotype-OVA), OVA-P_{200}-Isotype-P_{20}-TNE was also injected to control mice in the absence of adjuvant. Serum anti-OVA Ig reactivity was measured in 1, 2 and 3 wk later by ELISA. Each group consists of 5 mice. Each symbol represents the individual response and the bar represents the geometric mean. n=10 from two individual experiments.

4. Discussion and conclusion

Currently clinical applications of native protein antigen based vaccines are hampered by the lack of an effective delivery platform and their inability to initiate strong T cell immunity, a process that is vital for the development of immunity against evading pathogens. Encapsulation of protein antigen into a delivery vehicle to target specific DC for efficient induction of CTL and antibody would provide opportunities for further development of protein antigens in anti-viral vaccines and tumor immunotherapy [41]. Here, we report a novel TNE engineered with anti-Clec9A mAb to deliver antigen payloads for induction of $CD8^+$ and $CD4^+$ mediated immunity. We previously reported the design and construction of TNE, which we showed targeted $CD8^+$ DCs selectively in vivo by means of the Clec9A targeting mAb [35]. In this study, hydrophilic OVA was loaded into the oil core using the solid-in-oil nanodispersion method [42]. In this method, protein was first coated with hydrophobic surfactant molecules to form protein-surfactant complexes, which significantly increased its solubility in the oil phase, thus enabling its facile packaging into the TNE oil core by the time of emulsification. The particle size of OVA encapsulated TNE was under 200 nm. PEGylation imparted steric stability to the TNE oil core in isotonic conditions, as observed from the consistent size distribution when the same structure was exposed to isotonic PBS, indicating suitability for i.v. injection and intracellular delivery [43]. Moreover, OVA-encapsulated TNE (OVA-P_{200}-Ab-P_{20}-TNE) effectively mediated OVA presentation and cross-presentation, leading to antigen-specific $CD8^+$ and $CD4^+$ T cell proliferation and CTL activity, even when the delivered dose of OVA was only 5 μg and in the absence of adjuvant. Indeed delivery of 5 μg of OVA by P_{200}-Ab-P_{20}-TNE induced greater levels of T cell proliferation compared to the same amount of soluble OVA. OVA delivered by P_{200}-Ab-P_{20}-TNE induced significantly enhanced anti-OVA response over three weeks post immunization. Although native protein based vaccines generally induce strong humoral immune responses, cellular immune responses are often relatively poor. By encapsulating protein antigens into nanoparticulate vehicles we could induce both Ab and CTL responses. We observed that OVA-encapsulated nanoemulsion (OVA-P_{200}-Ab-P_{20}-TNE) induced substantial levels of CTL in vivo, while the same amount of soluble OVA did not. Previously, OVA-specific CTL, albeit at lower levels, were induced after i.v. or i.d. injection of OVA-conjugated nanoparticles without targeting Ab but not low doses of soluble OVA [44]. DCs are the major antigen presenting cells through both MHC class I and II pathways. We previously showed that OVA-P_{200}-Ab-P_{20}-TNE was efficiently taken up by CD8+ DCs and that its encapsulated antigen was subsequently cross-presented by MHC class I molecules to $CD8^+$ T cells [35].

Previously, antigen targeting to mouse Clec9A^{+} DCs via anti-mClec9A mAb led to antigen-specific CD4 and CD8 T cell proliferation [10, 15, 45-47]. The current data demonstrate an alternate method to deliver Ag to CD8^{+} DCs with similar outcomes for cross presenting to CD8^{+} T cells. Targeting antigen specifically to the Clec9A DC receptor using anti-Clec9A mAb modified P_{200}-Ab-P_{20}-TNE has manufacturing advantages over construction of recombinant Ag-mAb constructs and in the flexibility of the TNE system for addition of excipients such as immunomodulatory adjuvants or drugs. Importantly, the efficiency of TNE for cross-presentation was dependent on the density of Clec9A mAb that been engineered on the TNE surface. Therefore there exists an optimal density for targeting mAb below TNE surface-saturation levels, suggesting that formulation optimization would be important for translation of this technology to clinically-relevant antigens. The ability to optimize DC targeting TNE platforms by controlling targeting moiety density could have significant benefit to future clinical applications, especially in chronic viral infections, intracellular bacterial infections and tumors where CD4^{+} and CD8^{+} cell-mediated immunity are critical for disease control, and to extend applicability to patients with multiple MHC types where CTL peptide epitopes are not known.

Overall, the results presented here demonstrate that antigen delivered by TNE can be presented by both MHC I and II molecules, leading to CD4 and CD8 T cell activation in vivo. Our work lays a foundation on which to develop the TNE platform for vaccines to deliver both humoral and T cell mediated immunity.

[1] J. Banchereau, R.M. Steinman, Dendritic cells and the control of immunity, Nature, 392 (1998) 245-252.
[2] I. Mellman, R.M. Steinman, Dendritic Cells: Specialized and Regulated Antigen Processing Machines, Cell, 106 (2001) 255-258.
[3] A. Lanzavecchia, F. Sallusto, Regulation of T Cell Immunity by Dendritic Cells, Cell, 106 (2001) 263-266.
[4] R.M. Steinman, J. Banchereau, Taking dendritic cells into medicine, Nature, 449 (2007) 419-426.
[5] I. Caminschi, M.H. Lahoud, K. Shortman, Enhancing immune responses by targeting antigen to DC, Eur. J. Immunol., 39 (2009) 931-938.
[6] K. Shortman, S.H. Naik, Steady-state and inflammatory dendritic-cell development, Nat Rev Immunol, 7 (2007) 19-30.
[7] J.A. Villadangos, P. Schnorrer, Intrinsic and cooperative antigen-presenting functions of dendritic-cell subsets in vivo, Nat. Rev. Immunol., 7 (2007) 543-555.
[8] W. Jiang, W.J. Swiggard, C. Heufler, M. Peng, A. Mirza, R.M. Steinman, M.C. Nussenzweig, The receptor DEC-205 expressed by dendritic cells and thymic epithelial cells is involved in antigen processing, Nature, 375 (1995) 151-155.
[9] J. Idoyaga, N. Suda, K. Suda, C.G. Park, R.M. Steinman, Antibody to Langerin/CD207 localizes large numbers of CD8α+ dendritic cells to the marginal zone of mouse spleen, Proceedings of the National Academy of Sciences, 106 (2009) 1524-1529.
[10] I. Caminschi, A.I. Proietto, F. Ahmet, S. Kitsoulis, J.S. Teh, J.C.Y. Lo, A. Rizzitelli, L. Wu, D. Vremec, S.L.H. van Dommelen, I.K. Campbell, E. Maraskovsky, H. Braley, G.M. Davey, P. Mottram, N.V. De Velde, K. Jensen, A.M. Lew, M.D. Wright, W.R. Heath, K. Shortman, M.H. Lahoud, The dendritic cell subtype-restricted C-type lectin Clec9A is a target for vaccine enhancement, Blood, 112 (2008) 3264-3273.
[11] M.H. Lahoud, A.I. Proietto, F. Ahmet, S. Kitsoulis, L. Eidsmo, L. Wu, P. Sathe, S. Pietersz, H.-W. Chang, I.D. Walker, E. Maraskovsky, H. Braley, A.M. Lew, M.D. Wright, W.R. Heath, K. Shortman, I. Caminschi, The C-Type Lectin Clec12A Present on Mouse and Human Dendritic Cells Can Serve as a Target for Antigen Delivery and Enhancement of Antibody Responses, The Journal of Immunology, 182 (2009) 7587-7594.
[12] S. Zelenay, A.M. Keller, P.G. Whitney, B.U. Schraml, S. Deddouche, N.C. Rogers, O. Schulz, D. Sancho, C. Reis e Sousa, The dendritic cell receptor DNGR-1 controls endocytic handling of necrotic cell antigens to favor cross-priming of CTLs in virus-infected mice, The Journal of Clinical Investigation, 122 (2012) 1615-1627.
[13] J.-G. Zhang, Peter E. Czabotar, Antonia N. Policheni, I. Caminschi, S. San Wan, S. Kitsoulis, Kirsteen M. Tullett, Adeline Y. Robin, R. Brammananth, Mark F. van Delft, J. Lu, Lorraine A. O'Reilly, Emma C. Josefsson, Benjamin T. Kile, Wei J. Chin, Justine D. Mintern, Maya A. Olshina, W. Wong, J. Baum, Mark D. Wright, David C.S. Huang, N. Mohandas, Ross L. Coppel, Peter M. Colman, Nicos A. Nicola, K. Shortman, Mireille H. Lahoud, The Dendritic Cell Receptor Clec9A Binds Damaged Cells via Exposed Actin Filaments, Immunity, 36 (2012) 646-657.
[14] C. Huysamen, J.A. Willment, K.M. Dennehy, G.D. Brown, CLEC9A is a novel activation C-type lectin-like receptor expressed on BDCA3(+) dendritic cells and a subset of monocytes, Journal of Biological Chemistry, 283 (2008) 16693-16701.
[15] M.H. Lahoud, F. Ahmet, S. Kitsoulis, S.S. Wan, D. Vremec, C.N. Lee, B. Phipson, W. Shi, G.K. Smyth, A.M. Lew, Y. Kato, S.N. Mueller, G.M. Davey, W.R. Heath, K. Shortman, I. Caminschi, Targeting Antigen to Mouse Dendritic Cells via Clec9A Induces Potent CD4 T Cell Responses Biased toward a Follicular Helper Phenotype, J. Immunol, 187 (2011) 842-850.

[16] D. Sancho, Mour, xE, S. o, xE, Diego, O.P. Joffre, O. Schulz, N.C. Rogers, D.J. Pennington, J.R. Carlyle, C. Reis e Sousa, Tumor therapy in mice via antigen targeting to a novel, DC-restricted C-type lectin, The Journal of Clinical Investigation, 118 (2008) 2098-2110.
[17] L.C. Bonifaz, D.P. Bonnyay, A. Charalambous, D.I. Darguste, S.-I. Fujii, H. Soares, M.K. Brimnes, B. Moltedo, T.M. Moran, R.M. Steinman, In Vivo Targeting of Antigens to Maturing Dendritic Cells via the DEC-205 Receptor Improves T Cell Vaccination, The Journal of Experimental Medicine, 199 (2004) 815-824.
[18] T.S. Johnson, K. Mahnke, V. Storn, K. Schönfeld, S. Ring, D.M. Nettelbeck, H.J. Haisma, F. Le Gall, R.E. Kontermann, A.H. Enk, Inhibition of melanoma growth by targeting of antigen to dendritic cells via an anti-DEC-205 single-chain fragment variable molecule, Clinical cancer research : an official journal of the American Association for Cancer Research, 14 (2008) 8169-8177.
[19] J. Idoyaga, A. Lubkin, C. Fiorese, M.H. Lahoud, I. Caminschi, Y.X. Huang, A. Rodriguez, B.E. Clausen, C.G. Park, C. Trumpfheller, R.M. Steinman, Comparable T helper 1 (Th1) and CD8 T-cell immunity by targeting HIV gag p24 to CD8 dendritic cells within antibodies to Langerin, DEC205, and Clec9A, Proceedings of the National Academy of Sciences of the United States of America, 108 (2011) 2384-2389.
[20] P. Muttil, C. Prego, L. Garcia-Contreras, B. Pulliam, J. Fallon, C. Wang, A. Hickey, D. Edwards, Immunization of Guinea Pigs with Novel Hepatitis B Antigen as Nanoparticle Aggregate Powders Administered by the Pulmonary Route, AAPS J, 12 (2010) 330-337.
[21] H.Y. Chou, X.Z. Lin, W.Y. Pan, P.Y. Wu, C.M. Chang, T.Y. Lin, H.H. Shen, M.H. Tao, Hydrogel-delivered GM-CSF overcomes nonresponsiveness to hepatitis B vaccine through the recruitment and activation of dendritic cells, Journal of immunology (Baltimore, Md. : 1950), 185 (2010) 5468-5475.
[22] S. Raman, G. Machaidze, A. Lustig, U. Aebi, P. Burkhard, Structure-based design of peptides that self-assemble into regular polyhedral nanoparticles, Nanomedicine : nanotechnology, biology, and medicine, 2 (2006) 95-102.
[23] S. Babapoor, T. Neef, C. Mittelholzer, T. Girshick, A. Garmendia, H. Shang, M.I. Khan, P. Burkhard, A Novel Vaccine Using Nanoparticle Platform to Present Immunogenic M2e against Avian Influenza Infection, Influenza Research and Treatment, 2011 (2011).
[24] Y.Y. Hwang, K. Ramalingam, D.R. Bienek, V. Lee, T. You, R. Alvarez, Antimicrobial Activity of Nanoemulsion in Combination with Cetylpyridinium Chloride in Multidrug-Resistant Acinetobacter baumannii, Antimicrobial Agents and Chemotherapy, 57 (2013) 3568-3575.
[25] K. Matsuo, H. Koizumi, M. Akashi, S. Nakagawa, T. Fujita, A. Yamamoto, N. Okada, Intranasal immunization with poly(γ-glutamic acid) nanoparticles entrapping antigenic proteins can induce potent tumor immunity, Journal of Controlled Release, 152 (2011) 310-316.
[26] D. O'Hagan, T. Tsai, S. Reed, Emulsion-Based Adjuvants for Improved Influenza Vaccines, in: R. Rappuoli, G. Del Giudice (Eds.) Influenza Vaccines for the Future, Springer Basel, 2011, pp. 327-357.
[27] S. Calabro, M. Tortoli, B.C. Baudner, A. Pacitto, M. Cortese, D.T. O'Hagan, E. De Gregorio, A. Seubert, A. Wack, Vaccine adjuvants alum and MF59 induce rapid recruitment of neutrophils and monocytes that participate in antigen transport to draining lymph nodes, Vaccine, 29 (2011) 1812-1823.
[28] A. Seubert, E. Monaci, M. Pizza, D.T. O'Hagan, A. Wack, The Adjuvants Aluminum Hydroxide and MF59 Induce Monocyte and Granulocyte Chemoattractants and Enhance Monocyte Differentiation toward Dendritic Cells, The Journal of Immunology, 180 (2008) 5402-5412.
[29] L.R. Stanberry, J.K. Simon, C. Johnson, P.L. Robinson, J. Morry, M.R. Flack, S. Gracon, A. Myc, T. Hamouda, J.R. Baker Jr, Safety and immunogenicity of a novel nanoemulsion mucosal adjuvant W805EC combined with approved seasonal influenza antigens, Vaccine, 30 (2012) 307-316.

[30] T.G. Boyce, H.H. Hsu, E.C. Sannella, S.D. Coleman-Dockery, E. Baylis, Y. Zhu, G. Barchfeld, A. DiFrancesco, M. Paranandi, B. Culley, K.M. Neuzil, P.F. Wright, Safety and immunogenicity of adjuvanted and unadjuvanted subunit influenza vaccines administered intranasally to healthy adults, Vaccine, 19 (2000) 217-226.
[31] S. Laurent, S. Boutry, I. Mahieu, L. Vander Elst, R.N. Muller, Iron Oxide Based MR Contrast Agents: from Chemistry to Cell Labeling, CURRENT MEDICINAL CHEMISTRY, 16 (2009) 4712-4727.
[32] S. Mornet, S. Vasseur, F. Grasset, E. Duguet, Magnetic nanoparticle design for medical diagnosis and therapy, Journal of Materials Chemistry, 14 (2004) 2161-2175.
[33] S.M. Moghimi, A.C. Hunter, J.C. Murray, Long-Circulating and Target-Specific Nanoparticles: Theory to Practice, Pharmacological Reviews, 53 (2001) 283-318.
[34] D. Peer, J.M. Karp, S. Hong, O.C. FaroKhzad, R. Margalit, R. Langer, Nanocarriers as an emerging platform for cancer therapy, Nat. Nanotechnol., 2 (2007) 751-760.
[35] B.J. Zeng, Y.P. Chuan, B. O'Sullivan, I. Caminschi, M.H. Lahoud, R. Thomas, A.P.J. Middelberg, Receptor-Specific Delivery of Protein Antigen to Dendritic Cells by a Nanoemulsion Formed Using Top-Down Non-Covalent Click Self-Assembly, Small, 9 (2013) 3736-3742.
[36] W.W.J. Unger, A.J. van Beelen, S.C. Bruijns, M. Joshi, C.M. Fehres, L. van Bloois, M.I. Verstege, M. Ambrosini, H. Kalay, K. Nazmi, J.G. Bolscher, E. Hooijberg, T.D. de Gruijl, G. Storm, Y. van Kooyk, Glycan-modified liposomes boost CD4+ and CD8+ T-cell responses by targeting DC-SIGN on dendritic cells, Journal of Controlled Release, 160 (2012) 88-95.
[37] J.J. García-Vallejo, M. Ambrosini, A. Overbeek, W.E. van Riel, K. Bloem, W.W.J. Unger, F. Chiodo, J.G. Bolscher, K. Nazmi, H. Kalay, Y. van Kooyk, Multivalent glycopeptide dendrimers for the targeted delivery of antigens to dendritic cells, Molecular Immunology, 53 (2013) 387-397.
[38] K. Kawano, Y. Maitani, Effects of polyethylene glycol spacer length and ligand density on rolate receptor targeting of liposomal doxorubicin in vitro, J. Drug Deliv., 2011 (2010) 6.
[39] A. Yamada, Y. Taniguchi, K. Kawano, T. Honda, Y. Hattori, Y. Maitani, Design of folate-linked liposomal doxorubicin to its antitumor effect in mice, Clinical Cancer Research, 14 (2008) 8161-8168.
[40] A.F. Dexter, A.S. Malcolm, A.P.J. Middelberg, Reversible active switching of the mechanical properties of a peptide film at a fluid-fluid interface, Nat Mater, 5 (2006) 502-506.
[41] C.L. Hutchings, S.C. Gilbert, A.V.S. Hill, A.C. Moore, Novel Protein and Poxvirus-Based Vaccine Combinations for Simultaneous Induction of Humoral and Cell-Mediated Immunity, The Journal of Immunology, 175 (2005) 599-606.
[42] Y. Tahara, S. Honda, N. Kamiya, H. Piao, A. Hirata, E. Hayakawa, T. Fujii, M. Goto, A solid-in-oil nanodispersion for transcutaneous protein delivery, Journal of Controlled Release, 131 (2008) 14-18.
[43] R. Agarwal, K. Roy, Intracellular delivery of polymeric nanocarriers: a matter of size, shape, charge, elasticity and surface composition, Therapeutic delivery, 4 (2013) 705.
[44] P.J. White, F. Anastasopoulos, J.E. Church, C.Y. Kuo, B.J. Boyd, P.L.C. Hickey, L.S. Tu, P. Burns, A.M. Lew, W.R. Heath, G.M. Davey, C.W. Pouton, Generic construction of single component particles that elicit humoural and cellular immune responses without the need for adjuvants, Vaccine, 26 (2008) 6824-6831.
[45] J.M. den Haan, S.M. Lehar, M.J. Bevan, CD8(+) but not CD8(-) dendritic cells cross-prime cytotoxic T cells in vivo, The Journal of Experimental Medicine, 192 (2000) 1685-1695.
[46] J.L. Pooley, W.R. Heath, K. Shortman, Cutting edge: intravenous soluble antigen is presented to CD4 T cells by CD8- dendritic cells, but cross-presented to CD8 T cells by CD8+ dendritic cells, Journal of immunology (Baltimore, Md. : 1950), 166 (2001) 5327-5330.

[47] P. Schnorrer, E. Maraskovsky, G.T. Belz, F.R. Carbone, K. Shortman, W.R. Heath, J.A. Villadangos, G.M.N. Behrens, N.S. Wilson, J.L. Pooley, C.M. Smith, D. El-Sukkari, G. Davey, F. Kupresanin, M. Li, The dominant role of CD8+ dendritic cells in cross-presentation is not dictated by antigen capture, Proceedings of the National Academy of Sciences of the United States of America, 103 (2006) 10729-10734.

Chapter 7 Conclusions and future directions

Rational design of drug delivery system (DDS) has provided a solution to overcome the problems that many drugs have, such as poor water-solubility, rapid blood clearance and severe side effect. The application of nanotechnology to DDS has exerted tremendous impact on medicine in the past few decades. Nanocarriers hold great potential as drug delivery vehicles as they can be tailored to deliver unique drug combinations needed for personalized medical interventions, with a concurrent minimization of side effects in a cell-specific manner. There are over twenty nanocarrier-based therapeutic in clinical use, and numerous others are at various stage of development. Nanocarrier-based therapeutics, or nanomedicine, is expected to play increasingly important role in modern medicine landscape.

However, the development of nanocarriers to date still has drawbacks including low drug loading capacity and laborious manufacturing process and low in therapeutic efficiency. To this end, this doctoral work aims to develop a tailorable nanocarrier emulsion (TNE) through an entirely novel nano-engineering approach based on non-covalent self-assembly at the oil-water interface. A completely new concept of using a surface active protein surfactant DAMP4 as an anchor to display functional moieties on the surface of nanoemulsion was explored and developed in this doctoral project, by which the use of stringent chemistry that required for surface functionalization was substantially minimized. Surface active peptide AM1 stabilized oil-in-water emulsion provides a well-defined interface to facilitate self-assemble surface functionalization mediated by DAMP4. Meanwhile, incorporation of active components into the oil phase at the time of emulsion formation enables facile packaging. The TNE platform developed from this doctoral work was functionalized with PEG and a mAb against DCs specific receptor Clec9A. At the physiological level, PEGylation of nanocarrier increases *in vivo* half-life and enhance accumulation through passive targeting. Nanocarriers functionalized with site specific ligand increased target specificity and assisted in overcoming multiple cellular barriers through receptor-mediated endocytosis. At the molecular level, nanocarriers loaded with various drug combinations can further improve treatment efficacy by targeting multiple molecular pathways.

The experimental works discussed in this thesis were designed to explore the hypothesis of DAMP4 mediating TNE functionalization and solve obvious challenges along the way, through achieving the following aspects:

(i) Utilization of DAMP4 modified with polyethylene glycol (PEG) to investigate whether DAMP4 can display PEG at the interface and impart altered cell association to the nanoemulsion – This preliminary study evaluated the hypothesis stated in **Chapter 1** and highlighted the potential of using DAMP4 for TNE surface functionalization (**Chapter 3**);

(ii) Utilization of DAMP4 modified with monoclonal antibody (mAb) against the $CD8^+$ DCs specific receptor Clec9A to design a nanocarrier emulsion that able to target $Clec9A^+$ DCs – This study evaluate the robustness and effectiveness of Clec9A mAb functionalized TNE. The *in vivo* target specificity of $Clec9A^+$ DC targeting TNE was investigated (**Chapter 4**);

(iii) Targeting antigen to DCs by TNE – A model antigen was encapsulated into the oil core of TNE and the efficiency of TNE in delivering its payload to DCs was evaluated by measuring antigen-specific immune response (**Chapter 5** and **6**). The impact of Clec9A mAb molecule numbers presented on the TNE surface was also evaluated (**Chapter 6**).

The following sections will reiterate the important conclusions from this dissertation and give some prospective points for the future work of this research.

7.1. Summary of research findings

In **Chapter 3**, I described the design and development of PEGylated nanocarrier emulsion with enhanced immune evading ability through a simple top-down sequential addition of PEG modified DAMP4. This chapter aimed at evaluating the hypothesis of DAMP4 mediating TNE functionalization (introduced in **Chapter 1** in detail) through the construction of a PEGylated TNE. Here, we showed that simple mixing of AM1 stabilized TNE core with PEG-DAMP4 conjugate led to the non-covalent attachment of PEG to the surface of emulsion droplet. Addition of PEG-DAMP4 conjugate into the TNE system imparts steric stability to the TNE oil core in isotonic conditions, which enables intravenous injection and intracellular delivery application. PEGylation is a common strategy to increase "stealthiness" of nanocarrier by creating a steric barrier around the nanocarrier which against non-specific association with opsonins (Harris and Chess, 2003, Harris et al., 2001, Krystek et al.,

2011). An effective shielding of the nanocarrier with a PEG layer is of important to increase *in vivo* half-life. PEGylation of TNE through addition of PEG-DAMP4 to the TNE system reduces non-specific cell association compared to its non-PEGylated counterpart *in vitro*. In light of the results shown in this chapter, we confirmed the hypothesis that the integration of DAMP4 into the AM1 stabilized oil droplet surface would lead to the functional display of conjugated PEG at the interface of the TNE oil core. Non-specific cell association of TNE can be down-regulated to a minimum with appropriate shielding from self-assembled PEG using DAMP4 as an anchor. However, whether the PEG layer present on the TNE oil core surface reduce opsonins adsorption, and thereby complement activation and MPS clearance, need to be performed *in vivo* and I addressed this issue in the following chapters.

For therapeutic nanocarrier to maximize their efficacy, they need to arrive at the specific biological locations to release their payload. The active targeting of nanocarrier can be achieved by functionalization of a site specific ligand or mAb. The realization of the DCs are critical for initiation and control of innate and adaptive immune response, give rise to a number of strategies for target delivery antigen to DCs. Several studies have shown the delivery efficacy and efficiency of nanocarrier can be improved by engineering with a DCs targeting moiety on surface (Sehgal et al., 2014, Bandyopadhyay et al., 2011, Unger et al., 2012, Tel et al., 2013). To achieve targeting delivery, different DCs specific receptors had been studied with special interest to C-type lectin receptors (CRLRs), *e.g.* Clec9A (Caminschi et al., 2008, Huysamen et al., 2008, Idoyaga et al., 2011, Lahoud et al., 2011, Sancho et al., 2009, Schreibelt et al., 2012, Zelenay et al., 2012, Zhang et al., 2012). Chemical methods that most of the current Clec9A targeting strategies used for conjugating with vaccine antigen cannot guarantee site-specific conjugates and led to poor stoichiometry. In this PhD project, Clec9A mAb was conjugated to DAMP4 via genetic fusion approach and expressed as a recombinant fusion protein to eliminate the risk of mAb deactivation by extreme chemical conjugation condition. Leveraging the findings and method developed in **Chapter 3**, the design and development of $Clec9A^{+}$ DC targeting TNE (P_{200}-Ab-P_{20}-TNE) through the non-covalent "click" chemistry was discussed in **Chapter 4**. Using DAMP4 as an anchor to display mAb on the TNE surface, I was able to construct Clec9A targeting TNE for *in vitro* and *in vivo* study. The functionalization of TNE with anti-Clec9A mAb increased cell association to Clec9A-expressing cell line. With the array of Clec9A-targeted TNE formulated with different concentration of PEG, I evaluated the target specificity in relation to PEG density on TNE surface to Clec9A-expressing cell lines. As expected, increased PEG

density on TNE surface reduces the non-specific cell association and increases specificity towards Clec9A^{+} DCs. These results not only demonstrating the ability of the developed production method is capable of manipulating the target specificity by simple variation of TNE composition, but also showed the importance of maintaining an optimal balance of functional moieties on TNE surface.

Motivated by the need of developing an effective delivery system for biologics and vaccine, **Chapter 5** extended the studies in **Chapter 3** and **4** into the application of TNE for intracellular delivery of protein antigen. DCs are the most effective antigen-presenting cells that initiate and regulate antigen-specific immune responses. DCs internalize, process and present antigens to naïve T cells, therefore researchers have exploited DCs in an attempt to improve vaccine efficacy. In our study, hydrophilic ovalbumin (OVA) was loaded into the oil core using the solid-in-oil (S/O) nanodispersion method for enhanced solubility, which does not require any covalent conjugation that would damage the native properties of protein. OVA has been studied as a model antigen for a long time since many analysis tools have been developed, for example transgenic OT-I and OT-II mice which bear CD8^{+} and CD4^{+} T-cells respectively recognizing epitopes of the OVA (Hogquist et al., 1994, Barnden et al., 1998). Presentation of OT-I T cell specific OVA epitode ($OVA_{257-264,}$ SIINFEKL) by DCs to OT-I T cells leads to proliferation and differentiation of cytotoxic CD8^{+} T cells, while presentation of OT-II specific OVA epitode ($OVA_{323-339}$) to OT-II T cells results in proliferation and differentiation of cytokine producing CD4^{+} T cells. By using dot-blot assay, we showed that immunity of OVA protein was well preserved after it had been encapsulated within the TNE oil core. Exogenous antigens need to be cross-presented on MHC I molecules to CD8+ T-cells for their activation. As an initial test, here we showed that OVA-P_{200}-Ab-P_{20}-TNE was able to elicit antigen-specific OT-I T cell proliferation both *in vitro* and *in vivo.* In addition, results in this chapter further support the hypothesis that TNE will serve as an effective DDS platform for targeting DCs.

In **Chapter 6**, we examine the potential of TNE as vehicle for targeting antigen to Clec9A^{+} DCs *in vivo*. DC-based immunotherapy has been developed to the point where it is currently in the clinical trial phase (Apostolopoulos et al., 2014). However, such strategy also comes with problems such as the plasticity and complexity of DC maturation, shelf-life, high cost which restrict the translation of this therapeutic approach (Giannoukakis et al., 2011, Waeckerle-Men and Groettrup, 2005). Instead of manipulating DCs *ex vivo*, here we use a DCs targeting nanocarrier approach to apply the "*in situ* DC conditioning" concept to modulate immune response.

We analysed the immune response to model protein antigen OVA encapsulated within TNE (OVA-P_{200}-Ab-P_{20}-TNE). The primary activation of T-helper and cytotoxic T-cells (CTL) following immunization with OVA-P_{200}-Ab-P_{20}-TNE was studied *in vivo* by adoptive transfer OT-I and OT-II T cells into naïve mice. We showed that TNE is an effective antigen delivery system for induction of both CD4 and CD8 T cell immunity. Mice immunized with Clec9A$^+$ DCs targeting OVA-P_{200}-Ab-P_{20}-TNE showed enhanced antigen-specific CD4$^+$ and CD8$^+$ T cells response in spleen and lymph nodes, as compared to mice immunized with OVA encapsulated within the non-targeting TNE. Notably, targeting OVA to Clec9A$^+$ DCs via TNE resulted in sustained and enhanced anti-OVA response in three weeks post immunization. Whilst soluble OVA is weak at activating CD8 T cell or CTL response (Ke et al., 1995), herein we demonstrated that immunization with OVA-P_{200}-Ab-P_{20}-TNE in naïve mice leads to generation of functional effector CTL that selectively killed antigen-specific target cells, even when low dose of soluble OVA was delivered and in the absence of adjuvant. Both humoural and cell-mediated immune responses are essential elements required by novel vaccine design. Results from **Chapter 6** demonstrate potential of TNE in efficient induction of T cell immunity. More importantly, we showed that strong CD8$^+$ T cell response can be activated by antigen delivered by TNE, without the need for any chemical-based adjuvant, therefore circumventing any potential tolerability and safety issues. Questions regarding whether the ability of antigen carrying TNE for inducing antigen specific T cell immunity is dependent of the TNE formulation or the amount of antigen being encapsulated and delivered to DCs is of interest of this PhD project. We addressed this question by generating a panel of OVA-P_{200}-Ab-P_{20}-TNE which comprised varied molar ratios of OVA payload to targeting mAb, while keeping the composition of other components constant, and tested their efficacy in inducing OVA-specific T cell proliferation. We showed that the target specificity was partly dependent on the targeting mAb concentration within the TNE formulation, and the immunity responses could potentially be tuned by simply changing the concentration of the targeting mAb. Taken together, this chapter highlights the TNE platform as an effective antigen-delivery system to enhance CD8$^+$ and CD4$^+$ T cell immunity, hereby prove targeting delivery of protein antigen by TNE potentially an effective, adjuvant-free and simple platform for use as therapeutic vaccines to deliver both humoral and T cell mediated immunity.

7.2. Future direction

Evidently, this project is still at a nascent stage. Nonetheless, given the promising results thus far it should be worth to further explore and optimize the TNE platform for translation to clinical application in human. To accomplish this distant goal we will first have to improve the efficiency of the current TNE formulation. Reliable drug adsorption, distribution, metabolism, excretion and toxicity (ADME/T) are important properties critical for any drug development. Thus comprehensive pharmacokinetics and pharmacodynamics studies including an extensive toxicity analysis are required to evaluate and optimize the TNE delivery regime in vivo. In the studies described in the thesis, the dose of antigen was matched to a previously reported Clec9A targeting antigen that has been shown to stimulate a response (Caminschi et al., 2008, Lahoud et al., 2011). The relatively larger payload that is possible with TNE may allow for a reduced dose regime; therefore, a dose optimization study should be performed. In addition, by injecting mice with TNE that have been decorated with various amounts of anti-Clec9A mAb, we demonstrated that the efficiency of TNE for cross-presentation was partly dependent on the density of targeting moieties that been engineered on the TNE surface. Therefore there is an optimal density for targeting mAb below TNE surface-saturation levels that needs to be determined in the future studies.

Although TNE have been shown to be an effective vehicle for targeting antigen to Clec9A$^+$ DCs, those results were demonstrated by monitoring only cellular assays, *e.g.* antigen–specific CTL. In order to demonstrate translational significance of this delivery system, testing TNE in a disease model to show proof of concept will be essential. Clec9A have been shown to be a promising target for *in vivo* antigen delivery in human to increase the efficiency of vaccines against cancerous or infectious disease, targeting tumor antigen to Clec9A with adjuvant induced antitumor immunity in a mouse melanoma model (Schreibelt et al., 2012, Sancho et al., 2008). The TNE platform developed from this PhD project that is capable of highly specifically delivering protein antigen would potentially be a significant breakthrough in cancer treatment.

7.3. Conclusion thoughts

The results presented in this thesis add significant contributions to the continuing development of therapeutic nanocarriers. While functionally distinct, each of the aforementioned developments is structurally compatible with one another. The techniques for decorating TNE with PEG and mAb are

also compatible with other nanostructures, providing additional toolkit to the fledging field of nanotechnology and nanomedicine. The most significant results associated with this thesis centre around the exploitation of the application of protein surfactant DAMP4 as anchor for nanocarrier emulsion functionalization. This is the first time, to our best knowledge, that surface active peptide and protein has been utilized to prepare a nanoemulsion DDS with highly efficacious *in vivo* target specificity.

7.4. References

APOSTOLOPOULOS, V., PIETERSZ, G. A., TSIBANIS, A., TSIKKINIS, A., STOJANOVSKA, L., MCKENZIE, I. F. C. & VASSILAROS, S. 2014. Dendritic cell immunotherapy: clinical outcomes. *Clin Trans Immunol,* 3**,** e21.

BANDYOPADHYAY, A., FINE, R. L., DEMENTO, S., BOCKENSTEDT, L. K. & FAHMY, T. M. 2011. The impact of nanoparticle ligand density on dendritic-cell targeted vaccines. *Biomaterials,* 32**,** 3094-3105.

BARNDEN, M. J., ALLISON, J., HEATH, W. R. & CARBONE, F. R. 1998. Defective TCR expression in transgenic mice constructed using cDNA-based [agr]- and [bgr]-chain genes under the control of heterologous regulatory elements. *Immunol Cell Biol,* 76**,** 34-40.

CAMINSCHI, I., PROIETTO, A. I., AHMET, F., KITSOULIS, S., TEH, J. S., LO, J. C. Y., RIZZITELLI, A., WU, L., VREMEC, D., VAN DOMMELEN, S. L. H., CAMPBELL, I. K., MARASKOVSKY, E., BRALEY, H., DAVEY, G. M., MOTTRAM, P., DE VELDE, N. V., JENSEN, K., LEW, A. M., WRIGHT, M. D., HEATH, W. R., SHORTMAN, K. & LAHOUD, M. H. 2008. The dendritic cell subtype-restricted C-type lectin Clec9A is a target for vaccine enhancement. *Blood,* 112**,** 3264-3273.

GIANNOUKAKIS, N., PHILLIPS, B., FINEGOLD, D., HARNAHA, J. & TRUCCO, M. 2011. Phase I (safety) study of autologous tolerogenic dendritic cells in type 1 diabetic patients. *Diabetes care,* 34**,** 2026-2032.

HARRIS, J. M. & CHESS, R. B. 2003. Effect of pegylation on pharmaceuticals. *Nat Rev Drug Discov,* 2**,** 214-221.

HARRIS, J. M., MARTIN, N. E. & MODI, M. 2001. Pegylation - A novel process for modifying pharmacokinetics. *Clinical Pharmacokinetics,* 40**,** 539-551.

HOGQUIST, K. A., JAMESON, S. C., HEATH, W. R., HOWARD, J. L., BEVAN, M. J. & CARBONE, F. R. 1994. T cell receptor antagonist peptides induce positive selection. *Cell,* 76**,** 17-27.

HUYSAMEN, C., WILLMENT, J. A., DENNEHY, K. M. & BROWN, G. D. 2008. CLEC9A is a novel activation C-type lectin-like receptor expressed on BDCA3(+) dendritic cells and a subset of monocytes. *Journal of Biological Chemistry,* 283**,** 16693-16701.

IDOYAGA, J., LUBKIN, A., FIORESE, C., LAHOUD, M. H., CAMINSCHI, I., HUANG, Y. X., RODRIGUEZ, A., CLAUSEN, B. E., PARK, C. G., TRUMPFHELLER, C. & STEINMAN, R. M. 2011. Comparable T helper 1 (Th1) and CD8 T-cell immunity by targeting HIV gag p24 to CD8 dendritic cells within antibodies to Langerin, DEC205, and Clec9A. *Proceedings of the National Academy of Sciences of the United States of America,* 108**,** 2384-2389.

KE, Y., LI, Y. & KAPP, J. A. 1995. Ovalbumin injected with complete Freund's adjuvant stimulates cytolytic responses. *European Journal of Immunology,* 25**,** 549-553.

KRYSTEK, P., OOMEN, A. G., RAYAVARAPU, R. G., LEEUWEN, V. T. G., JONG, D. W. H., MANOHAR, S., LANKVELD, D. P. K. & VERHAREN, H. W. 2011. Blood clearance and tissue distribution of PEGylated and non-PEGylated gold nanorods after intravenous administration in rats. *Nanomedicine,* 6**,** 339-349.

LAHOUD, M. H., AHMET, F., KITSOULIS, S., WAN, S. S., VREMEC, D., LEE, C. N., PHIPSON, B., SHI, W., SMYTH, G. K., LEW, A. M., KATO, Y., MUELLER, S. N., DAVEY, G. M., HEATH, W. R., SHORTMAN, K. & CAMINSCHI, I. 2011. Targeting Antigen to Mouse Dendritic Cells via Clec9A Induces Potent CD4 T Cell Responses Biased toward a Follicular Helper Phenotype. *J. Immunol,* 187**,** 842-850.

SANCHO, D., JOFFRE, O. P., KELLER, A. M., ROGERS, N. C., MARTINEZ, D., HERNANZ-FALCON, P., ROSEWELL, I. & SOUSA, C. R. E. 2009. Identification of a dendritic cell receptor that couples sensing of necrosis to immunity. *Nature,* 458**,** 899-903.

SANCHO, D., MOUR, XE, O, S., XE, DIEGO, JOFFRE, O. P., SCHULZ, O., ROGERS, N. C., PENNINGTON, D. J., CARLYLE, J. R. & REIS E SOUSA, C. 2008. Tumor therapy in mice via antigen targeting to a novel, DC-restricted C-type lectin. *The Journal of Clinical Investigation,* 118**,** 2098-2110.

SCHREIBELT, G., KLINKENBERG, L. J. J., CRUZ, L. J., TACKEN, P. J., TEL, J., KREUTZ, M., ADEMA, G. J., BROWN, G. D., FIGDOR, C. G. & DE VRIES, I. J. M. 2012. The C-type lectin receptor CLEC9A mediates antigen uptake and (cross-)presentation by human blood BDCA3+ myeloid dendritic cells. *Blood,* 119**,** 2284-2292.

SEHGAL, K., RAGHEB, R., FAHMY, T. M., DHODAPKAR, M. V. & DHODAPKAR, K. M. 2014. Nanoparticle-Mediated Combinatorial Targeting of Multiple Human Dendritic Cell (DC) Subsets Leads to Enhanced T Cell Activation via IL-15–Dependent DC Crosstalk. *The Journal of Immunology,* 193**,** 2297-2305.

TEL, J., SITTIG, S. P., BLOM, R. A. M., CRUZ, L. J., SCHREIBELT, G., FIGDOR, C. G. & DE VRIES, I. J. M. 2013. Targeting Uptake Receptors on Human Plasmacytoid Dendritic Cells Triggers Antigen Cross-Presentation and Robust Type I IFN Secretion. *The Journal of Immunology,* 191**,** 5005-5012.

UNGER, W. W. J., VAN BEELEN, A. J., BRUIJNS, S. C., JOSHI, M., FEHRES, C. M., VAN BLOOIS, L., VERSTEGE, M. I., AMBROSINI, M., KALAY, H., NAZMI, K., BOLSCHER, J. G., HOOIJBERG, E., DE GRUIJL, T. D., STORM, G. & VAN KOOYK, Y. 2012. Glycan-modified liposomes boost CD4+ and CD8+ T-cell responses by targeting DC-SIGN on dendritic cells. *Journal of Controlled Release,* 160**,** 88-95.

WAECKERLE-MEN, Y. & GROETTRUP, M. 2005. PLGA microspheres for improved antigen delivery to dendritic cells as cellular vaccines. *Advanced Drug Delivery Reviews,* 57**,** 475-482.

ZELENAY, S., KELLER, A. M., WHITNEY, P. G., SCHRAML, B. U., DEDDOUCHE, S., ROGERS, N. C., SCHULZ, O., SANCHO, D. & REIS E SOUSA, C. 2012. The dendritic cell receptor DNGR-1 controls endocytic handling of necrotic cell antigens to favor cross-priming of CTLs in virus-infected mice. *The Journal of Clinical Investigation,* 122**,** 1615-1627.

ZHANG, J.-G., CZABOTAR, PETER E., POLICHENI, ANTONIA N., CAMINSCHI, I., SAN WAN, S., KITSOULIS, S., TULLETT, KIRSTEEN M., ROBIN, ADELINE Y., BRAMMANANTH, R., VAN DELFT, MARK F., LU, J., O'REILLY, LORRAINE A., JOSEFSSON, EMMA C., KILE, BENJAMIN T., CHIN, WEI J., MINTERN, JUSTINE D., OLSHINA, MAYA A., WONG, W., BAUM, J., WRIGHT, MARK D., HUANG, DAVID C. S., MOHANDAS, N., COPPEL, ROSS L., COLMAN, PETER M., NICOLA, NICOS A., SHORTMAN, K. & LAHOUD, MIREILLE H. 2012. The Dendritic Cell Receptor Clec9A Binds Damaged Cells via Exposed Actin Filaments. *Immunity,* 36**,** 646-657.

Appendix A

Receptor-Specific Delivery of Protein Antigen to Dendritic Cells by a Nanoemulsion Formed Using Top-Down Non-Covalent Click Self-Assembly

The entire Appendix A consists of the journal article published as:

ZENG, B. J., CHUAN, Y. P., O'SULLIVAN, B., CAMINSCHI, I., LAHOUD, M. H., THOMAS, R. & MIDDELBERG, A. P. J. 2013. Receptor-Specific Delivery of Protein Antigen to Dendritic Cells by a Nanoemulsion Formed Using Top-Down Non-Covalent Click Self-Assembly. *Small*, 9, 3736-3742.

The following modifications were made to the article:

- Page numbers of the original article were crossed out; and
- Page numbers consistent with those on the remainder of the thesis pages were inserted.

Receptor-Specific Delivery of Protein Antigen to Dendritic Cells by a Nanoemulsion Formed Using Top-Down Non-Covalent Click Self-Assembly

*B. J. Zeng, Y. P. Chuan, B. O' Sullivan, I. Caminschi, M. H. Lahoud, R. Thomas, and A. P. J. Middelberg**

Nanotechnology promises to make medicines better by enhancing control over their physical and biological properties, including cell selectivity.[1] Liposome nanocarriers and nanoparticles represent well-studied platforms for cell-specific delivery both in vitro and in vivo.[2] These systems can encode complex functionality, for example immune targeting and immune evasion, but often suffer from a lack of stability, limited cargo capacity, cellular processing through non-functional pathways, or a general loss of intended function simply due to the complexity of the in vivo environment.[3] At the other end of the drug delivery spectrum, emulsions and nanoemulsions have alreday found widespread use in clinical medicine but, in most cases, do not encode sophisticated function, for example the ability to specifically target a given cell population in vivo.[4] This limitation arises from the difficulty of engineering the emulsion interface, which is usually populated by mixed chemical species including surfactants, and is less physically and chemically defined than the solid counterpart. A nanoemulsion able to evade immune clearance to specifically target a sub-population of cells in vivo via a chosen receptor has not, to the best of our knowledge, been reported.

Here we report a new method for assembling a molecularly defined nano-sized oil-in-water emulsion that is able to target dendritic cells (DC) in a receptor-specific fashion to activate a specific T-cell response. Our approach employs non-covalent click self-assembly, building an emulsion from the interface up using top-down sequential reagent addition. The nanoemulsion is formed using recently-reported molecular approaches for emulsion interface design and stabilisation, and relies on mixing closely-matched designer biosurfactant peptides and proteins at the oil-water interface. By conjugating immune-evading poly-ethylene glycol (PEG) or receptor-specific antibody elements with biosurfactant protein, we show it is possible to present and tune the presence and function of the elements at the interface by simple ratioed sequential addition of reagents to the self-assembling mixture. In this work, intraperitoneal administration of an optimised nanoemulsion to mice confirmed specific uptake by the subset of DCs targeted by an anti-Clec9A monoclonal antibody, a receptor understood to facilitate enhanced $CD8^+$ T cell mediated vaccine responses as would be required for anti-viral or anti-tumor immunity.[5] This work introduces a new class of targeted and immune-evading nanocarrier made using only biological components and facile processes, assembled in a bottom-up fashion through simple top-down sequential reagent addition.

A tailorable nano-sized emulsion (TNE) formed by sequential reagent addition has recently been shown to effectively co-deliver curcumin and antigen to cells in vitro.[6] The reported TNE comprised a core that is a pharmaceutical-grade oil stabilized by a surface-active designer peptide AM1,[7] rendered stable in physiological conditions by electrostatic deposition of the antigen of interest onto the TNE outer surface. However, this approach requires that the cargo antigen perform both a biological (antigenic) and physical (emulsion stabilization) role, and limits scope for further nano-engineering of the TNE surface (e.g. for cell targeting). Here we decouple the biological and physical design criteria through a novel emulsion nano-engineering approach. Inspired by the chemical similarity of a recently-reported protein biosurfactant DAMP4 and its recently-determined mixing behaviour with a small peptide surfactant closely related to AM1,[8] we hypothesized that DAMP4 would integrate into the interface of a TNE core that had been stabilised with AM1. We further hypothesized that attachment of an unrelated molecule to DAMP4 would result in that molecule being carried to, and displayed on, the aqueous side of the oil-water interface. We show that both hypotheses proved correct, and that conjugation of DAMP4 to

B. J. Zeng, Dr. Y. P. Chuan, Prof. A. P. J. Middelberg
The University of Queensland
Australian Institute for Bioengineering and Nanotechnology
St Lucia QLD 4072, Australia
E-mail: a.middelberg@uq.edu.au
Dr. B. O'Sullivan, Prof. R. Thomas
The University of Queensland
Diamantina Institute
Princess Alexandra Hospital
Woolloongabba QLD 4102, Australia
Dr. I. Caminschi, Dr. M. H. Lahoud
The Walter and Eliza Hall Institute of Medical Research
Parkville, VIC 3052, Australia
Dr. I. Caminschi, Dr. M. H. Lahoud
Centre for Immunology
Burnet Institute, Melbourne, VIC 3004, Australia

DOI: 10.1002/smll.201300078

both a monoclonal antibody (Ab) and PEG resulted in functional display of those molecules at the interface separating the oil droplet from the aqueous bulk. We further explore the use of DAMP4 to create a tailorable nanocarrier emulsion (TNE) with enhanced mononuclear phagocyte system (MPS) evasion and DC targeting, through precise control of PEG and anti-Clec9A presentation at the emulsion surface.

As an initial test of this approach we sought to decorate an AM1-stabilised TNE core with PEG, a non-toxic, non-immunogenic, hydrophilic and highly elastic polymer approved by FDA for pharmaceutical use.[9] PEG creates a steric barrier that reduces phagocytosis and increases colloidal stability under physiological conditions. Under our first hypothesis, conjugation of PEG to DAMP4 and addition of the conjugate to a pre-formed emulsion should functionalize the AM1-coated oil-water interface with PEG. **Figure 1**a shows this idea schematically. PEG (white) chemically conjugated to DAMP4 (dark blue) is introduced to a solution

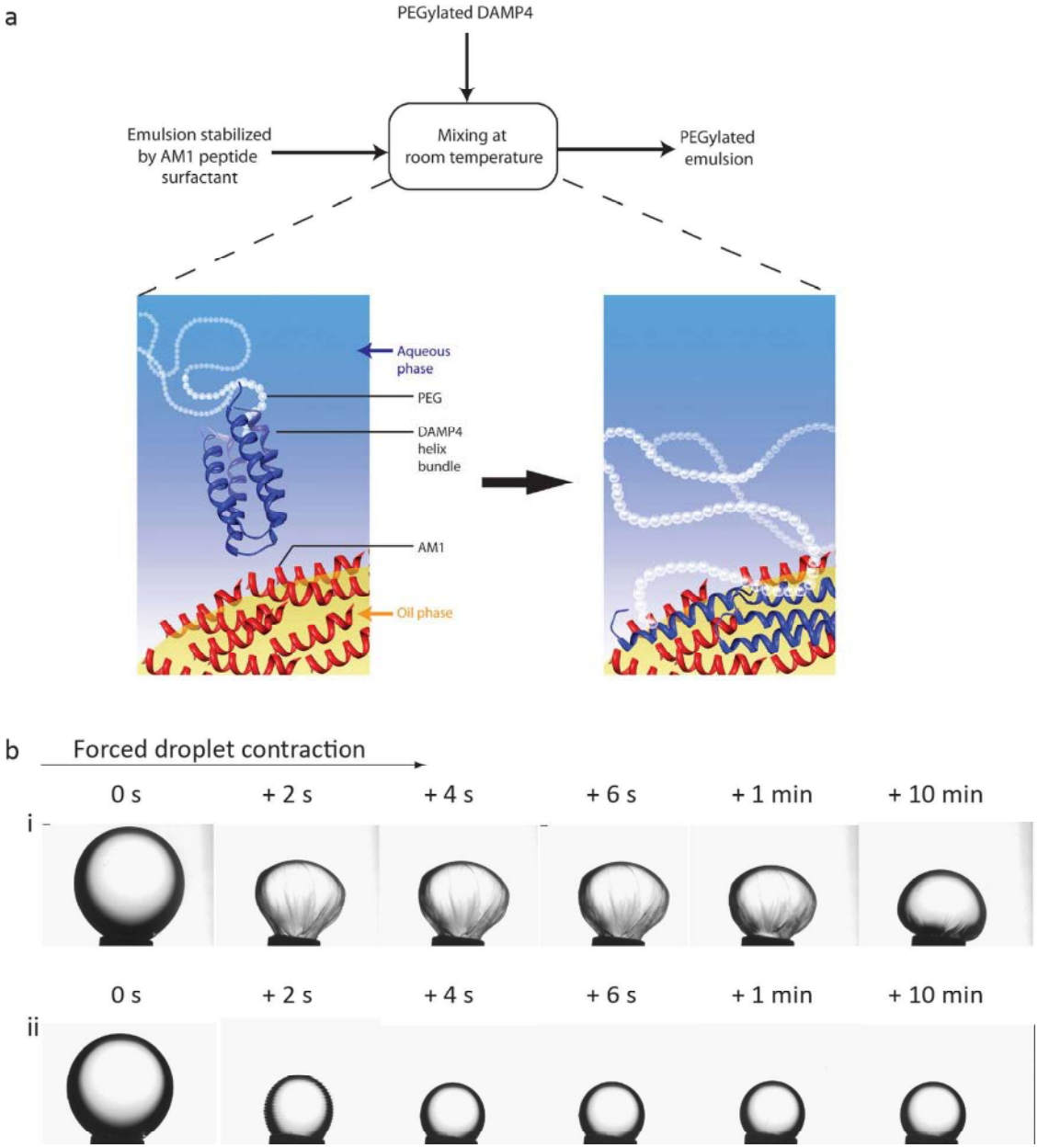

Figure 1. Decoration of the nanoemulsion oil-water interface with PEG by simple addition of PEGylated biosurfactant protein DAMP4 to an oil droplet previously formed in the presence of peptide surfactant AM1. a) Schematic representation of PEG (white) chemically conjugated to DAMP4 protein (dark blue) being introduced to a solution containing pre-formed nanoemulsion oil core (light yellow) stabilized by AM1 peptide (red), in aqueous buffer (light blue background). DAMP4 protein, which is chemically similar to AM1 peptide, is able to integrate into the oil-water interface formed between the core and the aqueous bulk. Prior conjugation of PEG to DAMP4 leads to its functional display at the interface through non-covalent molecular self-assembly. b) Photographs of a 10 min old Miglyol 812 bubble formed from an inverted needle in peptide AM1 solution, further aged for 30 min following the addition of either (i) PEGylated DAMP4 or (ii) HEPES buffer. Bubbles were subjected to a sudden contraction in volume and images were acquired using a drop shape tensiometer.

containing pre-formed TNE oil core (light yellow) stabilized by AM1 (red), in aqueous buffer (light blue background). The chemical similarity of DAMP4 and AM1 allows non-covalent interfacial coupling and hence integration of DAMP4 to the interface, with hydrophilic PEG projecting from its DAMP4 interfacial anchor into the aqueous phase surrounding the emulsion surface. We formed an oil bubble within an aqueous buffer solution comprising AM1 and allowed it to form a cohesive interfacial network at the oil-water interface.[6] PEGylated DAMP4 was then added to the buffer and aged for 30 min. When a sudden contraction of the bubble was imposed, the oil-water interface wrinkled as the bubble relaxed and the effect persisted for more than 10 min (Figure 1b i). In the absence of PEGylated DAMP4, the bubble relaxed to a spherical shape in less than 6 s (Figure 1b ii). The strikingly distinct interfacial behavior mediated by PEGylated DAMP4 is characteristic of an elastic interface,[10] likely due to the presence of the additional elastic PEG film connected to the oil-water interface by DAMP4, in keeping with our hypotheses.

We further tested the biological function of the TNE oil core modified with PEGylated DAMP4, by assessing whether the expected reduction in phagocytosis, due to core PEGylation, indeed occurred. We constructed a PEGylated TNE by adding 20 μM of PEGylated DAMP4 to a preformed 2% v/v AM1-stabilised TNE oil core (termed P_{20}-TNE, noting that the formulation comprises an AM1-stabilised core modified by addition of 20 μM PEG to the surrounding bulk aqueous phase), and co-cultured the emulsion with RAW264.7 macrophages for 2 h. Uptake of TNE was monitored with intensity of the DiI dye used to label the emulsion. Compared with uptake of a BSA-stabilized but non-PEGylated TNE,[6] uptake of P_{20}-TNE appeared to be reduced (**Figure 2**a), although significant uptake occurred in both cases. Further addition of 200 μM PEGylated DAMP4 to P_{20}-TNE created a modified TNE which notionally had a higher PEG surface coverage (P_{200}-P_{20}-TNE; *i.e.* P_{20}-TNE with a further 200 μM of PEG added to the surrounding bulk aqueous phase after prior addition of 20 μM PEG). In vitro testing confirmed that P_{200}-P_{20}-TNE exhibited reduced uptake by macrophages compared to P_{20}-TNE (Figure 2a), providing evidence that the core TNE is amenable to successive PEGylation via simple, top-down sequential addition of PEGylated DAMP4. Clearance by immune cells was investigated in vitro by co-culturing these TNEs with human peripheral blood mononuclear cells (hPBMC), predominantly comprising T and B cells, monocytes and dendritic cells (DCs). Figure 2b shows that uptake of P_{200}-P_{20}-TNE was consistently lower than that of the simple and previously-reported BSA-TNE across all of these cell types, with 40% and 20% reduction in internalization by monocytes and HLA-DR^{hi} $CD11c^+$ DCs, respectively. This result shows that the nanoemulsion, when appropriately covered with self-assembled PEG, is able to avoid non-specific cell uptake.

We next evaluated whether this top-down approach for sequential self assembly of components of the oil-water interface of the nanoemulsion could be applied to simultaneously down-regulate phagocytosis by generic immune cells

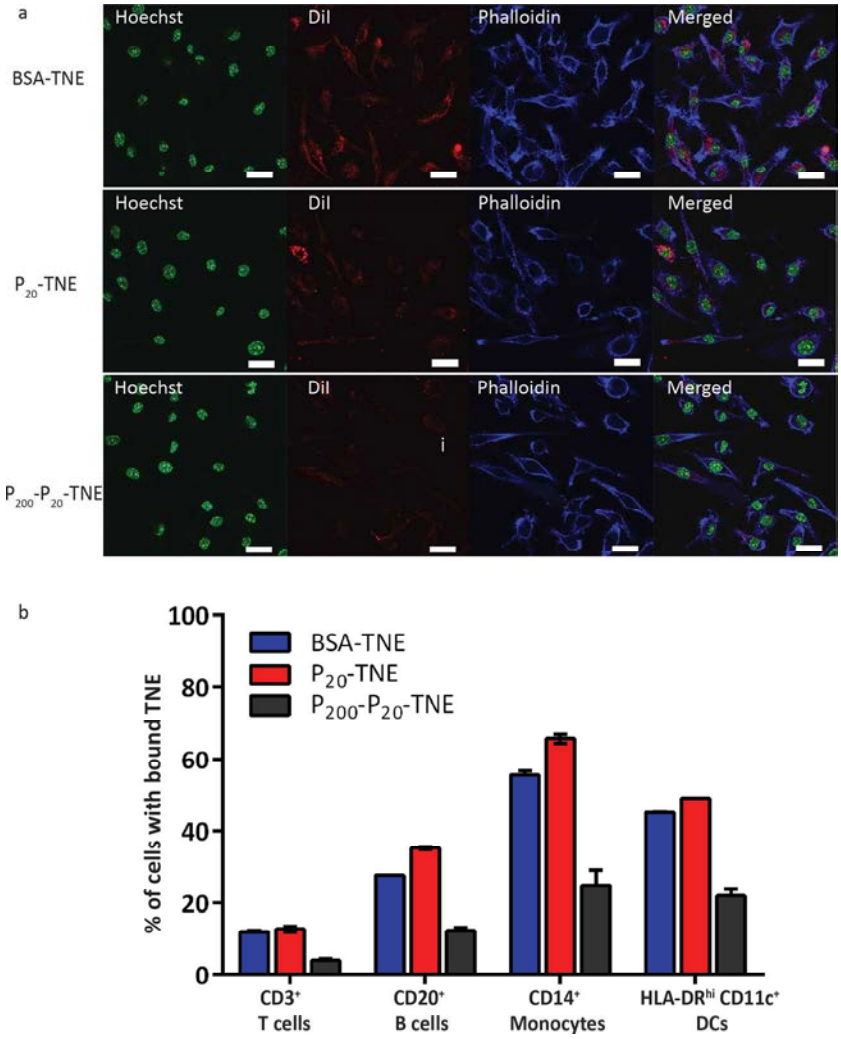

Figure 2. Biological function of self-assembled nanoemulsion after non-covalent coating with PEG using click self assembly. a) Confocal images showing uptake of BSA-TNE (a negative control reported previously, lacking PEG), P_{20}-TNE (an interface coated with a low amount of PEG) and P_{200}-P_{20}-TNE (nanoemulsion with a higher level of PEG interfacial coverage) by murine macrophage cell line (RAW264.7) after 2 h incubation. Nanoemulsions were labeled with fluorescent dye DiI (red). Cell nuclei were stained with Hoechst 33342 (green) and cell membrane was stained with Alexa Fluor® 647 conjugated phalloidin (blue). Scale bar 20 μm; b) Uptake of BSA-TNE, P_{20}-TNE and P_{200}-P_{20}-TNE by cell subpopulations within human peripheral blood mononuclear cells (PBMC). Gating strategy: T cells: $CD3^+$ $CD20^-$; B cells: $CD20^+$ $CD3^-$; monocytes: $CD14^+$, DCs: HLA-$DR^{hi}CD11c^+$. Results are expressed as mean with standard deviation (for N = 2), and demonstrate a clear down-redgulation of non-specific binding for PEGyalted nanoemulsions versus BSA-TNE.

small NANO MICRO

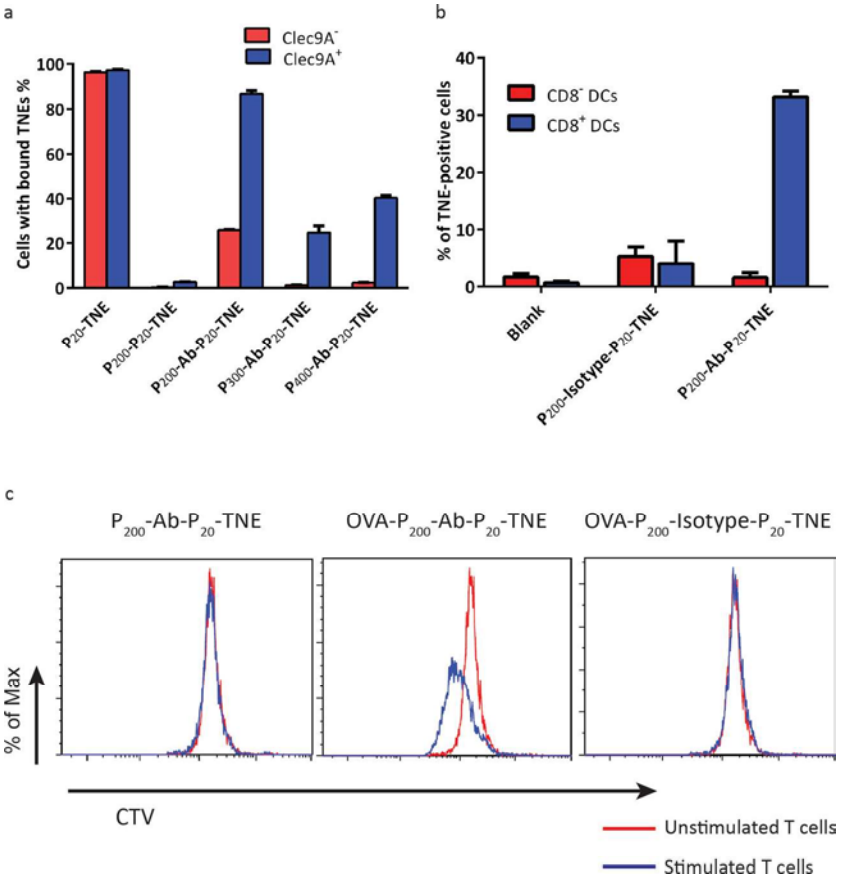

Figure 3. Immune evasive and active targeting characteristics of TNE. a) The percentage of Clec9A⁻ or Clec9A⁺ CHO-K1 cells bound with TNE calculated from flow cytograms showing the effects of increased PEG content in the Ab-P_{20}-TNE formulation. Results are shown as the mean of N = 3 experiments with standard deviation. b) In vivo cellular uptake of P_{200}-Ab-P_{20}-TNE and P_{200}-Isotype-P_{20}-TNE by CD8⁺ DC and CD8⁻ DCs. Results shown are mean and stanrad deviation from N = 2 experiments. c) In vitro proliferative response of CTV-labeled OT-I T cells to splenocytes pre-incubated with P_{200}-Ab-P_{20}-TNE, OVA-P_{200}-Ab-P_{20}-TNE or OVA-P_{200}-Isotype-P_{20}-TNE. CD8⁺ T cells proliferation was measured by CTV dilution after 4 days.

via PEGylation, and up-regulate specific delivery to target cells. We chose dendritic cells (DCs) as the model target cell, and an antibody against the highly DC-restricted receptor Clec9A[5b,5e] as the homing device on the nanoemulsion. DCs are unique in their ability as professional antigen presenting cells (APCs) to potently prime naïve T cells, making them an ideal drug-delivery target for enhanced vaccine efficacy or autoimmune disease treatments.[11] Targeted pharmaceutical delivery to DCs using an anti-Clec9A monoclonal antibody (mAb)[5b] previously yielded remarkable enhancement of biological efficacy, demonstrating that Clec9A is an excellent surface target for in situ DC delivery. Here, the anti-Clec9A mAb was first fused to DAMP4 (mAb-DAMP4) at the DNA level (see Experimental Section). A self-assembled nanoemulsion bearing the anti-Clec9A mAb and PEG on its surface was then created by adding 20 μM PEGylated DAMP4, 270 nM mAb-DAMP4 and 200 μM PEGylated DAMP4 to a pre-formed AM1-stabilised nanoemulsion, in a sequential order. The resulting nanoemulsion formed by non-covalent sequential self-assembly was termed P_{200}-Ab-P_{20}-TNE, enabling the sequence of additions to be easily identified.

The generic immune evasive and active targeting characteristics of P_{200}-Ab-P_{20}-TNE were evaluated in vitro using Chinese hamster ovary (CHO)-K1 cells with (Clec9A⁺) and without (Clec9A–) surface-expressed Clec9A receptors in a 1:10 number ratio (**Figure 3**a). P_{200}-Ab-P_{20}-TNE exhibited striking selectivity for Clec9A⁺ cells, binding to more than 85% of this subpopulation, which represented only 10% of the total population. Binding to Clec9A⁻ cells was significantly less (only 26%), even though these cells dominated the culture numerically. This result shows clear ability to target cells in a mixed population and in a receptor-specific fashion. As expected, P_{20}-TNE was present in over 95% of both the Clec9A⁺ and Clec9A– cells, showing no cell selectivity. P_{200}-P_{20}-TNE, on the other hand, almost completely avoided cell binding, likely due to the high PEG surface coverage on the TNE. These findings provided evidence that the anti-Clec9A mAb was connected to the oil-water interface of P_{200}-Ab-P_{20}-TNE by DAMP4 in a functional manner, and that presence of the mAb successfully up-regulated selectivity for targeted Clec9A-bearing CHO cells. These results suggest that cell selectivity could be adjusted by modifying the mAb to PEG ratio presented on the TNE surface. To test this theory, mAb-DAMP4 concentration was kept constant while varying the amount of PEGylated DAMP4 added in the sequential addition preparation method. Figure 3a shows that cell selectivity was increased in P_{300}-Ab-P_{20}-TNE and P_{400}-Ab-P_{20}-TNE, with the non-specific binding to Clec9A– cells almost abrogated. However, the enhanced selectivity was achieved at the expense of overall reduced binding, decreasing the binding to Clec9A⁺ cells to only 30-40%. Nonetheless, these results provide a very clear demonstration that the targeted nanoemulsion was able to very selectively target a specific set of cells in a mixed population of very similar cells, in a receptor-specific fashion. The ability to control for non-specific binding by simple variation of the amount of PEG versus targeting antibody also provides an elegant nanotechnology strategy to tune specificity and thus to control bio-distribution and pharmacokinetics.

We next investigated the in vivo distribution of P_{200}-Ab-P_{20}-TNE by injecting labeled emulsion into mice, and harvested splenocytes after 24 h. Clec9A is highly restricted to DCs and is selectively expressed by CD8⁺ conventional DCs and plasmacytoid DCs in mice[5b,5e] therefore allowing the Clec9A⁺ cells among the harvested cells to be tracked using the CD8 marker. Figure 3b shows that P_{200}-Ab-P_{20}-TNE associated selectively with the CD8⁺ DC sub-population; the emulsion was detected in >30% of the CD8⁺ DCs but in <2% of the CD8⁻ DCs. This finding supports the in vitro data,

demonstrating the excellent *in situ* targeted delivery capability of P_{200}-Ab-P_{20}-TNE. As expected, this level of striking cell selectivity was not exhibited by the control sample constructed in a similar way but using a non-specific isotype antibody instead of the anti-Clec9A mAb (P_{200}-Isotype-P_{20}-TNE). We also investigated whether the model antigen ovalbumin (OVA) delivered to $CD8^+$ cDCs via P_{200}-Ab-P_{20}-TNE was correctly processed through cellular compartments to cross-present to OVA-specific $CD8^+$ OT-I T cells. As demonstrated by dilution of CellTrace violet in Figure 3c, OVA encapsulated in P_{200}-Ab-P_{20}-TNE and incubated with splenocytes induced proliferation of OT-I T cells, while no T cell activation was observed for splenocytes stimulated with an equivalent nanoemulsion targeted with an isotype antibody (OVA-P_{200}-Isotype-P_{20}-TNE). This result confirmed that protein antigen specifically delivered to $CD8^+$ $Clec9A^+$ DCs via the P_{200}-Ab-P_{20}-TNE nanoemulsion was correctly processed and cross-presented to enable a cargo-specific $CD8^+$ T-cell response, following receptor targeting. Thus, the nanoemulsion was productively taken up by the target cell population in a receptor-targeted fashion, and was correctly processed by the target cells.

Overall, our work demonstrates that biocompatible designer nanoemulsions can be engineered using a new and simple top-down sequential addition approach. This approach of non-covalent click self-assembly by sequential top-down reagent addition is, to the best of our knowledge, entirely novel. It has been enabled by new methods of controlling the structure and composition of the emulsion interface, through the interfacial mixing of biosurfactant protein and peptide, linked to functional elements (antibody and PEG). The approaches reported in this paper potentially open a new direction for developing a new class of targeted nanocarrier system that could be tailored to enhance cell selectivity. As the equivalent molecule of mouse Clec9A was found to be selectively expressed by human BDCA-3^+ DCs,[5c] the current Clec9A targeting TNE platform has high potential for relevance to human clinical vaccine applications.[5c]

Experimental Section

Materials: AM1 (molar mass 2473, 95% purity) was custom synthesized by Genscript (Piscataway, NJ, USA) as reported previously.[7] Peptide concentration was determined by quantitative amino-acid analysis (Australian Proteome Analysis Facility, Sydney, NSW, Australia). Miglyol 812 was purchased from AXO Industry SA (Wavre, Belgium). 1,1′-Dioctadecyl-3,3,3′,3′-tetramethylindocarbocyanine perchlorate (DiI), Phalloidin-AlexaFluor 647, Hoechst 33342, CellTrace Violet and AlexaFluor 700-anti-CD20 were purchased from Molecular Probes (Victoria, Australia). 4-(2-Hydroxyethyl)-1-piperazineethanesulfonic acid (HEPES), albumin from chicken egg white (OVA) and zinc chloride ($ZnCl_2$) were purchased from Sigma-Aldrich (St Louis, MO, USA). mPEG-NHS (MW 5000, PDI <1.08, purity >95%) was purchased from Nanocs (Boston, MA, USA). RPMI-1640 and foetal calf serum (FCS) were purchased from GIBCO (Victoria, Australia). Ammonium chloride (NH_4Cl), potassium bicarbonate ($KHCO_3$), n-hexane and disodium salt of ethylenediaminetetraacetic acid (Na_2EDTA) were purchased from Ajax Finechem (NSW, Australia). Anti-CD8-eFluor780 was purchased from eBioscience (San Diego, CA, USA). APC-anti-HLA-DR, FITC-anti-CD3, PerCP5.5-anti-CD14, PE/Cy7-anti-I-A/I-E, PerCP5.5-anti-CD8, Pacific Blue-anti-CD19 and PE/Cy7-anti-CD11c were purchased from Biolegend (San Diego, CA, USA). Cithrol GMO HP was a gift from Croda Europe Ltd (Staffordshire, United Kingdom)

Mice: Mice were bred at the Diamantina Institute Biological Research Facility (BRF) at The University of Queensland under specific pathogen-free conditions. Experiments were approved by the UQ Animal Ethics Committee.

DAMP4 Expression, Purification and PEGylation: Expression and purification of DAMP4 followed published methods based on recombinant expression coupled with chromatographic purification and verification of identity by mass spectometry.[8b] To prepare PEGylated DAMP4, lyophilized DAMP4 was dissolved in HEPES (25 mM, pH 7.0) and a weighed amount of mPEG-NHS (see *Materials*) was added to the solution to give a molar ratio of mPEG:DAMP4 of 20:1. The reaction was allowed to incubate at 4 °C for 16 h. The resulting PEGylated DAMP4 was used without purification after verification of an increase in mass by conventional SDS-PAGE, which showed a yield >50% (data not shown).

Preparation of DAMP4 Fused with Antibody: The cDNA encoding heavy and light chains of (anti-Clec9A clone 24/04-10B4; rat IgG2a isotype control clone GL117) were amplified from the original hybridomas[5b] and cloned by RACE amplification as previously described.[12] The cDNA antibody heavy chains were subcloned into a pcDNA 3.1 vector modified to contain an Ala-Ala-Ala linker fused to DAMP4 cDNA. This construct enables the generation of a single a fusion protein where the C-terminal region of the heavy chain is fused to an alanine linker and DAMP4. The antibody light chains were cloned into pcDNA3.1. Plasmid DNA was prepared using the GigaPrep Plasmid DNA extraction kit (Qiagen, Hilden, Germany), and plasmids encoding the kappa chain, and the heavy chain linked to OVA were transiently co-transfected into freestyle 293F cells (Invitrogen) using 293Fectin transfection reagent as per manufacturer's recommendations. Culture supernatant containing the recombinant antibodies were harvested, and the antibodies purified by affinity chromatography using Protein G Sepharose. Recombinant antibodies were validated for their ability to bind Clec9A on transfectant cells as previously described.[5b]

Sudden Bubble Contraction Experiment: A drop shape tensiometer (DSA-10, Krüss GmbH, Hamburg, Germany) was used to record images. An 8 mL quartz cuvette (Hellma GmbH, Mülheim, Germany) was filled with AM1 peptide (5 μM) and zinc chloride (100 μM) in HEPES (25 mM, pH 7.0). An inverted needle fitted to a gas-tight glass syringe (SGE Analytical Science Pty Ltd, Ringwood, Australia) was submerged into the cuvette and Miglyol 812 was injected to form a droplet. Miglyol 812 droplets were first aged for 10 min before PEGylated DAMP4 (10 μM) or an equivalent volume of HEPES buffer (25 mM, pH 7.0) was added. Droplets were then aged for another 30 min before a sudden reduction in droplet volume was performed by withdrawing Miglyol 812 back into syringe.

TNE Preparation: To prepare TNE core, lyophilized AM1 (400 μM) was dissolved in 980 μL HEPES (25 mM, pH 7.0) containing $ZnCl_2$ (800 μM). Twenty microliter of Miglyol 812 was added to give an oil volume fraction of 2% (v/v). The mixture was homogenized using a Branson Sonifier 450 ultrasonicator for four 45 s bursts at 60 W. To prepare P_{20}-TNE, TNE (500 μL) was added to PEGylated DAMP4

small NANO MICRO

solution (500 μL, 40 μM) followed by 60 s of vigorous stirring using a magnetic stirrer. To prepare P_{200}-P_{20}-TNE, P_{20}-TNE (500 μL) was added to PEGylated DAMP4 solution (500 μL, 400 μM) followed by 60 seconds of vigorous stirring using a magnetic stirrer. For preparation of P_{200}-Ab-P_{20}-TNE, mAb-DAMP4 (36 μL, 3 μM) was added to P_{20}-TNE (200 μL) followed by 60 s of vigorous stirring using a magnetic stirrer, and subsequently Ab-P_{20}-TNE (200 μL) was added to PEGylated DAMP4 (200 μL, 400 μM), followed by 60 seconds of vigorous stirring. TNE size was measured by Malvern Zetasizer Nano ZS (Malvern, Worcestershire, UK) equipped with a He-Ne laser (633 nm). Data analysis was with DTS software (Malvern, version 6.2), using a non-negatively constrained least squares (NNLS) fitting algorithm. Dispersant refractive index and viscosity of the dispersant were assumed to be 1.45 and 1.02 cP, respectively. For each sample, 10 runs of 10s were performed. TNE size distribution was expressed as mean (nm) ± standard deviation and polydispersity index from three repeated measurements. The AM1-coated oil TNE core (dp = 163.8 ± 1.3 nm, PDI = 0.174) was measured to be smaller than both P_{20}-TNE (dp = 168.0 ± 1.0 nm, PDI = 0.170) and P_{200}-Ab-P_{20}-TNE (dp = 181.9 ± 0.166).

Analysis of In vitro Cell Uptake: RAW264.7 mouse macrophage cells were cultured in RPMI-1640 medium supplemented with FCS (5%, v/v). One day before the uptake experiment, cells (2.5×10^5 cells per well) were seeded into a 24-well flat bottom tissue culture plate (Greiner Bio-One, Frickenhausen, Germany) with 12-mm diameter glass slips and incubated at 37 °C with 5% CO_2 supplied. The following day, DiI labelled BSA-TNE (25 μL) or P_{20}-TNE (25 μL) or P_{200}-P_{20}-TNE (50 μL) was added to the corresponding well and co-cultured with cells for 2 h at 37 °C with 5% CO_2 supplied. Cells were fixed with 4% paraformaldehyde. Cell nuclei were stained with Hoechst 33342 and cell membrane was stained with Phalloidin-AlexaFluor 647. Mounted glass slips were imaged on an Apotome microscope (Carl-Ziess, Sydney, Australia). For in vitro uptake in human peripheral blood mononuclear cells (PBMC), cells (5×10^5 cells per well) were seeded into a 24-well flat bottom tissue culture plate in 1 mL of RPMI-1640 medium supplemented with FCS (5%, v/v). DiI labelled BSA-TNE (25 μL) or P_{20}-TNE (25 μL) or P_{200}-P_{20}-TNE (50 μL) was added to the corresponding wells and co-cultured with cells for 3 h at 37 °C with 5% CO_2 supplied. After washing with PBS, cells were stained with APC-anti-HLA-DR and PE/Cy7-anti-CD11c (DCs), FITC-anti-CD3 (T cells), PerCP5.5-anti-CD14 (monocytes) and Pacific Blue-anti-CD19 (B cells). Cell uptake was analysed on a Beckman Coulter Gallios Flow Cytometer.

Analysis of In vivo Specificity: Two hundred micro liter of DiI labelled P_{200}-Ab-P_{20}-TNE or P_{200}-Isotype-P_{20}-TNE was injected intraperitoneally into C57BL/6 mice. Twenty four hours post injection, spleens were removed and digested with Collagenase Type III (Worthington) for 25 min at room temperature. Digested tissue was passed through a cell strainer and then centrifuged at 800 *g* for 2 min before removing red blood cells by incubation in ACK lysis buffer (150 mM NH_4Cl, 1 mM $KHCO_3$, 0.1 mM Na_2EDTA). Single cell suspension was stained with anti-I-A/I-E-PE/Cy7, anti-CD11c-PerCP5.5 and anti-CD8-eFluor780. Cells were analysed on a Beckman Coulter Gallios Flow Cytometer. $CD8^+$ DCs were gated as I-A/I-$E^{hi}CD11c^+CD8^+$ and $CD8^-$ DCs were gated as I-A/I-$E^{hi}CD11c^+CD8^-$.

Preparation of OVA in Oil Dispersion: OVA solution (8 mg mL^{-1}) was prepared by dissolving OVA (80 mg) in ultrapure water (10 mL). Cithrol GMO HP solution (1%, w/v) was prepared by dissolving Cithrol GMO HP (200 mg) in hexane (20 mL). OVA solution (1 mL) and Cithrol GMO HP solution (2 mL) were transferred into a 20 mL glass vial, and mixed by using a homogenizer at 24,000 rpm for 5 min to form stable water in oil (w/o) emulsion. The resulting emulsion was frozen rapidly in dry ice for 2 h before being lyophilized for 24 h. The resulting OVA-Cithrol GMO HP pellet was dissolved in Miglyol 812 (3 mL), and used as oil phase for preparing OVA-P_{20}-Ab-P_{200}-TNE and OVA-P_{20}-Isotype-P_{200}-TNE.

In vitro Cross-Presentation Assay: To prepare splenocytes, spleen from C57BL/6 mouse was removed and digested with Collagenase Type III (Worthington) for 30 min at room temperature. Digested tissue was passed through a cell strainer and then centrifuged at 430*g* for 5 min before removing erythrocytes by incubation in ACK lysis buffer (150 mM NH_4Cl, 1 mM $KHCO_3$, 0.1 mM Na_2EDTA). OT-I cells were isolated from spleen and lymph nodes (LNs) of OT-I mice and purified using Miltenyi CD8α$^+$ T Cell Isolation Kit II (Miltenyi Biotec Australia Pty. Ltd., NSW, Australia). Purified OT-I cells were stained with CellTrace Violet for in vitro tracking.

Splenocytes were treated with Mitomycin C (Sigma-Aldrich, St Louis, MO, USA) to block cell division. Mitomycin C treated splenocytes (10^6 cells) were cultured with P_{200}-Ab-P_{20}-TNE, OVA-P_{200}-Ab-P_{20}-TNE or OVA-P_{200}-Isotype-P_{20}-TNE (50 μL) for 3 h at 37 °C with 5% CO_2. At the end of the incubation, splenocytes were washed three times with RPMI-1640 supplemented with FCS (5%, v/v) before being added to wells of a 96-well tissue culture plate at 5×10^5 cells per well in 100 μL RPMI-1640 medium supplemented with FCS (5%, v/v). 2.5×10^5 of OT-I cells in 100 μL RPMI-1640 medium supplemented with FCS (5%, v/v) were then added to each well and cultured for 4 days at 37 °C with 5% CO_2 supplied. Cells were harvested from 96-well plate and stained with PerCP5.5-anti-CD8. OT-I T cell proliferation was measured as a function of CellTrace Violet dye dilution after gating on $CD8^+$ T cells.

Acknowledgements

This research was supported by Australian Research Council Discovery Grants DP1093056 and DP120103683 (APJM), The Queensland Government 2010 Smart Futures Premier's Fellowship (APJM), and National Health and Medical Research Council of Australia (NHMRC) project grant 575546 (MHL, IC). This work was facilitated by The Queensland Government and Atlantic Philanthropies through construction of the AIBN and Diamantina Institute, and through Victorian State Government Operational Infrastructure Support and Australian Government NHMRC IRIIS.

[1] a) J. Bath, A. J. Turberfield, *Nat. Nanotechnol.* **2007**, *2*, 275; b) P. X. Guo, *Nat. Nanotechnol.* **2010**, *5*, 833; c) S. M. Metcalfe, T. M. Fahmy, *Trends. Mol. Med.* **2012**, *18*, 72; d) D. Peer, J. M. Karp, S. Hong, O. C. FaroKhzad, R. Margalit, R. Langer, *Nat. Nanotechnol.* **2007**, *2*, 751; e) V. P. Torchilin, *Adv. Drug Deliv. Rev.* **2006**, *58*, 1532.

[2] a) C. E. Ashley, E. C. Carnes, G. K. Phillips, D. Padilla, P. N. Durfee, P. A. Brown, T. N. Hanna, J. W. Liu, B. Phillips, M. B. Carter, N. J. Carroll, X. M. Jiang, D. R. Dunphy, C. L. Willman, D. N. Petsev, D. G. Evans, A. N. Parikh, B. Chackerian, W. Wharton, D. S. Peabody, C. J. Brinker, *Nat. Mater.* **2011**, *10*(5), 389; b) J. M. Hu, Y. F. Qian, X. F. Wang, T. Liu, S. Y. Liu, *Langmuir* **2012**, *28*(4), 2073; c) K. Kaaki, K. Herve-Aubert, M. Chiper,

A. Shkilnyy, M. Souce, R. Benoit, A. Paillard, P. Dubois, M. L. Saboungi, I. Chourpa, *Langmuir* **2012**, *28*(2), 1496; d) J. F. Kukowska-Latallo, K. A. Candido, Z. Y. Cao, S. S. Nigavekar, I. J. Majoros, T. P. Thomas, L. P. Balogh, M. K. Khan, J. R. Baker, *Cancer Res.* **2005**, *65*(12), 5317; e) Y. T. Liu, K. Li, J. Pan, B. Liu, S. S. Feng, *Biomaterials* **2010**, *31*(2), 330; f) A. Mathew, T. Fukuda, Y. Nagaoka, T. Hasumura, H. Morimoto, Y. Yoshida, T. Maekawa, K. Venugopal, D. S. Kumar, *Plos One* **2012**, *7*(3) e3216; g) S. T. Reddy, A. Rehor, H. G. Schmoekel, J. A. Hubbell, M. A. Swartz, *J. Control. Release* **2006**, *112*(1), 26; h) K. Shroff, E. Kokkoli, *Langmuir* **2012**, *28*(10), 4729; i) X. Ying, H. Wen, W. L. Lu, J. Du, J. Guo, W. Tian, Y. Men, Y. Zhang, R. J. Li, T. Y. Yang, D. W. Shang, J. N. Lou, L. R. Zhang, Q. Zhang, *J. Control. Release* **2010**, *141*(2), 183; j) M. Yoshida, R. Takimoto, K. Murase, Y. Sato, M. Hirakawa, F. Tamura, T. Sato, S. Iyama, T. Osuga, K. Miyanishi, K. Takada, T. Hayashi, M. Kobune, J. Kato, *Plos One* **2012**, *7*(7), e39545.

[3] a) A. Salvati, A. S. Pitek, M. P. Monopoli, K. Prapainop, F. B. Bombelli, D. R. Hristov, P. M. Kelly, C. Aberg, E. Mahon, K. A. Dawson, *Nat. Nanotechnol.* **2013**, *8*(2), 137; b) J. A. Kim, C. Aberg, A. Salvati, K. A. Dawson, *Nat. Nanotechnol.* **2012**, *7*(1), 62; c) E. Ruoslahti, S. N. Bhatia, M. J. Sailor, *J. Cell Biol.* **2010**, *188*(6), 759; d) M. J. Turk, D. J. Waters, P. S. Low, *Cancer Lett.* **2004**, *213*(2), 165.

[4] a) S. Ganta, M. Amiji, *Mol. Pharmaceutics* **2009**, *6*(3), 928; b) N. S. Santos-Magalhaes, A. Pontes, V. M. W. Pereira, M. N. P. Caetano, *Int. J. Pharm.* **2000**, *208*(1-2), 71; c) S. Khandavilli, R. Panchagnula, *J. Invest. Dermatol.* **2007**, *127*(1), 154; d) P. E. Makidon, A. U. Bielinska, S. S. Nigavekar, K. W. Janczak, J. Knowlton, A. J. Scott, N. Mank, Z. Y. Cao, S. Rathinavelu, M. R. Beer, J. E. Wilkinson, L. P. Blanco, J. J. Landers, J. R. Baker, *Plos One* **2008**, *3*(8), e2954; e) A. Myc, J. F. Kukowska-Latallo, A. U. Bielinska, P. Cao, P. P. Myc, K. Janczak, T. R. Sturm, M. S. Grabinski, J. J. Landers, K. S. Young, J. Chang, T. Hamouda, M. A. Olszewski, J. R. Baker, *Vaccine* **2003**, *21*(25-26), 3801.

[5] a) I. Caminschi, M. H. Lahoud, K. Shortman, *Eur. J. Immunol.* **2009**, *39*(4), 931; b) I. Caminschi, A. I. Proietto, F. Ahmet, S. Kitsoulis, J. S. Teh, J. C. Y. Lo, A. Rizzitelli, L. Wu, D. Vremec, S. L. H. van Dommelen, I. K. Campbell, E. Maraskovsky, H. Braley, G. M. Davey, P. Mottram, N. V. De Velde, K. Jensen, A. M. Lew, M. D. Wright, W. R. Heath, K. Shortman, M. H. Lahoud, *Blood* **2008**, *112*(8), 3264; c) I. Caminschi, K. Shortman, *Trends Immunol.* **2012**, *33*(2), 71; d) I. Caminschi, D. Vremec, F. Ahmet, M. H. Lahoud, J. A. Villadangos, K. M. Murphy, W. R. Heath, K. Shortman, *Mol. Immunol.* **2012**, *50*(1-2), 9; e) C. Huysamen, J. A. Willment, K. M. Dennehy, G. D. Brown, *J. Biol. Chem.* **2008**, *283*(24), 16693.

[6] Y. P. Chuan, B. Y. Zeng, B. O'Sullivan, R. Thomas, A. P. J. Middelberg, *J. Colloid Interface Sci.* **2012**, *368*(1), 616.

[7] A. F. Dexter, A. S. Malcolm, A. P. J. Middelberg, *Nat. Mater.* **2006**, *5*(6), 502.

[8] a) M. D. Dwyer, L. Z. He, M. James, A. Nelson, A. P. J. Middelberg, *J. R. Soc., Interface.* **2013**, *10*(80), 20120987; b) A. P. J. Middelberg, M. Dimitrijev-Dwyer, *Chem Phys Chem.* **2011**, *12*(8), 1426.

[9] J. M. Harris, R. B. Chess, *Nat. Rev. Drug Discov.* **2003**, *2*(3), 214.

[10] A. S. Malcolm, A. F. Dexter, J. A. Katakdhond, S. I. Karakashev, A. V. Nguyen, A. P. J. Middelberg, *ChemPhysChem* **2009**, *10*(5), 778.

[11] K. Shortman, M. H. Lahoud, I. Caminschi, *Exp. Mol. Med.* **2009**, *41*(2), 61.

[12] M. H. Lahoud, F. Ahmet, S. Kitsoulis, S. S. Wan, D. Vremec, C. N. Lee, B. Phipson, W. Shi, G. K. Smyth, A. M. Lew, Y. Kato, S. N. Mueller, G. M. Davey, W. R. Heath, K. Shortman, I. Caminschi, *J. Immunol.* **2011**, *187*(2), 842.

Received: January 9, 2013
Revised: March 12, 2013
Published online: April 18, 2013

Appendix B

Co-delivery of antigen and a lipophilic anti-inflammatory drug to cells via a tailorable nanocarrier emulsion

The entire Appendix B consists of the journal article published as:

CHUAN, Y. P., ZENG, B. Y., O'SULLIVAN, B., THOMAS, R. & MIDDELBERG, A. P. J. 2011. Co-delivery of antigen and a lipophilic anti-inflammatory drug to cells via a tailorable nanocarrier emulsion. *Journal of Colloid and Interface Science,* 368**,** 616-624.

The following modifications were made to the article:

- Page numbers of the original article were crossed out; and
- Page numbers consistent with those on the remainder of the thesis pages were inserted.

Journal of Colloid and Interface Science 368 (2012) 616–624

Contents lists available at SciVerse ScienceDirect

Journal of Colloid and Interface Science

www.elsevier.com/locate/jcis

Co-delivery of antigen and a lipophilic anti-inflammatory drug to cells via a tailorable nanocarrier emulsion

Yap Pang Chuan [a], Bi Yun Zeng [a], Brendan O'Sullivan [b], Ranjeny Thomas [b], Anton P.J. Middelberg [a,*]

[a] The University of Queensland, Australian Institute for Bioengineering and Nanotechnology, St. Lucia, QLD 4072, Australia
[b] The University of Queensland, Diamantina Institute for Cancer, Immunology and Metabolic Medicine, Level 4, R Wing, Princess Alexandra Hospital, Ipswich Rd., Woolloongabba, QLD 4102, Austraila

ARTICLE INFO

Article history:
Received 27 July 2011
Accepted 5 November 2011
Available online 22 November 2011

Keywords:
Drug delivery
Emulsion
Nanotechnology
Biosurfactant
Arthritis
Curcumin

ABSTRACT

Nanotechnology promises new drug carriers that can be tailored to specific applications. Here we report a new approach to drug delivery based on tailorable nanocarrier emulsions (TNEs), motivated by a need to co-deliver a protein antigen and a lipophilic drug for specific inhibition of nuclear factor kappa B (NF-κB) in antigen presenting cells (APCs). Co-delivery for NF-κB inhibition holds promise as a strategy for the treatment of rheumatoid arthritis. We used a highly surface-active peptide (SAP) to prepare a nanosized emulsion having defined surface properties predictable from the SAP sequence. Incorporating the lipophilic drug into the oil phase at the time of emulsion formation enabled its facile packaging. The SAP is depleted from bulk during emulsification, allowing simple subsequent addition of the drug-loaded oil-in-water emulsion to a solution of protein antigen. Decoration of emulsion surface with antigen was achieved via electrostatic deposition. *In vitro* data showed that the TNE prepared this way was internalized and well-tolerated by model APCs, and that good suppression of NF-κB expression was achieved. This work reports a new type of nanotechnology-based carrier, a TNE, which can potentially be tailored for co-delivery of multiple therapeutic components, and can be made using simple methods using only biocompatible materials.

1. Introduction

Increasing research in drug delivery is driven by a growing library of lipophilic candidates from drug discovery [1] and by new opportunities for simpler carrier design resulting from nanotechnology innovations [2]. With almost 40% of new therapeutic candidates and over 30% of pipeline drugs exhibiting poor water solubility [3], there is a tremendous need for systems able to deliver lipophilic molecules to their biological targets at meaningful therapeutic levels and in a way that can be tailored for specific biological outcomes. Carriers able to encapsulate poorly water-soluble drugs that have defined structure down to the nanoscale hold great promise for new drug delivery modalities [4].

Emulsion templating provides a sophisticated means to create nanocontainers for the delivery of lipophilic compounds. Using this approach, single or multiple polyelectrolyte layers are electrostatically deposited onto emulsion droplets preloaded with drugs [5–7] (Fig. 1a). In most cases organic solvents not approved for human injection, such as chloroform, are used to facilitate solubilization of the poorly water-soluble ionic surfactants needed to initiate deposition of the first layer [e.g. dioctadecyldimethylammonium bromide (DODAB) [6] and docusate sodium (AOT) [7]]. Removal of the templating core using organic solvents is also often required [5]. These inefficiencies necessitate tedious and time-consuming centrifugation and wash steps (Fig. 1a), and mandate stringent monitoring procedures to ensure removal of residual solvents down to levels that might be considered acceptable to the regulatory authorities.

A superior strategy for nanocarrier construction would involve the use of only biocompatible components in the preparation method, and sequential addition of components in such a way that their removal between individual steps in the process is not required for regulatory purposes. Here we report such a method which is inspired by innovations in the food sector, where emulsions have been prepared using only biocompatible components such as lecithins and food proteins [8,9] (Fig. 1b) or food-grade polyelectrolytes such as chitosan and alginate [10,11]. Specifically, we use a designer peptide surfactant AM1 [12] to develop a tailorable nanocarrier emulsion (TNE), and show efficient cellular uptake.

Peptide surfactants comprising a short helix-forming sequence based on the peptide Lac21 [13], such as AM1, have very high interfacial activity and rapid interfacial adsorption [14]. Rapid

* Corresponding author. Address: Australian Institute for Bioengineering and Nanotechnology, School of Chemical Engineering, The University of Queensland, St. Lucia QLD 4072, Australia. Fax: +61 7 3346 4197.
E-mail address: a.middelberg@uq.edu.au (A.P.J. Middelberg).

0021-9797/$ - see front matter © 2011 Elsevier Inc. All rights reserved.
doi:10.1016/j.jcis.2011.11.014

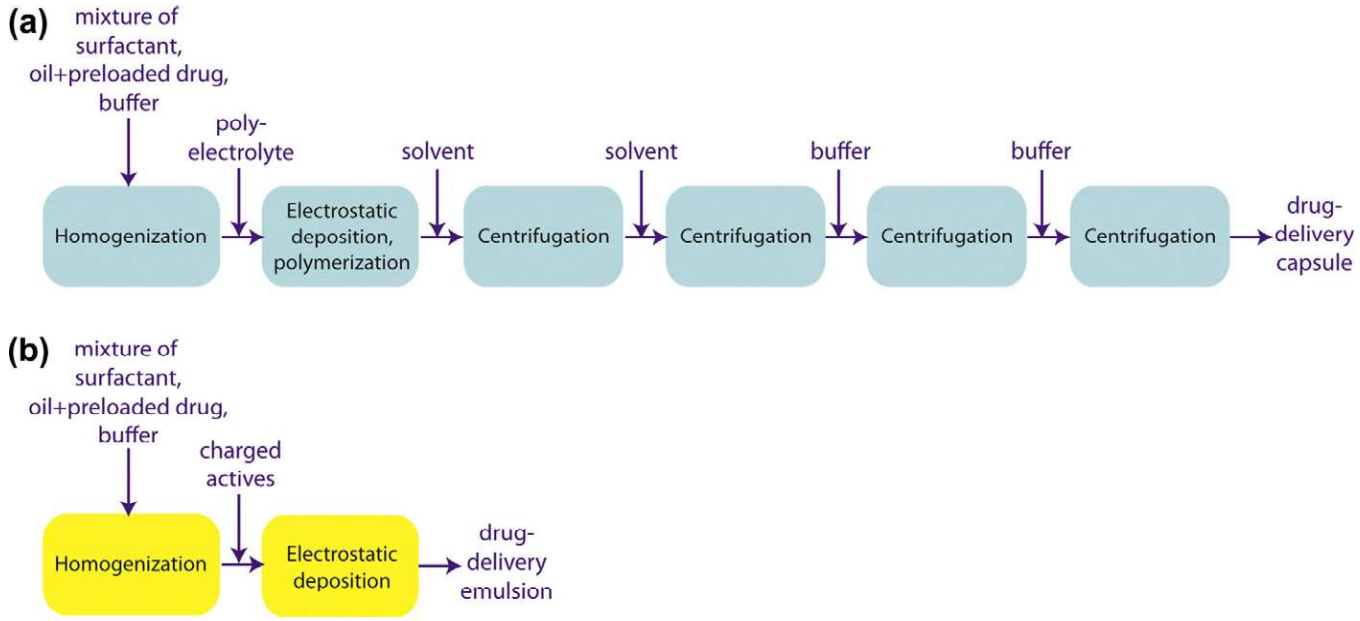

Fig. 1. Preparation of nanocarriers based on emulsion templating, when (a) organic solvents are required for surfactant solubilization and template removal; or (b) when only biocompatible materials are used.

adsorption of these highly surface active peptides (SAP) facilitates efficient interfacial coverage resulting in easy formation of a nano-scale emulsion having a narrow size distribution, while high interfacial activity ensures depletion of the peptide from the bulk aqueous phase, eliminating the need for a wash step following emulsion formation. Additionally, the properties of the emulsion interface are tunable by changing either the sequence of the peptide [15] or the buffer pH and ionic character [12,16], so that the mechanical behavior of the resulting nanocarrier can be tailored to resemble a conventional emulsion or a nanocapsule [17]. Advantageously, AM1 yields a precisely defined and understood interfacial structure [18,19] that can be molecularly tailored to facilitate further nanocarrier surface engineering, as might be needed for a specific biological application. The combination of a simple nanoscale emulsion formation method, along with the ability to tailor the mesoscopic and molecular character of the interface, makes this TNE approach potentially advantageous as a new platform for delivery, particularly for multiple-component therapy. Therapeutic components can be incorporated into the TNE interfacial membranes and be co-delivered with a small-molecule drug to designated biological sites.

Rheumatoid arthritis (RA) affects up to 1% of the global population, causing pain, impaired movement and a reduction in mean life expectancy by up to 10 years [20]. Recent findings suggest that a biologically efficient strategy for treating RA is by co-delivery of an antigen and a small-molecule inhibitor, such as curcumin, to antigen-presenting cells (APCs) [21,22]. We therefore investigated the design strategy of adsorbing an anionic antigen onto the positively-charged surface of a TNE, which also carries curcumin included in the oil at the time of emulsion formation. This approach was informed by studies that identified nuclear factor kappa B (NF-κB) as an attractive therapeutic target for RA [23]. NF-κB is a nuclear transcription factor that plays a key role in APCs in the initiation of immunity. Although suppression of NF-κB activity reduces chronic inflammation associated with auto-immune diseases, global inhibition of NF-κB is toxic and may result in increased susceptibility to infection [21,22]. Co-delivery of lipophilic NF-κB inhibitors together with autoimmune antigens by liposomes results in antigen-specific NF-κB suppression, which have been shown to reduce clinical signs of inflammatory arthritis in animal models [22].

In this work, a monodispersed, sub-200 nm AM1-based TNE is developed and used for the successful co-delivery of curcumin and an animal-model-relevant antigen [22] into APCs. The TNE was well-tolerated by the APCs investigated, and succeeded in inhibiting the expression of NF-κB in *in vitro* experiments. The TNE preparation method described here is simple, sequential and efficient, and opens a new approach for the co-delivery of antigens and lipophilic small molecules through nano-tailoring of emulsions.

2. Results and discussion

2.1. Formulation studies for curcumin encapsulation

Delivery of curcumin was a primary objective in this work. Therefore, the emulsion oil phase was chosen to maximize the amount of curcumin encapsulated, and to produce an emulsion with stability and physical properties suitable for delivery. Food-grade olive, canola and sunflower oils as well as Miglyol 812 were investigated for their ability to dissolve curcumin. Fig. 2 shows the reversed-phase high-pressure chromatography (RP-HPLC) analysis of curcumin solubilized in different oils. The RP-HPLC chromatograms consistently showed a broad peak with substantial shoulders, with overlap of several elution peaks. This finding was consistent with evidence that commercially available turmeric extracts were not pure, instead consisting of a number of curcuminoids including curcumin, demethoxycurcumin and bisdemethoxycurcumin [24]. Related studies on anti-inflammatory properties of curcumin had been performed using unpurified turmeric extracts containing these curcuminoids [22,25]. To allow direct comparison with these studies, the entire chromatography peak area from 5 to 10 min was included in the quantitation process. Curcumin solubility was the highest in Miglyol 812 (4.4 mg ml^{-1}), and significantly lower in the other oils investigated (0.9–1.0 mg ml^{-1}).

Therefore, Miglyol 812 was selected for subsequent investigation due to its superior ability to solubilize curcumin. We also analyzed the solubility of curcumin in water. Consistent with previous findings, the aqueous solubility of curcumin was below the detection limit of our RP-HPLC method.

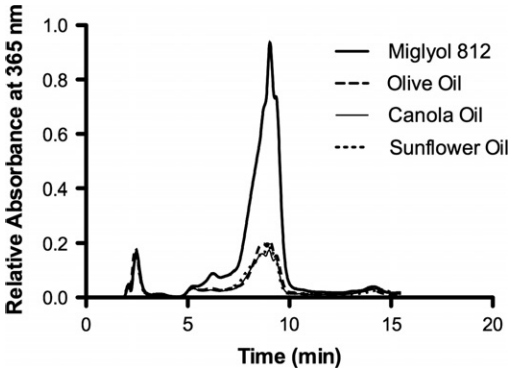

Fig. 2. Reversed-phase high pressure chromatography (RP-HPLC) analysis of saturated solutions of curcumin in Miglyol 812 as well as olive, canola and sunflower oils. Prior to analysis, excess curcumin was incubated in the oil candidates for 5 h at room temperature and centrifuged to produce saturated solutions.

2.2. Effects of oil-to-peptide ratio on emulsion characteristics

We subsequently investigated a range of oil-to-AM1 ratios that yielded emulsion droplets having different physical properties, in order to determine the best formulation for TNE assembly. Neutron reflectometry was previously used to characterize the film formed by AM1 self-assembly at the air–water interface [18], giving an interfacial AM1 molecular area of 380 Å^2 and a surface coverage of 55%. Based on these data, the theoretical dispersed phase concentration needed for the formation of sub-500 nm droplets, using 200–800 μM of AM1, was 1–3 v/v%. Therefore, we first used 2 v/v% Miglyol 812 to investigate the effect of AM1 concentration on the Z-averaged diameter (*d*) and zeta-potential of the emulsion droplets at pH 7.0. The AM1 surfactant, bearing two metal-binding histidine residues by design, binds zinc at neutral pH to form a film-like interfacial layer with increased mechanical properties. Taking advantage of this uniqueness of AM1, $ZnCl_2$ was added at twice the concentration of AM1 in all formulations to prepare emulsions with enhanced stability.

Fig. 3a shows that 50–1600 μM of AM1 was sufficient to produce highly monodispersed (polydispersity index, pdi < 0.2) emulsion droplets smaller than 300 nm at 2 v/v% Miglyol 812. Below 50 μM AM1, the droplet size increased significantly to 560 ± 17 nm, indicating that there was insufficient peptide available to adsorb at the oil–water interface to prevent coalescence of the droplets formed. The droplet size decreased to 165 ± 3 nm at 50 μM AM1, but remained relatively constant at 155 ± 3 nm when AM1 concentration was further increased from 100 to 400 μM. As the theoretical interfacial surface coverage of AM1 molecules at 330 μM on a 155 nm droplet was only 55%, it is possible that the change in AM1 concentration in the range of 100–400 μM only resulted in a change of surface coverage of peptide molecules instead of droplet size. Further increase in AM1 concentration to 1600 μM resulted in slightly larger droplets of 216 ± 7 nm. This counter-intuitive result suggested that the emulsification process under these conditions might be limited by the mixing energy provided, or that the critical concentration for maximum emulsifying capacity of AM1 had been reached. This critical concentration might be related to peptide aggregation in the bulk solution that was exacerbated at high concentration [26], thus reducing the effective amount of peptide available for interfacial stabilization. The solution viscosity might also be higher at high peptide concentration, resulting in an apparently larger droplet size. However, the likelihood of erroneous measurement due to changes in medium viscosity was minimized in our experiments by diluting the emulsion 100-fold prior to size measurements.

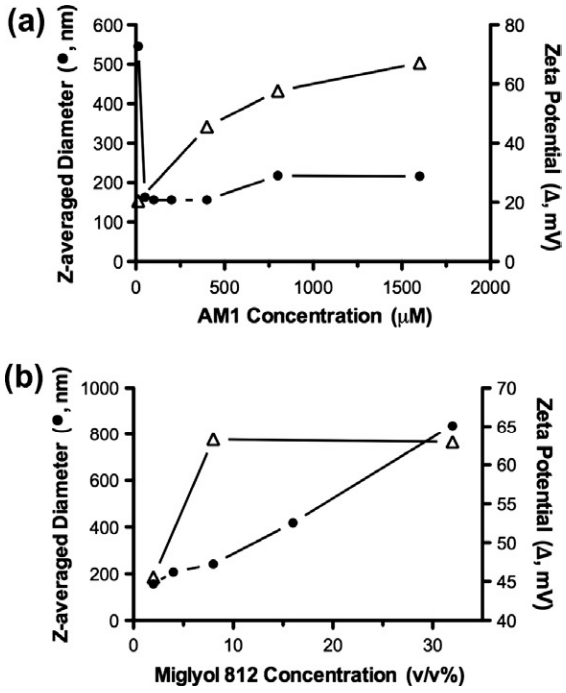

Fig. 3. Dependence of Z-averaged diameter and zeta potential of emulsion droplets on (a) AM1 concentration (2 v/v% Miglyol 812, $ZnCl_2$ at twice the concentration of AM1, 25 mM HEPES, pH 7.0); and (b) Miglyol 812 concentration (400 mM AM1, 800 mM $ZnCl_2$, 25 mM HEPES, pH 7.0).

Due to the positive charge of AM1 at pH 7 (theoretical isoelectric point = 8.5) and the zinc ions bound within the interfacial film formed by AM1 self-assembly, the emulsion droplets are positively charged. The droplet zeta potential increases gradually from 21 ± 1 to 67 ± 1 mV when AM1 concentration was increased from 12.5 to 1600 μM, possibly due to the presence of more AM1 molecules and zinc ions at the interface. Results in Fig. 3a suggested that the combination of 400 μM AM1, 800 μM $ZnCl_2$ and 2 v/v% Miglyol 812 would be suitable for TNE assembly. This formulation produced monodispersed droplets at 157 nm, and an adequately strong positive charge (46 ± 1 mV) for adsorption of anionic antigen.

We noted the possibility of manipulating the emulsion droplet size simply by varying the dispersed phase concentration, if needed. Fig. 3b shows the droplet size increase with oil loading. The Z-averaged diameter increased moderately from 157 to 241 ± 3 nm as Miglyol 812 concentration was increased from 2 to 8 v/v%. A more substantial change in droplet size from 241 ± 3 to 838 ± 17 nm was observed when Miglyol 812 concentration was increased from 8 to 32 v/v%. This biphasic trend was also observed in the droplet zeta potential, which was increased from 46 ± 1 to 63 ± 1 mV when Miglyol 812 concentration was increased from 2 to 8 v/v%, but remained relatively constant following further increase of oil concentration to 32 v/v%. The increase in droplet size with increased oil loading (Fig. 3b) could be due to limitation by (i) mixing energy, and/or (ii) surfactant coverage. The increase in zeta potential with increasing oil concentration from 2 to 8 v/v% suggested that surfactant coverage was not limiting under these conditions, and that mixing energy was the only limiting factor; the presence of more charged surfactant at the interface of larger droplets might have contributed to the zeta potential increase observed. However, both the surfactant coverage and homogenization energy might be limiting when the oil loading was further increased from 8 to 32 v/v%, resulted in the larger droplet size increase with increasing oil loading, and the different relationship between zeta potential change and droplet size.

2.3. Preparation of curcumin-loaded TNE

To prepare a loaded emulsion, curcumin was first dissolved to saturation in Miglyol 812. The resulting curcumin-containing oil was added to an AM1 solution [400 μM AM1 and 800 μM $ZnCl_2$ in 25 mM HEPES (pH 7.0)] to a final oil concentration of 2 v/v%, and homogenized. The resulting emulsion droplets loaded with curcumin had similar physical properties to those of unloaded droplets, as shown in Fig. 4. Loaded droplets had Z-averaged diameter and zeta potential of 157 ± 1 nm and 46 ± 1 mV, respectively. Repeated measurements over seven days indicated that the droplets were stable in water, with relatively little change in size and charge.

Bovine serum albumin (BSA) was selected as the model antigen for this study as it had been used successfully to induce inflammatory arthritis in an antigen-induced inflammatory arthritis (AIA) animal model [22]. The positively charged AM1 interfacial layer on the loaded emulsion (46 ± 1 mV) enabled electrostatic adsorption of anionic BSA, providing a simple strategy for incorporation of the antigen. The loaded emulsion was added slowly and with vigorous vortexing into 80 mg ml^{-1} of BSA. Sufficient mixing and a high BSA protein concentration were critical to ensure that the emulsion droplets were introduced into a protein-rich environment, which allowed the droplets to be coated rapidly before droplet collision. Inadequate mixing or lower BSA concentrations (<70 mg ml^{-1}) resulted in polydispersed emulsion size distributions with large droplets, possibly due to aggregate formation. Since the loaded emulsion was stable before addition of BSA, the aggregation at <70 mg ml^{-1} BSA might be due to bridging flocculation [27] as a result of BSA molecules adsorbing onto to the surfaces of more than one emulsion droplet. The transition through a low zeta potential region as BSA was absorbed onto the AM1 interface might also be prolonged at these lower BSA concentrations, contributing to the flocculation observed.

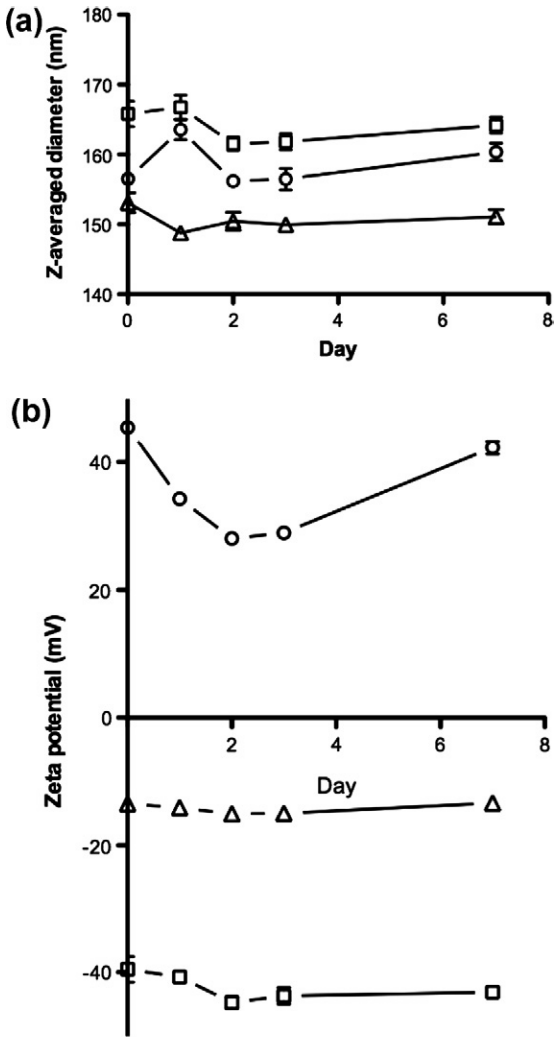

Fig. 4. (a) Z-averaged diameter and (b) zeta potential over 7 days of (circle) uncoated curcumin-loaded emulsion in water; (square) BSA-coated curcumin-emulsion in water; and (triangle) BSA-coated curcumin loaded emulsion in phosphate buffered saline (PBS, 137 mM NaCl, 2.7 mM KCl, 10 mM Na_2HPO_4, 2 mM KH_2PO_4, pH 7.4). Emulsions were stored at 4 °C and diluted at room temperature prior to analysis on test days.

Following the coating with BSA, the emulsion was slightly larger, but remained monodispersed at 166 ± 3 nm. The zeta potential of the emulsion surface decreased to −40 ± 4 mV (Fig. 4b) as a result of BSA adsorption. Charge reversal occurred because the total charge of the adsorbed BSA molecules was greater than that required to neutralize the net opposite charge on the droplet surface [27]. Fig. 4 shows that the BSA-coated emulsion was stable in water for up to seven days. Since this emulsion would later be applied in a physiological environment, we also performed stability tests in phosphate buffered saline (PBS, 137 mM NaCl, 2.7 mM KCl, 10 mM Na_2HPO_4, 2 mM KH_2PO_4, pH 7.4). The high ionic strength of PBS resulted in electrostatic screening, which decreased the magnitude and range of the electrostatic interactions between droplets. This phenomenon was evident from the change of coated droplet zeta potential from −40 ± 4 to −13 mV in the presence of salt. Despite the low electrostatic repulsion, the coated droplets were stable against flocculation, due to the steric barrier provided by BSA [28]. BSA-coated emulsion was stable in PBS for up to 7 days. In contrast, droplets not coated in BSA started to form large aggregates rapidly when diluted in PBS, due to decreased electrostatic repulsion and the presence of a moderately strong interfacial layer able to only slow rather than fully inhibit coalescence. We also measured the concentration of curcumin entrapped in the final TNE prepared by this method. RP-HPLC analysis indicated that the emulsion, after dilution and coating with BSA, carried up to 70 μg ml^{-1} (190 μM) of curcumin.

2.4. Extracellular release of curcumin from TNE

The release profile of curcumin from the TNE was investigated by separating the TNE via centrifugation into a top turbid layer containing the emulsion droplets, and a clear bottom layer containing free curcumin and BSA. The amount of free curcumin in the aqueous phase was measured with optical density at 425 nm [25] (Fig. 5, inset), and normalized against a control sample containing 70 μg ml^{-1} curcumin. Fig. 5 shows that 1.9% of curcumin was present in the aqueous phase 5 min after preparation. This amount detected might be due to curcumin that was not encapsulated during emulsion preparation, as well as curcumin that was released from the TNE in 5 min. An initial release of 8.6% was observed within the first hour, and a sustained release of curcumin up to 51.2 ± 2% was detected over 72 h.

2.5. Cytotoxicity of curcumin and TNE

Toxicity of BSA-coated emulsions was investigated *in vitro* using RAW 264.7 cells. After an 8 h incubation of emulsions with RAW 264.7 cells, viability of cells was determined by uptake of propidium iodide (PI). PI entered cells with compromised cellular membranes, forming highly fluorescent complexes with DNA by intercalation, thus allowing the quantitation of the proportion of dead cells using fluorescence detection. As a positive control, cultures were treated with 0.1 v/v% Triton X-100 to induce complete

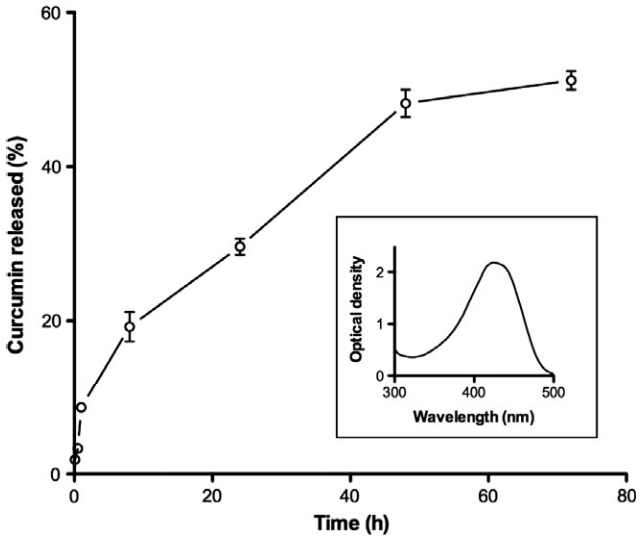

Fig. 5. Percentage of cumulative release of curcumin from BSA-coated curcumin loaded TNE over 3 days. Inset shows the UV–Vis spectrum of 70 μg ml^{-1} curcumin in 100% ethanol.

cell death (Fig. 6). Unloaded emulsion over a 20-fold dose range did not induce cell death. In contrast, emulsion loaded with curcumin induced noticeable cell death at the higher dose range. This was expected since NF-κB inhibition progressively reduces cell viability [29]. At 10- and 5-fold dilutions (19–38 μM curcumin) only 80 and 66% of cells, respectively, were viable compared to 89% in the absence of emulsion. The tolerance threshold of 19 μM of curcumin is within the range reported in the literature, although tolerance is often dependant on cell type. For example, while freshly-plated rat hepatocytes were able to tolerate up to 20 μM of curcumin [30], the same concentration resulted in 75% cell death of human pancreatic cancer cells [29]. Due to the cell-specific variance in toxicity and biological activity of curcumin, *in vitro* experiments in this study were performed on macrophages, a relevant model for APCs.

2.6. Curcumin delivery and downregulation of NF-κB

In order to study the internalization of emulsion by RAW 264.7 cells, the BSA-coated emulsion droplets were internally labeled with 1,1′-dioctadecyl-3,3,3′3′-tetramethylindocarbocyanine perchlorate (DiI). DiI is a red flourescent dye with low toxicity, which is preferentially integrated into Miglyol 812 due to its hydrophobicity, hence minimizing background signals from free dye in the aqueous phase. RAW 264.7 cells were incubated with either free DiI or DiI-labeled emulsion and examined by immunoflourescence microscopy. Incubation of cells with free DiI solution at 3 μg ml^{-1} resulted in faint staining of the cell membranes (data not shown), consistent with the function of the dye as a membrane tracer. In contrast, cells incubated with DiI entrapped in emulsion at the

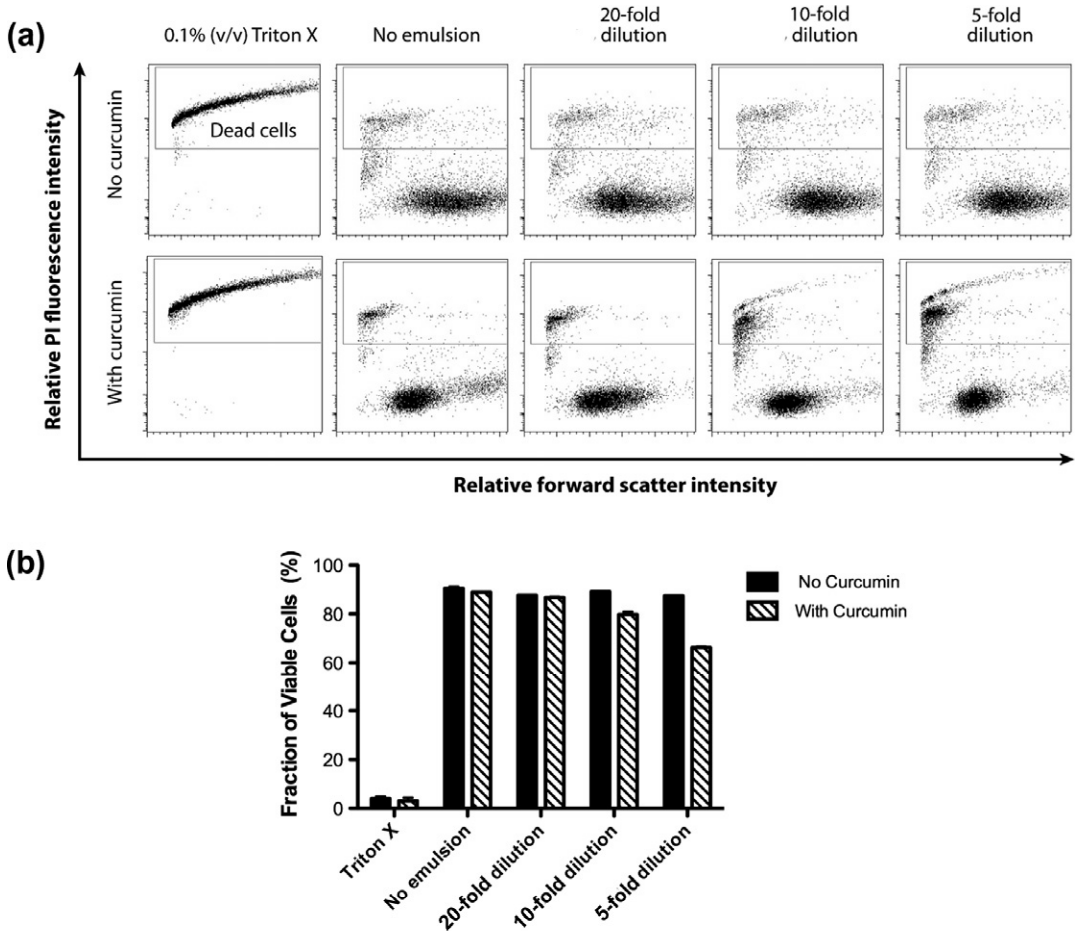

Fig. 6. Cytotoxicity profile of BSA-coated emulsion (400 mM AM1, 800 mM $ZnCl_2$, 25 mM HEPES, pH 7.0), unloaded and loaded with curcumin. (a) Flow cytograms showing the uptake of propidium iodide (PI) by RAW 264.7 cells after 8 h incubation with emulsions or 0.1 v/v% Triton X-100. Emulsions were added at 20-, 10- and 5-fold dilutions, with the corresponding curcumin concentration (for loaded emulsion) at 9.5, 19 and 38 μM, respectively. (b) Fraction of viable RAW 264.7 following incubation with emulsions or 0.1 v/v% Triton X-100, calculated using data from (a).

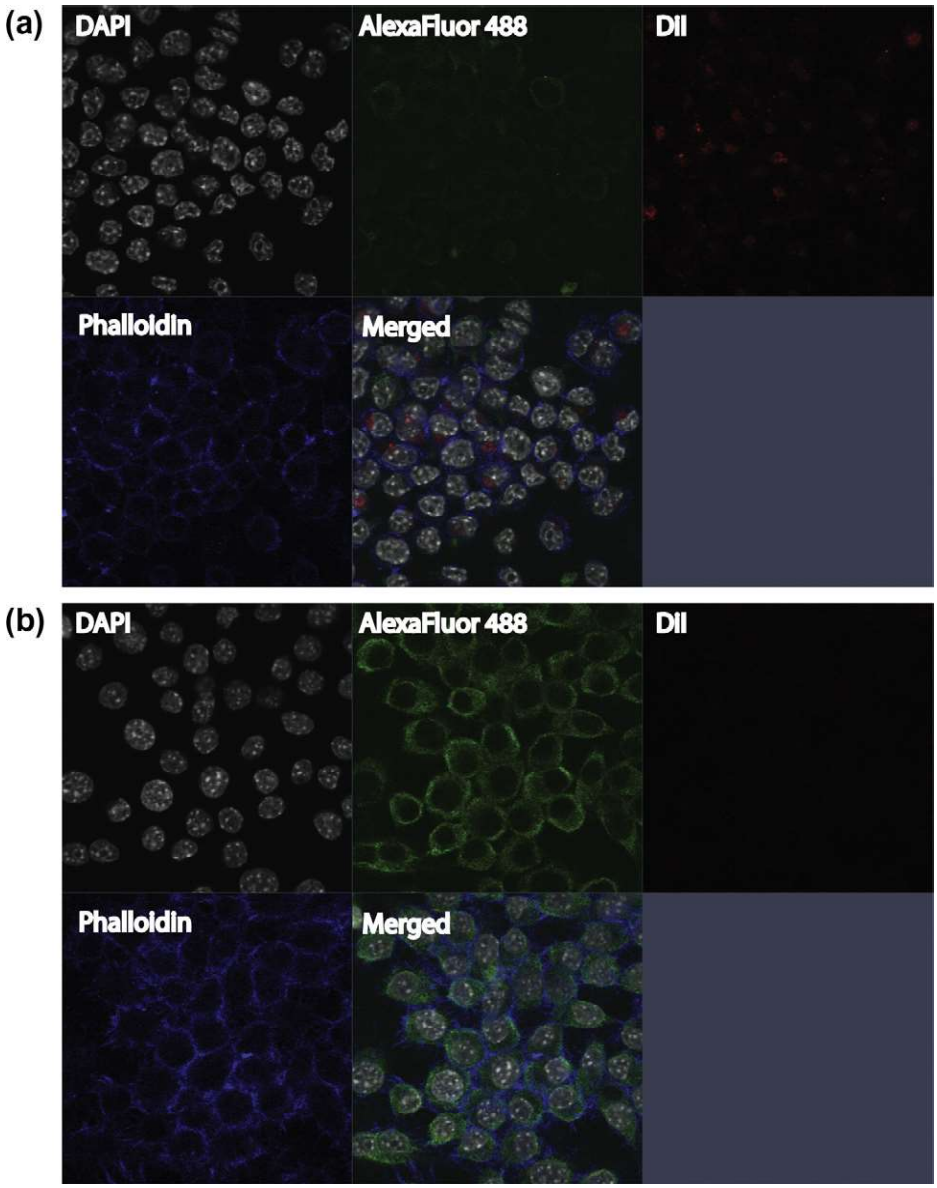

Fig. 7. Immunofluorescence microscopy showing the distribution of curcumin emulsion and relative level of NF-κB-p65 in LPS stimulated RAW 264.7 cells cultured (a) with BSA-coated curcumin-emulsion at a 10-fold dilution or (b) no emulsion. In (a), emulsion droplets were internally labeled with DiI (red) and incubated with RAW 264.7 cells for 30 min, after which 100 ng ml^{-1} of lipopolysaccharide (LPS) was added and the cell culture was incubated further for 2 h. Cells were stained with anti NF-κB-p65 and secondary Alexa Fluor 488 (green) antibodies. Cell nuclei and membranes were labeled with DAPI (gray) and phalloidin (blue), respectively. (For interpretation of the references to color in this figure legend, the reader is referred to the web version of this article.)

same concentration exhibited strong DiI fluorescence within the cell, appearing as groups of irregular bright spots (Fig. 7a). Notably the uptake distribution was uneven, with some cells showing a higher level of fluorescence than others. The irregular uptake pattern might result from differences in expression of uptake receptors within the cell line [31]. In summary these results indicate that the curcumin-emulsion droplets were efficiently internalized by RAW 264.7 cells.

Curcumin is a known anti-inflammatory compound capable of suppressing the activation and expression of NF-κB [22], a ubiquitous transcription factor that regulates inflammatory response. In this study, the expression level of NF-κB was assessed by immunofluorescent staining of cells with antibodies specific to subunits of the NF-κB family (p50, p52, p65/RelA, c-Rel and RelB). Lipopolysaccharide (LPS)-stimulated RAW 264.7 cell expressed high levels of cytoplasmic NF-κB-p65 (Fig. 7b). In contrast, cells incubated with BSA-coated curcumin-emulsion at a 10-fold dilution showed low level NF-κB-p65 fluorescent staining (Fig. 7a). These results supported the conclusion that the curcumin loaded-emulsion droplets were internalized by macrophages, and that the entrapped curcumin was released intracellularly and inhibited the expression of NF-κB *in situ*. Despite the heterogeneous internalization of emulsion by RAW 264.7 cells, NF-κB down-regulation occurred uniformly among the cells. This reduction was specific to p65, as reduced expression of p50, p52, RelB or c-Rel was not observed (data not shown), consistent with the findings that p65/p50 and p65/65 dimers are the most abundant forms of NF-κB in RAW264 cells [23]. The downregulation of p65 expression by emulsion-delivered curcumin (Fig. 7) demonstrated the potential of our delivery method to target inflammatory diseases.

In order to quantitate the inhibition of NF-κB-p65 expression by curcumin loaded emulsions in RAW264 cells, flow cytometry was

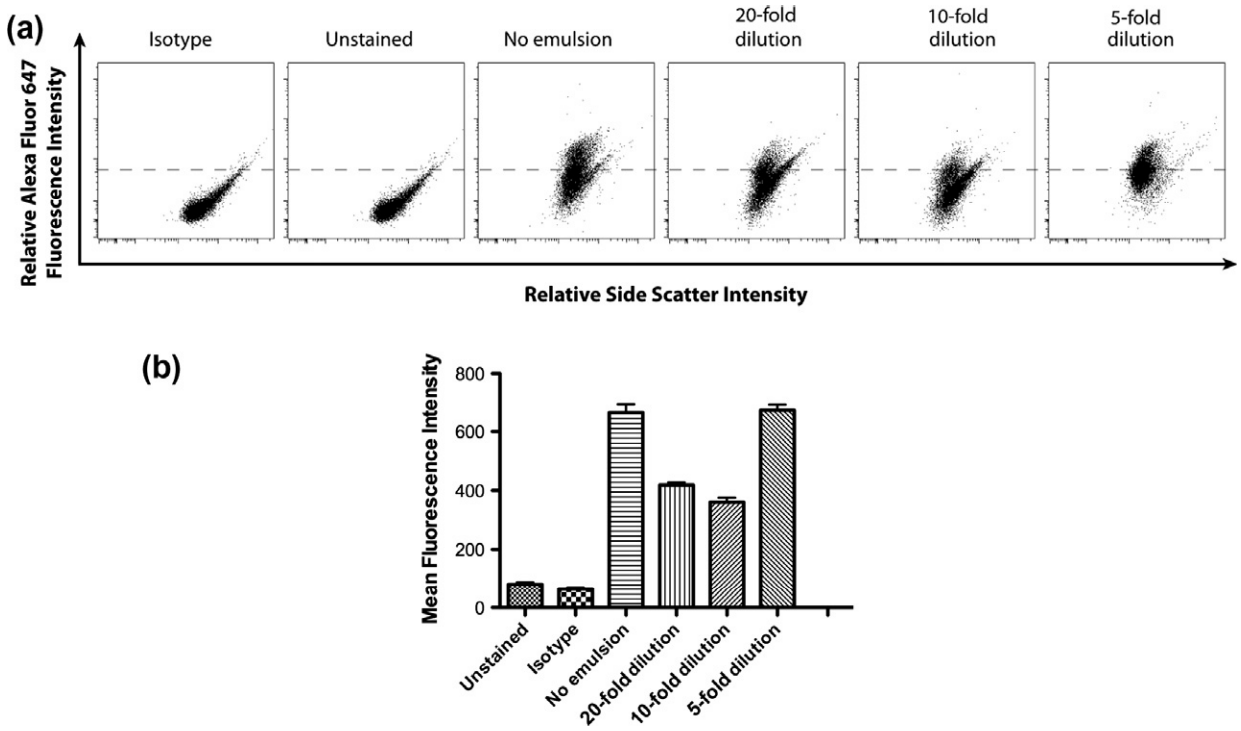

Fig. 8. Flow cytometry analysis of NF-κB-p65 level in RAW 264.7 cells cultured with BSA-coated curcumin-emulsion (400 mM AM1, 800 mM ZnCl2, 25 mM HEPES, pH 7.0) at 20-, 10- and 5-fold dilutions. Emulsion was incubated with cells for 30 min, after which 100 ng ml^{-1} of lipopolysaccharide (LPS) was added and the cells incubated for a further 2 h. (a) Flow cytograms showing NF-κB levels, detected as Alexa Fluor 647 fluorescence, in RAW 264.7 cells; (b) mean Alexa Fluor 647 fluorescence intensity calculated using data from (a).

used to measure NF-κB-p65 levels (Fig. 8). NF-κB expression was reduced by 35% when cells were cultured with curcumin-emulsion at a 20-fold dilution (19 μM curcumin). A further 11% decrease was observed when the dilution factor was decreased to 10-fold (9 μM curcumin), indicating that curcumin inhibited the expression of p65 in a dose-dependent manner. NF-κB expression was not reduced in cells incubated with curcumin loaded emulsion at a 5-fold dilution (38 μM Curcumin), relative to the untreated cells. This was due to a high level of cell death at this concentration of curcumin (Fig. 7, 34% cell death at this curcumin concentration).

3. Further discussion

Curcumin is an ideal lipophilic immunomodulatory compound with well-documented anti-cancer and anti-inflammatory properties [25,32]. While curcumin could be taken up by cells at low concentrations (0.2–1 μg ml^{-1}) *in vitro*, it is challenging to achieve such plasma concentration using free curcumin. For example, a 2 g dose of curcumin taken orally resulted in a serum concentration of less than 10 ng ml^{-1} [33]. This measured serum concentration was similar to the aqueous solubility of curcumin [34] (less than 11 ng ml^{-1}), thus indicating the lack of *in vivo* protein opsonization which could lead to increased bioavailability. Curcumin also degrades rapidly in aqueous systems, with up to 90% decomposition in phosphate buffer within 30 min [35]. Therefore, a myriad of studies have been conducted to create carriers for sustained and controlled release, and protection of this compound. These attempts include conjugation with phospholipids [36], and coating by polysaccharides [34] and polyelectrolytes [37]. Encapsulation of curcumin within a polymeric capsule has also been reported [29]. However, methods for producing these nanocarriers are complex and time-consuming, and may introduce undesirable side effects due to the use of alkaline conditions and organic solvents. Curcumin is readily dissolved in the oil phase of oil-in-water emulsions, thus making emulsion-based vehicles an attractive alternative delivery method. Entrapment in the oil phase may also protect administered curcumin from premature metabolism in the gastro-intestinal tract. Curcumin delivery by emulsion has been reported previously [25], but the non-ionic surfactant Tween 20 used in that study did not provide interfacial properties amenable to simple surface engineering. In contrast, the nanocarrier emulsion described in this study possess surface characteristics that are tailorable by modifying the designer peptide surfactant used.

There were at least two possible routes by which curcumin was delivered to the cells by the TNE. Fig. 5 shows that, during the 8-h incubation period, up to 19 ± 3% of the encapsulated curcumin might be released extracellularly into the culture medium, allowing direct uptake of curcumin. The curcumin-loaded TNE was also internalized by the cells (Fig. 7). A potential intracellular processing pathway of the internalized TNE is through the lysosomal pathway [38] leading to disruption of the emulsion at low pH [12], thus allowing release and partitioning of curcumin into the intracellular environment. For *in vivo* studies, the curcumin release rate from the TNE may need to be reduced to accommodate for the circulation time required to reach the intended biological sites. Within the context investigated in the current study, the optimum dose concentration of curcumin in RAW 264.7 is approximately 19 μM. By taking into account the appropriate dilution factor in an *in vivo* environment, the data obtained in this study may be used to guide future studies into developing a TNE for anti-inflammatory treatment.

4. Conclusions

A 166 ± 3 nm tailorable nanocarrier emulsion (TNE) was developed for the co-delivery of an anti-inflammatory drug (curcumin) and an animal-model-relevant antigen (bovine serum albumin,

BSA) using only biocompatible materials. To produce the TNE, a highly surface active peptide (SAP), AM1, was used to stabilize the curcumin-loaded emulsion and simultaneously charge the adsorption interface, enabling electrostatic adsorption of BSA. BSA simultaneously served as a model antigen and sterically stabilized the TNE under physiological conditions. The TNE was stable and well-tolerated by RAW 264.7 cells. Internalization of the emulsion successfully resulted in downregulation of NF-κB in a dose-dependent manner. The TNE reported here is ideally suited for studies using an antigen-induced arthritis model, in which arthritis develops in animals as a result of an immune response to methylated-BSA. The data presented here warrant future *in vivo* and animal studies, using antigen-specific models of autoimmune disease, to further explore the potential of TNEs as an effective and low-cost therapeutic delivery system for multiple-component therapy.

5. Experimental

5.1. Materials

AM1 peptide (molar mass 2473, 95% purity) was custom synthesized by GenScript Corporation (Piscataway, NJ, USA). Peptide concentration was determined by quantitative amino-acid analysis (Australian Proteome Analysis Facility, Sydney, Australia) on lyophilized samples. Miglyol 812 was a gift from Sasol (Rosebank, Johannesburg, South Africa). Canola (Gold'n), sunflower (Black and Gold) and olive (Coles Farmland) oils were consumer-grade products purchased from a local shop. Curcumin powder (94% purity, analytical grade) was a gift from Synthite Industrial Chemicals (Kolenchery, Kerala, India). Bovine serum albumin (BSA), poly(L-lysine) (PLL) and lipopolysaccharide (LPS) were purchased from Sigma–Aldrich (Castle Hill, Australia). 1,1′-dioctadecyl-3,3,3′3′-tetramethylindocarbocyanine perchlorate (DiI), goat anti-rabbit Alexa Fluor 488 antibody and Zenon Alexa Fluor 647 Rabbit labeling kit were from Molecular Probes (Victoria, Australia). Rabbit anti-NF-κB antibodies (p50, p52, p65/RelA, RelB, c-Rel) were from Santa Cruz Biotechnology, Inc. (Santa Cruz, CA, USA). RPMI-1640 medium was from Sigma. Goat serum, foetal calf serum (FCS) and penicillin/streptomycin/glutamine (PSG) were from GIBCO (Victoria, Australia). All other reagents were analytical grade.

5.2. Emulsion preparation

Lyophilized AM1 was dissolved in an appropriate amount of HEPES (25 mM, pH 7.0) to prepare AM1 solutions from 12.5 to 1600 μM, in which zinc chloride was added at twice the molar concentration of AM1. Miglyol 812 (2–32 v/v%) was added to the AM1/zinc chloride mixture and homogenized using a Branson Sonifier 450 ultrasonicator for two 60 s bursts at 30 W. To prepare curcumin-emulsion, excess curcumin powder was first added to Miglyol 812, incubated for 5 h at room temperature and centrifuged to produce a saturated solution. 2 v/v% of curcumin in Miglyol 812 was subsequently added to AM1 (400 μM) and zinc chloride (800 μM) in HEPES (25 mM, pH 7.0) to prepare emulsion as described above. To produce the BSA-coated emulsion, 500 μl of curcumin-loaded emulsion was added to 500 μl of 80 mg ml^{-1} BSA followed by 60 s of vigorous vortexing.

5.3. Particle size and zeta potential analysis

Emulsions were diluted 100-fold into water or phosphate buffered saline (PBS, 137 mM NaCl, 2.7 mM KCl, 10 mM Na_2HPO_4, 2 mM KH_2PO_4, pH 7.4) prior to analysis to avoid multiple scattering effects. Particle size and zeta potential measurements were performed using a Malvern Zetasizer Nano ZS (Malvern, Worcestershire, UK) equipped with a He–Ne laser (633 nm). Data analysis was with DTS software (Malvern, version 4.2), using a non-negatively constrained least squares (NNLS) fitting algorithm. Dispersant refractive index and viscosity of the dispersant were assumed to be 1.33 and 1.02 cP, respectively. For stability test, emulsions prepared were stored at 4 °C and diluted at room temperature prior to analysis on test days.

5.4. RP-HPLC

Curcuminoids were assayed by RP-HPLC using a Shimadzu system equipped with a Phenomenex Jupiter C-18 column (150 × 4.6 mm). The mobile phase was 90 v/v% acetonitrile, and 0.1 v/v% trifluoroacetic acid and 9.9 v/v% water. The flowrate was 1.0 ml min^{-1} and the detection wavelength was set at 365 nm. To determine the concentration of curcuminoids, a calibration curve was constructed using standards (5–1600 μg ml^{-1}) prepared by dissolving weighed amounts of curcumin powder in 100% ethanol.

5.5. Curcumin release assay

One milliliter of emulsion was centrifuged at 22,000*g*, 26 °C for 5 min. The bottom aqueous layer was extracted and analyzed with a Shimadzu UV-2450 UV–Vis spectrophotometer. UV–Vis spectra of samples obtained at different time points after preparation was compared to that of a control sample containing 70 μg ml^{-1} curcumin in 100% ethanol. The amount of curcumin relative to the control sample was measured with optical density at 425 nm [25].

5.6. Cell culture

Mouse leukaemic monocyte macrophage cell line (RAW 264.7) was used for evaluation of emulsion cytotoxicity and NF-κB expression by flow cytometry, as well as emulsion uptake with immunofluorescence microscopy. For flow cytometry experiments, RAW 264.7 cells were first transferred to 24-well plates (2×10^5 cells per well) 24 h after passaging, and cultivated at 37 °C and 5% CO_2 for 16 h in RPMI-1640 medium supplemented with 5 v/v% FCS and PSG, prior to further treatments. To prepare immunofluorescence microscopy slides, cells were cultivated in 12-well chamber slides (Lab-Tek, Roskilde, Denmark) instead of 24-well plates.

5.7. Cytotoxicity test

BSA-coated emulsions, with or without curcumin, were added to RAW 264.7 cells at 20-, 10- and 5-fold dilutions and incubated for 8 h. Cells were harvested by centrifugation and resuspended in 100 μl of PBS. The cell suspension was added with 5 μg ml^{-1} of propidium iodide (PI), incubated for 10 min and analyzed by a BD Biosciences FACSCanto flow cytometer.

5.8. NF-κB quantitation and immunoflurescence microscopy

BSA-coated emulsions (20-, 10-, 5-fold dilutions) were added to cells and incubated for 30 min, after which 100 ng ml^{-1} of lipopolysaccharide (LPS) was added for a further 2 h. For analysis of NF-κB by immunofluorescence microscopy, cells were cultured in chamber slides. After three washes with PBS, the cells were fixed with 4 w/v% paraformaldehyde for 15 min at room temperature. Fixed cells were washed three times with PBS, permeabilized with Tween 20 (0.5 v/v% in PBS) for 15 min, and blocked with blocking solution (10 v/v% goat serum and 0.5 v/v% Tween 20 in PBS) for 30 min. Rabbit anti-NF-κB-p65 antibody (200 μg ml^{-1}) was

incubated with treated and fixed cells in blocking solution for 1 h at room temperature. Cells were washed three times with Tween 20 (0.5 v/v% in PBS), and incubated with goat anti-rabbit-Alexa Fluor 488 antibody (200 μg ml^{-1}) for 30 min at room temperature. Excess antibody was washed off and the cells were stained with DAPI (200 ng ml^{-1}) for 10 min. After three washes with Tween 20 (0.5 v/v% in PBS), the chamber slide was disassembled according to manufacturer's instructions and mounted with fluorescent mounting medium. Mounted slides were imaged on an Apotome microscope (Carl-Ziess, Sydney, Australia).

For quantitation of NF-κB expression level, NF-κB-p65 antibody was labeled with Alexa Fluor 647 fluorophore using a Zenon kit according to the manufacturer's instructions. Labeled NF-κB-p65 antibody (200 μg ml^{-1}) was incubated with permeabilised and fixed cells in blocking solution for 1 h at room temperature. After excess antibody had been washed off with PBS, the cells were resuspended in 200 μl PBS and analyzed with a BD Biosciences FACSCanto flow cytometer.

References

[1] L.J. De Cock, S. De Koker, B.G. De Geest, J. Grooten, C. Vervaet, J.P. Remon, G.B. Sukhorukov, M.N. Antipina, Angew. Chem. Int. Ed. Engl. 49 (2010) 6954.
[2] O.C. Farokhzad, R. Langer, ACS Nano 3 (2009) 16.
[3] S. Riley, Bus. Insights Ltd., 2006, p. 25.
[4] B.J. Boyd, Expert Opin. Drug Delivery 5 (2008) 69.
[5] J.W. Cui, Y.J. Wang, A. Postma, J.C. Hao, L. Hosta-Rigau, F. Caruso, Adv. Funct. Mater. 20 (2010) 1625.
[6] D.O. Grigoriev, T. Bukreeva, H. Mohwald, D.G. Shchukin, Langmuir 24 (2008) 999.
[7] K. Szczepanowicz, H.J. Hoel, L. Szyk-Warszynska, E. Bielanska, A.M. Bouzga, G. Gaudernack, C. Simon, P. Warszynski, Langmuir 26 (2010) 12592.
[8] S. Ogawa, E.A. Decker, D.J. McClements, J. Agric. Food. Chem. 51 (2003) 2806.
[9] L. Moreau, H.J. Kim, E.A. Decker, D.J. McClements, J. Agric. Food. Chem. 51 (2003) 6612.
[10] P. Thanasukarn, R. Pongsawatmanit, D.J. McClements, Food Res. Int. 39 (2006) 721.
[11] J. Surh, D.J. McClements, Food Sci. Biotechnol. 17 (2008) 8.
[12] A.F. Dexter, A.S. Malcolm, A.P.J. Middelberg, Nat. Mater. 5 (2006) 502.
[13] R. Fairman, H.G. Chao, L. Mueller, T.B. Lavoie, L.Y. Shen, J. Novotny, G.R. Matsueda, Protein Sci. 4 (1995) 1457.
[14] A.P.J. Middelberg, C.J. Radke, H.W. Blanch, Proc. Natl. Acad. Sci. USA 97 (2000) 5054.
[15] A.F. Dexter, A.P.J. Middelberg, J. Phys. Chem. C111 (2007) 10484.
[16] A.S. Malcolm, A.F. Dexter, J.A. Katakdhond, S.I. Karakashev, A.V. Nguyen, A.P.J. Middelberg, ChemPhysChem 10 (2009) 778.
[17] E.O. Fridjonsson, T.C. Chandrasekera, A.J. Sederman, M.L. Johns, C.-X. Zhao, A.P.J. Middelberg, Soft Matter 7 (2011) 2961.
[18] A.P.J. Middelberg, L. He, A.F. Dexter, H.H. Shen, S.A. Holt, R.K. Thomas, J. R. Soc. Interface 5 (2008) 47.
[19] L.Z. He, A.S. Malcolm, M. Dimitrijev, S.A. Onaizi, H.H. Shen, S.A. Holt, A.F. Dexter, R.K. Thomas, A.P.J. Middelberg, Langmuir 25 (2009) 4021.
[20] M.C. Hochberg, Rheumatoid Arthritis, Mosby/Elsevier, Philadelphia, PA, 2009.
[21] E. Martin, B. O'Sullivan, P. Low, R. Thomas, Immunity 18 (2003) 155.
[22] C. Capini, M. Jaturanpinyo, H.I. Chang, S. Mutalik, A. McNally, S. Street, R. Steptoe, B. O'Sullivan, N. Davies, R. Thomas, J. Immunol. 182 (2009) 3556.
[23] B. O'Sullivan, A. Thompson, R. Thomas, Expert Opin. Ther. Targets 11 (2007) 111.
[24] B.K. Jadhav, K.R. Mahadik, A.R. Paradkar, Chromatographia 65 (2007) 483.
[25] X.Y. Wang, Y. Jiang, Y.W. Wang, M.T. Huang, C.T. Ho, Q.R. Huang, Food Chem. 108 (2008) 419.
[26] D. Thirumalai, D.K. Klimov, R.I. Dima, Curr. Opin. Struct. Biol. 13 (2003) 146.
[27] G.B. Sukhorukov, E. Donath, S. Davis, H. Lichtenfeld, F. Caruso, V.I. Popov, H. Mohwald, Polym. Adv. Technol. 9 (1998) 759.
[28] J. Rangsansarid, K. Fukada, J. Colloid Interface Sci. 316 (2007) 779.
[29] S. Bisht, M. Mizuma, G. Feldmann, N.A. Ottenhof, S.M. Hong, D. Pramanik, V. Chenna, C. Karikari, R. Sharma, M.G. Goggins, M.A. Rudek, R. Ravi, A. Maitra, A. Maitra, Mol. Cancer Ther. 9 (2010) 2255.
[30] N. Romiti, R. Tongiani, F. Cervelli, E. Chieli, Life Sci. 62 (1998) 2349.
[31] T. Ravasi, C. Wells, A. Forrest, N. Walsh, D.M. Underhill, B.J. Wainwright, A. Aderem, S. Grimmond, D.A. Hume, J. Immunol. 168 (2002) 1497.
[32] B.B. Aggarwal, A. Kumar, A.C. Bharti, Anticancer Res. 23 (2003) 363.
[33] G. Shoba, D. Joy, T. Joseph, M. Majeed, R. Rajendran, P.S.S.R. Srinivas, Planta Med. 64 (1998) 353.
[34] H.H. Tonnesen, M. Masson, T. Loftsson, Int. J. Pharm. 244 (2002) 127.
[35] Y.J. Wang, M.H. Pan, A.L. Cheng, L.I. Lin, Y.S. Ho, C.Y. Hsieh, J.K. Lin, J. Pharm. Biomed. Anal. 15 (1997) 1867.
[36] K. Maiti, K. Mukherjee, A. Gantait, B.P. Saha, P.K. Mukherjee, Int. J. Pharm. 330 (2007) 155.
[37] Z.G. Zheng, X.C. Zhang, D. Carbo, C. Clark, C.A. Nathan, Y. Lvov, Langmuir 26 (2010) 7679.
[38] F. Nielloud, G. Marti-Mestres, Pharmaceutical Emulsions and Suspensions, Marcel Dekker, New York, 2000.